

Revista **ALCONPAT**

Latin American Journal of Quality Control, Pathology and
Construction Recovery

DOI: <http://dx.doi.org/10.21041/ra.v10i1>
editorial.revista.alconpat@gmail.com

eISSN: 2007-6835

Volume 10

January - April 2020

Issue 1



Latin American Journal of Quality Control, Pathology and
Construction Recovery

<http://www.revistaalconpat.org>



ALCONPAT International

Founders members:

Liana Arrieta de Bustillos – **Venezuela**
Antonio Carmona Filho - **Brazil**
Dante Domene – **Argentina**
Manuel Fernández Cánovas – **Spain**
José Calavera Ruiz – **Spain**
Paulo Helene, **Brazil**

Board of Directors International:

President of Honor

Angélica Ayala Piola, **Paraguay**

President

Carmen Andrade Perdriz, **Spain**

Managing Director

Pedro Castro Borges, **Mexico**

Executive Secretary

José Iván Escalante García, **Mexico**

Technical Vice President

Enio Pazini Figueiredo, **Brazil**

Administrative Vice President

Luis Álvarez Valencia, **Guatemala**

Manager

Paulo Helene, **Brazil**

Revista ALCONPAT

Editor in Chief:

Dr. Pedro Castro Borges
Centro de Investigación y de Estudios Avanzados del
Instituto Politécnico Nacional, Unidad Mérida
(CINVESTAV IPN – Mérida)
Merida, Yucatan, **Mexico**

Co-Editor in Chief:

Dr. Francisco Alberto Alonso Farrera
Universidad Autónoma de Chiapas
Tuxtla Gutiérrez, Chiapas, México

Executive Editor:

Dr. José Manuel Mendoza Rangel
Universidad Autónoma de Nuevo León,
Facultad de Ingeniería Civil
Monterrey, Nuevo Leon, **Mexico**

Associate Editors:

Dr. Manuel Fernandez Canovas
Universidad Politécnica de Madrid.
Madrid, **Spain**

Ing. Raúl Husni

Facultad de Ingeniería Universidad de Buenos Aires.
Buenos Aires, **Argentina**

Dr. Paulo Roberto do Lago Helene
Universidade de São Paulo.
São Paulo, **Brazil**

Dr. José Iván Escalante García
Centro de Investigación y de Estudios Avanzados del
Instituto Politécnico Nacional (Unidad Saltillo)
Saltillo, Coahuila, **Mexico**.

Dr. Mauricio López.

Departamento de Ingeniería y Gestión de la Construcción,
Escuela de Ingeniería, Pontificia Universidad Católica de
Chile
Santiago de Chile, **Chile**

Dra. Oladis Troconis de Rincón
Centro de Estudios de Corrosión
Universidad de Zulia
Maracaibo, **Venezuela**

Dr. Fernando Branco Universidad
Técnica de Lisboa
Lisboa, **Portugal**

Dr. Pedro Garcés Terradillos
Universidad de Alicante
San Vicente, **Spain**

Dr. Andrés Antonio Torres Acosta
Instituto Tecnológico y de Estudios Superiores de
Monterrey, Querétaro
Querétaro, **Mexico**

Dr. Luiz Fernández Luco
Universidad de Buenos Aires –
Facultad de Ingeniería – INTECIN
Buenos Aires, **Argentina**

RAVIONI, January – April 2020

Message from the Editor in Chief

**JOURNAL OF THE LATIN-AMERICAN
ASSOCIATION OF QUALITY CONTROL,
PATHOLOGY AND RECOVERY OF
CONSTRUCTION**

<http://www.revistaalconpat.org>

We present the first issue of the tenth year of the ALCONPAT journal with great satisfaction.

The aim of the journal is to publish case studies within the scope of the Association, namely quality control, pathology and recovery of constructions, including basic and applied research, reviews and documentary research.

In 2019, a special session was held on the action of fire in concrete materials, elements and structures during CONPAT 2019, to honor Paulo Helene for his 70th anniversary and fruitful career. Consequently, and as part of the celebration, the V10 N1 of the RA is a special issue on topics related to the action of fire in honor of him.

The first work of this issue is by Carlos Brites and colleagues and aims to present and briefly discuss some essential issues about the action of fire in concrete structures and the possible harmful effects due to high temperatures. A brief review of the literature that deals with the behavior of concrete (seen as a material and as a structural element) was carried out when exposed to exceptional and severe thermal actions in a fire scenario, which contributes to demystifying some beliefs and doubts about the phenomenon of occurrence of spallings.

In the second work, Fabrício Bolina and colleagues discuss the fire resistance of vertical sealing systems composed of ceramic blocks with vertical holes at high temperatures. Masonry is widely used in the civil construction market because it is a low cost and high productivity system compared to conventional elements. The results were obtained with finite element computational models through Ansys Mechanical software, and calibrated with a real-scale experimental test, determining the fire resistance time (TRF) for different block geometries. The computational analyzes led to results that point to a limit for the efficiency of increasing the thickness of a wall to achieve high TRFs in relation to thermal insulation.

In the third article Dainer Marçal Dias and colleagues investigate the influence of the addition of polymeric fibers of polypropylene, polyester, polyamide, aramid and aramid pulp in the behavior of concretes subjected to high temperatures. The specimens with fiber additions at a rate of 2 kg / m³ were produced and subjected to high temperatures through oven tests and direct fire. Columns were also built and submitted to a live fire simulator, belonging to the Espírito Santo Fire Department - Brazil. The microstructural and mechanical properties were analyzed. It was noted that the fibers can influence the properties of concrete and

that fire tests with standard fire load can be an alternative or complement for the analysis of concrete subjected to high temperatures.

In the fourth article, by Carlos Alexandre Santos Sales et. al., the efficiency of surface protection of masonry structures sealed with intumescent ink in relation to mechanical resistance and thermal insulation was evaluated. Sixty masonry blocks with ceramic sealing were used. The temperature of the face directly exposed to the flame was on average 25% lower for the block with passive protection. The compressive strength of the passive protection blocks was approximately 70% greater than that of the unprotected blocks, after 60 minutes of direct flame exposure. More than 70% of the blocks without passive protection and exposed to flames had a compressive strength of 1.35 MPa, while 100% of the blocks with protection had values of 2.38 MPa, even after 60 minutes of exposure.

The fifth work of this issue is written by Francine Barcellos and colleagues, with the objective of evaluating the performance of composite slabs in a fire situation, correlating them with the project at normal temperature, according to NBR 14323 (ABNT, 2013), NBR 8800 (ABNT, 2008) and NBR 14762 (ABNT, 2010), through the heating curve of ISO 834 (ISO, 1999) and the distribution of slab temperatures obtained by using Ansys software. The computational models were calibrated according to the standard and extrapolated to other design scenarios, with different geometries, thicknesses and effective thicknesses of the concrete layer. As a result, the platform with recesses had a better performance in relation to the trapezoids, the thickness of the concrete layer being the predominant variable in the behavior of these slabs at high temperatures, due to their greater thermal stability.

In the sixth work, Carlos Brites and colleagues compare different fire-resistant cladding systems applied to reinforced concrete elements of one year of age and 1.5 cm of concrete cladding and evaluate the performance of these systems by visual inspection and verification. of the evolution of internal temperatures after fire simulations under the ISO 834 curve, using thermocouples for 120 minutes. The results showed very close correlations with the literature for cement-based mortar coatings, as well as particularities about plaster coatings and the possibility of using intumescent paints as passive protection in reinforced concrete elements.

In the seventh paper, Julia Menegon and colleagues evaluate the behavior of ceramic structural block walls at high temperatures. Blocks 14 and 19 cm wide were used, with compressive strengths of 7 and 10 MPa. The thicknesses of the joints, the mortar for settlement and the influence of coating on the exposed face were evaluated. Kiln temperatures were measured, inside and on the surface of the walls, the expansion of the blocks and the crushing of the joints. It could be inferred that the samples showed good performance, maintaining their tightness, insulation and mechanical resistance. The lateral restriction did not cause the blocks to be deployed, however, it was possible to

observe tension transfer for them for poorly flexible mortars. The 19 cm wide masonry and the coated ones presented better thermal performance.

The eighth article, by Paulo Helene and colleagues, makes a diagnosis that explains the mechanism of collapse, in just 80 minutes, of the Wilton Paes de Almeida building, which was surprising for the engineering of structural concrete. Previous fires, such as that of the Andraus Building, the Joelma and the Great Avenue, withstood more than 4 hours of fire without collapsing and are currently in use. To understand this unusual collapse, an experimental investigation of the characteristics and properties of the concrete and the reinforcement used in that structure was carried out, based on a "hypothetical structural project" that considered the actual characteristics of the materials used. Based on the diagnosis, recommendations were established so that cases like this do not recur.

The article that closes the edition is by Antonio Fernando Berto, who addresses the regulatory aspects related to fire safety and presents case studies of buildings in São Paulo that suffered the action of fire and its consequences. Berto discusses the fire safety that should be considered from the conception of the building, through the design and construction, to the operation and maintenance phase. In the design phase, the issue should be considered especially, since it establishes the basic structure of fire safety of the building. This should be based on a thorough knowledge of the relationships that exist with the provisions that give the building adequate levels of fire safety.

We are confident that the articles in this issue will constitute an important reference for those readers involved with questions of evaluations and characterizations of materials, elements and structures. We thank the authors participating in this issue for their willingness and effort to present quality articles and meet the established times.

On behalf of the Editorial Board

A handwritten signature in black ink, appearing to read 'Pedro Castro Borges', written over a circular stamp or seal.

Pedro Castro Borges
Editor in Chief



CONTENT

Página

REVIEW

C. Brites, M. Carvalho, P. Helene: Fire impacts on concrete structures. A brief review.

1 - 21

APPLIED RESEARCH

F. Bolina, B. Tutikian, J. Gonçalves, T. Souza, G. Manica: Numerical-experimental analysis of ceramic block masonry walls of different thickness at high temperatures.

22 – 35

D. M. Dias, J. L. Calmon, G. L. Vieira: Polymeric fiber reinforced concrete exposed to fire.

36 - 52

C. A. S. Sales, C. F. G. Nascimento, T. M. Silva, L. M. Barreto, A. C. Lordsleem Jr, W. A. Soares, P. Castro-Borges, E. C. B. Monteiro: Fire resistance of ceramic-masonry sealing blocks using intumescent paint protection.

53 - 68

F. Barcellos, F. Bolina, B. Tutikian: Numerical analysis of composite concrete and steel slabs section under fire situation.

69 - 78

BASIC RESEARCH

C. Brites, V. P. Silva, M. Carvalho, P. Helene: Performance of fire protective coatings in reinforced concrete elements submitted to high temperatures.

79 - 96

J. Menegon, Â. G. Graeff, L. C. P. Silva Filho: Structural masonry walls exposed to high temperatures with thermal expansion control.

97 - 113

DOCUMENTARY RESEARCH

P. Helene, J. Pacheco, D. Couto: Fire and Collapse of the Wilton Paes de Almeida Building in São Paulo, Brasil: lessons learned.

114 - 131

A. F. Berto: Fires in concrete structures - Significant case studies in São Paulo.

132 - 146



Fire impacts on concrete structures. A brief review

C. Britez^{1*}, M. Carvalho², P. Helene³ 

*Contact author: britez.consultoria@gmail.com

DOI: <http://dx.doi.org/10.21041/ra.v10i1.421>

Reception: 07/06/2019 | Acceptance: 11/11/2019 | Publication: 30/12/2019

ABSTRACT

This paper aims to present briefly discuss some essential topics about the impact of fire on concrete structures and the possible deleterious effects of high temperatures on the concrete material itself. A literature review was conducted, addressing the behavior of concrete (seen as a material and as a structural element) when exposed to exceptional and severe actions from a fire scenario, contributing to demystify some beliefs and doubts about the *spalling* phenomenon and the behavior of reinforced concrete under fire situations.

Keywords: fire; concrete structure; *spalling*.

Cite as: Britez, C., Carvalho, M., Helene, P. (2020), " *Fire impacts on concrete structures. A brief review*", Revista ALCONPAT, 10 (1), pp. 1 – 21, DOI: <http://dx.doi.org/10.21041/ra.v10i1.421>

¹ Pesquisador de Pós-Doutorado na Escola Politécnica da USP, Britez Consultoria, São Paulo, Brasil.

² Universidade Presbiteriana Mackenzie, São Paulo, Brasil.

³ Professor Titular da Escola Politécnica da USP, PhD Engenharia, São Paulo, Brasil.

Legal Information

Revista ALCONPAT is a quarterly publication by the Asociación Latinoamericana de Control de Calidad, Patología y Recuperación de la Construcción, Internacional, A.C., Km. 6 antigua carretera a Progreso, Mérida, Yucatán, 97310, Tel.5219997385893, alconpat.int@gmail.com, Website: www.alconpat.org

Responsible editor: Pedro Castro Borges, Ph.D. Reservation of rights for exclusive use No.04-2013-011717330300-203, and ISSN 2007-6835, both granted by the Instituto Nacional de Derecho de Autor. Responsible for the last update of this issue, Informatics Unit ALCONPAT, Elizabeth Sabido Maldonado, Km. 6, antigua carretera a Progreso, Mérida, Yucatán, C.P. 97310.

The views of the authors do not necessarily reflect the position of the editor.

The total or partial reproduction of the contents and images of the publication is strictly prohibited without the previous authorization of ALCONPAT Internacional A.C.

Any dispute, including the replies of the authors, will be published in the third issue of 2020 provided that the information is received before the closing of the second issue of 2020.

Ações e efeitos deletérios do fogo em estruturas de concreto. Uma breve revisão

RESUMO

Este artigo tem o objetivo de apresentar e discutir brevemente alguns tópicos essenciais sobre a ação do fogo nas estruturas de concreto e quais os eventuais efeitos deletérios das elevadas temperaturas no material concreto propriamente dito. Foi realizada uma revisão da literatura, abordando o comportamento do concreto (visto como um material e como um elemento estrutural) quando exposto às ações térmicas excepcionais e severas procedentes de um cenário de incêndio, contribuindo para desmistificar algumas crenças e dúvidas quanto ao fenômeno de ocorrência de *spalling* e ao comportamento de estruturas de concreto armado em situação de incêndio.

Palavras-chave: incêndio; estrutura de concreto; *spalling*.

Acciones y efectos nocivos del fuego sobre estructuras de hormigón. Una breve reseña

RESUMEN

Este artículo tiene como objetivo presentar y discutir brevemente algunos temas esenciales sobre la acción del fuego en las estructuras de concreto y los posibles efectos nocivos de las altas temperaturas en el material concreto. Se realizó una revisión de la literatura, que aborda el comportamiento del concreto (visto como un material y como un elemento estructural) cuando se expone a acciones térmicas excepcionales y severas de un escenario de incendio, lo que contribuye a desmitificar algunas creencias y dudas sobre el fenómeno de ocurrencia de *spalling* y el comportamiento de la estructura de hormigón armado en situación de incendio.

Palabras clave: fuego; estructuras de hormigón; *spalling*.

1. INTRODUCTION

In terms of the design of structures and of the exceptional action of fire, when compared to other (unprotected) building materials, concrete has a number of attributes, as it can be seen in Figure 1. In this context, it is emphasized that there are two main components responsible for the positive performance of concrete in fire conditions: the first related to the intrinsic properties of the material and the second to its functionality when inserted in the overall structure.

Unprotected construction materials	Fire resistance	Ease of combustion	Contribution to fire loads	Temperature rise rate at cross section	Fire protection (intrinsic of the material)	Ease of rehabilitation	Protection for escape and firemen
WOOD	LOW	HIGH	HIGH	VERY LOW	VERY LOW	NULL	LOW
STEEL	VERY LOW	NULL	NULL	VERY HIGH	LOW	LOW	LOW
CONCRETE	HIGH	NULL	NULL	LOW	HIGH	HIGH	HIGH

Figure 1. Summary of the performance of (unprotected) building materials under fire (translated from Jacobs, 2007).

Concrete is non-combustible and has a low temperature rise rate along its cross section, so in most structural systems the material can be used without any additional fire protection.

In this article, some essential topics about the action of fire on concrete structures and the possible deleterious effects of high temperatures on the concrete material itself are briefly presented and discussed.

2. ASPECTS OF CONCRETE UNDER FIRE SITUATION

2.1 Fire, concrete and burning event

In Brazil, ABNT NBR 13860:1997 has the following definition: “**Fire** is the combustion process characterized by the emission of heat and light”. However, according to Seito et al. (2008), despite major advances in fire science, there is still no global consensus to define fire because there is no clear agreement on the definitions of major international standards in force.

Seito et al. (2008) clarifies that a theory known as the Fire Triangle was initially formulated, which was formed by three fundamental elements: the fuel, the oxidizer (oxygen) and the heat. According to this theory, the removal of any of these elements from the triangle would be directly responsible for extinguishing the fire.

On the other hand, with the discovery of the *halon* extinguishing agent¹, the theory was reformulated, being known today as Fire Tetrahedron (Figure 2). In turn, the Fire Tetrahedron consists of the following elements: heat, oxidizer, fuel and chain reaction.

Heat is the element used to start a fire, maintain and increase its spread. Oxidizer (oxygen) is required for combustion and is present in the air surrounding us. Fuel is the propagating element of fire and can be solid, liquid or gaseous. The chain reaction makes the burning process self-sustaining. Basically, the radiated heat from the flames reaches the fuel and it is broken down into smaller particles, which combine with oxygen and burn, radiating heat back into the fuel, thus forming a constant (self-sustaining) cycle.

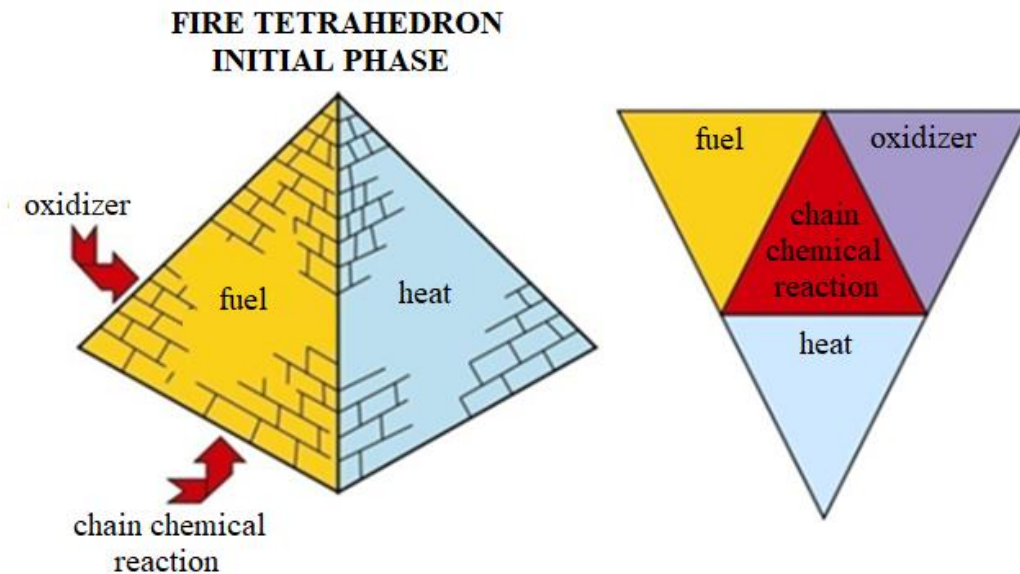


Figure 2. Fire tetrahedron (adapted from Seito et al., 2008).

Concrete (exclusively as a material) is recognized for its good behavior at high temperatures due to its thermal characteristics such as: incombustibility and low thermal conductivity. In addition,

¹ *Halon* (halogenated hydrocarbon) is an extinguishing agent for chemical compounds formed by halogen elements (fluorine, chlorine, bromine and iodine). It was banned by the Montreal Protocol for being harmful to the ozone layer. The Montreal Protocol, in turn, is an international treaty in which the signatory countries undertake to replace ozone-depleting substances.

concrete does not release toxic gases when heated and the elements have greater mass and volume when compared to other materials such as the elements of metal and wood structures, i.e. potentially resist longer.

It can be said, therefore, that concrete is not a fundamental element of Fire Tetrahedron because it is not a solid fuel. In a fire event, concrete suffers the consequences of the burning of any flammable material, whether solid, liquid or gaseous. Generally, in commercial and residential buildings, this flammable charge comes from solid cellulosic base materials such as doors, furniture, office supplies, carpeting, curtains, etc.

In general, several studies conservatively point out that a more exposed portion of concrete loses approximately 25% of its original compressive strength when heated at temperatures around 300°C and approximately 75% when this temperature reaches 600°C inside.

In addition to the reduction in strength, precursor research by Abrams (1971) and Neville (1981) indicated that concretes considered normal² suffered high thermal gradients when exposed to fire and there was a strong tendency for hot surface layers to detach from the cooler layers inside the element. This type of detaching is known worldwide as *spalling*.

Fire generally starts in small proportions and its growth depends on the first ignited³ item, the fire performance characteristics of materials in the vicinity of this ignited item, and its distribution in the environment (Seito et al., 2008).

Costa & Silva (2003) and Costa (2008) describe that, in general, the curve that represents the temperature variation in a real fire is characterized by two well-defined branches (one ascending and one descending) with three phases delimited by two points (Figure 3): flashover⁴ and maximum temperature. These three phases are explained below.

- **Ignition:** heating stage at the beginning of the fire, with gradual temperature growth, with minimal influence of compartment characteristics and without risk to human life or heritage by structural collapse. This stage is also known as pre-flashover and ends at the instant known as flashover.
- **Flashover:** stage characterized by a sudden change in temperature growth. At this stage all combustible material in the compartment is combusted. The temperature of the hot gases is above the 300°C level until reaching the peak of the curve, usually with temperatures above 1000°C.
- **Cooling:** stage that represents the gradual temperature reduction of the gases in the environment, after the complete extinguishing of the combustible material present in the compartment. Without new fire loads to feed the flames, heat loss begins, i.e. the gradual cooling of the fire.

² It is understood in this text that concretes considered “normal” (or conventional) are those with compressive strength below 50MPa, as recommended by the Portland Cement Association (PCA), recorded in High Strength Concrete (published in 1994 by Farny and Panarese) and adopted in this text.

³ From the verb to ignite (to ignite, to burn, to turn into fire).

⁴ Flashover can be defined as: instant of generalized inflammation, although there is no consensus in Brazilian literature about this translation. The use of the English term flashover is popular in Brazil and abroad.

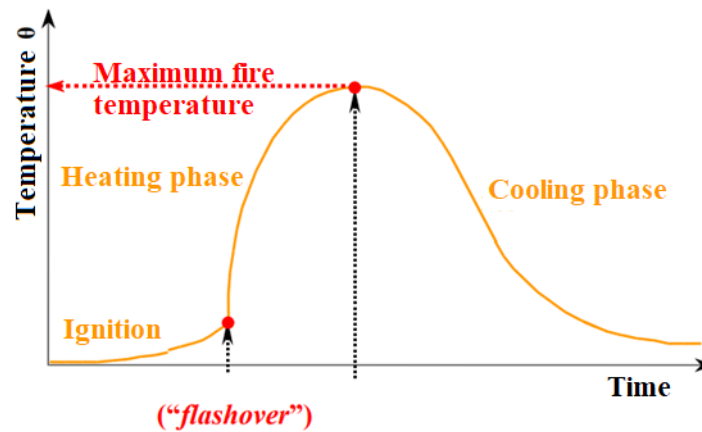


Figure 3. Main phases of a real fire (Costa & Silva, 2003).

In general, the simulation of real or natural fire in a structure is quite complex and can be quite unique, as each fire has its particularities, which depend directly on the heating rate, the maximum temperature reached and the duration of the fire event.

Considering this situation, Costa & Silva (2003, 2006) observed that, to facilitate the determination of the thermal action in the structures, mathematical fire models were formulated to describe the variation of the room temperature as a function of the fire time.

The temperature-time relation, in these specific cases, can be represented by "temperature-time curves" or "fire curves", which are standardized and popularly known as the "standard fire curve".

2.2 Standard fire simulation curves

These are standard curves adopted in experimental and laboratory fire resistance tests to standardize the tests and provide enough support to analyze and compare the results, once the fire simulation was normalized (Costa e Silva, 2006).

In this perspective, when the minimum resistance time of the structural elements is determined by means of the standard fire curve, it is referred to as the **Fire Resistance Required Time** or simply by the acronym **TRRF** (ABNT NBR 14432 in Brazil: 2001).

TRRF is a standardized minimum period which assumes that a given structure will maintain its performance functions during a fire scenario simulated by a standard curve.

In general, this period is expressed in 30-minute intervals with predetermined values, depending on several factors (*fib*, 2007): type of occupation/use, height and number of floors of the building, number of people to be evacuated, room dimensions, escape routes/emergency exits and available protection systems (extinguishers, automatic showers, among others).

Figure 4 shows the temperature profiles that simulate three standard fire scenarios that are commonly used in experimental studies, as follows: (a) the tunnel fire scenario; (b) the one caused by hydrocarbon-based materials and (c) the one caused by buildings (by cellulosic materials).

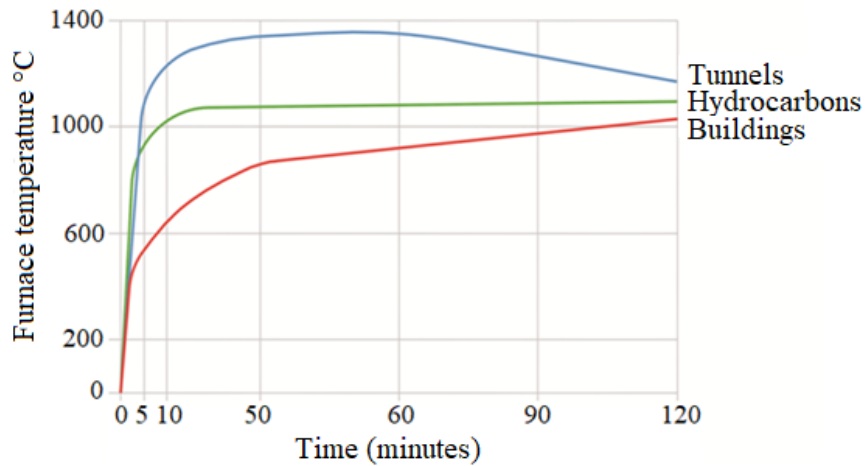


Figure 4. “Idealized” curves for three fire simulation scenarios: tunnels, hydrocarbons and buildings - cellulosic materials - up to 120 minutes (The Concrete Center, 2004).

The three most widespread idealized and standardized curves in the technical field used in experimental studies involving fire scenario simulations caused by cellulosic-based materials in concrete elements are the curves: ISO 834, ASTM E119 and JIS A 1304 (Phan, 1996). These curves are very similar and can be seen, overlapping, in the Figure 5. Tunnel and hydrocarbon standard curves will not be addressed in this article and can be consulted in Leonardo Da Vinci Pilot Project: Handbook 5 (2005).

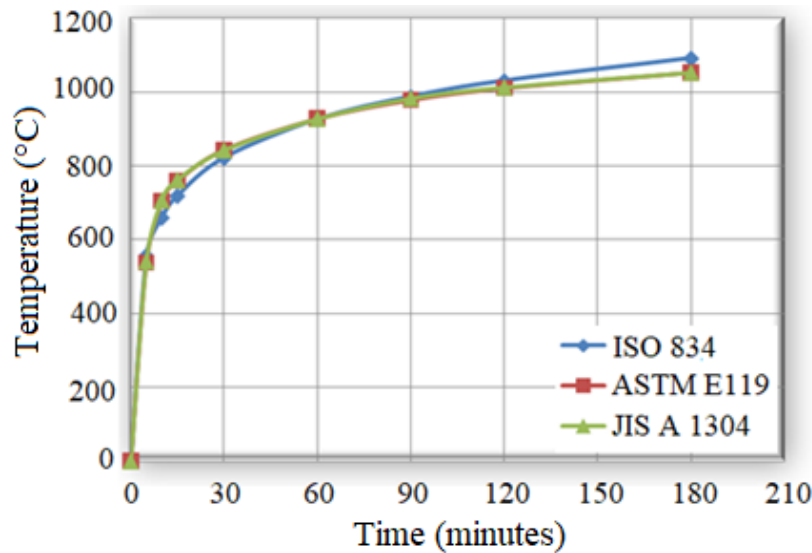


Figure 5. Standard fire curves (adapted from Phan, 1996).

The ISO 834 curve is one of the most used in international experimental studies, being also adopted in Brazil - transcribed in ABNT NBR 5628:2001. This curve specifies that the sample must be subjected to a temperature rise inside the furnace, given by the following logarithmic equation (Equation 1):

$$\theta - \theta_0 = 345 \log_{10} 8(t + 1) \tag{Equation 1}$$

Where:

t = time, expressed in minutes (min);

θ = furnace inside temperature at time t, expressed in Celsius degrees (°C);

θ₀ = initial temperature inside the furnace, expressed in Celsius degrees (°C).

Other standard curves for flammable materials (ASTM E1549, RWS and RABT) have been modeled for fire severity and have been internationally recommended for special situations (Costa, 2008). There are also fire curves called “natural curves”, parameterized by the amount of combustible material (fire load), the degree of ventilation and the thermal and physical characteristics of the compartmental materials. These curves are simplified models of the real fire and will not be covered in this article and can be consulted in Leonardo Da Vinci Pilot Project: Handbook 5 (2005).

2.3 Temperature distribution inside the concrete

Heat is the energy that is being transferred from one system to another because of a temperature difference. Basically, there are three classic heat transfer mechanisms: conduction, convection, and radiation.

In conduction, thermal energy is transferred through interactions between atoms or molecules, although there is no transport of these atoms or molecules, only the displacement of energy. In convection, energy is transported in the form of heat through direct mass transport. In radiation, thermal energy is carried through space in the form of electromagnetic waves moving at the speed of light.

In a fire event there is a combination of these three heat transfer mechanisms, however, within the concrete mass there is a predominance of **conduction heat flux**.

In this context, the calculation of the development of a temperature field in the cross section of a structural concrete element exposed to fire involves solving the classical *Fourier* differential equation (Equation 2):

$$\frac{\partial}{\partial x} \left(\lambda_{\theta} \frac{\partial \theta}{\partial x} \right) + \frac{\partial}{\partial y} \left(\lambda_{\theta} \frac{\partial \theta}{\partial y} \right) + \frac{\partial}{\partial z} \left(\lambda_{\theta} \frac{\partial \theta}{\partial z} \right) + Q = \rho \cdot c_{\theta} \frac{\partial \theta}{\partial t}$$

(Equation 2)

In which:

λ_{θ} : is the thermal conductivity of the material (W/m °C);

$\rho \cdot c$: is the specific volumetric heat of the material (product of specific mass and absolute specific heat) (J/kg °C);

x, y e z: the Cartesian coordinates of the three-dimensional system;

Q: is the internal heat rate generated on the material;

$\partial\theta$: is the temperature gradient in the direction of heat flow;

t: time (s).

Internal heat generation Q can be considered 0 (zero) for non-combustible materials (such as concrete). The boundary conditions (on the surface of the element) are expressed in terms of heat flow equations and the thermal properties of the material depend on the type and quantity of materials used in concrete mix design (Leonardo Da Vinci Pilot Project: Handbook 5, 2005).

To exemplify the behavior of the temperature field evolution as a function of time in a concrete element, we present the computer simulation study by Ongah, Mendis & Sanjayan (2002) in high strength concrete walls (Figure 6) with only one side exposed to fire. The graph indicates the significant thermal gradient inside the material (concrete) according to a heat flow model that numerically simulates the fire scenario.

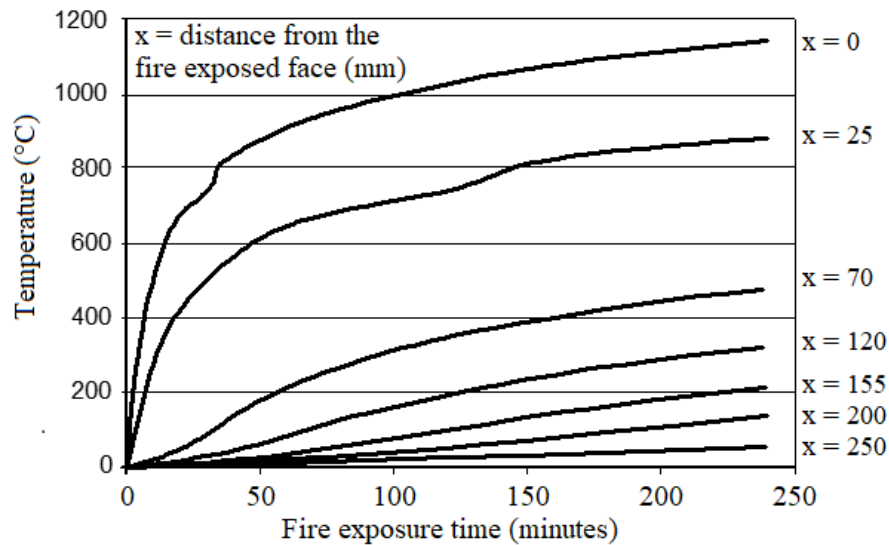


Figure 6. Temperature field evolution in a high strength concrete wall as a function of fire exposure time (Ongah, Mendis & Sanjayan, 2002).

Another way to present the temperature evolution inside a concrete element, prescribed by the main international codes, can be seen in Figure 7. In this case, the instantaneous curves of standardized times as a function of the temperature and depth of the surface exposed to fire are presented, this is a very common model adopted by researchers and in the codes of various countries.

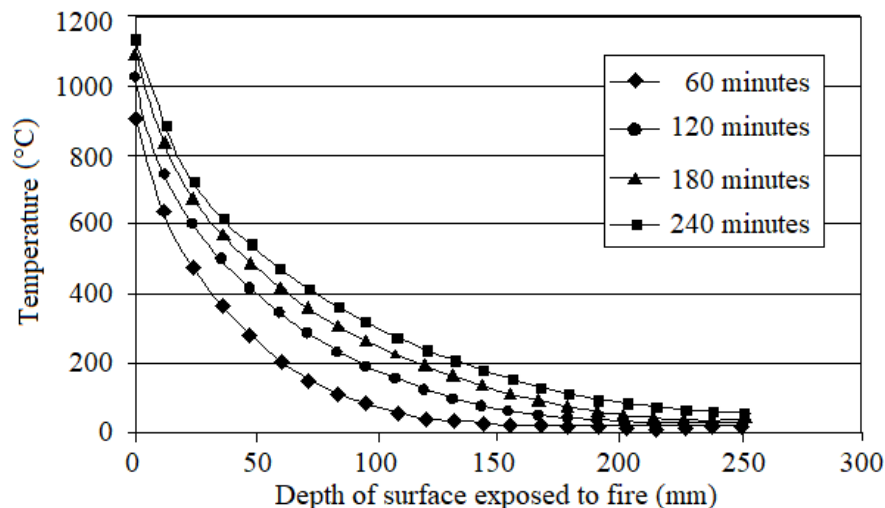


Figure 7. Calculated temperature distribution as a function of the depth of surface exposed to fire and fire exposure time, by using a numerical model (Ongah, Mendis & Sanjayan, 2002).

2.4 Changes in microstructure of concrete material at high temperatures

Precise analysis of the behavior of changes in the microstructure of a concrete sample is considered quite complex, as each concrete has its uniqueness due to the vast alternatives of materials and available additions, as well as the use of different mix design techniques. It is also noteworthy that at high temperatures, anisotropy and concrete material heterogeneity become much more evident. Obviously, some reactions are more striking given the prior knowledge of the lithological aspects of the aggregates, additions and the type of cement employed in concrete mix design. As specifically to the lithological nature of the aggregate, Figure 8 shows the marked difference in behavior (thermal stability) of various aggregates as a function of temperature increase.

In the context of microstructure, Taylor (1990) mentions that due to its low thermal conductivity and high specific heat, concrete provides good protection to steel in fire situation, however, it can be severely damaged due to thermal actions that harm mainly the cement paste. He highlights that at low temperatures, the cement paste expands when heated, but from 300°C, a contraction occurs, associated with water loss. At this stage, aggregates continue to expand, and the resulting internal stresses can lead to loss of strength, cracking and flaking. Some phenomena are more explicit, quartz elements, for example, expand sharply at 573 °C due to a polymorphic transformation of crystallization and calcite contracts from 900 °C due to its generalized decomposition.

Taylor (1990) also describes the thermal effects on cement paste, and points out that: below 500°C, carbonation and dilation of the matrix pores occur mainly; between 450 and 550°C, the decomposition of C-S-H, and at 600°C, the decomposition of CaCO₃, providing CaO, which may eventually rehydrate during the cooling phase.

Specifically regarding the role of water, Kalifa et al. (2000) note that the excessive water contained in saturated Portland cement pastes contributes to the formation of significant pressure gradients in the concrete pore network during mass transfer (water evaporation) and, consequently, in the increase of cracking due to contraction of the paste.

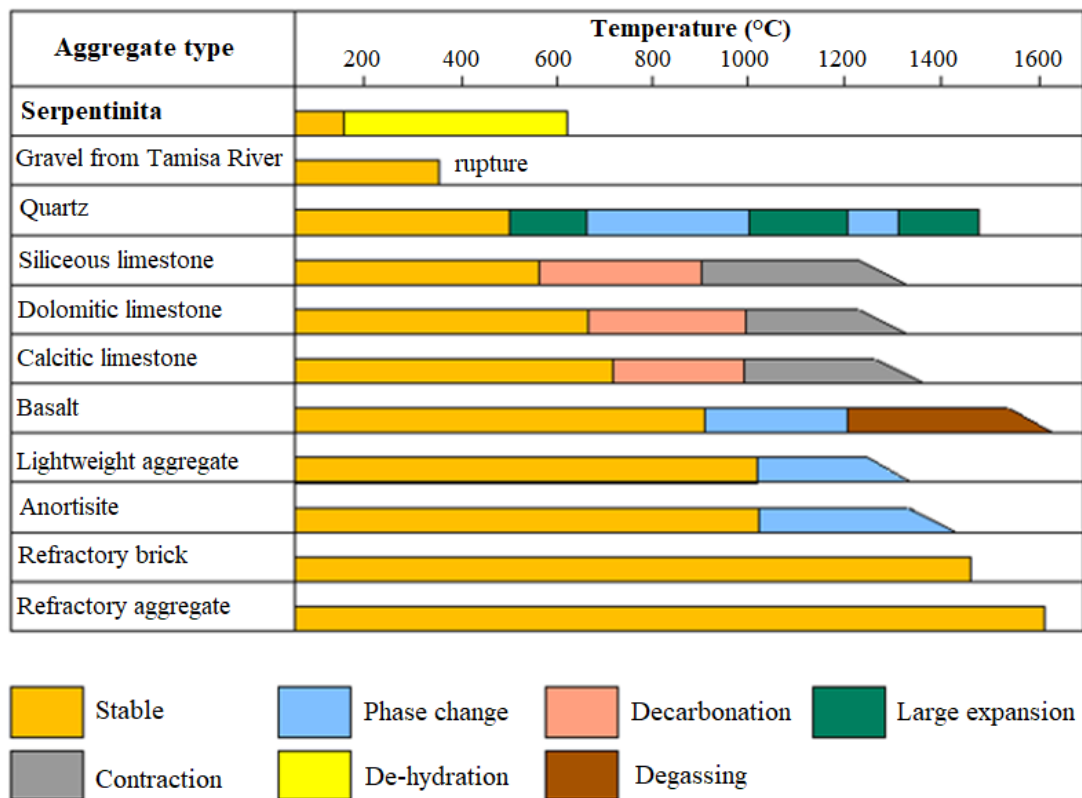


Figure 8. Behavior of various aggregates during heating (adapted from *fib*, 2007).

Regarding this, despite the significant physicochemical changes that occur in the cement paste, as well as the role of water in the mix, *fib* (2007) points out that at high temperatures it is the aggregates that can really govern the thermal behavior of concrete, when they are considered exclusively as a composite material. The main reasons for this theory are based on the following considerations:

- aggregates generally occupy a significant volume of concrete, between 60% and 80% of the volume of normal concrete;
- variations in aggregate properties during heating can have a significant effect on concrete performance at high temperatures. The thermal conductivity of concrete, for example, is greatly

influenced by the lithological nature of the aggregate;

- each type of aggregate reacts differently to heat. The main factor in the behavior of heated concrete is the chemical and physical stability of the aggregate;
- aggregates are also responsible for restricting any expansion and contraction of the cement paste during heating.

In general, the physical-chemical process of concrete, involving the interaction between aggregates and cement paste, in a fire situation, can be simplified as shown in Figure 9.

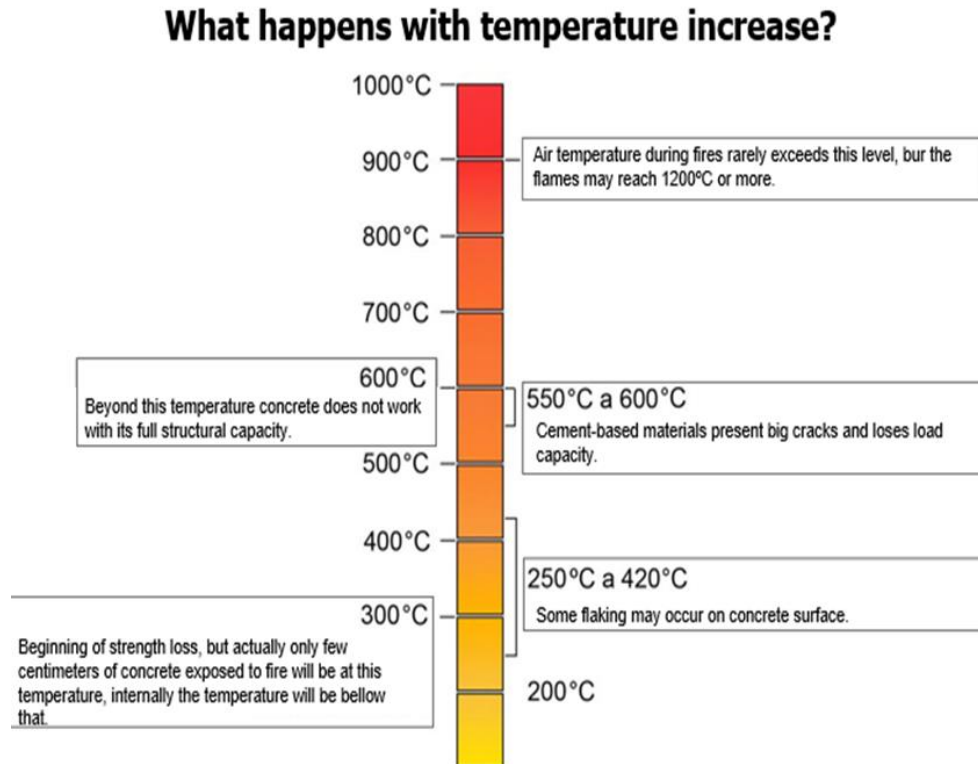


Figure 9. Physical-chemical process of concrete in fire situation (adapted from Jacobs, 2007).

As for reinforced concrete itself, Cánovas (1988) *apud* Costa (2008) notes that after 100°C, the reduction in adhesion between steel bars and concrete may occur due to the increase and duration of heating, and that above 600°C there may be a significant loss of adherence. It is noteworthy that the microstructural changes in the steel bars are not part of the scope of this article, but can be consulted in other references, namely: Holmes et al. (1982), Cabrita Neves, Rodrigues & Loureiro (1996) and Purkiss (1996).

2.5 Flaking of concrete at high temperatures (*spalling*)

The term spalling is internationally known and standardized in leading international codes and research. The physical phenomenon known as spalling (Figure 10) can be defined as explosive, and for some even called violent/explosive, flaking of layers or concrete pieces from the surface of a structural element when exposed to high temperatures and rapid heating rates, both characterized by a fire scenario (*fib*, 2007).



Figure 10. Example of explosive spalling occurred in high strength concrete column $f_{ck} = 83$ MPa (Kodur et al., 2005).

It should be clarified, however, that spalling is not a mechanism of failure or structural collapse of the element. The phenomenon may be mild or severe and, as a result, may or may not lead to rapid loss of cross section, which could trigger a structural collapse mechanism, such as traditional failures caused by compression, flexion or shear.

The extent, severity and nature of spalling can be very variable and unpredictable. The phenomenon may be insignificant in quantity and consequence when small punctures occur; however, it can be severe and compromise the fire resistance of the element due to the peeling of large portions of concrete, exposing the reinforcement and decreasing its structural capacity due to the respective reduction of the cross section.

In order to simplify and classify the spalling phenomenon, *fib* (2007) proposed to group it into six categories, namely⁵:

- aggregate *spalling*;
- explosive *spalling*;
- superficial *spalling*;
- *spalling* per delamination;
- edge *spalling* and
- post-cooling *spalling*.

Of all categories explosive spalling is the most severe in a fire situation. As discussed in *fib* (2007), this type of spalling can result in explosive and subsequent breakdowns of concrete layers, generally reaching thicknesses between 25 and 100 mm, depending on each specific case.

According to Khoury & Anderberg (2000) and *fib* (2007), the occurrence of each type of spalling is influenced by several factors, such as strength, age, type and size of aggregates, moisture content and the water vapor permeability of the material; the maximum temperature and the heating rate of thermal actions; the shape and size of the cross section, the presence of cracks, the steel rate, the arrangement (configuration) of the reinforcement, the presence of polypropylene fibers and the loading intensity of the structural element. The influence of these factors can be briefly observed in Chart 1⁶.

⁵ The terms in the six categories proposed by *fib* (2007) were interpreted and translated by the authors of this article.

⁶ Some terms of the original table proposed by *fib* (2007) were interpreted and translated by the authors of this article.

Chart 1. Different categories of spalling and their respective influencing agents (*fib*, 2007).

Spalling classification	Time of occurrence (probabilistic)	Nature	Sound aspects	Severity	Main influences*
Aggregate	between 7 and 30 minutes	cracking	small pops (popcorn type)	superficial	H, A, S, D W
Edge	between 30 and 90 minutes	nonviolent	none	may be severe	T, A, Ft, R
Superficial	between 7 and 30 minutes	violent	occurrence of cracking/creaking	may be severe	H, W, P, Ft
Explosive	between 7 and 30 minutes	violent	loud bangs / explosions	severe	H, A, S, Fs, G, L, O, P, Q, R, S, W, Z
Delamination	when concrete becomes friable (loses strength capacity)	nonviolent	none	may be severe	T, Fs, L, Q, R
Post-cooling	during and after moisture absorption cooling	nonviolent	none	may be severe	T, Fs, L, Q, R, W1, AT

*The acronyms used in the original document were preserved (*fib*, 2007), according to the following caption to avoid confusion with acronyms already used in the national language (from Brazil).

Subtitle:

A = aggregate thermal expansion, D = aggregate thermal diffusivity, Fs = concrete shear stress, Ft = concrete tensile stress, G = concrete age, H = heating rate, L = load / restraint, O = heating profile, AT = aggregate type, P = permeability, Q = cross-sectional shape (geometry), R = reinforcement, S = aggregate size, T = maximum temperature, W = moisture content, Z = cross-section size, W1 = moisture absorption.

2.5.1 Spalling in high strength concrete

When dealing with high strength concrete subjected to high temperatures, particular attention is given to the explosive spalling phenomenon. This type of spalling is theoretically originated by the formation of water vapor pressure in the pores inside a concrete mass during its heating.

According to Kodur et al. (2005), high strength concrete is more susceptible to this water vapor pressure formation, mainly due to its low permeability to water vapor when compared to normal strength concrete.

It is observed, however, that the theory widespread in the international literature is based on the precursor studies of Shorter & Harmanthy (1965) apud *fib* (2007) and internationally known as “moisture clog model”. According to this theory, the extremely high water vapor pressure within the concrete mass generated during fire exposure cannot be overflowed due to the low permeability of the high strength concrete.

According to Kodur et al. (2005), at 300 °C this pressure can reach values equal to or higher than 8MPa, being high to be resisted by the high strength concretes that have a tensile strength, in general, of the order of 5MPa to 7MPa.

In accordance with the theory formalized by Shorter & Harmanthy (1965) apud *fib* (2007), extensive research by Phan (2002) showed that the occurrence of explosive spalling was actually related to the inability of certain high-strength concretes to leak pressure from free water and chemically combined water that are vaporized with the temperature rise inside the concrete mass. In his experiments, Phan (2002) observed that an alternative to minimize the effects of internal pressure formation on concrete can be conceived by introducing polypropylene fibers into concrete mixtures, and this fact has been proven in extensive research involving high strength concrete specimens. It was possible to characterize the behavior of the high strength concrete with respect to the internal pressure formation aspects, being considered equivalent to the normal strength concrete, when at high temperatures, simply by the introduction of polypropylene fibers. This fact was verified by studying the pore pressure exerted on these two types of concrete (normal and high strength), coming from the high temperatures that can be reached in a fire, as shown in Figure 11 (Phan, 2002).

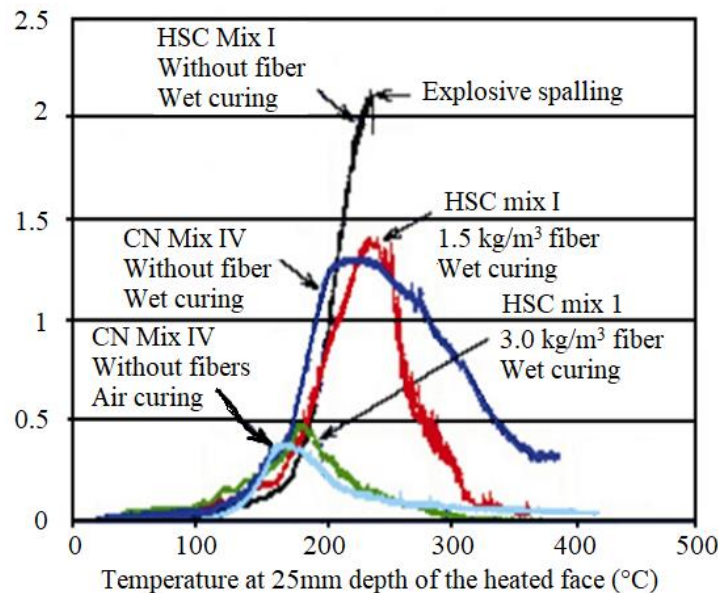


Figure 11. Equivalent pressure of the two concrete types (CN: normal and HSC: high strength) with the introduction of polypropylene fibers into high strength concrete (at high temperatures) (Phan, 2002).

However, Phan (2002) pointed out that there are significant inconsistencies when associated only with pore pressure formation with the explosive spalling phenomenon, mainly because there are other fundamental factors that may influence the experimental programs in general. Only the introduction of polypropylene fibers does not necessarily guarantee the integrity of the concrete at high temperatures, and there may be other influencing agents, such as the type and size of the sample itself (specimens or structural elements).

2.5.1.1 The effect of reinforcement (reinforced concrete)

The experimental studies conducted by Professor Ph.D. Venkatesh Kodur⁷, while still linked to the NRC-CNRC National Research Council Canada, had a significant impact on research and development, especially regarding high strength concrete in fire conditions.

Kodur et al. (2000) tested columns, under load, of normal and high strength concrete with 305mm x 305mm cross section and 3810mm height. The normal concrete columns had 34MPa strength

⁷ Professor Ph.D. Venkatesh Kodur is currently linked to the Center for Structural Fire Safety and Diagnostics of the Michigan State University Department of Civil & Environmental Engineering.

and the high strength ones 83MPa, both at 28 days of age.

In an extensive experimental program, Kodur et al. (2000) highlighted some innovative guidelines involving structural elements, submitted to fire resistance tests, which contributed considerably to a better performance of high strength concrete in fire situation. The main guidelines were based on procedures adopted for column confinement, as discussed below.

The main recommendation concerns the arrangement (configuration) of the transverse reinforcement (stirrups) with a hook-shaped locking (confinement) at 135° at the edge of the element and the corresponding reduction in stirrup spacing, which is approximately 0.75 times the usual required for normal concrete. The modifications proposed by Kodur et al. (2000) and also summarized in Kodur et al. (2005) can be seen in Figure 12.

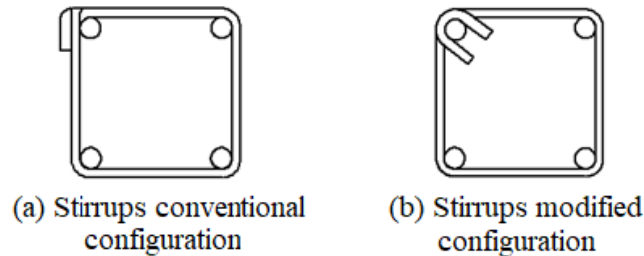


Figure 12. High strength concrete column stirrups conventional configuration (a) and modified configuration (b) (Kodur et al., 2005).

The positive result of Kodur's et al. (2005) proposal is evident when looking at the two high-strength concrete elements of Figure 13, after the respective fire resistance verification experiments performed under the same test and material conditions. It is also important to note that in these samples there was no addition of polypropylene fibers in the concrete mix, only the modification in the arrangement (configuration) of the reinforcement (indicated in Figure 12).

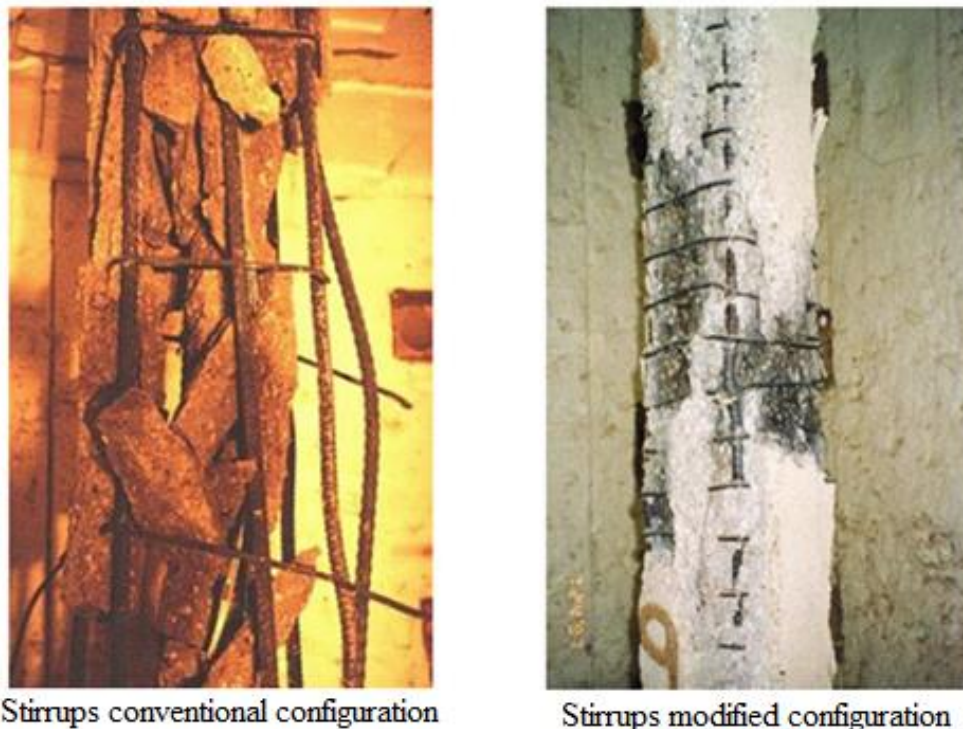


Figure 13. Results obtained after test under the high temperatures: (a) conventional configuration of the high strength column reinforcement and (b) modified configuration (Kodur et al., 2005).

In short, according to Kodur et al. (2005), high strength concrete may actually be more susceptible to spalling when compared to normal strength concrete (fact recurrent for compressive strengths above 70 MPa). However, this phenomenon can be substantially minimized when some guidelines are adopted. As noted by Kodur et al. (2000), the moisture content of the concrete, the aggregate type and the cross-sectional size of the element are also relevant, besides the previous proposal of modification in the transverse reinforcement. They also point out that, in practice, the higher the moisture content of the concrete mix, the more intense and severe the spalling phenomenon.

2.5.1.2 Age effect

Morita et al. (2002) conducted extensive research to evaluate two parameters: (a) the influence of water/cement ratio on spalling intensity and (b) the influence of different reinforcement configurations of reinforced high strength concrete elements to minimize spalling effect, with and without the addition of polypropylene fibers in the concrete mix.

To evaluate the influence of water/cement ratio on spalling intensity, various types of concrete elements (with different w/c ratios) were tried, always at two different ages: two months old and one year old; without varying the dimensions of the structural element (70cm x 70cm x 140cm) and the thickness of the concrete cover (5cm). The fire simulation was performed according to the requirements of the ISO 834 curve over a predetermined period of 180 minutes (3h).

In Figure 14 it is possible to observe the considerable difference as a function of the age of the concrete element for equivalent water/cement ratio values (for example: w/c = 0.375 and w/c = 0.449).

The experiment conducted by Morita et al. (2002) seems to contribute to highlight how much the conducted research may be limited to evaluate spalling severity in concrete elements at premature ages, since the occurrence of this type of phenomenon depends significantly on the time factor (sample age).

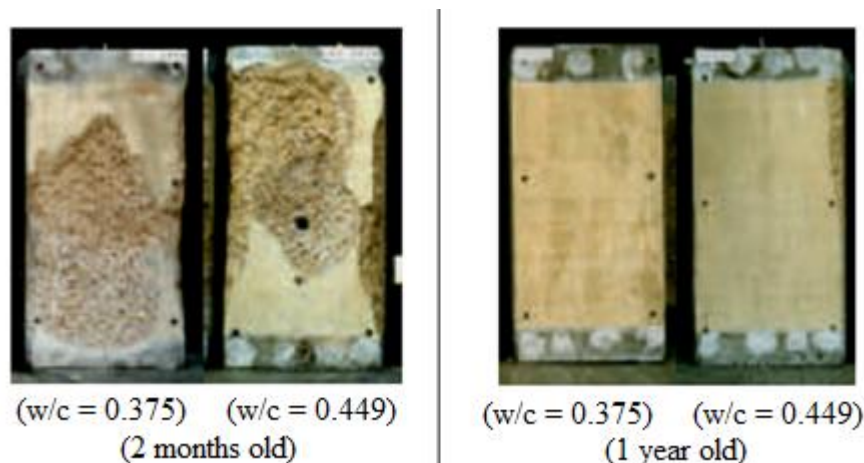


Figure 14. Reinforced concrete columns after fire simulation experiment (180min): effect of water/cement ratio and age on the occurrence of spalling phenomenon, 70cm square cross-section (Morita et al., 2002).

Recently in Brazil (Britez, 2011), an experiment was carried out involving a large column, prototype of the high strength colored reinforced concrete columns of the e-Tower building - world record in compressive strength at the time (Helene & Hartmann, 2003) - , with advanced age of eight years.

At the time, the results showed that the high strength concrete behaved in an upright manner (Figure 15) under fire, with 95% of its cross-sectional area maintained after the fire simulation test (only 5% effectively reduced by spalling). In addition, it was found in this experiment that the use of iron oxide-based pigment (colored concrete) also acted as an excellent colorimetric indicator (natural

thermometer), helping to evaluate the post-fire structure.

The tested column (140 MPa f_{ck}) had a cross section of 70cm x 70cm, 2m high, 25mm average cover thickness; and was tested with three faces exposed to fire for a period of 180min (3h), without loading, with fire simulation characterized by the ISO 834 curve at the IPT Fire Safety Laboratory in São Paulo.

In addition to advanced age, Britetz (2011) pointed out that other factors may have contributed positively to the good performance, such as the type of coarse aggregate used in the original concrete mix (basalt), as well as the cross-sectional size and reinforcement configuration.

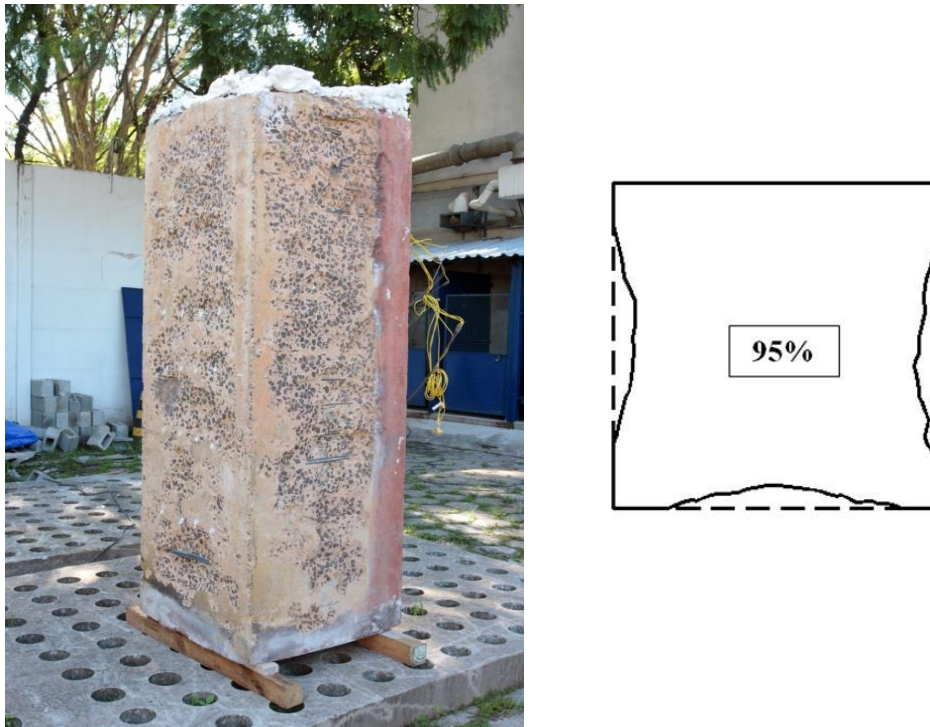


Figure 15. Column integrity and preserved cross-sectional detail after 180min (3h) test (showing the small cross-sectional reduction by spalling) (Britetz, 2011).

2.5.1.3 The effect of load intensity

Although important and standardized, the tests carried out on **specimens** (cubic or cylindrical) and even on large **structural elements** (columns, beams and slabs), with loading increments and restrictions, are not yet enough for a real simulation of the behavior of concrete when inserted into a **structural system**, where other effects occur during a fire, such as nodes dilations/stretching, deformations and generalized displacements of all concrete elements exposed to fire.

For obvious reasons associated with the costs involved and the complexity of carrying out these types of experiments, it is not common practice to simulate thermal experimental programs in a prototype building for structural element evaluation. However, such a widely publicized essay at the time was held in September 2001 at the Cardington Large Building Test Facility (LBTF)⁸. The prototype building of the Cardington project had seven floors, a total height of 25.2m and occupied an area of 675m² distributed in 7.5m x 7.5m square compartments, which in plan formed a rectangle with four compartments in one direction and three in another. A perspective of the Cardington project prototype building can be seen in Figure 16.

⁸ The *Cardington Large Building Test Facility (LBTF)* was located within the *BRE's (Building Research Establishment) Cardington Laboratory* in Cardington, Bedford, approximately 70 km north of London, England. The laboratory was an area formed by an extensive hangar, which allows testing at a useful height of up to 50m in a wind-protected environment (Chana & Price, 2003).



Figure 16. Perspective of the reinforced concrete prototype structure designed for the Cardington fire simulation experiment (Chana & Price, 2003).

The prototype building had no beams and was characterized by a construction system consisting of columns and flat and massive slabs, which were 25cm thick, the internal columns 40cm x 40cm square cross section and the end columns 40cm x 25cm. The columns had a 40mm concrete cover thickness and were designed using high strength concrete ($f_{ck} = 103\text{MPa}$ at 28 days age), containing limestone aggregates, silica and 2kg of polypropylene fiber per cubic meter of concrete.

As described by Chana & Price (2003), the fire simulation took place in a region occupied by four compartments in a total area of 225m^2 with a height of 4.25m (ceiling height) on the ground floor of the building. Intentionally, an internal column was exposed on all four faces and some of its end partially, as observed in the plan of Figure 17. The experiment also involved ventilation openings projected on the outer walls of the compartments to be ignited, as well as the loading simulation. The slabs were evenly loaded with sandbags for a load of 3.25kN/m^2 (325kgf/m^2) and in the column region additional bags were positioned to simulate an axial stress of 925kN (92.5tf).

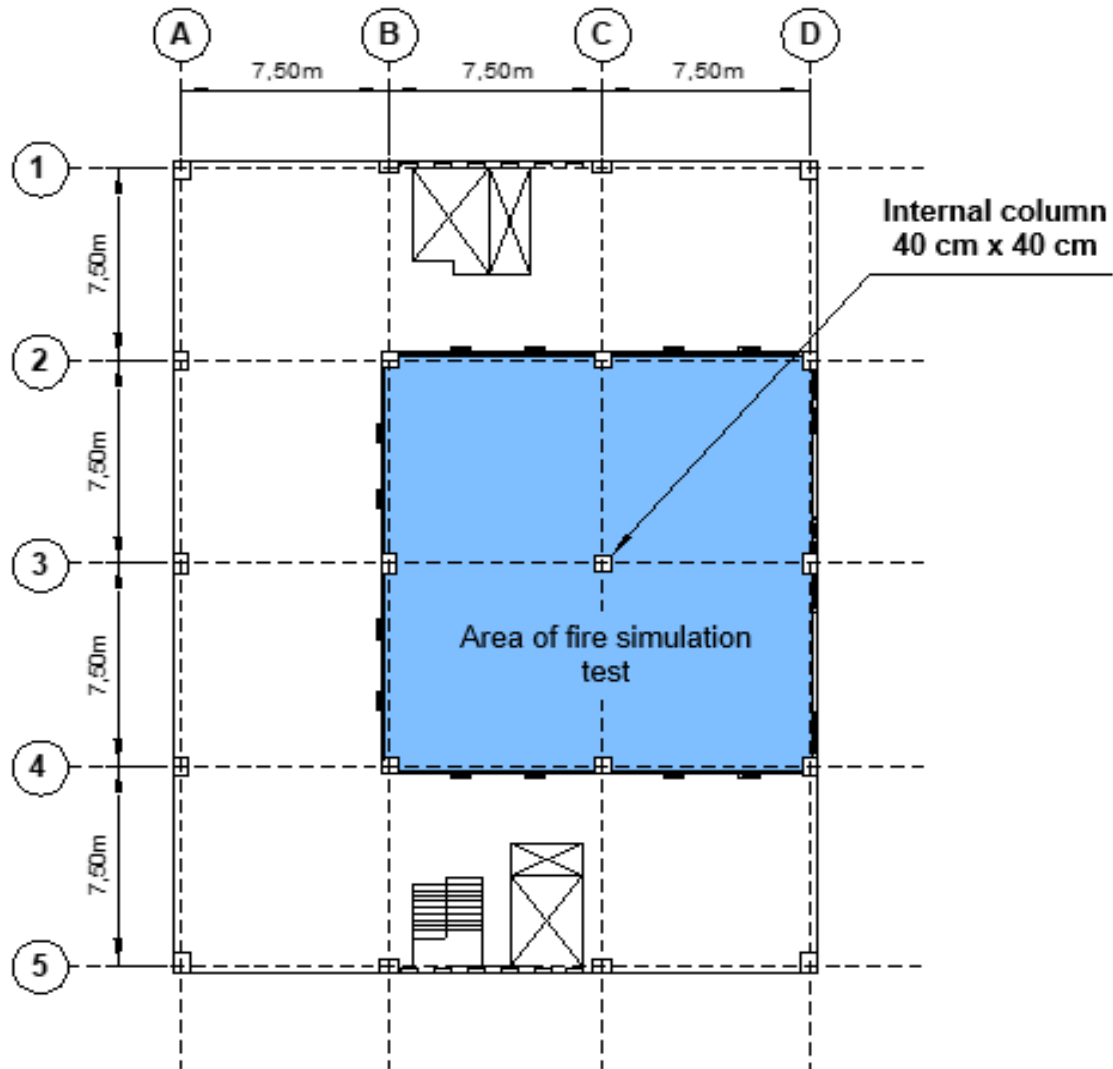


Figure 17. Plan of the prototype structure in reinforced concrete indicating the area under fire simulation (Chana & Price, 2003).

The fire was simulated by the burning of flammable material consisting of wooden pallets, positioned in the compartments to produce a thermal load of 40kg/m^2 (720MJ/m^2), compatible with a typical commercial office fire load, for example.

During the fire simulation, in the first 10 minutes of the experiment, there was the occurrence of low intensity, superficial spalling characterized by a discreet popping sound. However, after this period and for a further 15 minutes, the intensity was much higher, indicating a probable explosive spalling, which was later found mainly on the slab (ceiling) of the burning compartments ($f_{ck} = 74$ MPa). After 25 minutes, spalling occurrences decreased significantly. The extent and severity of the occurrence of the spalling phenomenon after the experiment can be observed in Figure 18.



Figure 18. Detail of extent and severity of slab spalling ($f_{ck} = 74$ MPa) after fire simulation. Highlighting, observe the integrity conditions of the high strength concrete column ($f_{ck} = 103$ MPa) (Chana & Price, 2003).

Regarding the integrity aspect of the high strength concrete, Chana & Price (2003) observed that the columns ($f_{ck} = 103$ MPa at the test) behaved satisfactorily, with low intensity spalling, negligible from the safety and structural stability point of view, even considering the effects of loading, bonding, among other normal attributes of a concrete structure in service state. They also added that, in this specific case, there may also have been a positive contribution of the addition of polypropylene fibers in the concrete mix (in the columns).

The researchers also concluded that the structural integrity of the slabs ($f_{ck} = 74$ MPa) was maintained despite widespread spalling and deflections of up to 7.8cm, which did not compromise safety because, as noted, no slabs collapsed and all continued to support the loads. distributed of 325kgf/m². In this context, it is noteworthy that in the case of solid slabs no polypropylene fibers were introduced in the concrete mix.

3. CONCLUSIONS

1. It is considered that the text, in general, potentially contributes to demystify some beliefs and doubts about the phenomenon of spalling, one of the main circumstances of the material at high temperatures.
2. Within the focus of fire characterized by cellulose based materials, even high intensity, it can generally be concluded that a reinforced concrete structure behaves better than that observed in small specimens as well as larger structural elements behave better than small structural elements, as well as structural elements in dry environments and with advanced age resists better to fire than newly built and wet ones.
3. Although the scenario of a burnt-out concrete structure is very bleak and makes strong negative impressions, in light of engineering, the problem may be more aesthetic than structural. However, of course, the structure must be inspected by a qualified specialist, based on technical and experimental resources to properly characterize the residual properties of the reinforced concrete structure.
4. It is difficult to imagine, in principle, the decision to demolish (may occur more due to social commotion or lack of property insurance) a reinforced concrete structure that has been

subjected to high temperatures from a fire scenario. Corrective interventions for repairs and structural rehabilitation are much more common and recurrent, provided they are backed by detailed technical expertise, consent of related public agencies and interest of the building owner.

4. REFERENCES

- Abrams, M. S. (1971), “*Compressive strength of concrete at temperatures to 1600F*”. American Concrete Institute, Special Publication, V 25, p.33-58.
- American Concrete Institute (2008), *ACI 318-08: building code requirements for reinforced concrete*. Farmington Hills: ACI.
- American Concrete Institute (1989), *ACI 216R-89: guide for determining the fire endurance of concrete elements*. Farmington Hills: ACI.
- American Society for Testing and Materials (2007), *E 119-07: standard test methods for fire of building construction and materials*. West Conshohocken: ASTM.
- Associação Brasileira de Normas Técnicas (1997), *NBR 13860: glossário de termos relacionados com a segurança contra incêndio*. Rio de Janeiro: ABNT.
- Associação Brasileira de Normas Técnicas (2001), *NBR 14432: exigência de resistência ao fogo de elementos construtivos de edificações – Procedimento*. Rio de Janeiro: ABNT.
- Associação Brasileira de Normas Técnicas (2001), *NBR 5628: componentes construtivos estruturais: determinação da resistência ao fogo*. Rio de Janeiro: ABNT.
- Britez, C. A. (2011), “*Avaliação de pilares de concreto armado colorido de alta resistência, submetidos a elevadas temperaturas*”. Tese (Doutorado em Engenharia), Escola Politécnica, Universidade de São Paulo, São Paulo: USP, 252 f.
- Cabrita Neves, I.; Rodrigues, J. P. C.; Loureiro, A. P. (1996), “*Mechanical properties of reinforcing and prestressing steels after heating*”. *Journal of Materials in Civil Engineering*, 8 (4), p.189-194, [https://doi.org/10.1061/\(ASCE\)0899-1561\(1996\)8:4\(189\)](https://doi.org/10.1061/(ASCE)0899-1561(1996)8:4(189))
- Chana, P.; Price, B. (2003), “*The Cardington fire test*”. *Concrete*, 37 (1), p. 28-33, Jan.
- Costa, C. N. (2008), “*Dimensionamento de elementos de concreto armado em situação de incêndio*”. Tese (Doutorado em Engenharia), Escola Politécnica, Universidade de São Paulo, São Paulo: USP, 405 f.
- Costa, C. N.; Silva, V. P. (2003), “*Dimensionamento de estruturas de concreto armado em situação de incêndio: métodos tabulares apresentados em normas internacionais*”. In: V Simpósio EPUSP sobre Estruturas de Concreto, 5, 2003, São Paulo.
- Costa, C. N.; Silva, V. P. (2006), “*Revisão histórica das curvas padronizadas de incêndio*”. In: Seminário Internacional NUTAU: Tecnologia de Durabilidade, São Paulo: NUTAU-USP.
- Costa, C. N.; Silva, V. P. (2004), “*Considerações sobre a segurança das estruturas de concreto em situação de incêndio*”. In: Seminário Internacional NUTAU: Demandas Sociais, Inovações Tecnológicas e a Cidade, 2004, São Paulo: NUTAU-USP. Disponível em: www.lmc.ep.usp.br/people/valdir/fire_safety/Nutau2004_concreto.pdf. Acesso em: nov. 2007.
- Costa, C. N.; Figueiredo, A. D.; Silva, V. P. (2002), “*Aspectos tecnológicos dos materiais de concreto em altas temperaturas*”. In: Seminário Internacional NUTAU 2002. Sustentabilidade, Arquitetura e Desenho Urbano. São Paulo: NUTAU/FUPAM/FAUUSP.
- European Committee for Standardization (2003), *Eurocode 2: design of concrete structures: part 1-2: general rules: structural fire design*. prEN 1992-1-2. Brussels, Belgium, 106 p.
- Farny, J. A.; Panarese, W. C. (1994). “*High-strength concrete*”. Skokie, Ill.: Portland Cement Association, 53 p.
- (fib) Fédération Internationale Du Béton (2007), “*Fire design of concrete structures – materials, structures and modeling – State-of-art report*”. Lausanne, fib. 97 p. (Bulletin d’information, 38).
- Helene, P.; Hartmann, C. T. (2003), “*HPCC in Brazilian office tower*”. *Concrete International*, v. 25, n. 12, p. 64-68, Dec. 2003.

- Holmes, M.; et al. (1982), “*The effects of elevated temperatures on the strength properties of reinforcing and prestressing steels*”. Structural Engineer, v. 60B, p. 7-13.
- Jacobs, J. -P. (2007), “*Comprehensive fire protection and safety with concrete*”. Brussels: European Concrete Platform. 30p. Disponível em: http://www.britishprecast.org/publications/documents/06-Fire_brochure-3004071.pdf. Acesso em: 22 Jun. 2011.
- Kalifa, P.; Menneveau, F.-D.; Quenard, D. (2000), “*Spalling and Pore Pressure in HPC at High Temperatures*”. Cement and Concrete Research, 30 (12), [https://doi.org/10.1016/S0008-8846\(00\)00384-7](https://doi.org/10.1016/S0008-8846(00)00384-7)
- Khoury, G. A.; Anderberg, Y. (2000), “*Concrete spalling review*”. [S.l.]: FSD, 2000. 60 p. Report submitted to the Swedish National Road Administration.
- Kodur, V. K. R.; et al. (2000), “*Experimental studies on the fire endurance of high-strength concrete columns*”. Canada: IRC/NRC, 146p. (NCR-CNRC Internal Report 819).
- Kodur, V. K. R.; et al. (2005), “*Guidelines for fire resistance design of high-strength concrete columns*”. Ottawa, Ontário, Canadá: IRC/NRC. (Report NRCC-47729). Disponível em: <<http://irc.nrc-cnrc.gc.ca/pubs/fulltext/nrcc47729/>>. Acesso em: nov. 2007.
- Leonardo Da Vinci Pilot Project CZ/02/B/F/PP-134007 (2005), “*Handbook 5: design of buildings for the fire situation*”. Luxembourg: European Commission. Implementation of Eurocodes.
- Morita, T.; et al. (2002), “*An estimation method for fire resistance of reinforced concrete elements considering spalling*”. Proceedings of the 1st Fib Congress. p. 119-128.
- Neville, A. M. (1981), “*Properties of concrete*”. 3rd ed. London; Marshfield, Mass.: Pitman. 779 p.
- Ongah, R.; Mendis, P. A.; Sanjayan, J. G. (2002), “*Fire performance of high strength reinforced concrete walls*”. In: Proceedings of the Australasian Conference On The Mechanics Of Structures And Materials, 17, Gold Coast, Austrália. Lisse: Balkema, p. 199-204. Disponível em: http://www.civenv.unimelb.edu.au/aptes/publications/Fire-HSC_walls.pdf. Acesso em: nov. 2007.
- Phan, L. T. (2002), “*High-strength concrete at high temperature: an overview*”. In: Building and fire research laboratory. Gaithersburg: National Institute of Standard and Technology, Disponível em: <http://www.fire.nist.gov/bfrlpubs/build02/PDF/b02171.pdf>. Acesso em: nov. 2007.
- Phan, L. T. (1996), “*Fire performance of high-strength concrete: a report of the state-of-the-art*”. In: Building and fire research laboratory. Gaithersburg: National Institute of Standard and Technology, NISTIR 5934. Disponível: <http://www.fire.nist.gov/bfrlpubs/build96/art075.html>. Acesso em: nov. 2007.
- Purkiss, J. A. (1996), “*Fire safety engineering design of structures*”. Oxford: Butterworth-Heinemann, 369 p.
- Seito, A I.; et al. (2008), “*A segurança contra incêndio no Brasil*”. São Paulo: Projeto. 496 p.
- Taylor, H. F. W. (1990), “*Cement chemistry*”. London: Academic Press, 475 p.
- The Concrete Centre (2004), “*Concrete and fire: using concrete to achieve safe, efficient buildings and structures*”. Camberley, Surrey, England. Disponível em: <http://www.mace.manchester.ac.uk/project/research/structures/strucfire/DataBase/References/Concrete%20&%20Fire%203557%20lo%20res.pdf>. Acesso em: nov. 2007.

Numerical-experimental analysis of ceramic block masonry walls of different thickness at high temperatures

F. Bolina¹ , B. Tutikian^{1*} , J. Gonçalves¹ , T. Souza¹ , G. Manica¹ 

*Contact author: btutikian@terra.com.br

DOI: <http://dx.doi.org/10.21041/ra.v10i1.415>

Reception: 01/05/2019 | Acceptance: 11/11/2019 | Publication: 30/12/2019

ABSTRACT

The study discusses the fire resistance of vertical sealing systems composed of ceramic bricks with vertical holes at high temperatures. The masonry sealing construction system is widely used in the Brazilian construction market because it is a low cost and high productivity system compared to conventional elements. The results were obtained with finite element computational models, using the Ansys Mechanical software, calibrated by a real scale experimental test, determining the fire resistance time (FRT) for different block geometries. The computational analysis led to results that point to a limit in efficiency of the wall thickness increase in order to reach a high FRT in relation to the thermal insulation.

Keywords: fire resistance time; fire; compartmentation.

Cite as: Bolina, F., Tutikian, B., Gonçalves, J., Souza, T. Manica, G. (2020), "Numerical-experimental analysis of ceramic block masonry walls of different thickness at high temperatures", Revista ALCONPAT, 10 (1), pp. 22 – 35, DOI: <http://dx.doi.org/10.21041/ra.v10i1.417>

¹ Universidade do Vale do Rio dos Sinos, São Leopoldo, Brasil.

Legal Information

Revista ALCONPAT is a quarterly publication by the Asociación Latinoamericana de Control de Calidad, Patología y Recuperación de la Construcción, Internacional, A.C., Km. 6 antigua carretera a Progreso, Mérida, Yucatán, 97310, Tel.5219997385893, alconpat.int@gmail.com, Website: www.alconpat.org

Responsible editor: Pedro Castro Borges, Ph.D. Reservation of rights for exclusive use No.04-2013-011717330300-203, and ISSN 2007-6835, both granted by the Instituto Nacional de Derecho de Autor. Responsible for the last update of this issue, Informatics Unit ALCONPAT, Elizabeth Sabido Maldonado, Km. 6, antigua carretera a Progreso, Mérida, Yucatán, C.P. 97310.

The views of the authors do not necessarily reflect the position of the editor.

The total or partial reproduction of the contents and images of the publication is strictly prohibited without the previous authorization of ALCONPAT Internacional A.C.

Any dispute, including the replies of the authors, will be published in the third issue of 2020 provided that the information is received before the closing of the second issue of 2020.

Análise numérico-experimental de paredes de alvenaria de bloco cerâmico com diferentes espessuras em altas temperaturas

RESUMO

O estudo discute sobre a resistência ao fogo de sistemas de vedação vertical compostos por blocos cerâmicos com furos verticais em altas temperaturas. O sistema construtivo de vedação em alvenaria é amplamente utilizado no mercado da construção civil no Brasil por tratar-se de um sistema de baixo custo e alta produtividade em comparação aos elementos convencionais. Os resultados foram obtidos com modelos computacionais de elementos finitos, através do software Ansys Mechanical, calibrados por ensaio experimental em escala real, determinando-se o tempo de resistência ao fogo (TRF) para diferentes geometrias de blocos. As análises computacionais levaram a resultados que apontam um limite para eficiência do aumento de espessura de uma parede para se atingir TRF elevados em relação ao isolamento térmico.

Palavras-chave: tempo de resistência ao fogo; incêndio; compartimentação.

Análisis numérico-experimental de paredes de mampostería con bloques de cerámica de diferentes espesores en altas temperaturas.

RESUMEN

Este estudio discute la resistencia al fuego de sistemas de sellado vertical compuestos por bloques cerámicos con agujeros verticales en altas temperaturas. La albañilería es ampliamente utilizada en el mercado de la construcción civil por tratarse de un sistema de bajo costo y alta productividad en comparación con los elementos convencionales. Los resultados fueron obtenidos con modelos computacionales de elementos finitos a través del software Ansys Mechanical, calibrados por ensayo experimental de resistencia al fuego a escala real, determinándose el tiempo de resistencia al fuego (TRF) para diferentes geometrías de bloques. Los análisis computacionales llevaron a resultados que apuntan un límite para la eficiencia del aumento de espesor de una pared para alcanzar altos TRF en relación con el aislamiento térmico.

Keywords: albañilería estructural; incendio; compartimentación.

1. INTRODUCTION

In 1974, the fire of the Joelma building, located in São Paulo, Brazil, highlighted the risk of fire due to the absence of horizontal and vertical compartmentation. Compartmentation of areas is a fire safety feature and its main purpose is to contain the action of fire in order to restrict the area and thus the development of the flames, as well as to protect the dwellers from the action of fire for a determined period. Masonry walls and partitions can promote compartmentation between rooms, mitigating the spread of fire and smoke between environments. (MARCATTI et al., 2008). With the growing need to build with quality and safety, especially due to the Brazilian Standard of Performance of Housing Buildings, NBR 15575 (ABNT, 2013) taking effect, the need to verify the performance of building systems in terms of (a) sustainability, (b) habitability and (c) security gained strength. According to NBR 15575 (ABNT, 2013), among the systems that must meet these conditions, the vertical sealing system must follow minimum fire requirements. In addition, compartmentation requirements are demanded by state fire department regulations in Brazil, which reinforces this need and requires designers to meet these standards.

It is common to associate fire resistance of masonry elements with their thickness, but other factors must be considered, such as the amount of air layers contained in the blocks. There is a complex temperature distribution in the section of these elements that should be further investigated due to

the different heat conduction mechanisms in them. Masonry also varies by region of manufacture, and by changing available constituent materials and local manufacturing processes. (ZSEMBERY, 2013).

For the project of masonry in fire situation, Eurocode 6 (EN 1996-1-2, 2005) allows two types of sizing methods. One uses fixed data, which provides the minimum required wall thickness dimension to obtain the fire resistance time. The second method, through calculation that considers the material failure modulus when exposed to high temperature, defines the element specifications according to temperature, slenderness rate and deformation due to restricted thermal expansion. (RIGÃO, 2012).

Considering that NBR 15220 (ABNT, 2003) uses the apparent thermal conduction simplification and presents a coefficient for the thermal conduction of the confined air much lower than that of ventilated air, it may be deduced that the reason for this reduction is due to convection and thermal radiation transport that occurs between the faces that generate this confinement. It may also be assumed that the explanation for the difference in apparent thermal conduction values in Bai's (2017) tests is related to the fact that their samples with smaller alveoli have a larger number of cavities, resulting in more convection and thermal radiation phenomena occurring within the sample.

Laboratory tests are performed to understand the performance of vertical sealing systems in a fire situation and, consequently, make their use feasible. In Brazil, the standard that regulates the fire resistance tests of these systems is NBR 5628 (ABNT, 2001) for walls with structural function and NBR 10636 (ABNT, 1989) for walls without structural function. According to the standards, the tests must be performed in real scale, turning the process costly, which, added to the limited number of vertical furnaces in Latin America, makes the technical collection in this area limited. (RIGÃO, 2012).

Therefore, the development of theoretical models and computer simulations is necessary to evaluate the behavior of masonry in a fire situation. In these analyses, heat transmission and mechanical behavior are factors that occur in a three-dimensional plane. However, most existing models are based on two-dimensional approaches, based on a macroscopic scale, preventing proper analysis of convective and radiative heat transmission within the ceramic blocks. (NGUYEN et al., 2009).

Aiming to make computational analysis more representative, computational models should be calibrated with data obtained through experimental tests. The available results on vertical sealing system tests approach the items of tightness (T), thermal insulation (I) and mechanical resistance (R), which makes it difficult to perform an advanced computational model, which requires a few other relevant information. (NGUYEN; MEFTAH, 2012).

Therefore, this work evaluated the influence of ceramic block geometry with vertical holes on the fire resistance of vertical sealing systems in fire situations, using computer assisted models, calibrating them through results of fire resistance tests in real scale experimental walls, elaborated according to NBR 5628 (ABNT, 2001). The study was divided into five stages: (1) introduction; (2) experimental program; (3) numerical analysis; (4) results and discussion; and (5) conclusion.

2. EXPERIMENTAL PROGRAM

2.1 Wall prototype construction

The wall used as a calibration object was named P1. This system has dimensions consisting of 3,15 x 2,80m and was built in a metal gantry in laboratory, as shown in Figure 1.

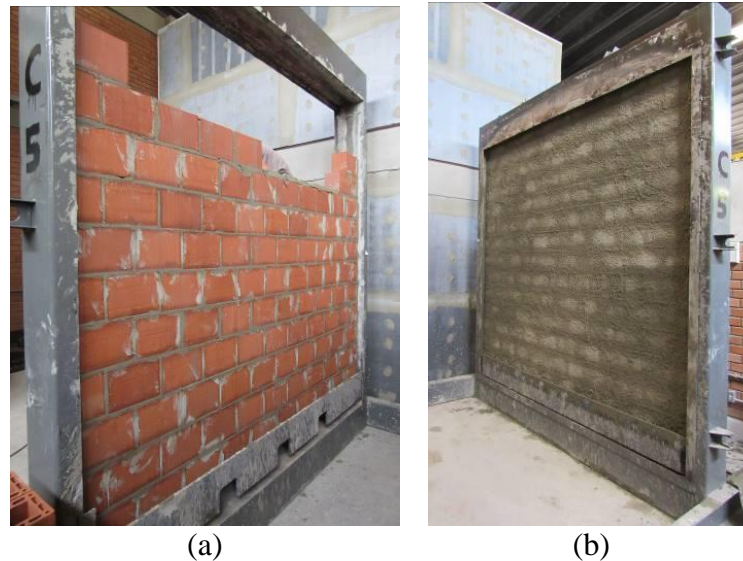


Figure 1. Constructive sequence of wall P1.

For the execution of the experimental test wall, ceramic blocks with f_{bk} 8 MPa were used, containing vertical holes and dimensions of 14 x 19 x 29 cm, and also with laying mortar joint of cement, sand and lime, with 4 MPa of medium compressive strength, in addition to aerator additives, hydration stabilizer and water retainer.

2.2 Instrumentation

To evaluate the wall temperature throughout the test, five thermocouples were used in the face exposed to the fire and five thermocouples in the unexposed face, placed in its surface, as shown in Figure 2. Also, five thermocouples were added along the block section, as shown in Figure 3.

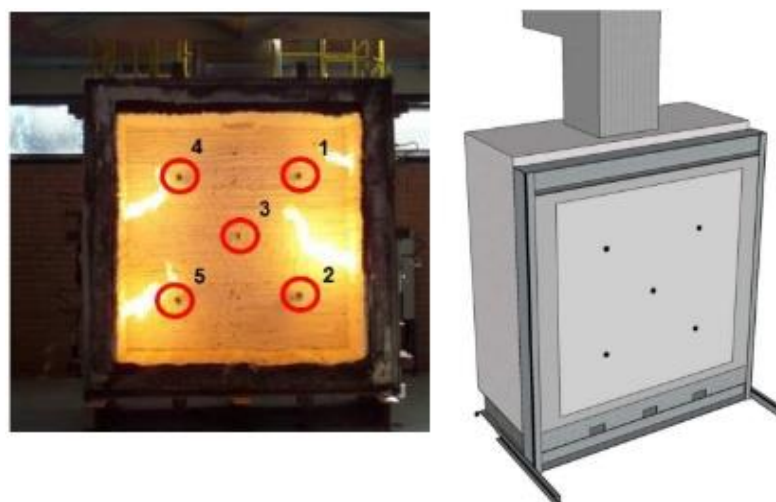


Figure 2. External thermocouples.

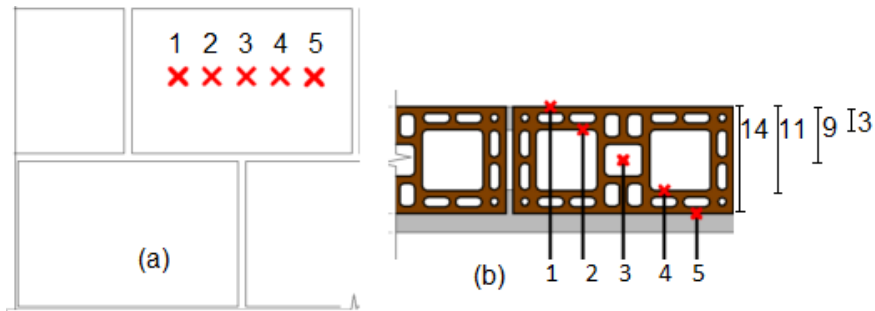


Figure 3. Location of internal thermocouples on blocks in (a) section and (b) plan.

2.3 Vertical furnace

The test was performed at Unisinos' Fire Safety Laboratory. The wall was tested after 56 days of curing in a vertical furnace. The furnace has four burners arranged according to Figure 4, controlled by two thermocouples that allow the measurement of temperature evolution by ISO 834 (2014). Figure 4 also shows the wall mounting and installation sequence in the test furnace. The furnace has a chimney that regulates the flow of gases generated by the heating and the internal pressure throughout the test, as well as thermal insulation composed by ceramic fiber blanket and four gas burners, digitally controlled by a digital control center.

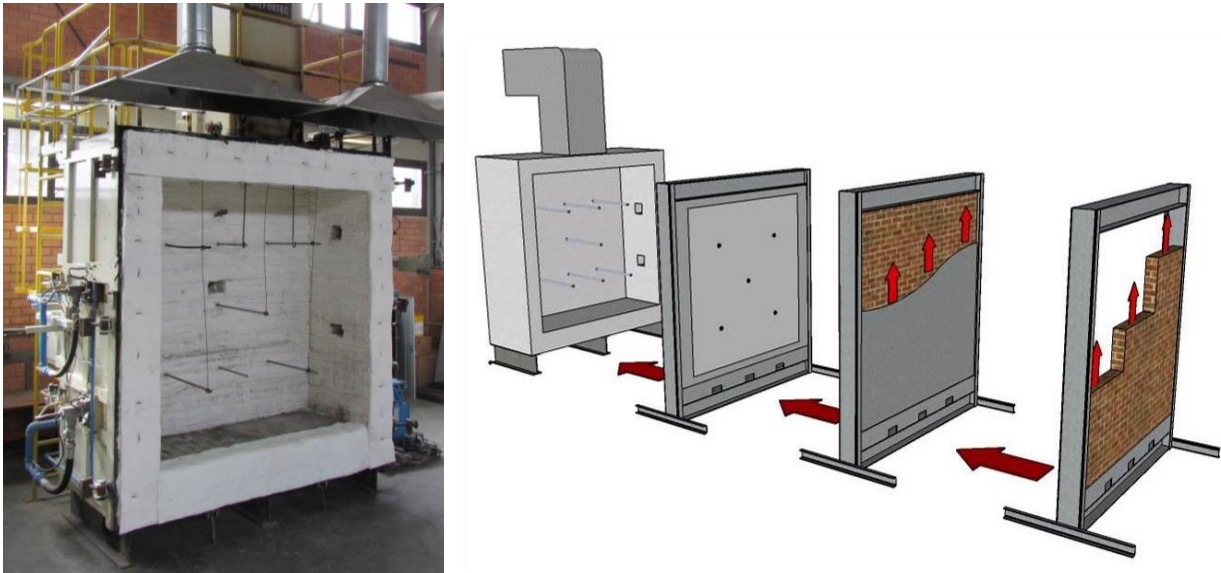


Figure 4. Detail of system coupling to vertical furnace.

3. NUMERICAL ANALYSIS

3.1 Analysis premises

For the elaboration of the computational model, the Ansys Mechanical Transient Thermal program was used. In this program, a mesh of elements was generated, as shown in Figure 5. Each division displayed in the block section represents a finite element to be calculated, so that the program performs a series of smaller calculations and groups them to present the final result.

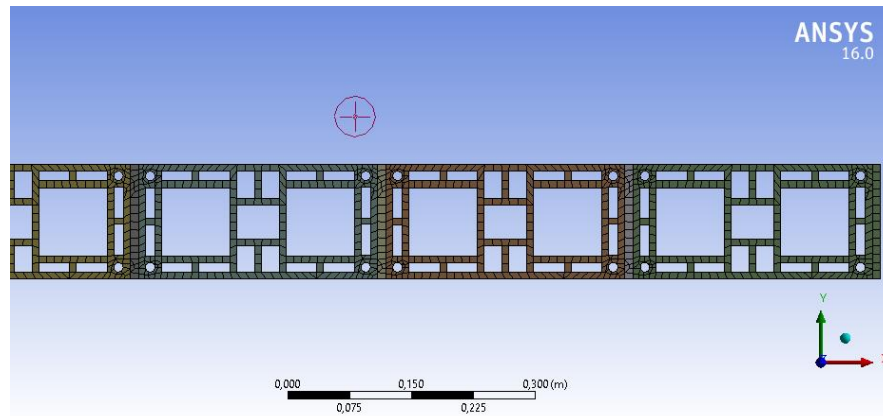


Figure 5. Hypothetical computational mesh for computational analysis.

The finite elements generated by the program for the analysis were QUAD_4 type, which generates four nodes and represents close square shapes. The minimum and maximum size of each element was determined manually, being the smallest possible element with 1 mm side and the largest possible element with 50 mm side. The mortar was considered as an inert element, with complete interaction with the block. The thermal conductivity of the block was given as a function of the temperatures extracted from the experimental model. This simulation was made in 2 dimensions, with the sole purpose of considering the isotherms of the blocks under analysis.

With the calculation mesh, the temperature curve to which the wall should be exposed was inserted, following the curve given by ISO 834 (ISO, 2014). The initial temperature defined for the computational analysis was the same as that used in the experimental test, 20°C.

3.2 Parameters obtained in experimental calibration

To perform the experimental analysis, it was necessary to use parameters related to the thermal properties of the materials involved, that is: density, specific heat and thermal conductivity coefficient. The parameters defined for the calibration are presented in Table 1.

Table 1. Parameters defined for the calibration.

Parameter	Value		
	Density (kg/m ³)	Thermal conductivity (W.C/m)	Specific heat (J.C/kg)
Air	1,125	0,025	1005
Mortar	1709	0,9	1550
Block	1200	2,5	880

For the definition of the convection values, considering its variability with the increase in temperature, the block was divided into two regions, as shown in Figure 6, and for each one of them a thermal conductivity coefficient value was assigned according to the evolution of the test time, when temperatures rose. The coefficients used are shown in Table 2.

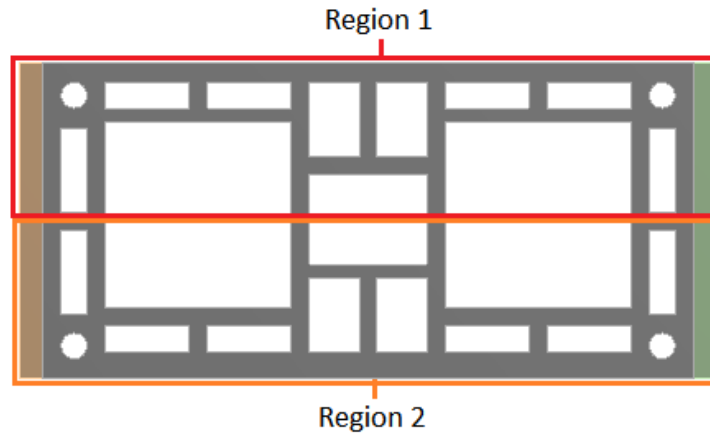


Figure 6. Regions defined for convection coefficients.

Table 2. Thermal convection coefficients.

Block region	Test time			
	30 min	60 min	120 min	240 min
Region 1	30 (W.C/m)	14 (W.C/m)	9 (W.C/m)	4 (W.C/m)
Region 2	0,7 (W.C/m)	20 (W.C/m)	6 (W.C/m)	0,5 (W.C/m)

These values were extracted from the experimental model and inserted in the computational simulation.

3.3 Temperature reading points

The temperature reading points in the block were the same as those experimentally defined, as shown in Figure 7. Thermocouples 3 and 4, which are not shown in Figure 7, were used to measure the results of air temperature in the computational modeling.

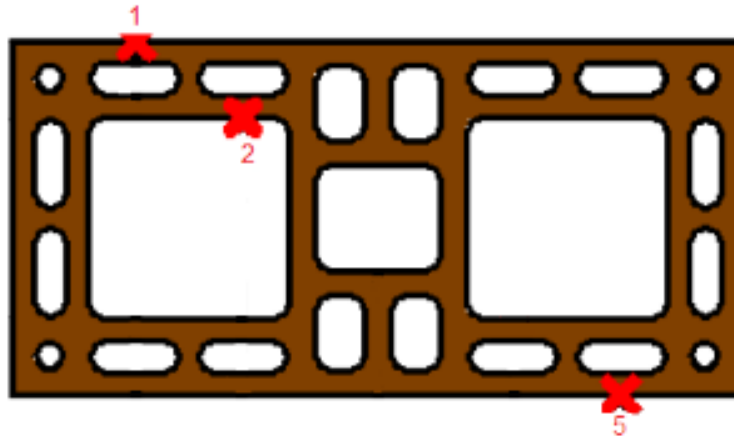


Figure 7. Points considered in the blocks' temperature measurement.

3.4 Calibration and validation of the computational model

For the validation of the computational model, through the experimental analysis in vertical furnace, the variables considered were the parameters of density, thermal conductivity, specific heat and thermal convection, which were extracted from the test. Through these reports, the computational model was calibrated with experimental data, as shown in Table 3.

Table 3. Temperatures reached in the calibration model.

Points	Time			
	30 min	60 min	120 min	240 min
At point 1	833 °C	945 °C	1047 °C	1151 °C
At point 2	321 °C	608 °C	701 °C	846 °C
At point 3	46 °C	95 °C	237 °C	417 °C

The validation of the model occurred through the values obtained in the numerical analysis with the experimental analysis.

3.5 Extrapolation of experimental results

With the calibration performed according to the experimental result, the process of computational extrapolation for different block geometries began. For this, three commercial thicknesses of 11,5, 14 and 19 cm of ceramic blocks were used. For each of these thicknesses, three blocks were defined, varying the number of alveoli and, therefore, percentage of voids. Three distinct geometries were proposed, but the thickness of the internal walls of the block were constant, with 9 mm externally and 8 mm internally, as shown in Figure 8.

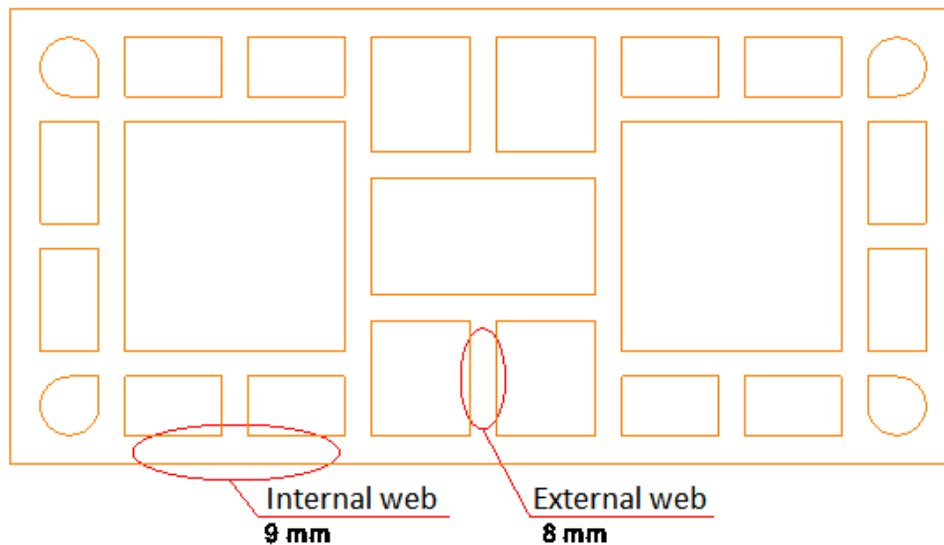


Figure 8. Internal and external walls of the blocks.

The 11,5 cm thick block family was called BL1; 14 cm thick BL2; and the 19 cm thick BL3. The percentage variations of voids within the same block family were calculated using the ratio between gross area and net area, and referred to as indexes I, II and III. Figure 9 details the blocks used in this study. The blocks were named sequentially BL1 to BL3. It is observed that the blocks with II index (BL1-II, BL2-II and BL3-II) are found in the market, the commercial ones. From there, it has been proposed blocks with smaller and slightly larger alveoli, those with I index (BL1-I, BL2-I and BL3-I), and blocks with larger alveoli and in small quantity, those with III index (BL1-III, BL2-III e BL3-III).

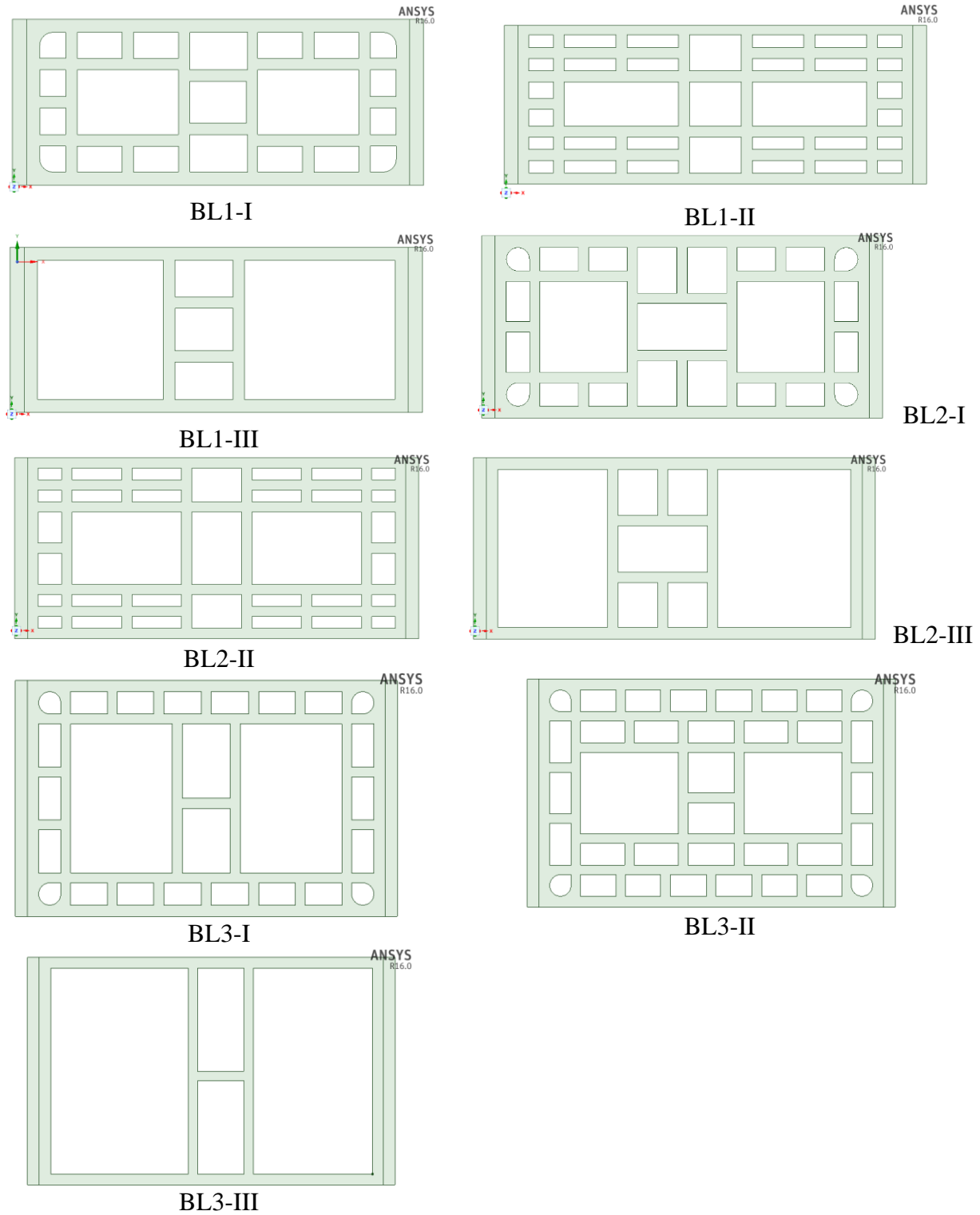


Figure 9. Used blocks.

Table 4 shows the nomenclatures, measurements and void volume (%) calculated for each type of ceramic block.

Table 4. Blocks used in simulations.

Block name	Dimensions (cm)	Total voids (%)
BL1-I	11,5 x 19 x 26,5	54,24
BL1-II	11,5 x 19 x 26,5	43,72
BL1-III	11,5 x 19 x 26,5	71,42
BL2-I	14 x 19 x 26,5	54,2
BL2-II	14 x 19 x 26,5	58,6
BL2-III	14 x 19 x 26,5	72,82
BL3-I	19 x 19 x 26,5	64,36
BL3-II	19 x 19 x 26,5	57,39
BL3-III	19 x 19 x 26,5	79,03

3.6 Times of analysis of block isotherms

The isotherms of the blocks in the computational program were calculated at 30, 60, 90, 120, 180 and 240 minutes. To define the Fire Resistance Time (FRT) of each block, the limit temperature of 200°C (180+20°C) on the unexposed face to the fire for an isolated thermocouple was defined with base on the precepts of NBR 10636 (ABNT, 1989).

4. RESULTS AND DISCUSSION

Due to the predominant criterion of FRT definition being the temperature of the unexposed face of the block, these measurements were used for the analysis, with the limit temperature of 200 °C on the unexposed face. Block isotherms were collected in the computational program at 30, 60, 90, 120, 180 and 240 minutes. Figure 10 presents the isotherms of some of the blocks used in this study and Figure 11 displays the comparison among all the blocks, with variation in geometry, percentage of voids and thicknesses.

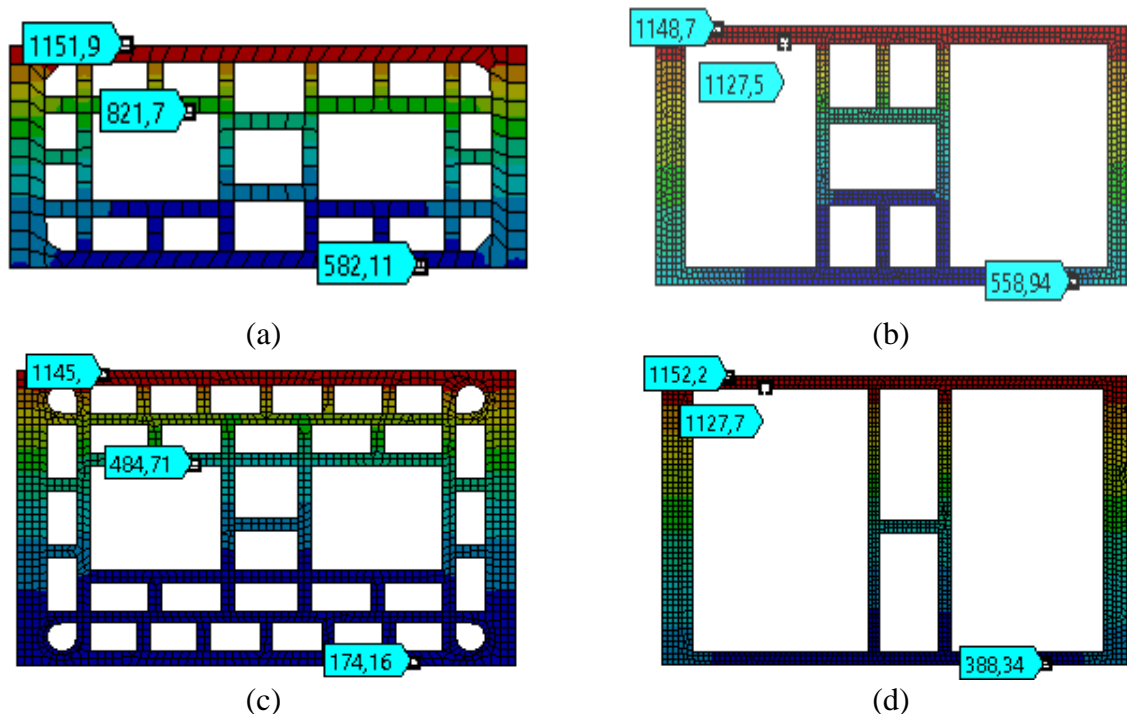


Figure 10. Block isotherms of (a) BL2-I, (b) BL2-III, (c) BL3-II and (d) BL3-III at 180 minutes.

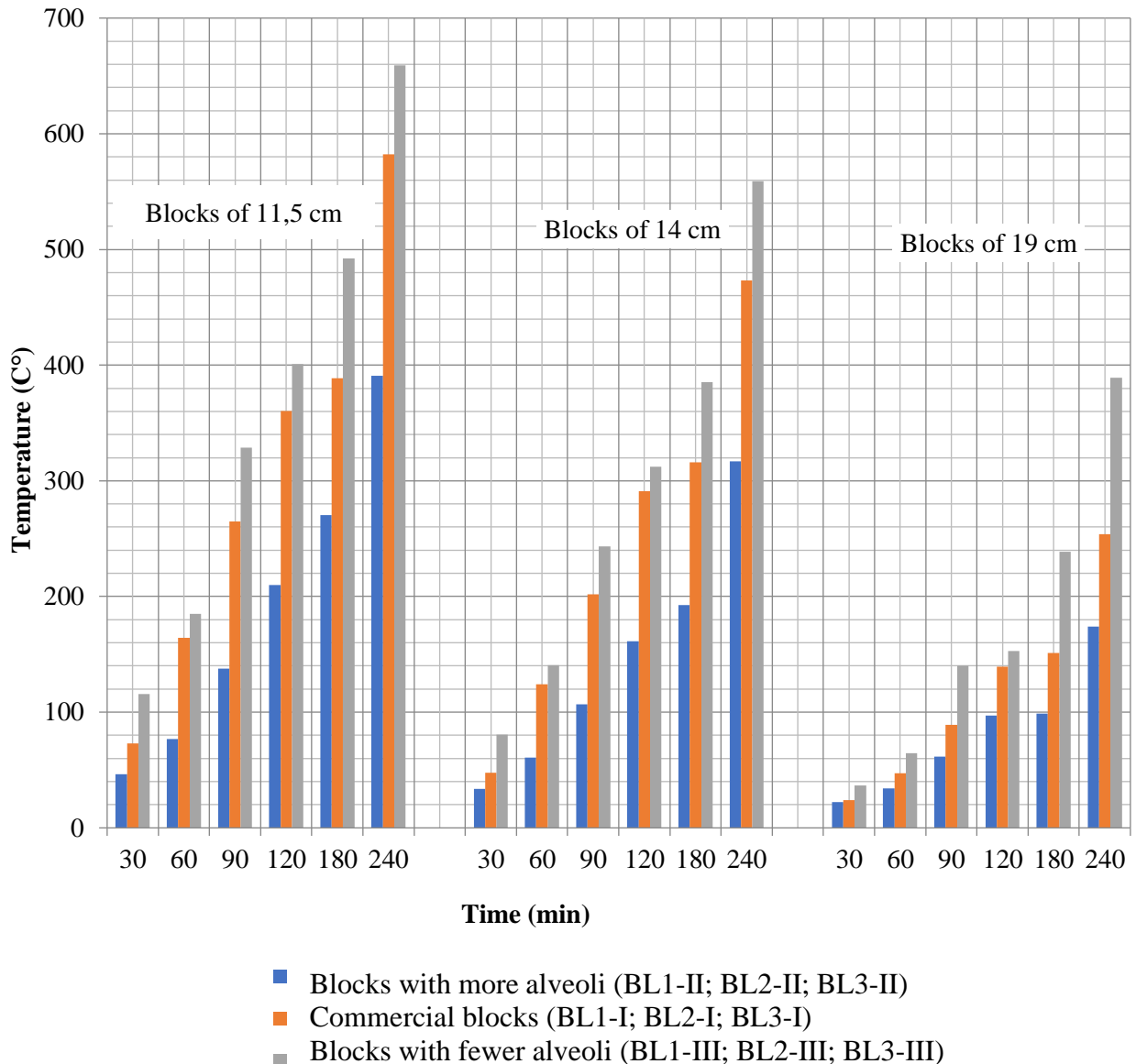


Figure 11. Comparison among the temperatures on the unexposed faces of all tested blocks.

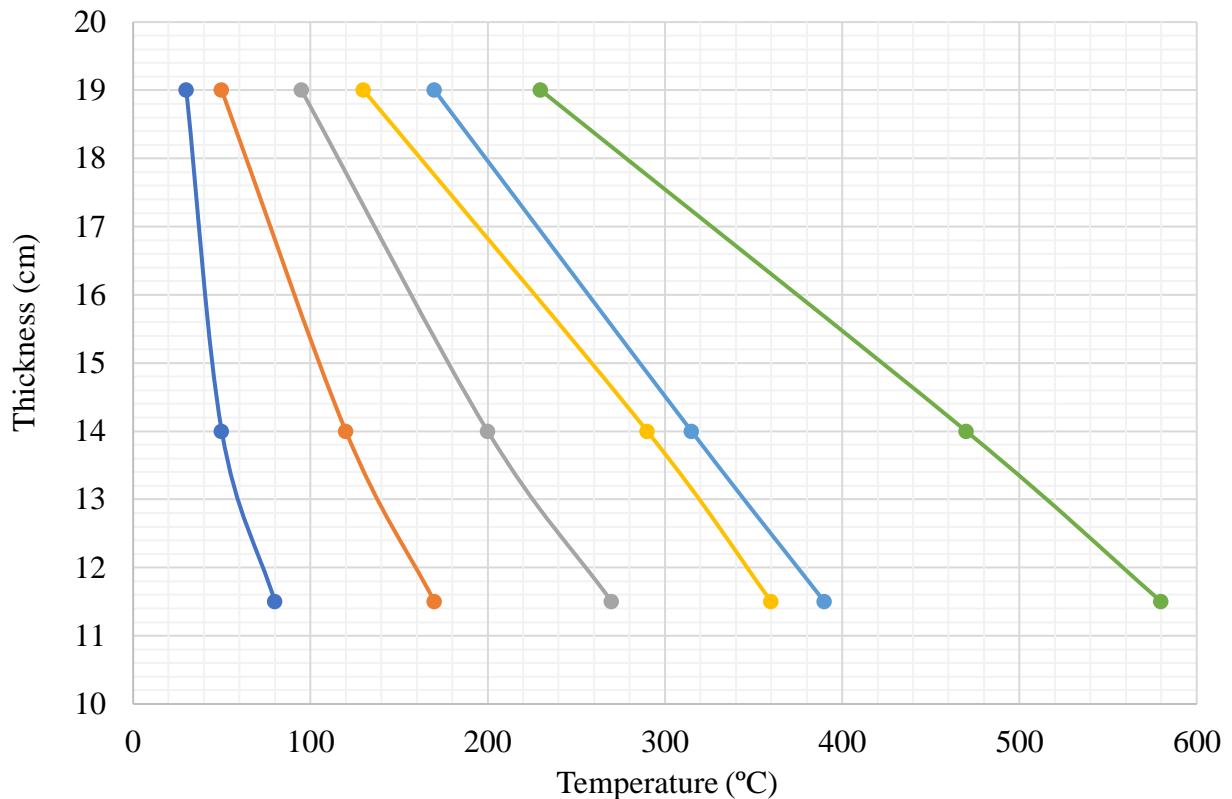
According to Figure 11, it is possible to determine that the alveoli have a great influence on the thermal insulation of the blocks, especially at higher temperatures. It was observed that choosing a block with a larger number of alveoli may be a more effective option, rather than choosing a thicker block, when high FRT is desired, which corroborates with what was concluded by Lee (2017), as to the fact that the influence of the alveoli in a block becomes practically null at low temperatures. Considering the response of the models, it was found that, at higher temperatures, the convective and irradiative phenomena that occur inside the blocks are more relevant than the thermal conduction, which occurs through the material. This is stressed in NBR 15220 (ABNT, 2003), where it defines confined air as an excellent thermal insulator.

From the results of Figure 11, it was possible to extrapolate the void values required to meet a thermal insulation time (TIT) for each type of block, presented in Table 5. Extrapolation was made by only performing adjustments in the shape of the block, based on the one that had been calibrated by experimental means.

Table 5. TIT determination from the percentage of voids in a block.

Block thickness	Maximum percentage of voids for FRT in minutes					
	30	60	90	120	180	240
11,5 cm	79,11%	86,64%	45,95%	42,17%	40,25%	30,95%
14 cm	81,73%	80,71%	62,89%	58,30%	53,08%	45,96%
19 cm	84,90%	84,90%	84,90%	84,90%	74,02%	59,62%

For comparison purpose, temperature evolution curves of the unexposed face of the Index II blocks were generated, in order to compare the influence of the block’s thicknesses, presented in Figure 12.



● 30 min ● 60 min ● 90 min ● 120 min ● 180 min ● 240 min

30 min: $L = 23,843e^{-0.01T}$ $R^2 = 0,9787$	60 min: $L = 22,768e^{-0.004T}$ $R^2 = 0,9948$	90 min: $L = 24,566e^{-0.003T}$ $R^2 = 0,9985$	120 min: $L = 25,136e^{-0.002T}$ $R^2 = 0,9869$	180 min: $L = 26,21e^{-0.002T}$ $R^2 = 0,9907$	240 min: $L = 26,337e^{-0.001T}$ $R^2 = 0,9912$
---	--	--	---	--	---

Figure 12. Block curves of BL1-II, BL2-II and BL3-II

From these curves it was possible to determine the thickness related to TIT desired in a sealing wall, shown in Table 6.

Table 6. TIT determination from block thickness.

Minimum thickness for FRT						
FRT (min)	30	60	90	120	180	240
Thickness (cm)	11,5	11,5	14	19	19	-

Table 6 presents minimum wall thicknesses that meet the requirements in Eurocode 6 (EN 1996-1-2, 2005), reinforcing the validation of the parameters used. Through observation of the data generated from the analysis of the influence of the block thickness, it is possible to verify that this factor has a good influence on lower TITs. However, after 90 minutes, this parameter tends to have a lower TIT increment rate.

5. CONCLUSIONS

In this work, the fire resistance of ceramic blocks used for structural masonry was analyzed through the finite element method using the Ansys Mechanical program. The blocks tested by the software were molded into an uncoated configuration and with 1 cm mortar joints, varying only the thickness and number of alveoli in each simulation.

The computational analyses led to results that point to a limit in the efficiency of the wall thickness increase to reach high FRTs in relation to the thermal insulation. It was also possible to demonstrate thermal insulation gain by increasing the number of alveoli within a block. Thus, it was possible to verify the importance of convection and thermal radiation processes in fire safety, which are more relevant than the thermal conduction of the assessed material.

When an analysis is performed only regarding the block thicknesses, the results converge towards what is presented in Eurocode 6 project table (EN 1996-1-2, 2005). When considering the number of alveoli, the potential gain in thermal resistance without varying the thickness of a block meets the concepts of thermal comfort that are presented in NBR 15220. This fact reinforces the relevance of using this concept in the elaboration of a Brazilian standard for projects of structural masonry in fire situation.

6. REFERENCES

- Associação Brasileira de Normas Técnicas (1989). *ABNT NBR 10636: Paredes divisórias sem função estrutural - Determinação da resistência ao fogo - Método de ensaio*. Rio de Janeiro.
- Associação Brasileira de Normas Técnicas (2001). *ABNT NBR 5628: Componentes construtivos estruturais - Determinação da resistência ao fogo*. Rio de Janeiro.
- Associação Brasileira de Normas Técnicas (2013). *ABNT NBR 15575: edificações habitacionais: desempenho*. Rio de Janeiro.
- Associação Brasileira de Normas Técnicas (2003). *ABNT NBR 15220: Desempenho térmico de edificações*. Rio de Janeiro.
- Bai, G. et al. (2017). *Study on the Thermal Properties of Hollow Shale Blocks as Self-Insulating Wall Materials*. *Advances in Materials Science and Engineering*. 2017(ID 9432145), p. 12. DOI: <https://doi.org/10.1155/2017/9432145>
- Ehrenbring, H. Z., Quinino, U., Oliveira, L. S., Tutikian, B. F. (2019), *Experimental method for investigating the impact of the addition of polymer fibers on drying shrinkage and cracking of concrete*. *Structural Concrete*. 20(3), 1064–1075. DOI: <https://doi.org/10.1002/suco.201800228>.
- European Committee Standardization (2005). *Eurocode 6: Design of masonry structures: Part 1-2: General rules – Structural fire design*. Brussels.
- Gil, A., Pacheco, F., Christ, R., Bolina, F. L., Khayat, K. H., Tutikian, B. F. (2017), *Comparative study of concrete panels' fire resistance*. *ACI Materials Journal*. 114(5), 755-762.
- International Organization for Standardization (2014). *ISO 834-11: Fire resistance tests - Elements of building construction - Part 11: Specific requirements for the assessment of fire protection to structural steel elements*. Switzerland.
- Lee, L. S. H., Jim, C. Y. (2017). *Subtropical summer thermal effects of wirerope climber green walls with different air-gap depths*. *Building and Environment*, v. 126, p. 1–12. DOI: <https://doi.org/10.1016/j.buildenv.2017.09.021>

- Marcatti, J., Coelho Filho, H. S., Berquó Filho, J. E. (2008), *Compartimentação e afastamento entre edificações*. In: SEITO, A. I. et al (Coord.). A segurança contra incêndio no Brasil. São Paulo: Projeto Editora. p. 496. ISBN:978-85-61295-00-4
- Nguyen, T. D. et al. (2009), *The behaviour of masonry walls subjected to fire: Modelling and parametrical studies in the case of hollow burnt-clay bricks*. Fire Safety Journal. 44(4), p. 629–641. DOI: <https://doi.org/10.1016/j.firesaf.2008.12.006>
- Nguyen, T. D., Meftah, F. (2012), *Behavior of clay hollow-brick masonry walls during fire. Part I: Experimental analysis*. Fire Safety Journal. 52. p. 55–64. DOI: <https://doi.org/10.1016/j.firesaf.2012.06.001>
- Pacheco, F., Souza, R., Christ, R., Rocha, C., Silva, L., Tutikian, B. F. (2018), *Determination of volume and distribution of pores of concretes according to different exposure classes through 3D microtomography and mercury intrusion porosimetry*. Structural Concrete. 19(2). p. 1419–1427. DOI: <https://doi.org/10.1002/suco.201800075>
- Rigão, A. O. (2012), *Comportamento de pequenas paredes de alvenaria estrutural frente a altas temperaturas*. 142 f. Dissertação (Mestrado) - Curso de Engenharia Civil, Universidade Federal de Santa Maria, RS, Brasil.
- Zsembery, S., Lawrence, S. (2013), *Manual 2 - The Properties of Clay Masonry*. Think Brick. Austrália.

Polymeric fiber reinforced concrete exposed to fire

D. M. Dias^{1*} , J. L. Calmon¹ , G. L. Vieira¹ 

*Contact author: dainerdias@gmail.com

DOI: <http://dx.doi.org/10.21041/ra.v10i1.426>

Reception: 01/07/2019 | Acceptance: 27/11/2019 | Publication: 30/12/2019

ABSTRACT

The aim of this work was to investigate the influence of the addition of polypropylene, polyester, polyamide, aramid and aramid pulp fibers on the behavior of concretes subjected to high temperatures. For that, test specimens with fiber additions were made at a rate of 2 kg/m³ and submitted to temperatures in furnace, as well as to high temperatures through direct fire test. Columns were also built and subjected to a live fire simulator belonging to the Espírito Santo Fire Department - Brazil. Microstructural and mechanical properties were analyzed. It has been observed that the fibers may influence the properties of the concrete and that fire tests with standard fire load may be an alternative or complementary analysis of concrete subjected to elevated temperatures.

Keywords: Reinforced concrete; polymeric fibers; high temperatures; fire; mechanical properties.

Cite as: Dias, D. M., Calmon, J. L. Vieira, G. L. (2020), “*Polymeric fiber reinforced concrete exposed to fire*”, Revista ALCONPAT, 10 (1), pp. 36 – 52, DOI: <http://dx.doi.org/10.21041/ra.v10i1.426>

¹ Federal University of Espírito Santo, Vitória-ES, Brazil.

Legal Information

Revista ALCONPAT is a quarterly publication by the Asociación Latinoamericana de Control de Calidad, Patología y Recuperación de la Construcción, Internacional, A.C., Km. 6 antigua carretera a Progreso, Mérida, Yucatán, 97310, Tel.5219997385893, alconpat.int@gmail.com, Website: www.alconpat.org

Responsible editor: Pedro Castro Borges, Ph.D. Reservation of rights for exclusive use No.04-2013-011717330300-203, and ISSN 2007-6835, both granted by the Instituto Nacional de Derecho de Autor. Responsible for the last update of this issue, Informatics Unit ALCONPAT, Elizabeth Sabido Maldonado, Km. 6, antigua carretera a Progreso, Mérida, Yucatán, C.P. 97310.

The views of the authors do not necessarily reflect the position of the editor.

The total or partial reproduction of the contents and images of the publication is strictly prohibited without the previous authorization of ALCONPAT Internacional A.C.

Any dispute, including the replies of the authors, will be published in the third issue of 2020 provided that the information is received before the closing of the second issue of 2020.

Concreto reforçado com fibras poliméricas exposto ao fogo

RESUMO

O objetivo desse trabalho foi investigar a influência da adição de fibras poliméricas de polipropileno, poliéster, poliamida, aramida e polpa de aramida no comportamento de concretos submetidos a temperaturas elevadas. Para tanto, corpos de prova com adições de fibras a uma taxa de 2kg/m^3 foram produzidos e submetidos a mufla, bem como a altas temperaturas através de teste de fogo direto em grelha. Protótipos também foram construídos e submetidos a simulador de incêndio real pertencente ao Corpo de Bombeiros do Espírito Santo - Brasil. Propriedades microestruturais e mecânicas foram analisadas. Observou-se que as fibras podem influenciar as propriedades do concreto e que os ensaios de teste de fogo com carga de incêndio padrão podem ser uma alternativa ou complementar análise de concreto submetido a temperaturas elevadas.

Palavras-chave: Concreto reforçado; fibras poliméricas; altas temperaturas; incêndio; propriedades mecânicas.

Hormigón reforzado con fibras poliméricas expuesto al fuego

RESUMEN

El objetivo de este trabajo fue investigar la influencia de la adición de fibras poliméricas de polipropileno, poliéster, poliamida, aramida y pulpa de aramida en el comportamiento de hormigones sometidos a temperaturas elevadas. Las probetas con adiciones de fibras a una tasa de 2 kg/m^3 fueron producidas y sometidas a altas temperaturas a través de pruebas en horno y de fuego directo. También se construyeron columnas y se sometieron a un simulador de incendios en vivo perteneciente al Departamento de Bomberos de Espírito Santo - Brasil. Se analizaron las propiedades microestructurales y mecánicas. Se observó que las fibras pueden influir en las propiedades del concreto y que los ensayos de fuego con carga de incendio estándar pueden ser una alternativa o complemento para el análisis de hormigón sometido a temperaturas elevadas.

Palabras clave: Concreto reforzado; fibras poliméricas; altas temperaturas; fuego; propiedades mecánicas.

1. INTRODUCTION

Large fires have already severely compromised various structures throughout history (Metha and Monteiro, 2008). Structural fire safety is one of the most important considerations that should be applied in constructions (Khalaf and Huang, 2016). The behavior of concrete under the action of aggressive agents has long been the subject of studies in the fields of technology and durability of concretes (Petrucci, 1981).

Ma et al. (2015), Haddad et al. (2008), Cree et al. (2013) and Park and Yim (2016) showed that the high temperature is known to seriously damage the micro and the mesostructure of the concrete, what causes a general mechanical decay and even harmful effects at the structural level due to the cracking of the concrete and the exposure of the steel to the flames in case of fire.

The behavior of a real fire is very different from most furnace tests. In a performance-based approach, a more realistic representation of fire can be used, what consists of a heating phase followed by a cooling phase until it returns to room temperature (Gernay and Franssen, 2015). Real fire tests are important to understand the true behavior of concrete in fires, since conventional laboratory tests do not always reflect the behavior of this pathological situation. Just as the fire resistance of constructed structures is greater than that predicted from tests on individual element

(Lennon et al., 2007), it is observed that traditional methods of testing materials are more conservative than fire tests.

The use of fibers in concrete has become popular, mainly because of the resistance to cracking, plastic retraction and increased tenacity, and, more specifically, the polymeric fibers give the concrete a better post-cracking behavior, prevent and control the formation and propagation of cracks and also avoid the phenomenon of spalling (Alhozaimy et al., 1996; Kurtz and Balaguru, 2000; Ezziane et al., 2015; Poon et al., 2004). Already Pai and Chandra (2013) said a better understanding of the concepts behind fiber reinforcement, new manufacturing methods and new types of organic fibers have led researchers to conclude that synthetic and natural fibers can reinforce concrete.

In a fire, the fibers melt at a certain temperature, which assists in the release of water vapor through the pores (Pliya et al., 2011). The additional porosity and the small channels created by the melting of the polypropylene fibers can decrease the internal vapor pressure in the concrete and reduce the probability of spalling (Noumowe, 2005), especially in high strength concrete.

Lee et al. (2012) remember that the addition of fibers to concrete has been suggested by several researchers since the first documents discussed the fire resistance of concrete, like the ACI report in 1919 (ACI, 2019). However, the discussion about the positive influence of polymer fibers on the mechanical properties of concrete is not yet finalized because, although some studies indicate that fibers do not significantly influence or worsen the properties of a reference concrete, other studies have shown the opposite, before and after. After being subjected to high temperatures, the fibers can improve the mechanical properties of concrete, as demonstrated by Shihada (2011) and Drzymala et al. (2017).

Studies have shown that polypropylene fibers are effective in mitigating spalling in concretes exposed to high temperatures (Ezziane et al., 2015; Xiao and Falkner, 2006; Behnood and Ghandehari, 2009; Bangi and Horiguchi, 2012; Akca and Zihnioglu, 2013) and that the addition of polypropylene fibers is the most widely used method in preventing spalling in high strength concrete. Song et al. (2005) evaluated the effects of addition of nylon and polypropylene fibers and showed that the compressive strength of the concretes increased, respectively, 12.4% and 5.8% when compared to the concrete without fibers. Regarding to polyester fibers, and depending on the percentage used, the addition of fibers may contribute to the increase of the compressive strength of the concrete, as Suresh et al. (2014) concluded. In an ideal dosage, the polyester fibers improved the compressive strength and flexural tensile strength of the concrete exposed to high temperatures in the range of 150-250°C during intervals of 1,2 or 3 hours (Sekhar and Raju, 2017). The addition of polyester fibers in the concrete can contribute to a failure delay of normal concrete when subjected to a sustained temperature range of 25 to 400 ° C (Suresh et al., 2014). Aramid fiber is still uncommon for the construction industry (Çavdar, 2013), showing that it can be better studied. Therefore, due to the existing gaps and the importance of the theme, the objective of this work was to investigate the influence of the addition of polypropylene, polyester, polyamide, aramid and aramid pulp fibers in the behavior of concretes subjected to elevated temperatures through different tests. For that, test specimens with fiber additions were made at a rate of 2 kg/m³. The samples were submitted to temperatures of 300°C, 500°C and 700°C in furnace, as well as at high temperatures through direct fire test. Short columns were also built and subjected to fire through a live fire simulator belonging to the Espírito Santo Fire Department - Brazil. Compressive strength, flexural tensile strength, splitting tensile strength, mass loss and ultrasonic pulse velocity tests were subsequently performed.

2. EXPERIMENTAL PROGRAM

2.1 Materials and mix proportions

For the preparation of the concrete, Portland cement CP III 40 RS, according to classification in standard (ABNT, 2018) was used. Natural sand of fineness modulus of 1.92 and maximum dimension of 2.4 mm was used as fine aggregate. Two types of granitic aggregate were used in the concrete as coarse aggregate, one of maximum size of 19 mm and one with 9 mm. A superplasticizer was used in the preparation of the concretes. Fibers were used at a dosage of 2 kg/m³. Such a dosage was mainly aimed at reducing the possibility of spalling and followed a tendency extracted from the study of the state-of-the-art of better fiber consumption (Poon et al., 2004; Behnood and Ghandehari, 2009; Kim et al., 2013; Lourenço et al., 2011; Bei and Zhixiang, 2016), where the best results were obtained with rate at or very close to it. Typical fiber properties are shown in Table 1.

Table 1. Properties of fibers

Fiber	Diameter (µm)	Length (mm)	Modulus of elasticity (GPa)	Tensile strength (GPa)	Density (g/cm ³)	Melting point (°C)
Polypropylene	12	12	9.0	0.5	0.91	160
Polyester	20-25	15	8.2	0.3 – 0.5	1.34	235
Polyamide (Nylon 6.6)	30	12	5.0	0.9	1.14	260
Aramid (Kevlar 29/49)	14	12	65/125	2.8	1.44	427-482
Aramid pulp Kevlar	2-13	0.5-1.0	65/125	2.8	1.45	423

2.2 Specimen preparations

The proportion of the materials used to concrete mixtures is show in Table 2. Six concretes were produced, the reference without fibers (NF), polypropylene fiber reinforced concrete (PP), polyester fiber reinforced concrete (POL), polyamide fiber reinforced concrete (NY), aramid fiber reinforced concrete (AR) and aramid pulp fiber reinforced concrete (AP).

Table 2. Mix proportions

Material	NF	PP	POL	NY	AR	AP
Cement (kg/m ³)	340	340	340	340	340	340
Fine aggregate (kg/m ³)	770	770	770	770	770	770
Coarse aggregate 9 mm (kg/m ³)	300	300	300	300	300	300
Coarse aggregate 19 mm (kg/m ³)	842	842	842	842	842	842
Water (l/ m ³)	170	170	170	170	170	170
Superplasticizer (l/ m ³)	2,85	2,85	2,85	2,85	2,85	2,85
w/c	0,5	0,5	0,5	0,5	0,5	0,5
Fiber (kg/m ³)	0	2	2	2	2	2
Slump (mm)	190	30	50	70	60	20
Density (kg/m ³)	2471	2439	2455	2457	2460	2452

Cylindrical and prismatic specimens were molded according to NBR 5738 (ABNT, 2015a). The fresh concrete mixtures were tested for workability by slump test according to NBR NM 67 (ABNT, 1998). Reinforced concrete short columns with cross section of 20x20cm and height of 1.35m were made soon after.

The specimens remained in moist cure for 28 days. After this period, the specimens were kept in a controlled environment (climatic chamber) for 7 days more with a constant temperature of 23°C and a relative humidity of 77%, close to the reality found in the state of Espírito Santo - Brazil. As the tests of high temperatures are influenced by the humidity and considering that the goal was to test the concrete as close to reality as possible, temperature and humidity control was performed. Conditioning specimens with the objective of providing the internal moisture condition similar to constructed buildings is indicated by ASTM E119 (ASTM, 2018).

2.3 Heating procedures

Before the mechanical tests, the specimens were submitted to high temperature tests in furnace and direct fire. In the furnace, the maximum temperatures reached for analysis were 300, 500 and 700°C. These temperature ranges analyzed (intervals where important transformations take place in concrete) follow a trend found in the state-of-the-art like, for example, Xiao and Falkner (2006), Shihada (2011), Suresh et al. (2014) and Yermak et al. (2017). In a previous study Dias et al. (2017) observed that at higher temperatures concretes lost their structural capacity.

Regarding spalling, a phenomenon that occurs with concrete subjected to high temperatures, factors such as aggregate type, samples size, presence of additives, strength concrete and, mainly, heating rate, influence the appearance or not of spalling. In most cases a temperature higher than 700°C is required to spalling. However, temperatures above 500°C, added to other characteristics, are enough. For example, Akca and Zihnioglu (2013) said that explosive spalling was observed especially in nonfibrous specimens and began after 500°C.

As the real fires in compartments, within its phases, presents an apex point and soon after the decay comes (Hartin, 2018), in the tests performed, after reaching the maximum stipulated temperature, the furnace was turned off. The heating rate used was 10°C/min and the cooling was at room temperature for 24 hours. The furnace tests followed methodologies commonly found in the state-of-the-art for this type of laboratory tests (Ezziane et al., 2015; Poon et al., 2004; Pliya et al., 2011; Shihada, 2011; Pai and Chandra, 2013; Xiao and Falkner, 2006; Behnood and Ghandehari, 2009; Akca and Zihnioglu, 2013; Suresh et al., 2014; Sekhar and Raju, 2017; Bei and Zhixiang, 2016; Choumanidis et al., 2016; Srikar et al., 2016; Yermak et al., 2017).

In order to obtain results that could be compared with furnace heating, direct fire tests were also performed according to ISO 834-R (ISO, 2015). To perform the test, the specimens were placed vertically on a steel grill of dimensions of (500x500) mm in a height of 100mm of the combustible material, leaving space between them to have direct contact with the fire. In the tests with real fire, as found in (Shihada, 2011), the fuel material used was wood. The amount of wood used in each test was calculated based on a standard low-risk fire load of 300 MJ/m² commonly found in apartments in Brazil (Espírito Santo, 2009; São Paulo, 2011; ABNT, 2000), considering the caloric potential of 19 MJ/kg of wood in each burn. To start the burning, alcohol was used. Two K-type thermocouple sensors were placed in the device to gauge the temperature evolution. The Espírito Santo Fire Department – Brazil (CBMES) supported with knowledge and protective equipment in the realization of the real fire test. This test lasted 80 min, which practically coincided with the end of the combustible material, and the cooling was ambient. The furnace test and the fire test can be seen in Fig. 1

An imaging infrared thermometer was used before, during and after the high temperature tests. Mechanical tests of compressive strength, flexural tensile strength, splitting tensile strength were performed after the high temperature tests. Ultrasonic pulse velocities and mass loss were performed before and after the submission to high temperature.

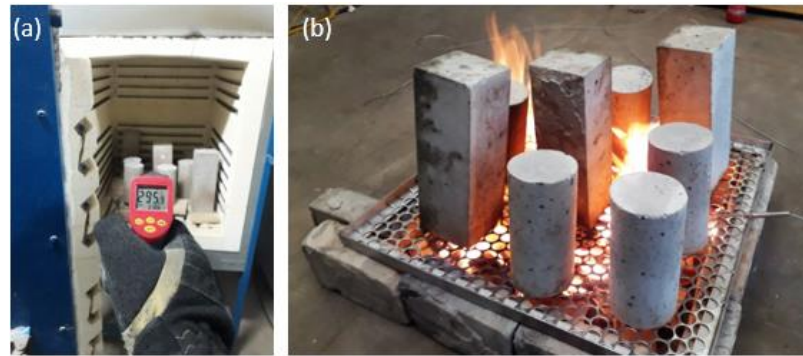


Fig. 1. Temperature rise through furnace (a) and grill fire test (b).

Aiming to complement the analysis, especially of the spalling, tests were carried out with real fire in the short columns through one of the CBMES's live fire simulators. The chosen module provides extreme fire behavior within the first few minutes of fire. Ventilation was controlled through the front doors. The fire load stipulated was also low risk using plywood and pallets. The arrangement of the fire load and the columns in the simulator can be seen in Fig. 2. The mounting followed firing patterns of the fire brigades and aimed to provide reality in the evolution of fire and uniformity of firing. Type k thermocouple sensors were inserted at 0.8m and 1.6m high in the container to gauge the internal temperature and a sensor was monitoring the external temperature. A firefighter with all the necessary personal protective equipment started this simulation. See Fig. 3 for a sequence of photos of the test run.



Fig. 2. Chosen simulator (a), device assembly (b) and sensor arrangement (c).



Fig. 3. Real fire simulation in columns

2.4 Test procedures

Compressive strength, flexural tensile strength, splitting tensile strength, mass loss and ultrasonic pulse velocity (UPV) tests were subsequently performed. Macro and microscale analysis were also performed on the specimens.

The verification of the concrete submitted to high temperatures began with visual analysis, observing spalling, cracks and changes of color. Images of fragments of specimens at a depth of 1cm were generated through a scanning electron microscope (SEM), aiming to verify the interfacial transition zone between the aggregate and the mortar matrix, and especially the interaction of the fibers in the concrete and the permanence or not of them in relation to the high temperatures.

The concrete specimens were subjected to the compressive strength test following the procedure of NBR 5739 (ABNT, 2007) after being submitted to high temperatures. The flexural tensile strength was carried out in accordance with the standards found in NBR 12142 (ABNT, 2010), in which it this test method covers the determination of the flexural strength of concrete by the use of a simple beam with third-point loading. In order to complement the analysis of the destructive mechanical tests, the splitting tensile strength test was also carried out. The test followed the regulations of NBR 7222 (ABNT, 2011).

The mass loss was obtained by the ratio between the difference of the mass of the test specimen before and after being subjected to high temperature and the mass before burning, the result being presented in percentage. The non-destructive tests to determine the propagation velocity of longitudinal waves obtained by ultrasonic pulses through concrete specimens were performed based on NBR 8802 (ABNT, 2013), where direct transmission between the transducers was used.

3. RESULTS

It was performed a statistical analysis of the results obtained in the tests to verify if there is a statistical difference in a 95% confidence interval, which reflects a level of significance of 0.05. The analysis of variance (ANOVA) was used, followed by the Tukey's multiple comparisons test. At first, the results of high temperatures in the furnace were analyzed separately and in a second moment the comparison with the fire test was carried out.

There was no spalling in any test specimens tested. As temperature and humidity were controlled in the cure, it was verified that under normal climatic conditions found in Espírito Santo - Brazil the spalling was mitigated, even in the case of concretes with strengths greater than 50 MPa - concrete class II (ABNT, 2015b).

From an overall analysis, as will be seen in the following topics, greater percentage losses were observed after the 500°C range. This is explained by the fact that heat passes through the interior of the test specimen and by the transformations of the microstructure of the concrete occurring during heating and are more damaging after this range (Ma et al., 2015; Castellote et al., 2004; EN Eurocode, 2004; Khoury, 1992).

3.1 Microstructure of the concrete

From the generated images, the interaction of the fibers was considered satisfactory. In the furnace tests in the range of 700°C it was not observed the presence of fibers in any concrete, which was to be expected, since the melting point of the all fibers did not exceed 500°C, as seen in Table 1.

The Fig. 4 shows the concretes after being subjected to a temperature of 500°C in furnace.

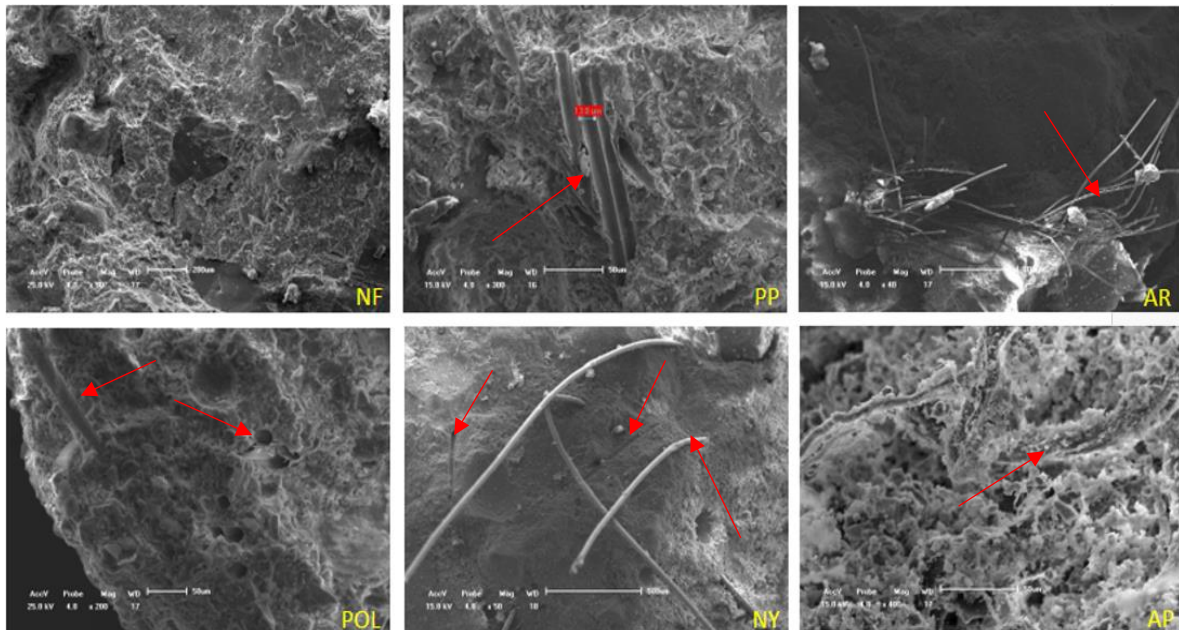


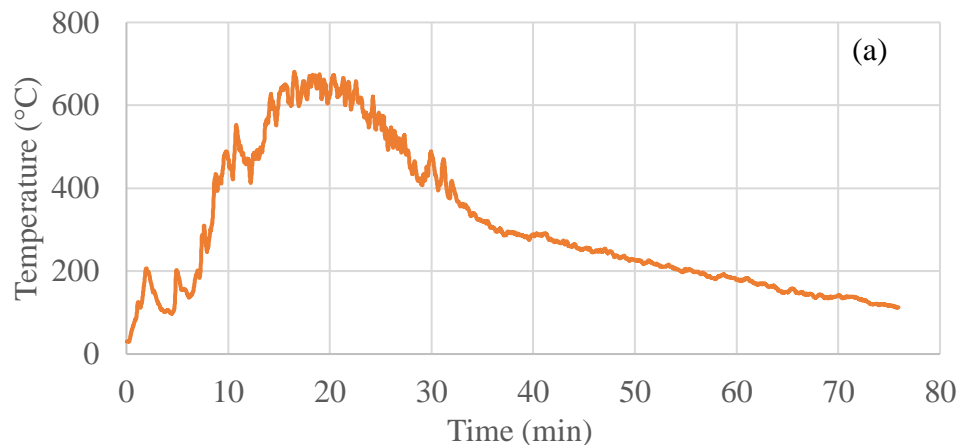
Fig. 4. SEM of concretes after being subjected to a temperature of 500°C

It is observed that PP and POL did not contain more fibers after 500°C, that the AR and AP did not lose the fibers in their totality and in the NY there was the partial fusion of the fibers. The temperature applied was 500°C, but it is worth remembering that the heat in the concrete goes through conduction and that is the reason why some fibers of the inner part of the NY remained and others not, that is, at the analyzed point the internal temperature of the concrete was close to 260°C. The arrows in Fig. 4 show this information.

Later it will be seen that NF and AP were the concretes that presented spalling in the live fire simulator test. Correlating with the MEV test it is verified that the lack of porosity to release water vapor influenced the spalling of NF. In the AP, the high fibrillation of the aramid pulp, the surface concentration and the fact that it did not melt were determinant factors for not increasing the porosity of the concrete. More explanations will be given in the topic of Fire test in live fire simulator.

3.2 Fire test

The type K thermocouple sensors gauged the behavior of real temperature evolution over time in the grill fire test and live fire simulator test. It is observed that the behavior is quite different from the standard ISO 834 curve of an electric furnace. Such a difference can be seen in Fig. 5.



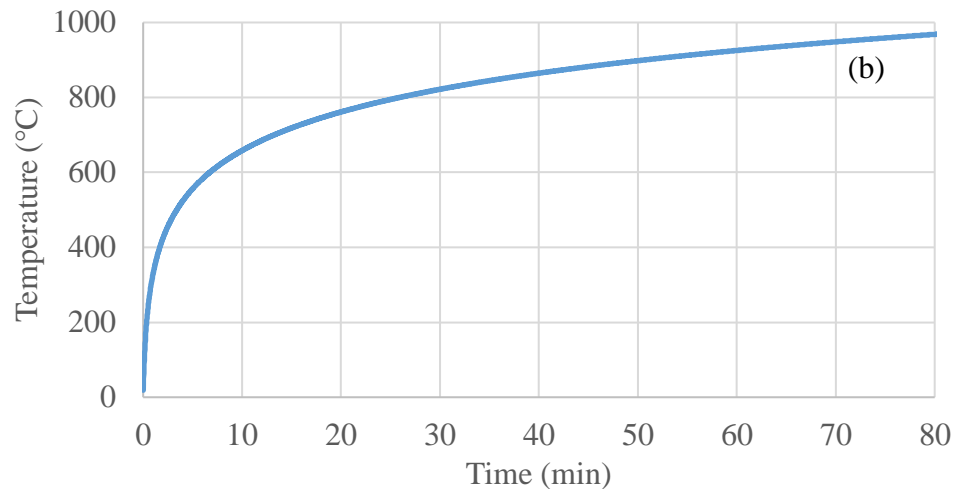


Fig. 5. Temperature x time in the grill fire test (a) and ISO 834 (b) curve

As shown in the graph, in the grill fire test there were the phases of the compartment burning, in other words, the tests showed the ignition point, growth phase, with or without generalized burning, apex and decay due to lack of material fuel. A behavior different from that found in furnace assays. Another divergent point is the heating pattern of the specimen. Heat is passed by conduction to the specimen. In a fire, the fire front most of the time has a pattern. In furnace burning all sides transfer energy equally to the test specimen. In Fig. 6 it is observed in thermograph images how the heat is passed in the two types of tests performed.

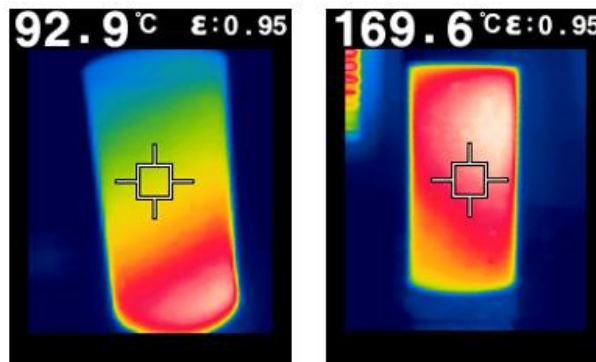


Fig. 6. Thermographic images of the specimens in cooling phase, immediately after burning on grill fire test (a) and immediately after being subjected to 500°C in furnace (b)

The Fig. 6(a) shows a well-defined temperature gradient, showing hotspots in the lower part of the specimen, where the fire load was concentrated. Already Fig. 6(b) shows that the heating of the specimen is almost uniform, which was expected, the furnace heat on all sides. Most real fires have a definite fire front, i.e. grill fire test was most effective in this aspect.

Another important information is that even the grill reaching temperatures higher than the furnace at 500 ° C, for example, the temperature of the specimen face in furnace was bigger than the specimen in grill, showing that the radiated thermal energy of the furnace is higher.

Tests of concrete submitted to elevated temperatures through electric furnaces can be reproducible, but do not represent the reality of a compartment fire and are much more severe than fire tests with finite charge material.

3.3 Compressive strength

The compressive strength data of the concretes tested in furnace were submitted to ANOVA. It was observed that the isolated effect of the concrete type (NF, PP, POL, NY, AR and AP) and the temperature variation (23, 300, 500 and 700°C) were significant, as well as the interaction between the two variables. Fig. 7a shows the compressive strength as a function of the temperature of the concretes analyzed.

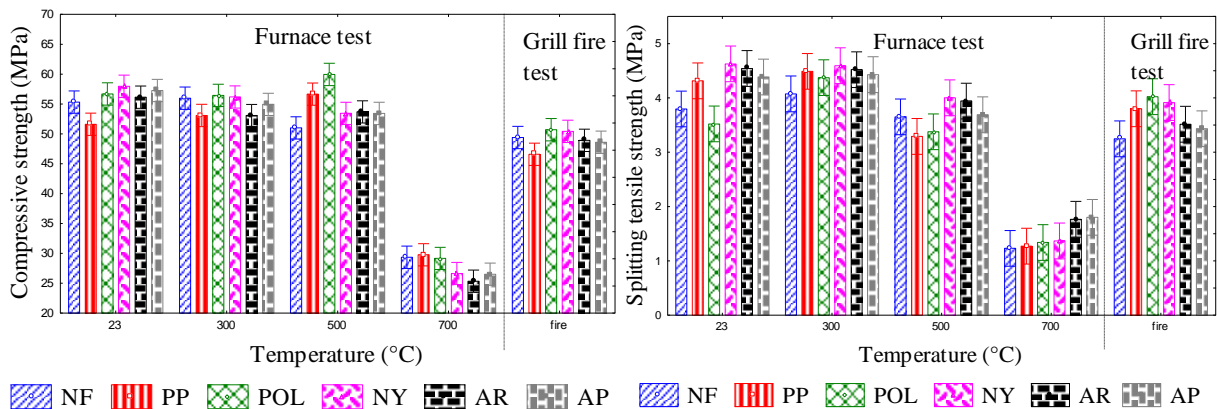


Fig. 7. Compressive strength (a) and splitting tensile strength (b) as a function of the temperature in the furnace and in the grill fire test.

Analyzing the furnace test, it is observed that from 23°C to the 500°C range there is almost no change in the compressive strength. At 700°C there is an average fall of approximately 50.2% of this mechanical property when compared to ambient temperature. This behavior can be explained by the range of temperature that occurs the important transformations in the concrete, as shown by Castellote et al. (2004).

After ANOVA it is concluded that there is a difference between the concrete groups submitted to different temperatures, however, only with this analysis it is not possible to point out if the difference occurs within the group or between the groups. A multiple comparison test can be used when there is a difference as it completes the analysis by comparing and then showing the result of all combinations of mean pairs. Tukey's multiple comparisons test was used.

After the Tukey's multiple comparisons test conclude that:

- The compressive strength of the NF did not change until the 300°C range. The PP presented the same behavior;
- The resistance of the POL did not change until 500°C;
- Up to 300°C the NY compressive strength is the same. Between 300-500°C there was no change in resistance. The AP had the same behavior;
- For the AR between 300-500°C the compressive strength is the same, as the value at room temperature is the same as at 500°C.

Analyzing the grill fire test, the results show that the effect of high temperature through furnace is more severe to concrete. Although the final temperature of the fire test reaches almost 700°C, the obtained values of compressive strength in furnace at 700°C are an average of 55% of the grill fire test results.

3.4 Flexural tensile strength

When performing the ANOVA, it was observed that the fibers and the temperature independently influence the behavior of flexural tensile strength in the concrete. The temperature was the variable of greatest impact followed by concrete type (addition of fibers), but the interaction between these two sources of variation, concrete type and temperature, was not significant, since the P value was higher than 0.05.

3.5 Splitting tensile strength

It was observed that there was no change in the result up to the range of 300°C and after that, when compared to the ambient temperature, the average value of the splitting tensile strength down 12.9% in the range of 500°C and 65.2% at 700°C.

It presented significance when the variation sources of concrete type and temperature were analyzed independently, as well as the interaction between the variables was significant with a 95% of confidence interval. Fig. 7b shows the graph of the splitting tensile strength as a function of temperature.

It was observed that NY, AR and AP had higher averages than NF, PP and POL. Even though it is a test that may present greater variations of results than the other two tests presented previously (compressive strength and flexural tensile strength), it is worth pointing out that the fiber characteristics may have influenced the results. It is verified that over again the temperature was the variable with the greatest impact. After multiple comparisons tests, it is verified that at 700°C there is no difference between the analyzed concretes. It is suggested that the orientation of the fibers may have interfered in the results, because in this test the POL obtained the lowest average result while the AR obtained the highest. In the compressive strength test this logic was inverted, in other words, the POL obtained the highest average result and the AR the worst. Because these cylindrical specimens were molded under the same conditions, it is hypothesized that the orientation of the fibers may have influenced the result. It is verified that the results obtained in grill fire test are close to those obtained in furnace at 500°C.

3.6 Mass loss

The mass loss results were significant for a 95% confidence interval.

From the 300 ° C the temperature already influences the loss of mass of the concretes tested. Both in this temperature range, where the great mass loss corresponds to the free water, and at 700 ° C, where all free water has already been released, many chemical transformations have already occurred, considerable cracks have already appeared and the concrete has already lost a large part of its structural characteristic [4].

In the range of 500 ° C it is verified that NF obtained the smaller loss of mass than the other concretes. This temperature range is enough to melt a large part of the fibers, providing the expected increase in pores, but not yet enough to perform all the chemical transformations of the concrete. The graph of mass loss as a function of temperature is in Fig. 8a.

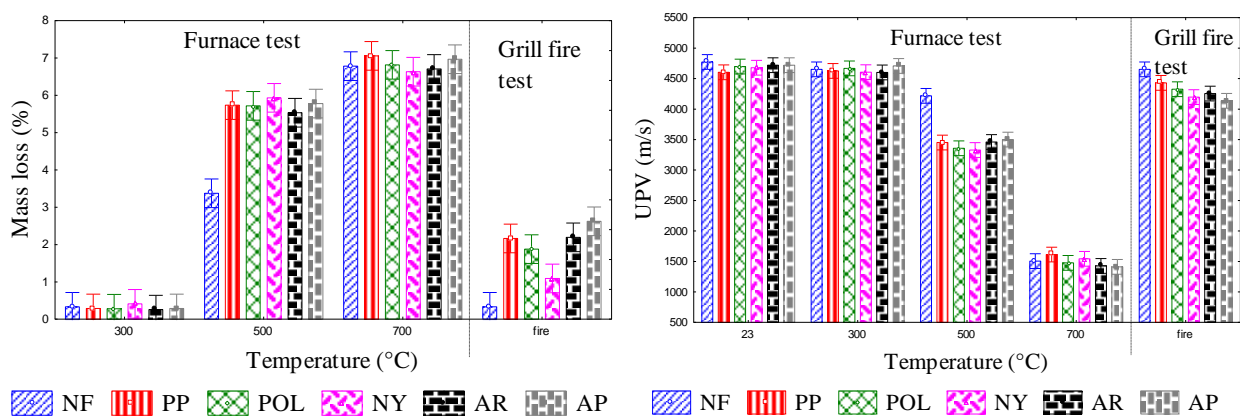


Fig. 8. Loss of mass (a) and UPV (b) as a function of temperature.

Although the final temperature of the grill fire test reaches almost 700°C, the concrete presents less loss than the concrete at 500°C in furnace, as can be seen in the results of mass loss and UPV.

3.7 Ultrasonic pulse velocity

Fig. 8b shows the result of UPV. It is suggested the existence of cracks and even increase of the pores with the addition of temperature.

By graphical analysis it was verified that up to 300°C there was no increase of cracks capable of presenting differences in the ultrasound analysis. The method of non-destructive testing to determine the speed of propagation of longitudinal waves, obtained by ultrasonic pulses through a component of concrete, its main applications detection of internal concreting flaws, depth of cracks and other imperfections (ABNT, 2013). Due to the heating rate, the maximum temperature reached and the cooling used, at 300 ° C, no moisture loss was detected. At 500°C the NF exhibited higher velocity than the concrete with fibers and the temperature of 700°C was enough to have the same result in all the concretes analyzed.

These numbers show that temperature is not the only variable that significantly influences the results of the same concrete after severe conditions, since heat flow, fire front and fire load are essential to determine behavior. Furnace tests, which are important for the sake of comparison, do not represent the reality of a real fire and other tests, such as the fire test, may complement the analysis.

3.8 Fire test in live fire simulator

In the Fig.9 are shown the temperature indices as a function of time of each of the sensors that monitored the fire in the live fire simulator.

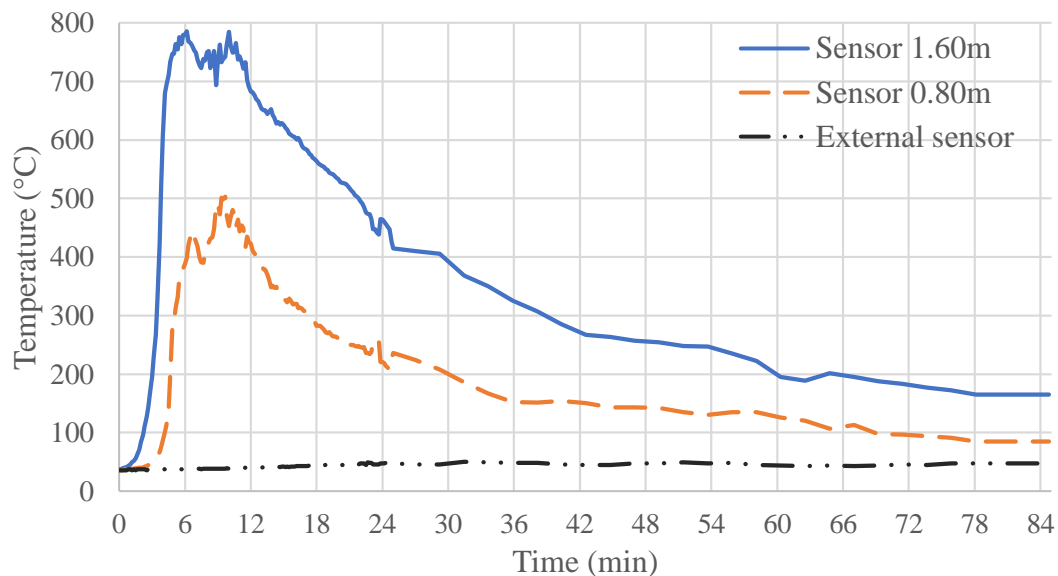


Fig. 9. Temperature vs time in the live fire simulator for the three sensors.

The mean temperature in the sensor outside the container was 42°C. It was observed that, in fact, the fire had an extreme behavior in the simulator, since in just 6 minutes after the fire began the temperature in the container reached its maximum range of 786°C in the sensor located at 1.60m. The first 2 minutes were of slow burning only in the center of the ignition of the material and of much release of white smoke (water vapor from the wood). With 4 minutes of simulation there was already widespread burning of the center pallets and flame touching the ceiling. Up to 5 minutes it was clear the release of white smoke starting to turn gray. From there, the behavior began to change.

In 6 minutes, the smoke was already light gray and already taking up the whole door. At that moment, it began to burn the wood from the bottom. At 10 minutes it occurred the general burn in the wood of the bottom and of the ceiling. At 11 minutes the smoke generated was already blurred, almost a khaki brown, which is an incomplete burning characteristic, which means, there was still a lot of combustible material being carried in the smoke. So much so that at this time of the test until the 12 minutes the smoke was burned with, even, the appearance of flames out of the container (this moment is called “flash”). That is why you can see almost a second peak of temperature rise in the upper sensor. After widespread burning, at 13 minutes the smoke was dark gray. At 23 minutes, slow burning only in the center (the reminder of the combustible material). Thereafter the temperature curve continues to decline. This is a real behavior of a fire.

After the test and the total cooling of the site, the visual analysis of each column was performed in the following day. Fig. 10 shows the columns side by side. The signs made in the columns show the displacements that happened in some of the concretes.



Fig. 10. Columns after being subjected to the fire and focus in NF and AP post fire, showing the top (a), center (b) and base (c).

It was observed that NF exhibited the highest spalling, followed by AP. AR also showed a small spalling at the base. The pillars of PP and POL did not present spalling, that is, the damages were not observed in the visual analysis. These concretes only showed a burning mark from the wood. At least one phase of each pillar showed this soot mark, a very common feature found in fires due to incomplete burning of combustible materials.

From this analysis conclude that the polymeric fibers decrease the incidence of spalling in the concrete and that the fibers with lower melting temperature are more efficient, because they melt at lower temperatures and open pores, thus releasing water vapor inside the concrete.

High performance polymeric fibers, such as aramid, were not efficient in the spalling aspect. Aramid pulp, being smaller and creating more nets and fiber interlacements, did not melt before the 500°C range and did not release pores, offering resistance to the concrete. This fact was essential for the appearance of spalling.

Fig. 10 also shows the detail of the most affected pillars. Both surface and edge spalling were observed in NF and AP too. As the main influences, besides the presence of the fiber in the case of PA, can mention the concrete permeability, thermal expansion of the aggregate, presence of steel and heating rate.

4. CONCLUSIONS

Based on the results of this experimental study, the following conclusions are drawn:

- Fire test with standard fire load may be an alternative or complementary analysis of concrete subjected to high temperatures, since the furnace tests do not represent faithfully the conditions found in a real fire in a compartment.
- Temperature is not the only variable that significantly influences concrete results after severe conditions, as heat flow, fire front and fire load are essential to determine the behavior, indicating that complementary testing is important for broad analysis.
- Polymeric fibers decrease the incidence of spalling in concrete and fibers with lower melting temperature (polypropylene and polyester) are more efficient because they melt at lower temperatures and open pores, thereby releasing water vapor into concrete. The polymeric fibers considered as high performance, as in the case of aramid, were not efficient in the spalling aspect.
- Although the grill fire test reached a temperature close to 700°C, the concrete showed less cracking than concrete in furnace at 500°C.
- In the mechanical tests performed after 700°C the results obtained were the same for all concretes, confirming that all the important transformations in the concrete have already happened, the fibers have already melted, and important cracks are already presented in this temperature range.
- The live fire simulator provided the most extreme behavior of the fire and it was possible to observe the spalling of concrete of some columns, showing an indication that type of cure, size of test specimen, presence of fibers and type of burning influence the behavior of the concrete exposed to fire.

5. ACKNOWLEDGEMENTS

The authors are grateful for the support provided by Espírito Santo Fire Department (CBMES), the Construction Materials Testing Laboratory (LEMAC) of the Civil Engineering Department of the Federal University of Espírito Santo (UFES) and Concrevit. In addition, a thanks to the Foundation for Support to Research and Innovation of Espírito Santo (FAPES) for the financial support to carry out this research.

6. REFERENCES









- ABNT Brazilian association of technical standards. (1998). *NBR NM 67: Concrete - Slump test for determination of the consistency*. Rio de Janeiro.
- ABNT Brazilian association of technical standards. (2000). *NBR 14432: Fire-resistance requirements for building construction elements - Procedure*. Rio de Janeiro.
- ABNT Brazilian association of technical standards. (2007). *NBR 5739: Concrete - Compression test of cylindrical specimens - method of test*. Rio de Janeiro.
- ABNT Brazilian association of technical standards. (2010). *NBR 12142: Concrete - Determination of tension strength in flexure of prismatic specimens*. Rio de Janeiro.
- ABNT Brazilian association of technical standards. (2011). *NBR 7222: Concrete and mortar - Determination of the tension strength by diametrical compression of cylindrical test specimens*. Rio de Janeiro.
- ABNT Brazilian association of technical standards. (2013). *NBR 8802: Hardened concrete — Determination of ultrasonic wave transmission velocity*. Rio de Janeiro.
- ABNT Brazilian association of technical standards. (2015a). *NBR 5738: Procedure for molding and curing concrete test specimens*. Rio de Janeiro.
- ABNT Brazilian association of technical standards. (2015b). *NBR 8953: Concrete for structural use - Density, strength and consistence classification*. Rio de Janeiro.
- ABNT Brazilian association of technical standards. (2018). *NBR 16697: Portland cement - Requirements*. Rio de Janeiro.
- ACI Committee on Fireproofing (2019). Report of committee on fireproofing (1919).

- Akca, A. H., Zihnioglu, N.Ö. (2013). *High performance concrete under elevated temperatures*. Constr. Build. Mater. 44, 317–328. <https://doi.org/10.1016/j.conbuildmat.2013.03.005>
- Alhozaimy, A. M., Soroushian, P., Mirza, F. (1996). *Mechanical properties of polypropylene fiber reinforced concrete and the effects of pozzolanic materials*. Cem. Concr. Compos. 18, 85–92. [https://doi.org/10.1016/0958-9465\(95\)00003-8](https://doi.org/10.1016/0958-9465(95)00003-8)
- ASTM International. (2018). *ASTM E119-18a, Standard Test Methods for Fire Tests of Building Construction and Materials*. <https://doi.org/10.1520/E0119-18A>
- Bangi, M. R., Horiguchi, T. (2012). *Effect of fibre type and geometry on maximum pore pressures in fibre-reinforced high strength concrete at elevated temperatures*. Cem. Concr. Res. 42, 459–466. <https://doi.org/10.1016/j.cemconres.2011.11.014>
- Behnood, A., Ghandehari, M. (2009). *Comparison of compressive and splitting tensile strength of high-strength concrete with and without polypropylene fibers heated to high temperatures*. Fire Saf. J. 44, 1015–1022. <https://doi.org/10.1016/j.firesaf.2009.07.001>
- Bei, S., Zhixiang, L. (2016). *Investigation on spalling resistance of ultra-high-strength concrete under rapid heating and rapid cooling*. Case Stud. Constr. Mater. 4, 146–153. <https://doi.org/10.1016/j.cscm.2016.04.001>
- Castellote, M., Alonso, C., Andrade, C., Turrillas, X., Campo, J. (2004). *Composition and microstructural changes of cement pastes upon heating, as studied by neutron diffraction*. Cem. Concr. Res. 34, 1633–1644. [https://doi.org/10.1016/S0008-8846\(03\)00229-1](https://doi.org/10.1016/S0008-8846(03)00229-1)
- Choumanidis, D., Badogiannis, E., Nomikos, P., Sofianos. (2016). *The effect of different fibres on the flexural behaviour of concrete exposed to normal and elevated temperatures*. Constr. Build. Mater. 129, 266–277. <https://doi.org/10.1016/j.conbuildmat.2016.10.089>
- Cree, D., Green, M., Noumowé, A. (2013). *Residual strength of concrete containing recycled materials after exposure to fire: A review*, Constr. Build. Mater. 45, 208–223. <https://doi.org/10.1016/j.conbuildmat.2013.04.005>
- Çavdar, A. (2013). *The effects of high temperature on mechanical properties of cementitious composites reinforced with polymeric fibers*, Compos. Part B Eng. 45 (2013) 78–88. <https://doi.org/10.1016/j.compositesb.2012.09.033>
- Dias, D., Calmon, J., Degen, M. (2017). *Concreto reforçado com fibras poliméricas submetido a temperaturas elevadas*. In: Congresso Brasileiro do Concreto-2017, 59, 2017, Bento Gonçalves, RS. Anais... São Paulo: IBRACON.
- Drzymała, T., Jackiewicz-rek, W., Tomaszewski, M., Kuś, A. (2017). *Effects of High Temperature on the Properties of High Performance Concrete (HPC)*, Proc. Eng. 172, 256–263. <https://doi.org/10.1016/j.proeng.2017.02.108>
- European Standard (2004). *EN 1992-1-2: Eurocode 2 – Design of Concrete Structures. Part 1.2: General Rules – Structural Fire Design*, p. 97.
- Espírito Santo. Corpo De Bombeiros Militar Do Estado. (2009). *Norma Técnica 04 – Carga de incêndio*. Vitória: CBMES.
- Ezziane, M., Kadri, T., Molez, L., Jaubertie, R., Belhacen, A. (2015). *High temperature behaviour of polypropylene fibres reinforced mortars*. Fire Saf. J. 71, 324–331. <https://doi.org/10.1016/j.firesaf.2014.11.022>
- Gernay, T., Franssen, J.M. (2015). *A performance indicator for structures under natural fire*. Eng. Struct. 100, 94–103. <https://doi.org/10.1016/j.engstruct.2015.06.005>
- Haddad, R. H., Al-Saleh, R. J., Al-Akhras, N. M. (2008). *Effect of elevated temperature on bond between steel reinforcement and fiber reinforced concrete*. Fire Saf. J. 43, 334–343. <https://doi.org/10.1016/j.firesaf.2007.11.002>
- Hartin, E. (2008). *Extreme Fire Behavior: Understanding the Hazards*. 2008. Access in: <<http://cfbt-us.com/pdfs/ExtremeFireBehavior.pdf>>. Acess 17 fev. 2018.
- ISO 834-1:1999 (2015). *Fire-Resistance Tests – Elements of Building Construction – Part 1: General Requirements*.
- Khalaf, J., Huang, Z. (2016). *Analysis of the bond behaviour between prestressed strands and concrete in fire*. Constr. Build. Mater. 128, 12–23. <https://doi.org/10.1016/j.conbuildmat.2016.10.016>

- Khoury, G. A. (1992). *Compressive strength of concrete at high temperatures : a reassessment*. Magazine of Concrete Research 44 (161), 291–309.
- Kim, Y., Lee, T., Kim, G. (2013). *An experimental study on the residual mechanical properties of fiber reinforced concrete with high temperature and load*. Mater. Struct. 46, 607–620. <https://doi.org/10.1617/s11527-012-9918-y>
- Kurtz, S., Balaguru, P. (2000). *Postcrack creep of polymeric fiber-reinforced concrete in flexure*. Cem. Concr. Res. 30, 183–190. [https://doi.org/10.1016/S0008-8846\(99\)00228-8](https://doi.org/10.1016/S0008-8846(99)00228-8)
- Lee, G., Han, D., Han, M.C., Han, C. G., Son, H. J. (2012). *Combining polypropylene and nylon fibers to optimize fiber addition for spalling protection of high-strength concrete*. Constr. Build. Mater. 34, 313-320. <https://doi.org/10.1016/j.conbuildmat.2012.02.015>
- Lennon, T., Rupasinghe, R., Canisius, G., Waleed, N., Matthews, S. (2007). *Concrete structures in fire – Performance, design and analysis*. BRE 1-81.
- Lourenço, L. A. P., Barros, J. A. O., Alves, J. G. A. (2011). *Fiber reinforced concrete of enhanced fire resistance for tunnel segments*.
- Ma, Q., Guo R., Zhao, Z., Lin, Z., He, K. (2015). *Mechanical properties of concrete at high temperature-A review*. Constr. Build. Mater. 93, 371–383. <https://doi.org/10.1016/j.conbuildmat.2015.05.131>
- Mehta, P. K., Monteiro, P. J. M. (2008). *Concrete: Microstructure, Properties, and Materials*. 3ed. <https://dx.doi.org/10.1036/0071462899>
- Noumowe, A. (2005). *Mechanical properties and microstructure of high strength concrete containing polypropylene fibres exposed to temperatures up to 200 °c*. Cem. Concr. Res. 35, 2192–2198. <https://doi.org/10.1016/j.cemconres.2005.03.007>
- Pai, S., Chandra, K. L. (2013). *Analysis of polyester fibre reinforced concrete subjected to elevated temperatures*. International Journal of Civil, Structural, Environmental and Infrastructure Engineering Research and Development (IJCSEIERD) 3 (2013) 1–10.
- Park, S.-J., Yim, H. J. (2016). *Evaluation of residual mechanical properties of concrete after exposure to high temperatures using impact resonance method*. Constr. Build. Mater. 129, 89–97. <https://doi.org/10.1016/j.conbuildmat.2016.10.116>
- Petrucci, E. G. R. (1981). *Concreto de cimento Portland*. 8 ed. Rio de Janeiro: Editora Globo.
- Pliya, P., Beaucour, A. L., Noumowé. (2011). *Contribution of cocktail of polypropylene and steel fibres in improving the behaviour of high strength concrete subjected to high temperature*. Constr. Build. Mater. 25, 1926–1934. <https://doi.org/10.1016/j.conbuildmat.2010.11.064>
- Poon, C. S., Shui, Z. H., Lam, L. (2004). *Compressive behavior of fiber reinforced high-performance concrete subjected to elevated temperatures*. Cem. Concr. Res. 34, 2215–2222. <https://doi.org/10.1016/j.cemconres.2004.02.011>
- São Paulo. Corpo De Bombeiros Militar Do Estado. (2011). *Instrução Técnica 14 - Carga de incêndio nas edificações e áreas de risco*. São Paulo.
- Sekhar, M. P., Raju, K. (2017). *A Study on Effect of Mechanical Properties of Recron 3S Fibre Concrete on Different Grades Exposed to Elevated Temperatures*. International Journal for Innovative Research in Science & Technology 4, 41–46.
- Shihada, S. (2011). *Effect of polypropylene fibers on concrete fire resistance*. J. Civ. Eng. Manag. 17, 259–264. <https://doi.org/10.3846/13923730.2011.574454>
- Song, P. S., Hwang, S., Sheu, B. C. (2005). *Strength properties of nylon- and polypropylene-fiber-reinforced concretes*. Cem. Concr. Res. 35, 1546–1550. <https://doi.org/10.1016/j.cemconres.2004.06.033>
- Srikar, G., Anand, G., Prakash, S. Suriya. (2016). *A Study on Residual Compression Behavior of Structural Fiber Reinforced Concrete Exposed to Moderate Temperature Using Digital Image Correlation*. Int. J. Concr. Struct. Mater. 10, 75–85. <https://doi.org/10.1007/s40069-016-0127-x>
- Suresh, N., Bindiganavile, V., Prabhu, M. (2014). *Compressive Behaviour of Polyester Fiber Reinforced Concrete Subjected To Sustained Elevated Temperature*. International Journal of Emerging Technology and Advanced Engineering 4, 220–224.

- Xiao, J., Falkner, H. (2006). *On residual strength of high-performance concrete with and without polypropylene fibres at elevated temperatures*. Fire Saf. J. 41, 115–122. <https://doi.org/10.1016/j.firesaf.2005.11.004>
- Yermak, N., Pliya, P., Beaucour, A. L., Simon, A., Noumowé, A. (2017). *Influence of steel and/or polypropylene fibres on the behaviour of concrete at high temperature: Spalling, transfer and mechanical properties*. Constr. Build. Mater. 132, 240–250. <https://doi.org/10.1016/j.conbuildmat.2016.11.120>

Fire resistance of ceramic-masonry sealing blocks using intumescent paint protection

C. A. S. Sales¹ , C. F. G. Nascimento¹ , T. M. Silva² , L. M. Barreto² , P. C. Lordsleem Jr.² , W. A. Soares² , P. Castro-Borges³ , E. C. B. Monteiro^{1,2*} 

*Contact author: eliana@poli.br

DOI: <http://dx.doi.org/10.21041/ra.v10i1.417>

Reception: 01/07/2019 | Acceptance: 27/11/2019 | Publication: 30/12/2019

ABSTRACT

The efficiency of surface protection of sealing masonry structures with intumescent ink was evaluated in relation to mechanical resistance and thermal insulation. Sixty ceramic sealing masonry blocks were used. The temperature of the face directly exposed to the flame was on average 25% lower for the block with passive protection. The compressive strength of the blocks with passive protection was about 70% higher than the unprotected blocks, after 60 minutes of direct exposure to the flame. More than 70% of the blocks without passive protection and that were exposed to flame had compressive resistance of 1.35 MPa, while 100% of the blocks with protection had values 2.38 MPa, even after 60 minutes of exposure.

Keywords: masonry; fire; passive protection; intumescent paints; resistance.

Cite as: Sales, C. A. S., Nascimento, C. F. G., Silva, T. M., Barreto, L. M., Lordsleem Jr., A. C., Soares, W. A. Castro-Borges, P., Monteiro, E. C. B. (2020), “*Fire resistance of ceramic-masonry sealing blocks using intumescent paint protection*”, Revista ALCONPAT, 10 (1), pp. 53 - 68, DOI: <http://dx.doi.org/10.21041/ra.v10i1.417>

¹ Departamento de Engenharia Civil, Universidade Católica de Pernambuco, Recife-PE, Brasil.

² Departamento de Engenharia Civil, Universidade de Pernambuco, Recife-PE, Brasil.

³ Centro de Investigación y de Estudios Avanzados (CINVESTAV) Unidad Mérida, México.

Legal Information

Revista ALCONPAT is a quarterly publication by the Asociación Latinoamericana de Control de Calidad, Patología y Recuperación de la Construcción, Internacional, A.C., Km. 6 antigua carretera a Progreso, Mérida, Yucatán, 97310, Tel.5219997385893, alconpat.int@gmail.com, Website: www.alconpat.org

Responsible editor: Pedro Castro Borges, Ph.D. Reservation of rights for exclusive use No.04-2013-011717330300-203, and ISSN 2007-6835, both granted by the Instituto Nacional de Derecho de Autor. Responsible for the last update of this issue, Informatics Unit ALCONPAT, Elizabeth Sabido Maldonado, Km. 6, antigua carretera a Progreso, Mérida, Yucatán, C.P. 97310.

The views of the authors do not necessarily reflect the position of the editor.

The total or partial reproduction of the contents and images of the publication is strictly prohibited without the previous authorization of ALCONPAT Internacional A.C.

Any dispute, including the replies of the authors, will be published in the third issue of 2020 provided that the information is received before the closing of the second issue of 2020.

Resistência ao fogo de blocos de alvenaria cerâmica de vedação utilizando proteção de tinta intumescente

RESUMO

Avaliou-se a eficiência da proteção superficial de estruturas de alvenaria de vedação com tinta intumescente em relação à resistência mecânica e ao isolamento térmico. Foram utilizados 60 blocos cerâmicos de alvenaria de vedação. A temperatura da face diretamente exposta à chama foi em média 25% inferior para o bloco com a proteção passiva. A resistência à compressão dos blocos com proteção passiva foi cerca de 70% superior aos blocos sem proteção, após 60 minutos de exposição direta a chama. Mais de 70% dos blocos sem proteção passiva e que foram expostos a chama tiveram resistência a compressão de 1,35 MPa, enquanto 100% dos blocos com proteção tiveram valores de 2,38 MPa, mesmo após 60 minutos de exposição.

Palavras-chave: alvenaria; incêndio; proteção passiva; tintas intumescentes; resistência.

Resistencia al fuego de bloques de albañilería cerámica de sellado utilizando protección de tinta intumescente

RESUMEN

Se evaluó la eficiencia de la protección superficial de las estructuras de mampostería de sellado con tinta intumescente en relación con la resistencia mecánica y el aislamiento térmico. Se utilizaron sesenta bloques de mampostería de sellado cerámico. La temperatura de la cara directamente expuesta a la llama fue en promedio un 25% menor para el bloque con protección pasiva. La fuerza de compresión de los bloques con protección pasiva fue aproximadamente 70% mayor que la de los bloques sin protección, después de 60 minutos de exposición directa a la llama. Más del 70% de los bloques sin protección pasiva y expuestos a llamas tenían una resistencia a la compresión de 1,35 MPa, mientras que el 100% de los bloques con protección tenían valores de 2,38 MPa, incluso después de 60 minutos de exposición.

Palabras clave: albañilería; incendio; protección pasiva; pinturas intumescentes; resistencia.

1. INTRODUCTION

The fires are present in the history of several cities in the world. In some of them, they have come to carry out significant changes in the urban design and the constructive characteristics of its buildings in urban scale, that is, reaching hundreds or thousands of structures, putting at risk the life of thousands of people (FREITAS, 2014).

In Brazil, knowledge about fire safety in buildings became a matter of importance only after two major national tragedies: the fires in the Andraus and Joelma buildings both in the city of São Paulo: the first in 1972 with sixteen deaths and the second in 1974 with one hundred and eighty-nine people dead.

National fire safety regulations and standards state that walls and sealing elements must have a certain fire resistance time, which varies with the type of building and the total height. The material performance suggestions offered by most of these codes are usually based on empirical knowledge; however, such materials indicate a much higher fire resistance when tested in the laboratory. As the ceramic blocks have good fire performance, it is expected that a wall constructed with such blocks also has good fire resistance.

According to NBR 14432 (2000), fire resistance can be defined as the property of a building element to resist the action of fire for a certain period of time, maintaining its structural safety, water tightness, and thermal insulation.

The fire resistance of the walls is very important for fire safety, since high-rise buildings fires were found to be initiated by smoke, heat, and flames, which made it difficult to abandon the building and allowed the fire to spread rapidly (ONO, 2007).

Andreini and Sassu (2011) argue that a masonry wall does not produce smoke or toxic gases, but using ceramic blocks becomes a good alternative to minimize the fire propagation, providing both thermal insulation and stability to the building. However, few studies have been found on the fire resistance of masonry walls with ceramic blocks, which involved only 14 cm thick walls (THOMAZ and HELENE, 2000).

Nguyen and Meftah (2012) reinforce that the studies to determine the mechanical characteristics of these materials are carried out in laboratories, with empirical results resulting in more expensive structures (NADJAI *et al.*, 2006).

The passive protection against fire is constituted by means of protection incorporated in the building and that does not require any type of activation for its operation in a fire. Some examples of passive protection are the control of finishing and coating materials, protection of leakage routes, compartmentalization and risk isolation (SEITO *et al.*, 2008).

Thus, measures must be implemented in the fire protection and some of them are the intumescent paints that were developed long ago - the first patent is from 1938 and the principles that govern its action are already very well known. Intumescent coatings are widely used in the protection of steel structures for periods of thirty and sixty minutes, and their use for ninety minutes has increased in some countries.

Due to the lack of technical information offered by most manufacturers of intumescent paints, in relation to the compressive strength of ceramic blocks after exposure to fire, in accordance with regulation or often generalized information and also because of few scientific researches found in the literature, the purpose of this paper was to study fire resistance, with the application of passive protection of intumescent paint, in the sealing ceramic masonry blocks, after direct exposure to flame. In this way, the efficiency of the passive protection with respect to the mechanical resistance and the thermal insulation can be verified.

1.1 Factors influencing fire performance of masonry walls

The fire performance of a masonry wall depends on several factors. Firstly, factors related to the type of block used in the masonry are highlighted, including the characteristics of the material used and the geometry of the blocks (THOMAZ; HELENE, 2000).

In addition to the block, the constructive characteristics such as the type of laying joints, coatings, and filling of the castings also influence fire resistance (THOMAZ; HELENE, 2000); (MEYER, 2006). Finally, Meyer (2006) presents some factors related to the structural stability of the wall, such as the slenderness index, the applied load, and the presence of eccentricities.

1.2 Passive protection

Obtaining the fire safety conditions requires adequate means of combat, aiming at not allowing the structural collapse of the building, facilitating the escape of the users and ensuring the approach and entry into the building for combat actions (COELHO, 2010).

Passive protection is the set of protection measures against fire situations incorporated in the building construction. It should, therefore, be foreseen by the architect. Building fire performance is independent of any external action (SEITO, *et al.*, 2008). The main means of passive protection are: emergency exits (location, quantity, and design), reaction to fire of finishing and coating materials, fire resistance of the building elements, smoke control, and separation of buildings.

1.3 Intumescent paints

Intumescent paints have long been developed - the first patent is from 1938 - and the principles governing their performance are already well known. Since its inception, and in particular over the

last twenty years, its use has grown. The term intumescent derives from the Latin "tumescere", which means to initiate, to expand.

Intumescence occurs by the reaction of active components under the influence of heat, producing a significant expansion. These active or intumescent components often expand their initial thickness applied (typically 60x greater) when heated, producing a carbonaceous mass which protects any substrate on which the coating has been applied.

Intumescent coatings have the following ingredients: a catalyst which decomposes under the effect of heat, producing a mineral acid (such as phosphoric acid; ammonium polyphosphate is the catalyst commonly used); a carbonizing agent, such as starch, which combines with the mineral acid to form a carbonaceous mass; a binder, or resin, which softens at a predetermined temperature; a foam agent that decomposes together with the binder melt, releasing large volumes of nonflammable gases. These gases include carbon dioxide, ammonia, and water vapor.

The production of these gases promotes the swelling of the carbonaceous mass, generating carbonaceous foam, which expands about 60x (or more) the original volume of the paint, promoting the thermal protection. The use of these products corresponds, in certain countries, to more than 40% of the market for thermal protection in multi-storey buildings.

1.4 Structural performance in fire situation

In a fire situation, there is a need to minimize the risk of building structural collapse. The materials used in the structure and subdivisions must be in accordance with the TRRF - Required Time of Fire Resistance, according to NBR 14432 (2000). Specific standards should also be met for the type of structure in question. For other types of structure, NBR 15575 (2013) establishes that the corresponding Eurocode must be met in its last edition.

2. MATERIALS AND METHOD

2.1 Materials and equipment

The materials used were: sixty (60) sealing masonry blocks with 8 horizontal holes and dimensions (9 cm x 19 cm x 19 cm), purchased in the Recife trade, state of Pernambuco; Butane Gas Torch (Flame Temperature 1200 °C); BENETECH Infrared Thermometer Model GM300 (Temperature: -50 °C to 380 °C); Salvterm 1200 K digital thermometer (Temperature: -50 °C to 1350 °C) with surface sensor (6.5 mm diameter stem by 260 mm in length); CKC-333® Intumescent paint; Foam roller for intumescent paint application; Personal Protective Equipment: mask, protective glove, and goggles; Laboratory Protection: Portable Dry Chemical Powder Fire Extinguisher (4 kg).

2.2 Characterization of test specimens

The 60 specimens were distributed in 4 groups (types) of 15 blocks, the first two groups being used as reference base for the analysis of compressive strength (saturated and unsaturated condition). Figure 1 presents the organization chart with the summary of the assays, as well as the detail of the experimental execution by type.

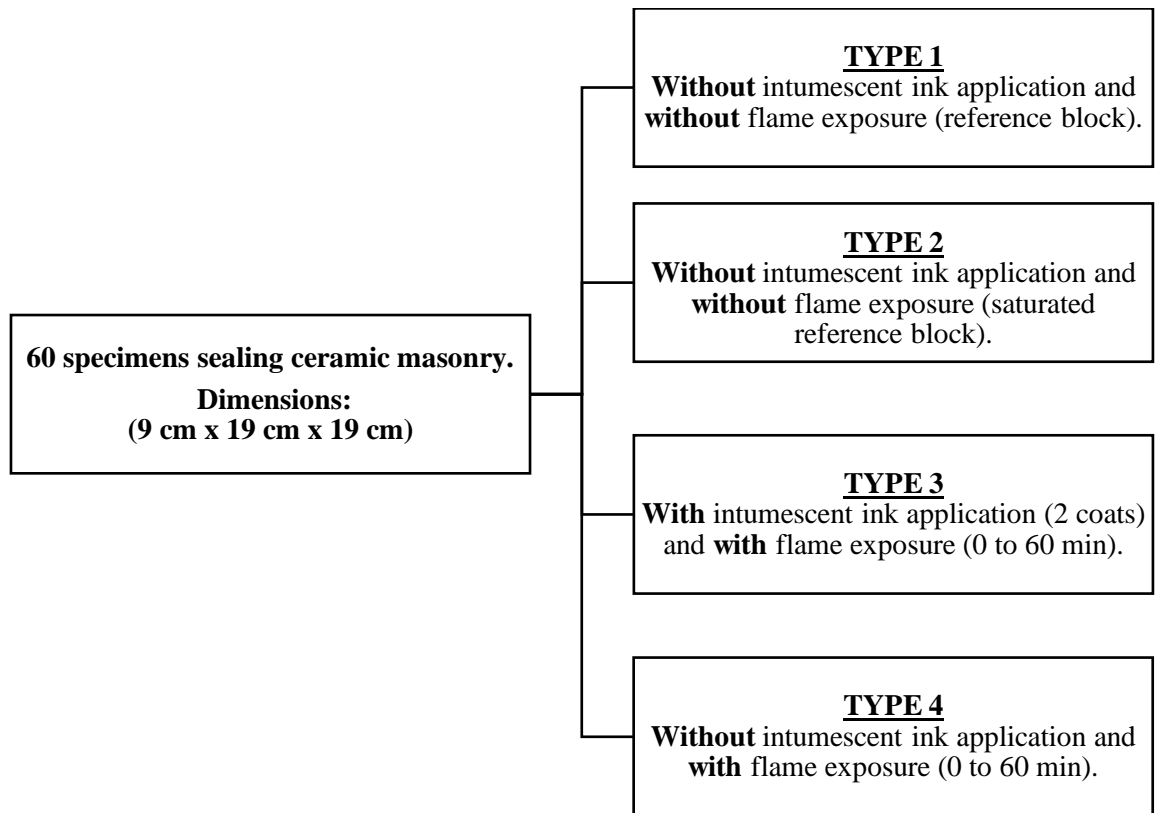


Figure 1. Experimental planning.

It is important to note that the experiment is a simulation for comparison and analysis of the behavior of sealing blocks with and without passive protection paint, that despite of having the NBR 10636/89 as a parameter, the methodology applied in the experiment conducted in this research is not associated with the standard cited and with the ISO 834, so in this way, it is not possible to attest the time of resistance to fire (TRF) of samples in accordance with the standards. It is also interesting to note that the time of exposure to fire defined for groups 3 and 4 was 60 minutes due to the limitations of fuel cost. That was the time indicated by the manufacturer as a protection time for 2 coats of paint. It is also twice the minimum time required for structural walls up to five pavements, according to the performance standard.

It is important to mention that there are significant differences between assays for the sealing system, prisms, and individual blocks, as well as that the coatings also influence the tests.

The analysis will be performed on the sealing ceramic block, without any type of coating other than the intumescent paint protection (Type 3). In addition to simulating conditions in many low-income housing units, it also simulates the most extreme condition of the material in the event of a fire.

The application of the flame as well as the temperature measurements were carried out in the geometric center of all the faces, in order to find the highest values to which they were exposed, with the fuel can at a distance of 20 centimeters from the exposed blocks. The average room temperature during the tests was 33°C.

2.2.1 Type 1 Block (reference block – unsaturated) and Type 2 (reference block – saturated)

The 15 blocks characterized as Type 1 are those used as reference for the compressive strength effect. For these blocks, no passive protections or exposure to any type of flame were applied, being kept at room temperature.

The 15 blocks characterized as Type 2, unlike the previous model, were tested after a 24h water immersion. Reception, preparation, conditioning of the specimens, and procedures are in accordance with ABNT NBR 15270-1, ABNT NBR 15270-2, and ABNT NBR 15270-3 standards showed in Figure 2.

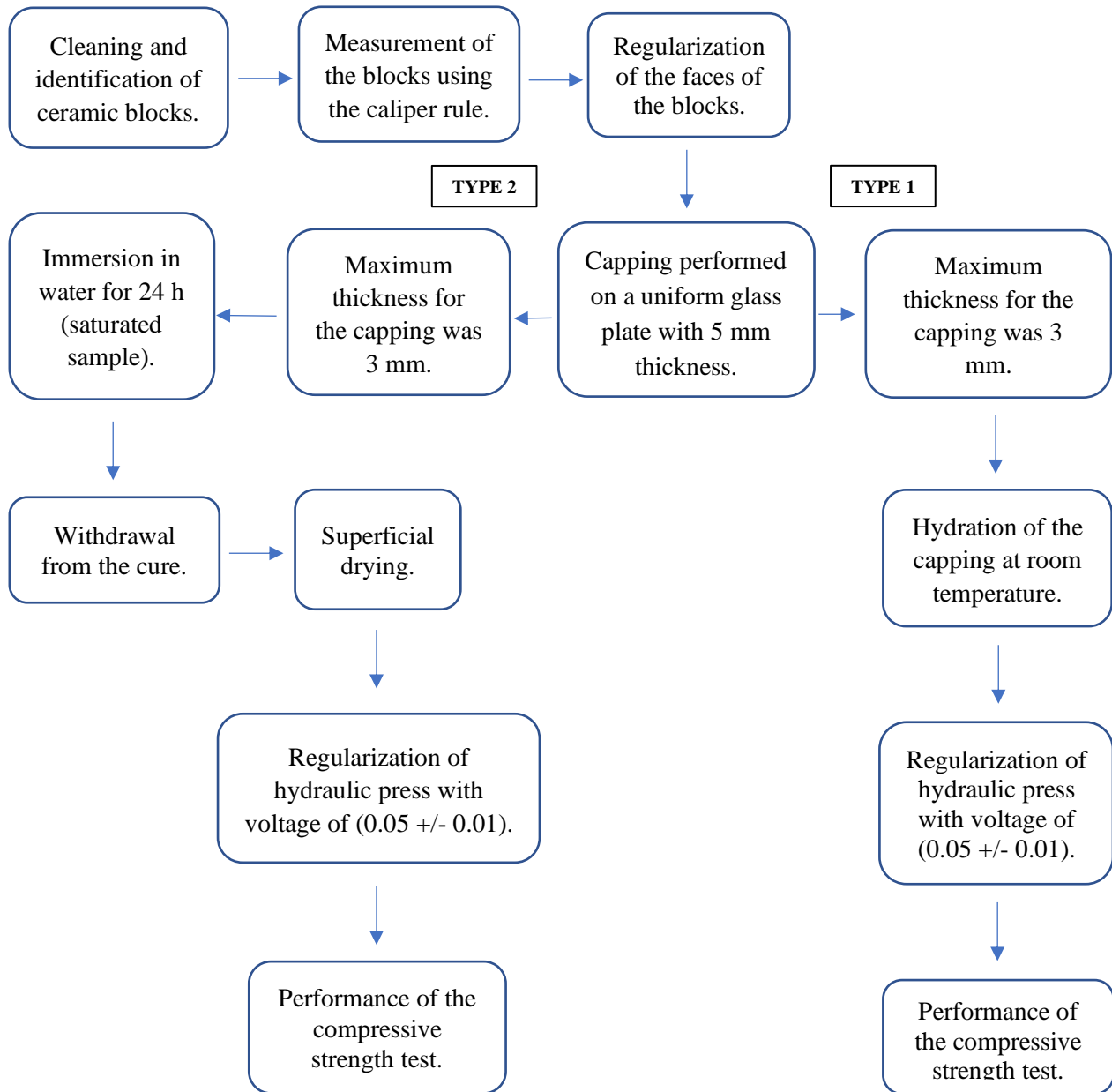


Figure 2. Receipt, preparation and packaging of blocks.

2.2.2 Type 3 Block (with intumescent paint application and direct flame exposure) and Type 4 Block (without intumescent paint application and direct exposure to flame)

In the 15 blocks called Type 3, the initial characterization and preparation (capping) procedures, identical to those already described for Type 1 (Figure 3), were performed; however, in this type of block, 2 (two) coats of intumescent paint were applied (Figure 4), as described below, in addition to directly exposing each block to the flame for 60 minutes showed in Figure 5.



Figure 3. Capping of ceramic blocks.



Figure 4. Application of intumescent paint.



Figure 5. Direct exposure to type 3 block flame (with intumescent paint).

Then, the temperature of the face directly affected by the flame (1), the temperature of the face immediately opposite (2), through the first septum of the block, and the temperature of the face of the block without application of intumescent paint (3) were measured.

In addition to the temperature survey to verify the thermal insulation efficiency, after the exposure to the flame, the blocks were taken to the hydraulic press for the purpose of checking the compressive strength and the maximum load supported.

The paint chosen for the test was the CKC-333 intumescent paint, which was selected on the basis of the range of international certifications. Also, it was the only brand, among those available in the national market, willing to support this research, forwarding sample to test.

The intumescent paint CKC-333 is an acrylic, non-toxic, odorless, anti-mold and anti-fungal water-based coating. At approximately 200 °C, it initiates a volumetric expansion process, preventing the temperature rise in concrete, masonry, and drywall elements.

On the other hand, for the 15 (fifteen) blocks characterized as Type 4, initial characterization and preparation (capping) procedures like those already described for Type 1 were performed; however, no passive protection was applied by intumescent paint, with 60 minutes of direct exposure to the flame.

The temperatures were then measured at the same locations as the Type 3 blocks. After temperature rise, the blocks were brought to a hydraulic press for the purpose of checking the compressive strength and maximum supported load.

Type 3 and Type 4 blocks were subjected to one hour of direct flame incidence and, before being brought to the hydraulic press, to verify the compressive strength and maximum load supported (Figure 6), the temperatures were calibrated on the faces directly affected by the flame; on the face immediately opposite, through the first septum; and the farthest face from the flame application.

The experimental procedure for Type 4 blocks was identical to that performed with Type 3 blocks; however, these specimens did not receive passive protection by intumescent paint showed in Figure 7.



Figure 6. Compressive strength



Figure 7. Blocks without passive protection.

3. RESULTS AND DISCUSSION

To determine the resistance and the standard deviation of Type 1 blocks, Equations 1 and 2 were used, respectively.

$$\bar{R}_1 = \frac{1}{n} \sum_{i=1}^{15} R_i \rightarrow \bar{R}_1 = 2,484 MPa ; \quad (1)$$

$$s = \sqrt{\frac{\sum_{i=1}^n (R_i - \bar{R})^2}{n-1}} \rightarrow s \cong 0,70 \quad (2)$$

To determine the maximum and minimum resistances considering the previously calculated values for the mean and standard deviation, Equation 3 was used.

For $k = 3$

$$\bar{R}_1 \pm 3s \rightarrow 2,484 \pm 3.(0,70) \Rightarrow R_{1\min} = 0,40 MPa \text{ e } R_{1\max} = 4,57 MPa \quad (3)$$

Where k is the time coefficient of variation in seconds.

To determine the standard deviation and the maximum supported load of Type 1 blocks, Equations 3 and 4 were used, respectively.

$$s = \sqrt{\frac{\sum_{i=1}^n (c_i - \bar{c})^2}{n-1}} \rightarrow s \cong 10,23 \quad (4)$$

For $k = 3$

$$\bar{C}_{1\max} \pm 3s \rightarrow 39,997 \pm 3.(10,23) \Rightarrow \bar{C}_{1\max\min} = 9,30 KN \text{ e } \bar{C}_{1\max\max} = 70,69 KN \quad (5)$$

To determine the strength and standard deviation of Type 2 blocks, Equation 1 and 2 respectively were used.

$$\bar{R}_2 = \frac{1}{n} \sum_{i=1}^{15} R_i \rightarrow \bar{R}_2 = 2,036MPa;$$

$$s = \sqrt{\frac{\sum_{i=1}^n (R_i - \bar{R})^2}{n-1}} \rightarrow s \cong 0,46$$

Considering the previously calculated values for mean and standard deviation, according to Equation 3:

$$\bar{R}_2 \pm 3s \rightarrow 2,036 \pm 3.(0,46) \Rightarrow R_{2min} = 0,66MPa \text{ e } R_{2máx} = 3,41MPa$$

To determine the maximum load average, the standard deviation, and the maximum and minimum loads supported by Type 2 blocks, Equations 6, 7, and 8 were used, respectively.

$$\bar{C}_{2max} = \frac{1}{n} \sum_{i=1}^{15} C_i \rightarrow \bar{C}_{2max} = 33,505KN; \tag{6}$$

$$s = \sqrt{\frac{\sum_{i=1}^n (c_i - \bar{c})^2}{n-1}} \rightarrow s \cong 10,23 \tag{7}$$

$$\bar{C}_{2max} \pm 3s \rightarrow 33,505 \pm 3.(7,47) \Rightarrow \bar{C}_{2maxmin} = 11,20KN \text{ e } \bar{C}_{2maxmáx} = 55,81KN \tag{8}$$

Taking into consideration the three standard deviations, it is observed that all values for the compressive strength and supported maximum load of Type 1 and 2 blocks are to be considered as representative, calculated according to Equations 9 and 10, respectively. Comparing the average values of the compressive strengths and the maximum supported loads of types 1 and 2:

$$\frac{\bar{R}_1 - \bar{R}_2}{\bar{R}_1} = \frac{2,484 - 2,036}{2,484} = 0,18 \text{ ou } 18\% \tag{9}$$

$$\frac{\bar{C}_1 - \bar{C}_2}{\bar{C}_1} = \frac{39,997 - 33,505}{39,997} = 0,16 \text{ ou } 16\% \tag{10}$$

The analysis of variance (ANOVA) was performed for a single factor, which for Types 1 and 2 are distinguished by the saturated condition or not, through analysis of MS Excel 2016 software. The data of compressive strength resulted in Table 1.

Table 1. ANOVA (Compressive strength - Types 1 and 2).

Variation Source	SQ	gl	MQ	F	P-value	F critical
Among groups	1.506	1	1.50662	4.3395	0.046486	4.19597
Within the groups	9.721	28	0.34719			

It can be verified that since the P-value found (0.046) is lower than the stipulated significance level of 5% (0.05) or, in a different analysis, the value of F (4.33) was found to be greater than the $F_{critical}$ (4.19), the null hypothesis (H_0) was rejected, in which the means would be equal.

In this way, it can be affirmed that the saturated and unsaturated conditions influence the results obtained for the compressive strength. By performing the same representativity check of the collected data for the type 3 and type 4 blocks, it was verified that, for three standard deviations, all the data are significant, as shown in Tables 2 and 3.

Table 2. Mean values and standard deviations for Type 3 blocks.

Data	TYPE 3 (With Flame Exposure and With Protection)						
	Temperature (60' exposure)					Cmax(KN)	R(MPa)
	Td(°C)	Ti1(°C)	Ti2(°C)	ΔT1(°C)	ΔT2(°C)		
Mean (X)	938.067	187.000	40.920	751.067	897.147	37.993	2.380
Standard Deviation (s)	54.61	10.62	2.00	57.89	54.21	7.19	0.42
X+3s	1101.89	218.85	46.91	924.75	1059.79	59.55	3.64
X-3s	774.25	155.15	34.93	577.39	734.50	16.44	1.12

Table 3. Mean values and standard deviations for Type 4 blocks.

Data	TYPE 4 (With Flame Exposure and Without Protection)						
	Temperature (60' exposure)					Cmax(KN)	R(MPa)
	Td(°C)	Ti1(°C)	Ti2(°C)	ΔT1(°C)	ΔT2(°C)		
Mean (X)	1166.33	509.73	92.82	656.60	1073.51	21.86	1.34
Standard Deviation (s)	34.16	30.46	5.39	44.78	35.09	5.81	0.35
X+3s	1268.81	601.12	108.98	790.95	1178.78	39.28	2.40
X-3s	1063.86	418.35	76.66	522.25	968.24	4.45	0.29

By initially evaluating the temperature of the face directly affected by flame, it can be seen that temperatures vary approximately 25% in average terms, according to Equation 11.

$$\frac{\bar{T}_{ds} - \bar{T}_{dc}}{\bar{T}_{dc}} = \frac{1166,33 - 938,07}{938,07} = 0,2433 \text{ ou } 24,33\% \quad (11)$$

When analyzing the faces immediately opposite to the flame application, the temperature variation between the protected and unprotected blocks has average values 172% higher when the blocks do not have passive protection, as shown in Equation 12.

$$\frac{\bar{T}_{fos} - \bar{T}_{foe}}{\bar{T}_{foe}} = \frac{509,73 - 187,00}{187,00} = 1,7258 \text{ ou } 172,58\% \quad (12)$$

Figures 8 and 9 show the results for the behavior of the faces of the blocks when exposed and not exposed to the flame and how the protective paint influences this process.

TEMPERATURE OF THE OPPOSITE FACE TO THE FLAME

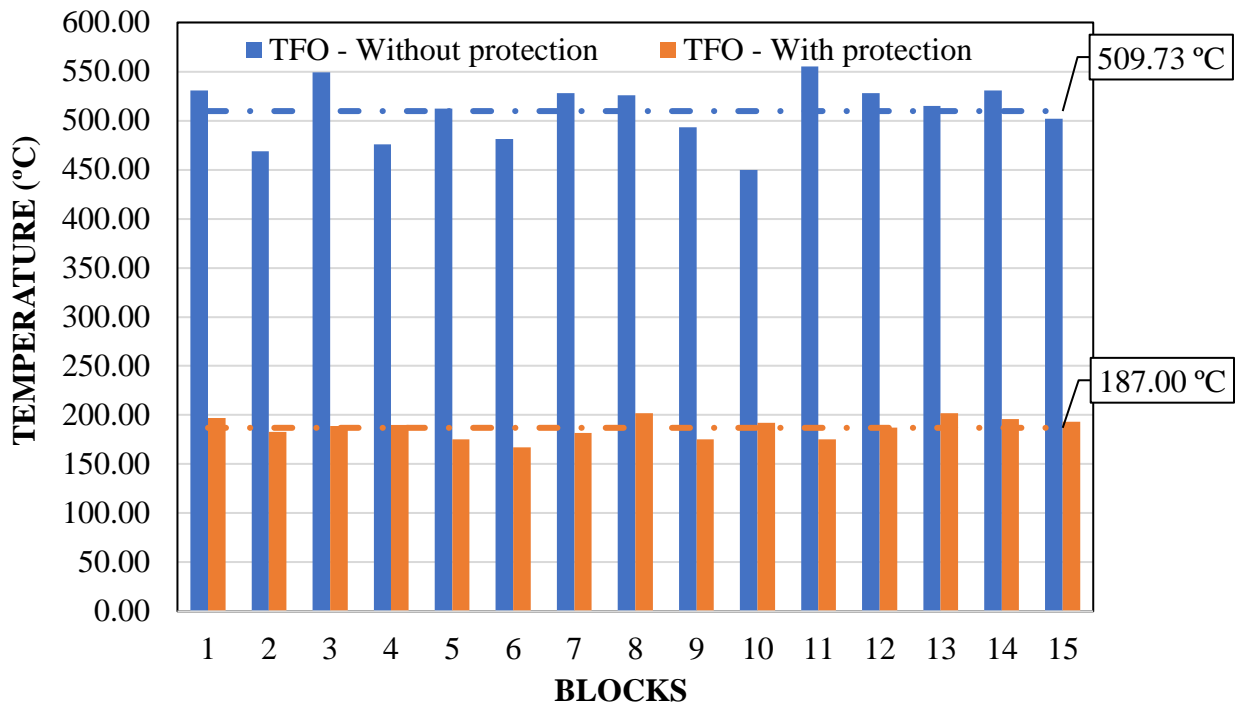


Figure 8. Comparison of the temperatures of the immediately opposing faces for the blocks with and without passive protection, types 3 and 4 respectively.

TEMPERATURE OF THE OPPOSITE FACE

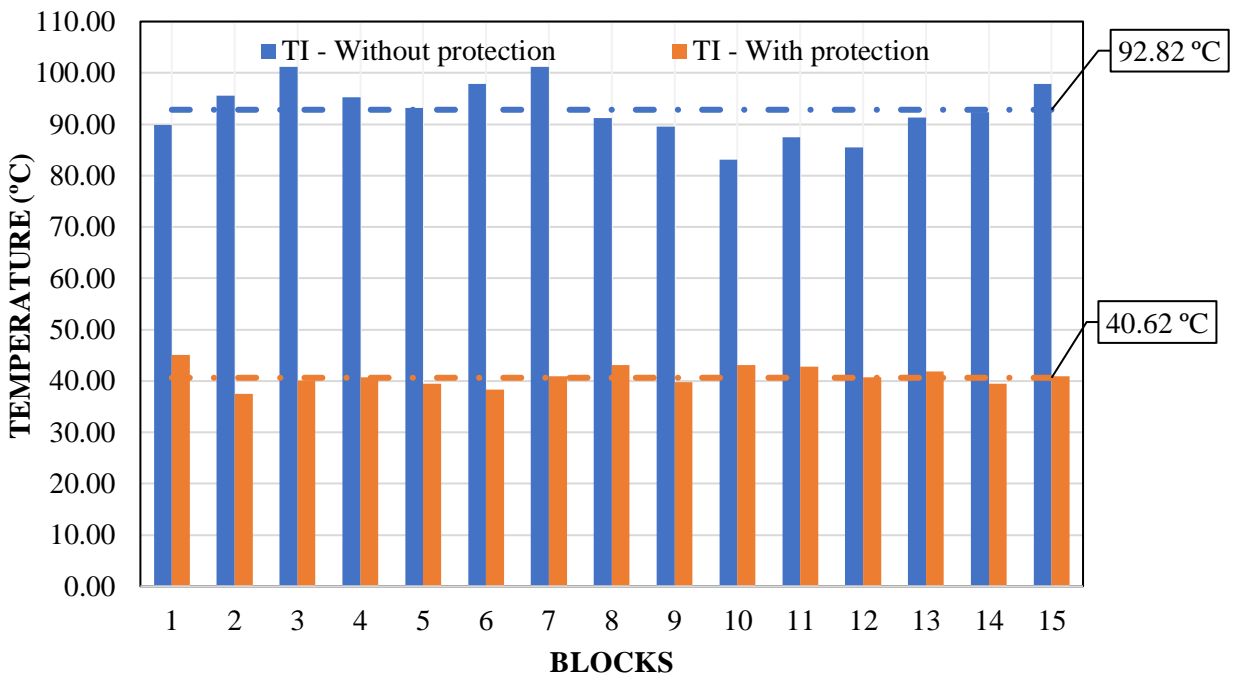


Figure 9. Comparison of the temperatures in the opposite faces for the blocks with and without passive protection, types 3 and 4 respectively.

This minor difference between the temperature variations on the farthest opposite face must occur due to the natural thermal insulation that the air between the septa provides to the block. It is verified that none of the blocks with passive protection reached temperatures higher than 46 °C. Equation 13 was then used to determine the percentage of this variation.

$$\frac{\bar{T}_{is} - \bar{T}_{ic}}{\bar{T}_{ic}} = \frac{92,82 - 40,62}{40,62} = 1,285 \text{ ou } 128,50\% \quad (13)$$

By performing analysis of variance for the temperature factor of types 3 and 4, considering the temperatures of each measured face and for all groups, the P value is lower than the stipulated significance level of 5% (0.05), as well as the value of F is less than F_{critical} .

Thus, the null hypothesis (H_0), in which the means would be equal, is rejected. Therefore, it can be stated that the values are different and the conditions with and without passive protection make the samples different.

Equations 14 and 15 were used in the comparison of the compressive strength and the maximum load capacity between the blocks with and without passive protection.

$$\frac{\bar{R}_c - \bar{R}_s}{\bar{R}_s} = \frac{2,38 - 1,34}{1,34} = 0,776 \text{ ou } 77,6\% \quad (14)$$

$$\frac{\bar{C}_c - \bar{C}_s}{\bar{C}_s} = \frac{37,993 - 21,860}{21,860} = 0,738 \text{ ou } 73,8\% \quad (15)$$

After the exposure to fire, during the 60-minute period, compressive strength in unprotected blocks decreased on average 70. Their maximum load capacity, when compared to blocks with passive protection, decreased 67%.

It is also possible to compare the values of compressive strength and load capacity between the protected blocks and the Type 1 blocks, which were those that had higher values of strength and load capacity; they were chosen as reference as shown in Equations 16 and 17.

$$\frac{\bar{R}_1 - \bar{R}_3}{\bar{R}_1} = \frac{2,484 - 2,38}{2,484} = 0,042 \text{ ou } 4,2\% \quad (16)$$

$$\frac{\bar{C}_1 - \bar{C}_3}{\bar{C}_1} = \frac{37,997 - 37,993}{37,997} = 0,000105 \text{ ou } 0,011\% \quad (17)$$

Comparing the average values of the compressive strength, a small variation of 5% is observed. However, the null value of variation for the average maximum load capacity does not bring the same individual analysis regarding the resistance defined by the standard, since there is a great variation in the values seen in Figures 10 and 11.

It is verified that for the significance level determined at 5%, as well as the F_{critical} , the resistance values are relevant because of the application or not of passive protection, making the sample data different.

COMPRESSIVE STRENGTH OF BLOCKS WITH AND WITHOUT PASSIVE PROTECTION

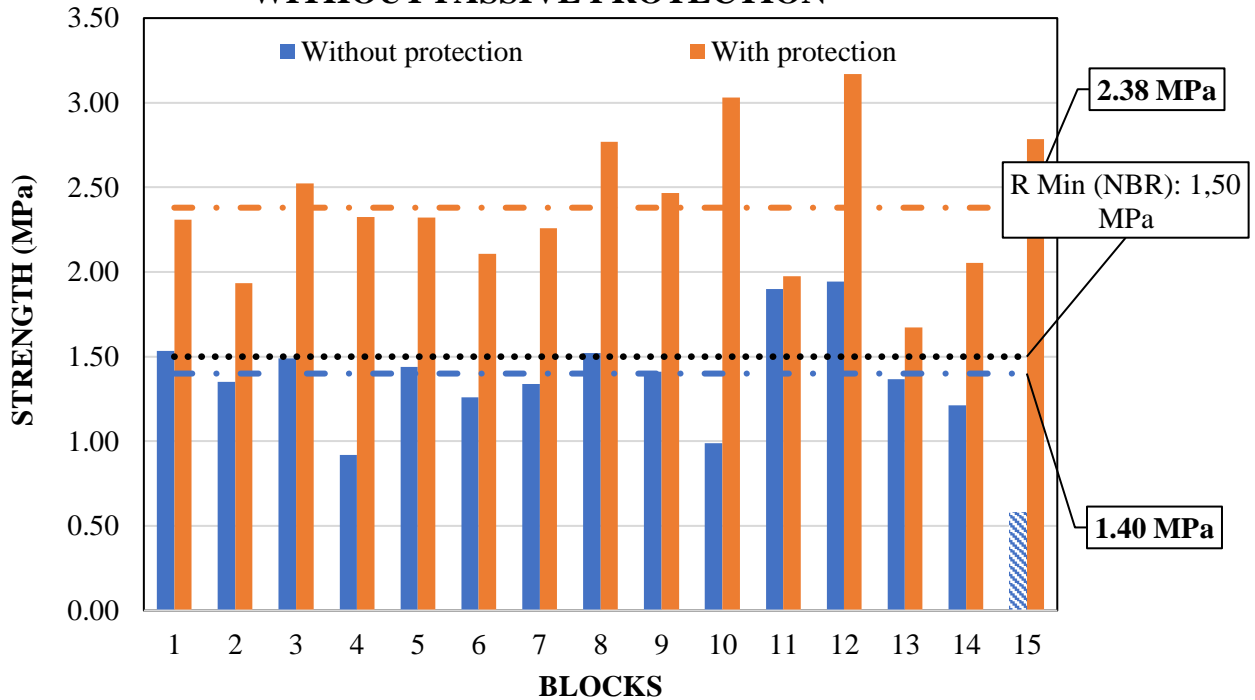


Figure 10. Compressive Strength: comparison between blocks with and without passive protection (types 3 and 4).

COMPRESSIVE STRENGTH: COMPARISON BETWEEN REFERENCE BLOCKS AND BLOCKS WITH PASSIVE PROTECTION

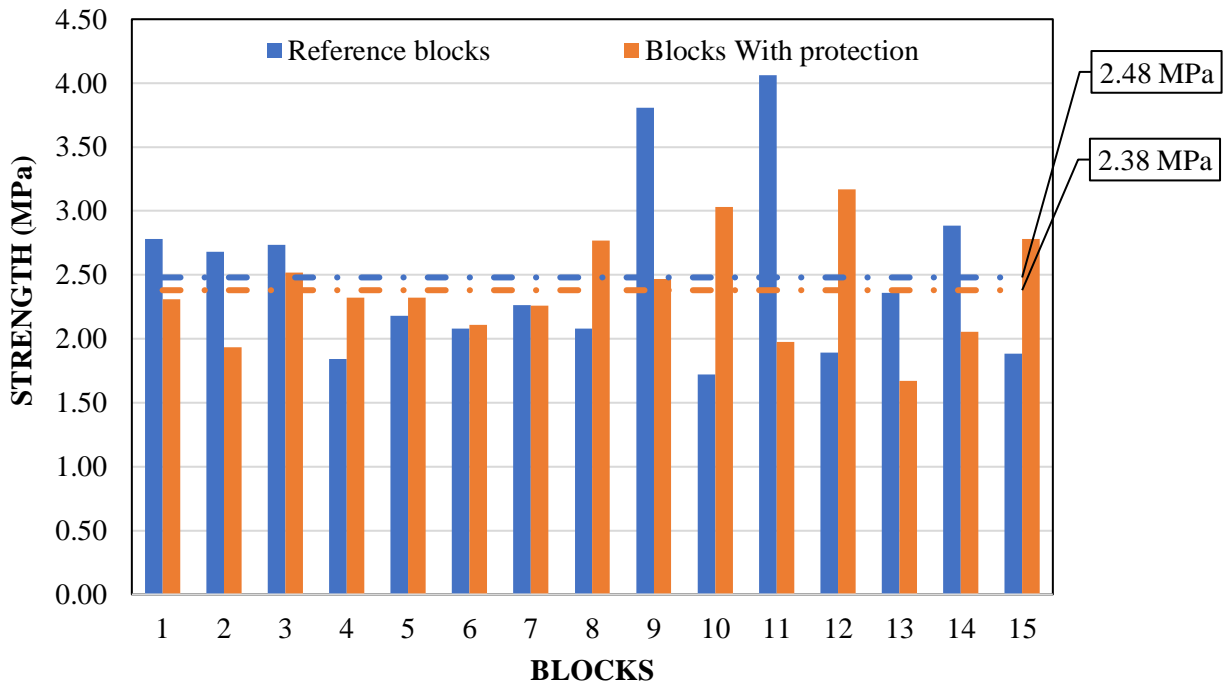


Figure 11. Compressive Strength: comparison between Reference Blocks and Blocks with Passive Protection.

It is verified that the P-value is lower than the stipulated significance level of 5% (0,05), as well as the value of F is lower than $F_{critical}$. It can be affirmed that the values are different and the conditions with and without passive protection make the samples different showed in Table 4.

Table 4. Data Summary (compressive strength - types 3 and 4)

Variation Source	SQ	gl	MQ	F	P-value	F critical
Among groups	8.03833	1	8.03833	53.794	5.50E-08	4.19597
Within the groups	4.18399	28	0.14943			

It was verified that, even after 60 minutes of direct flame incidence in the Type 3 blocks (passive protected by intumescent paint), the average values of compressive strength as well as maximum load capacity suffered small variation, below 5 %, when compared to the values obtained from the reference blocks showed in Table 5. Besides the excellent thermal insulation efficiency, the structural parameters of the blocks were maintained. Due to this small variation, the variance analysis test was performed again to verify if the means were different.

Table 5. ANOVA (Compressive Strength - types 1 and 3)

Variation Source	SQ	gl	MQ	F	valor-P	F crítico
Among groups	0,081	1	0,08112	0,24575	0,62395	4,19597
Within the groups	9,242	28	0,33009			

Thus, as the P-value found (0.624) is well above the stipulated significance level of 5% (0.05) or, in a different analysis, the value of F (0.245) found is lower than the $F_{critical}$ (4.19), then the null hypothesis (H_0), in which the means would be equal, was accepted. Therefore, the sets of reference blocks, which were not exposed, and the set of blocks protected by intumescent paints, after 60 minutes of exposure, are considered identical.

In addition, according to the NBR 15270 (2005) - *Ceramic Components - Part 1 - Ceramic Blocks for Sealing Masonry - Terminology and requirements*, regarding the minimum compressive strength for sealing blocks with horizontal holes, all blocks with passive protection (Type 3) have remained in compliance with the normative requirement, which requires at least 1,5 MPa. For the 15 blocks without passive protection (Type 4), 11 (eleven) blocks had lower resistance than required by the Brazilian standard and 2 (two) were very close to that value.

In terms of cost-effectiveness, it can be said that the retardant materials and passive protection were benefited by the greater employment and dissemination in Brazil. A consequence was the decrease in costs. Nowadays, it is possible to carry out the treatment of fabrics at BRL 7.00/m² and intumescent paintings at BRL 17.00/m². Varnished woods, being a more noble material, of high technology, and also produced in the United Kingdom, are priced at BRL 30-35/m². For the product used in this research, the cost was of approximately BRL 45/m².

Considering that currently the coatings used in new or renovation projects cost up to BRL 350/m², the use of retardants and passive protection materials is justified. As a percentage, passive protection of a complete building, including its common areas, is no more than 0.3% of its total budget. If all internal coatings used by architects and decoration are included, it will not exceed on average 0.6% of the cost of the building.

4. CONCLUSIONS

From the results obtained and their respective analyses, it is concluded that the surface protection provided by intumescent paints showed a reduction in the thermal gradient of the wall in a fire situation and better mechanical efficiency after exposure to fire. The following highlights are

presented from the analyses performed:

- When comparing the compressive strength values and maximum load capacity of the blocks chosen as reference (types 1 and 2), a variation in the values below 18%, in medium terms, in unsaturated and saturated conditions, was observed.
- The temperature of the face directly exposed to the flame, measured at its most unfavorable point, was on average 25% lower than the blocks with passive protection.
- After the incidence of the flame for 60 minutes and when analyzing the temperatures of the immediately opposite faces, it was found a difference of more than 170% in the blocks without the painting. This can indicate that there is a reduction of the thermal gradient in the blocks with the intumescent paint.
- The compressive strength and maximum load capacity of the blocks with passive protection were about 70% higher than the unprotected blocks after 60 minutes of direct exposure to the flame. More than 70% of the blocks without passive protection and that were exposed to the flame had compressive strength of 1.35 MPa. This value is lower than the minimum stipulated by the Brazilian standard (1.50 MPa), while 100% of the blocks with protection had resistance to 2.38 MPa, even after 60 minutes of exposure.

5. ACKNOWLEDGEMENT

The present paper was carried out with the support of the Coordination for the Improvement of Higher Education Personnel - Brazil - (CAPES) - Financing Code 001.

This research is of great relevance to the scientific/academic community and would not be possible without the collaboration of all participants.

6. REFERENCES

- Andreini, M., Sassu, M. (2011), *Mechanical Behaviour of Full Unit Masonry Panels Under Fire Action*. Fire Safety Journal, v. 46, n. 7, p. 440– 450.
- Associação brasileira de normas técnicas (2000). *NBR 14432: Exigências de resistência ao fogo de elementos construtivos de edificações – Procedimento*. Rio de Janeiro.
- Associação brasileira de normas técnicas (2005). *NBR 15270: Componentes cerâmicos Parte 1: Blocos cerâmicos para alvenaria de vedação – Terminologia e requisitos*. Rio de Janeiro.
- Associação brasileira de normas técnicas (2005). *NBR 15270: Componentes cerâmicos Parte 2: Blocos cerâmicos para alvenaria estrutural – Terminologia e requisitos*. Rio de Janeiro.
- Associação brasileira de normas técnicas (2005). *NBR 15270: Componentes cerâmicos Parte 3: Blocos cerâmicos para alvenaria estrutural e de vedação – Método de ensaio*. Rio de Janeiro.
- Associação brasileira de normas técnicas (2013). *NBR 15575: Edificações habitacionais – Desempenho Parte 4: Requisitos para os sistemas de vedações verticais internas e externas*. Rio de Janeiro.
- Associação brasileira de normas técnicas (2013). *NBR 14323: Projeto de estruturas de aço e de estruturas mistas de aço e concreto de edifícios em situação de incêndio*. Rio de Janeiro.
- Câmara Brasileira da Indústria da Construção (CBIC) (2013), *Desempenho de edificações habitacionais: guia orientativo para atendimento à norma ABNT NBR 15575/2013*. Fortaleza, Gadioli Cipolla Comunicação.
- Coelho, A. L. (2010), *Incêndios em edifícios*. Editora Orion, primeira edição – outubro de 2010.
- Meyer, U. (2006), *Extended Application Rules for the fire performance of masonry walls*. In: 7th International Masonry Conference, Londres. Disponível em: < <http://www.masonry.org.uk/> >. Acesso em: 28 de abril de 2019.
- Nadjai, A. et al. (2006), *Compartment Masonry Walls in Fire Situations*. Fire Technology, v. 42,

n. 3, p. 211-231.

Nguyen, T. D., Meftah, F. (2012), *Behavior of Clay Hollow-Brick Masonry Walls During Fire: part 1: experimental analysis*. Fire Safety Journal, v. 52, p. 55-64.

Freitas, L. (2014), *Segurança em boates aumenta após um ano da tragédia em Santa Maria*. Disponível em: <<https://diariodonordeste.verdesmares.com.br/editorias/metro/seguranca-em-boates-aumenta-apos-um-ano-da-tragedia-em-santa-maria-1.799643>> Acesso em: 28 de abril de 2019.

Ono, R. (2007), *Parâmetros para garantia da qualidade do projeto de segurança contra incêndio em edifícios altos*. Ambiente Construído. Porto Alegre, v. 7, n. 1, p. 97-113.

Seito, A. I. et al. (2008). *A Segurança contra Incêndios no Brasil*. São Paulo: Projeto Editora. p 496,497.

Thomaz, E., Helene, P. (2000), *Qualidade no projeto e na execução de alvenaria estrutural e de alvenarias de vedação em edifícios*. Boletim Técnico da Escola Politécnica da USP, BT/PCC/252. São Paulo: EPUSP, 31 p.

Numerical analysis of composite concrete and steel slabs section under fire situation

F. Barcellos¹, F. Bolina², B. Tutikian^{2*}

*Contact author: btutikian@terra.com.br

DOI: <http://dx.doi.org/10.21041/ra.v10i1.448>

Reception: 29/07/2019 | Acceptance: 11/12/2019 | Publication: 30/12/2019

ABSTRACT

This work aims to evaluate the performance of composite slabs under fire, correlating them to the project at normal temperature, according to NBR 14323 (ABNT, 2013), NBR 8800 (ABNT, 2008) and NBR 14762 (ABNT, 2010).), through the heating curve of ISO 834 (ISO, 1999) and distribution of slab temperatures obtained by using Ansys software. The computational models were calibrated according to the standard and extrapolated to other design scenarios, with different geometries, thicknesses and effective thicknesses of the concrete layer. As results, the steel deck with recesses had better performance in relation to the trapezoids, being the thickness of the concrete layer the preponderant variable in the behavior of these slabs at high temperatures, due to their greater thermal stability.

Keywords: fire safety; composite slabs; steel; concrete.

Cite as: Barcellos, F., Bolina, F., Tutikian, B. (2020), "Numerical analysis of composite concrete and steel slabs section under fire situation", Revista ALCONPAT, 10 (1), pp. 69 – 78, DOI: <http://dx.doi.org/10.21041/ra.v10i1.448>

¹ Master student in Graduate Program of Architecture and Urbanism, Universidade do Vale do Rio dos Sinos, São Leopoldo, Brazil.

² it Performance, Universidade do Vale do Rio dos Sinos, São Leopoldo, Brazil.

Legal Information

Revista ALCONPAT is a quarterly publication by the Asociación Latinoamericana de Control de Calidad, Patología y Recuperación de la Construcción, Internacional, A.C., Km. 6 antigua carretera a Progreso, Mérida, Yucatán, 97310, Tel.5219997385893, alconpat.int@gmail.com, Website: www.alconpat.org

Responsible editor: Pedro Castro Borges, Ph.D. Reservation of rights for exclusive use No.04-2013-011717330300-203, and ISSN 2007-6835, both granted by the Instituto Nacional de Derecho de Autor. Responsible for the last update of this issue, Informatics Unit ALCONPAT, Elizabeth Sabido Maldonado, Km. 6, antigua carretera a Progreso, Mérida, Yucatán, C.P. 97310.

The views of the authors do not necessarily reflect the position of the editor.

The total or partial reproduction of the contents and images of the publication is strictly prohibited without the previous authorization of ALCONPAT Internacional A.C.

Any dispute, including the replies of the authors, will be published in the third issue of 2020 provided that the information is received before the closing of the second issue of 2020.

Análise numérica das características da seção de lajes mistas de aço e concreto em situação de incêndio

RESUMO

Este trabalho busca avaliar o desempenho de lajes mistas de aço e concreto em situação de incêndio, correlacionando-as ao projeto em temperatura ambiente, conforme NBR 14323 (ABNT, 2013), NBR 8800 (ABNT, 2008) e NBR 14762 (ABNT, 2010), através da curva de aquecimento da ISO 834 (ISO, 1999) e distribuição de temperaturas obtidas segundo o software Ansys. Os modelos computacionais foram calibrados pela norma e extrapolados computacionalmente. Foram analisadas lajes com chapas trapezoidais de diferentes geometrias e com camadas de concreto variadas. Como resultados, as chapas com reentrâncias apresentaram melhor desempenho face às trapezoidais, sendo a espessura da camada de concreto preponderante no comportamento destas lajes ao incêndio, visto a sua maior estabilidade térmica.

Palavras-chave: segurança contra incêndio; lajes mistas; aço; concreto.

Análisis numérico de la sección de losas de hormigón compuesto y acero bajo incendio

RESUMEN

Este trabajo tiene como objetivo evaluar el rendimiento de las losas compuestas bajo fuego, correlacionándolas con el proyecto a temperatura normal, de acuerdo con NBR 14323 (ABNT, 2013), NBR 8800 (ABNT, 2008) y NBR 14762 (ABNT, 2010), a través de la curva de calentamiento de ISO 834 (ISO, 1999) y la distribución de las temperaturas de losas obtenidas utilizando el software Ansys. Los modelos computacionales fueron calibrados de acuerdo con el estándar y extrapolados a otros escenarios de diseño, con diferentes geometrías, espesores y espesores efectivos de la capa de concreto. Como resultado, la plataforma con rebajes tuvo un mejor rendimiento en relación con los trapecios, siendo el espesor de la capa de hormigón la variable preponderante en el comportamiento de estas losas a altas temperaturas, debido a su mayor estabilidad térmica.

Palabras clave: seguridad contra incendios; losas compuestas; acero; hormigón.

1. INTRODUCTION

The concrete and steel slabs have some constructive advantages in comparison with traditional systems. They offer a work platform during the structure's execution, speed of construction, increase in local and global stability of steel structures, height reduction in beams and self-weight reduction in structures (Craveiro, 2010; Liang, 2015). Although it is a highly used solution, the steel sensibility to fire require more attention in project (Li; Wang, 2013). The sensibility of steel materials to high temperatures grounds this discussion. In these composite slabs, the steel deck slenderness can promote failure in little time and sudden break (Li et.al., 2017).

The analysis of composite structures submitted to high temperature elaborated in Building Research Establishment during the 90's, in Cargindton, England, were motivated by fires in tall buildings, as One Meridian Plaza, in the USA (1991), and BroadGate, in England (1990), with the composite slabs showing a superior performance than the expected, with no collapse (Selamet; Bolukbas, 2016). Its interaction with beams and its loads redistribution promoted a mobilization of the membrane action (Nguyen et.al., 2015), improving its resistance to fire. Discussions arised about the standards conservatism (Bailey et.al., 2000) in face of the noted phenomenon – of difficult prediction in design level (Gillie et.al., 2001) – and demonstrated that steel structures have an inherent fire resistance not identified in simulations and/or at numerical verifications (Omer et.al., 2009).

In the Cardington studies, it was identified that the steel deck geometry has an important part in the temperature distribution in the slab, influencing its fire resistance (Li et al, 2017). The steel deck embossments make that the local humidity takes longer to evaporate, decreasing the global concrete temperatures. The steel deck thickness does not influence the slab temperatures, because its small dimension makes that the average temperature is practically equal in every case, with similar values (Li, Wang, 2013).

Concrete has a great influence over the composite slabs exposed to fire behavior. Due to its low thermal conductivity, the greater the thickness of its layer, the smaller it's the consequence of high temperatures in the slab, presenting a better fire resistance (Li, Wang, 2013). The membrane action becomes more developed in these cases. The concrete spalling tends to be mitigated in composite slabs because of the steel deck barrier (Costa et al, 2002; Wang, 2002).

The verification of composite concrete and steel structures under fire situation is made by NBR 14323 (ABNT 2013), that has a strong inspiration in EN 1994-1-1 (EN, 2005). It specifies that the design of this structures under fire situation must be done in the Ultimate Limit State (ULS), not being necessary its verification in the Service Limit State (SLS). The standard proposes the sizing can be done through laboratory results or analytical methods.

The structural verification of slabs under fire situation goes through three criteria: tightness, thermal insulation and bearing capacity. NBR 14323 (ABNT 2013) considers the tightness criteria is complied with the presence of the steel deck. The thermal insulation criteria are determined by the effective thickness of the slab. Its bearing capacity is determined through a global plastic analyses, considering the positive and negative moments generated by the specified loading and obtained through the bending moment diagram.

According to the standard, the contribution proportioned by the steel deck in the moment of resisting is calculated by the sum of the contribution of each element of the steel deck, according to Equation 1, in which A_{efi} is the effective area of the i part in cm^2 , d_i is the distance from the gravity center of part i to the neutral line in the section of the slab in cm , f_{yk} is the steel yield strength in kN/cm^2 and $k_{y,\theta i}$ is the steel resistance reduction coefficient according to the indicated temperature for the element, calculated through the coefficients indicated in the standard regarding the time required of fire resistance (TRFR) at 60, 90 and 120 minutes. For the calculation of the neutral line position in relation to the upper face of the slab the Equation 2 is utilized, in which f_{ck} is the concrete compressive resistance in kN/cm^2 , $k_{c,\theta}$ is the concrete resistance reduction coefficient according to the temperature and b_w is the slab width.

$$M_{Rd,faço} = \sum A_{efi} d_i f_{yk} k_{y,\theta i} \quad (1)$$

$$y_p = \frac{\sum A_{efi} f_{yk} k_{y,\theta i}}{0,85 f_{ck} k_{c,\theta} b_w} \quad (2)$$

The contribution proportioned by the concrete is calculated according to the Equation 3, in which $A_{ef,c}$ is the concrete contributing area above the neutral line in cm^2 , d is the distance to the gravity center of the concrete compressed area to the neutral line in cm , f_{ck} is the concrete compressive resistance in kN/cm^2 and $k_{c,\theta}$ is the concrete resistance reduction coefficient according to the temperature, as the standard indicates for a TRFR of 60, 90 and 120 minutes.

$$M_{Rd,c} = A_{ef,c} d f_{ck} k_{c,\theta} \quad (3)$$

The slab final moment of resistance is calculated as the sum of the steel deck and concrete moment of resisting. The shear is not considered in this standard, motive by which its evaluation will not be realized in this paper.

Although studies acknowledge the importance of steel sheet geometry and thickness (Li et.al., 2017; Li, Wang, 2013), and the existence of several geometries and thickness available, they are not taken into account in the thermal insulation, otherwise the minimum effective thickness of the concrete layer, according to NBR 14323 (ABNT 2013), deserving further investigation.

Therefore, this paper aims to analyze the behavior of composite concrete and steel slabs under fire situation, addressing the influence of the geometry and thickness of the steel deck and the thickness of the concrete to the time of resistance under fire, through a numerical analysis, calculating the slab temperature utilizing a computational tool, Ansys, taking the sizing criteria and verification of Brazilian and European standards.

2. METHOD

The numerical verification was made based on the NBR 8800 (ABNT, 2008), NBR 14323 (ABNT, 2013), NBR 15200 (ABNT, 2012), EN 1992 (CEN, 2010) and EN 1994 (CEN, 2004) equations. As NBR 14323 (ABNT 2013) presents limited design orientations for different TRFR, it was necessary to realize a computational analysis to extrapolation of results through the software Ansys utilizing a standard fire curve defined in ISO 834 (ISO, 1999), as required in NBR 14323 (ABNT, 2013) for structural analysis under fire situation.

The proposed response variables are the concrete layer thickness, the geometry and thickness of steel deck. The evaluation was made in order to explore the values of one variable while the other two have their fixed values. Effective concrete thickness of 80 mm, 90 mm, 100 mm, 110 mm, 120 mm, 130 mm, 140 mm and 150 mm were evaluated. The geometry of the steel deck consisted of two trapezoidal and one with embossments sections, according to Figure 1, and the studied steel deck thicknesses were 0,80 mm, 0,95 mm and 1,25 mm.

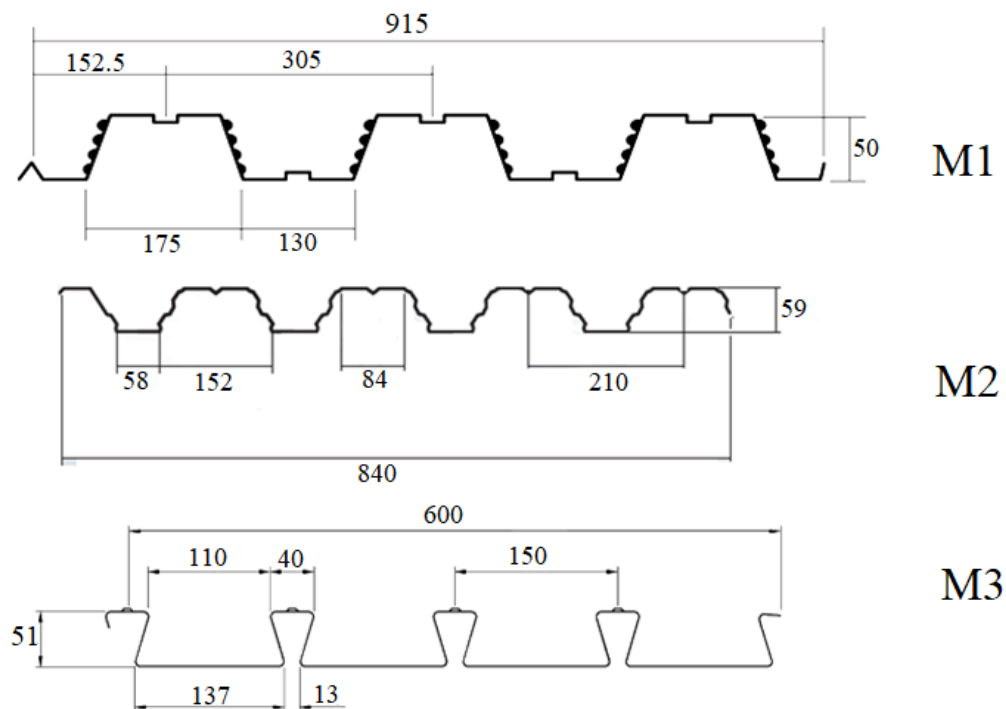


Figure 1. Steel deck models (in mm).

For denomination of the studied models, the order of the nomenclature was chosen as the first letter M followed by the number of the steel deck model, the letter F followed by the steel deck thickness and the letter C followed by the effective concrete thickness in millimeters. The Figure 2 shows an example of the nomenclature utilized in this paper.

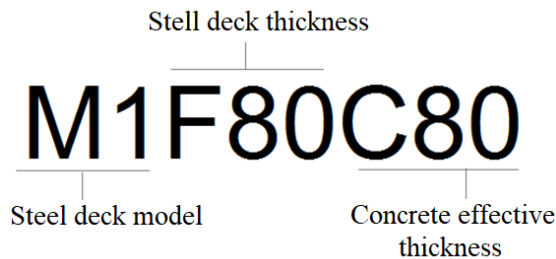


Figure 2. Nomenclature

As control variables, and for analysis of the slabs of this study, the values of steel and concrete under high temperatures were adopted, as seen in Table 1. The slab model studied is unidirectional and simply supported, forming isostatic elements, with 1-meter of width and 3-meter span. The supports were considered perpendicular to the ribs. There isn't formation of membrane action compressive strength due to the simply supported model that allows horizontal movements. Also, it was not considered the constructive analysis, as the steel deck must support the total load during the concrete curing period. It was not considered the utilization of negative bending reinforcement in this study, and the positive reinforcement was constituted by the steel deck.

Table 1. Steel and concrete properties under high temperatures.

	Steel properties	Concrete properties
Characteristic Strength	As Table 1 of NBR 14323 (ABNT, 2013)	As Table 1 of NBR 15200 (ABNT, 2012)
Poisson's ratio	0,3	0,15
Modulus of elasticity	As Table 1 of NBR 14323 (ABNT, 2013)	As EN 1994-1-2 (EN, 2005)
Thermal conductivity	As item E.4 of Annex E of NBR 14323 (ABNT, 2013)	As item C.3 of Annex C of NBR 15200 (ABNT, 2012)
Specific heat	As item E.43 do Annex E of NBR 14323 (ABNT, 2013)	As item C.2 of Annex C of NBR 15200 (ABNT, 2012)
Specific mass	7850 kg/m ³	2500 kg/m ³

The TRFR studied were: 15, 30, 45, 60, 90, 120, 150 and 180 minutes. As NBR 14323 (ABNT 2013) provides the coefficients for steel deck temperature calculation only for TRFR of 60, 90 and 120 minutes, was utilized the software Ansys to obtain the TRFR elements temperature not provided by the standard, calibrating the extrapolations with the values presented by standard. Ansys utilizes the finite element method in its analysis, with meshing and analyzing their intersection points. This tool was employed to analyze the temperature distribution in the section exposed to a standard fire curve ISO 834 (ISO, 1999). The convection coefficient used was 25 W/m².K. The thermal emissivity of the materials was not considered. Temperature collection was done using Ansys Temperature Probe tool. To measure the steel deck temperature, the exposed faces to fire were selected, adopting as the measurement point the average plane of the respective element that composes the steel deck. In the concrete temperature measurement, the compressed portion of the section was considered.

3. RESULTS

Figure 3, Figure 4 and Figure 5 show the average temperature in the superior face of concrete, above the neutral line.

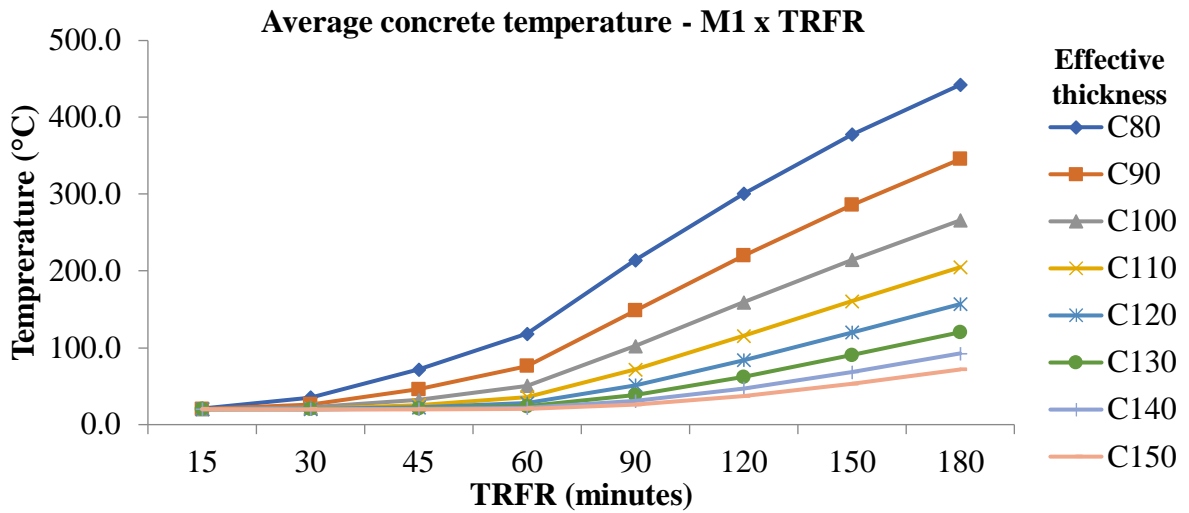


Figure 3. Average concrete temperature in steel deck model M1

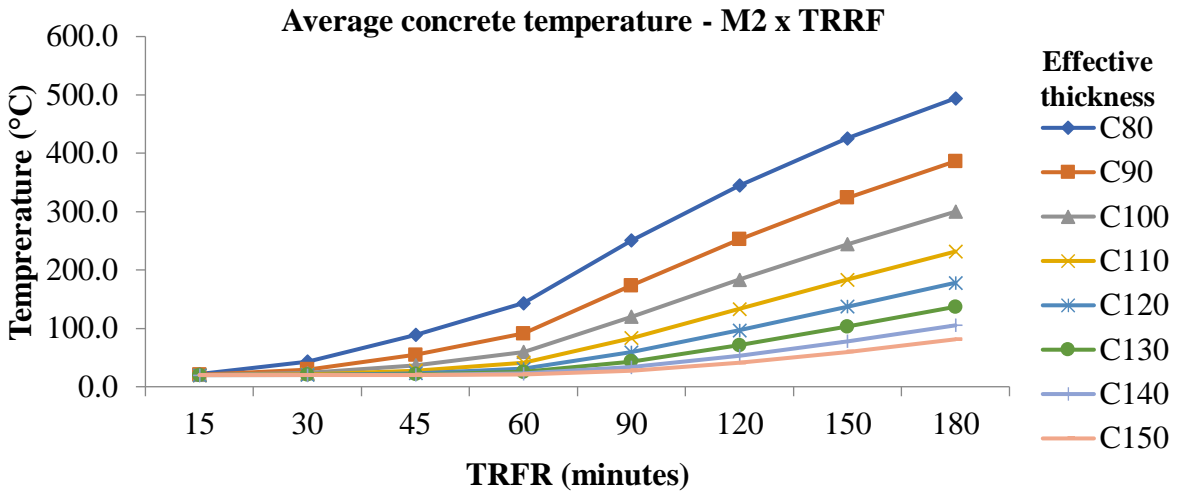


Figure 4. Average concrete temperature in steel deck model M2

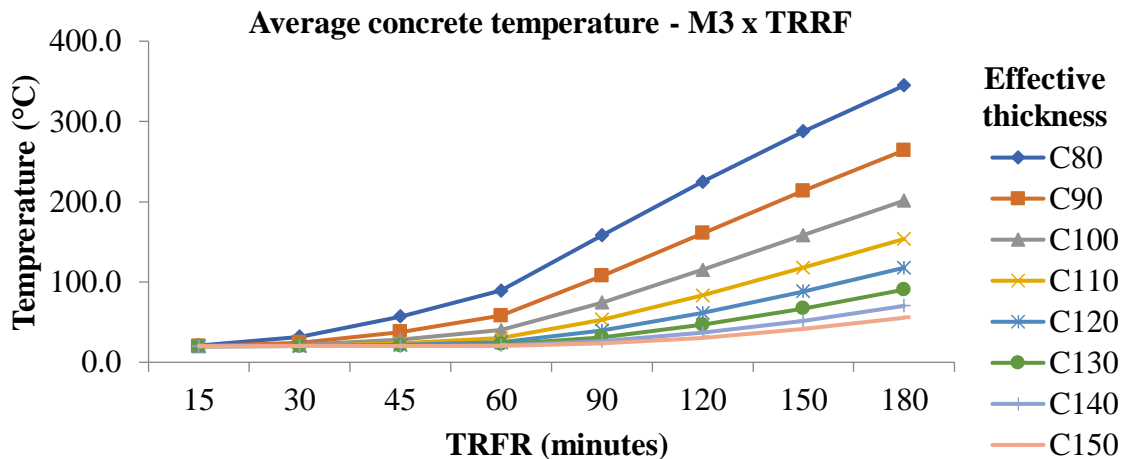


Figure 5. Average concrete temperature in steel deck model M3.

It is noticed that, only at 60 min of exposure, the temperature variation is larger and more significant in the first four thicknesses, exceeding 100°C and compromising its resistance. At 180 min, only the model M1 with concrete thickness of 14 and 15 cm, the model M2 with concrete thickness of 15 cm and model M3 with concrete thickness of 13 to 15cm do not reach 100°C. In the other thicknesses, temperatures reached 494.5°C, with a reduction coefficient of 0.61. This behavior of concrete thermal insulation can be explained by its low thermal conductivity and high specific heat, which in the face of fire exposure requires high temperature and duration for heat to be transferred along its thickness. Analyzing the steel deck temperature when verified its geometry under high temperature exposure, the obtained temperatures are similar in the bottom flange and the web, as expected, given the high thermal conductivity of steel.

The Tables 2, 3 and 4 show the resistance reduction factors in the different parts of the steel deck. The geometry of the M3 model has the largest temperature variation in the elements, showing the smallest temperatures on the top flange and the highest in the bottom flange and web amount the studied models. As consequence, this model has the biggest reduction factor in the top flange and the smallest in the bottom flange and web. This variation is within a range of 133°C and is influenced by the area and form of exposure, which, because of the re-entrant model, ends up isolating the top flange and leaving a larger exposure area on the bottom flange, which is transferred to the web.

Table 2. Top flange resistance reduction factors

Model	15 min	30 min	45 min	60 min	90 min	120 min	150 min	180 min
M1	1,00	0,72	0,42	0,25	0,12	0,08	0,06	0,05
M2	1,00	0,79	0,47	0,30	0,15	0,09	0,08	0,07
M3	1,00	0,89	0,64	0,43	0,22	0,13	0,10	0,09

Table 3. Bottom flange resistance reduction factors

Model	15 min	30 min	45 min	60 min	90 min	120 min	150 min	180 min
M1	1,00	0,65	0,34	0,20	0,09	0,06	0,05	0,04
M2	1,00	0,61	0,28	0,16	0,08	0,05	0,05	0,05
M3	1,00	0,52	0,24	0,14	0,07	0,05	0,05	0,04

Table 4. Web resistance reduction factors

Model	15 min	30 min	45 min	60 min	90 min	120 min	150 min	180 min
M1	1,00	0,65	0,34	0,20	0,09	0,06	0,05	0,04
M2	1,00	0,61	0,28	0,16	0,08	0,05	0,05	0,05
M3	1,00	0,52	0,24	0,14	0,07	0,05	0,05	0,04

The steel deck temperature did not suffer a significative variation with the change of thickness, due to the high thermal conductivity of steel and reduced dimensions of steel deck. In NBR 14323 (ABNT, 2013) calculation model, only the steel deck geometry influences de temperature variation and it is the same for all thicknesses of the same model. This procedure was confirmed by Ansys verification, as the variation did not exceed 1% amount of the thicknesses.

Correlating the variables that influence the slab strength at high temperatures (steel deck geometry and concrete layer thickness) and averaging these values with the steel deck thickness, it can be stated that the differences in temperature as a function of geometry are more significant in the smaller concrete thicknesses, decreasing as thickness increases as shown in Figure 6. Despite this, the advantage of the M3 model over the other models has always been observed. As the TRFR increased, the temperature difference relative to the thickness of the concrete layer decreased.

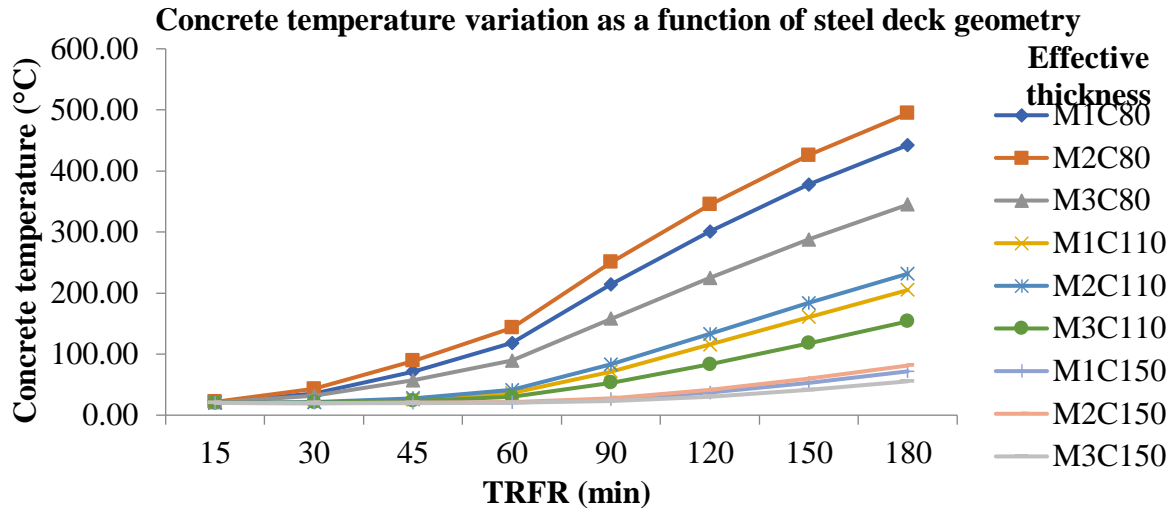


Figure 6. Concrete temperature variation as a function of steel deck geometry

The model M1 presents a similar geometry to model M2, as shown in Figures 7 and 8, which makes the temperature variation between these two models smaller. The most significant variation is between the models M2 and M3 geometry, the first has the highest temperature and the second the lowest temperature among the models studied. This is because the M2 model geometry exposes more to its top flange, making it easier for the temperature to reach higher values in the concrete. The model M3 is re-entrant, which allows the heat to concentrate in the bottom flange and difficult the access of hot air in the top flange, as shown in Figure 9. The isotherms also show how the temperature advances in the slabs, and in the M3 model they behave steadily, forming straight lines, while in the other two models they form waves.

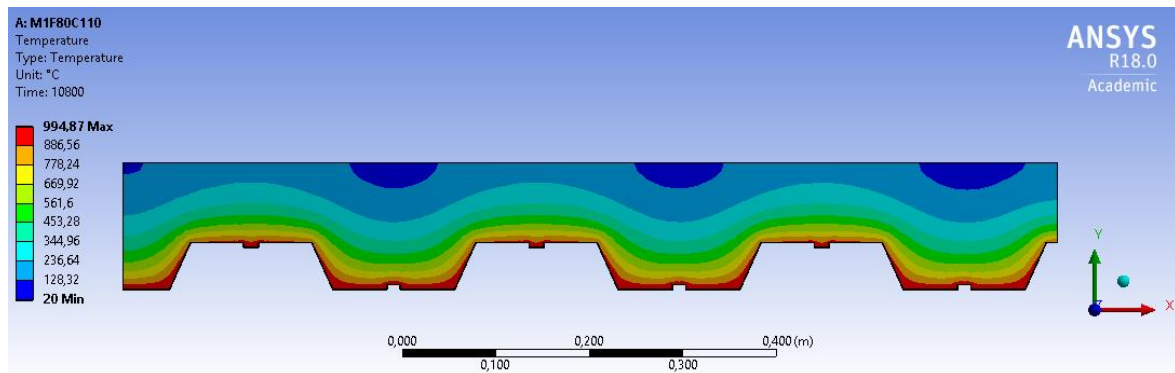


Figure 7. M1F80C110 with TRRF of 180 minutes

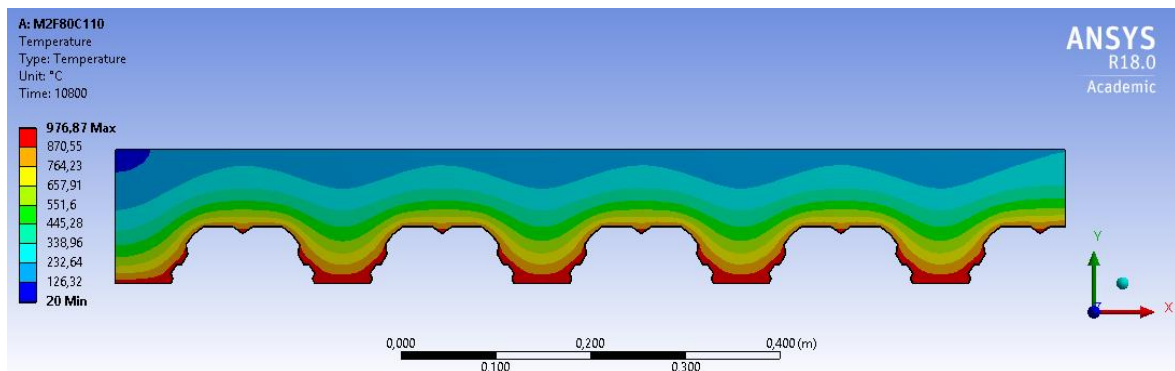


Figure 8. M2F80C110 with TRRF of 180 minutes

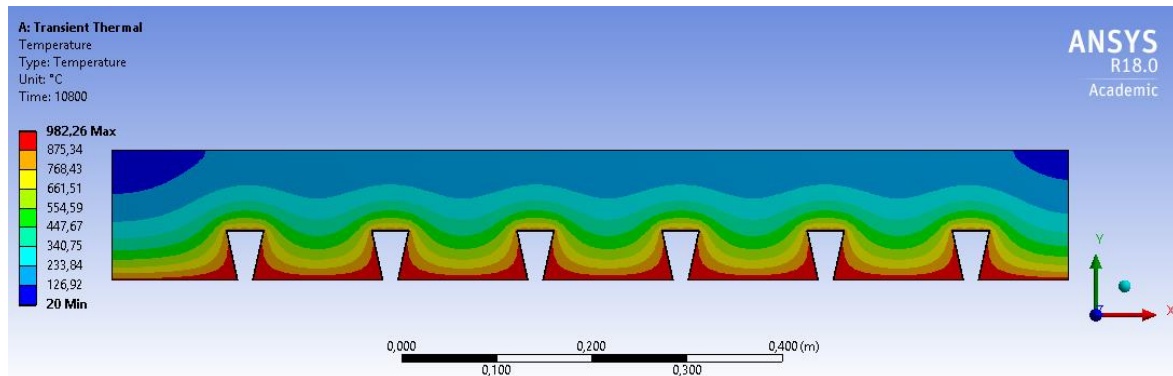


Figure 9. M3F80C110 with TRRF of 180 minutes

The variable that most influenced the temperature was the steel deck geometry, specifically the M3 model with re-entrant, having the best performance among the studied models. This was due to the larger unitary steel area of these elements and higher concrete consumption – with higher thermal stability - in the ribs.

The effective concrete layer thickness was also influent. Because the concrete has low thermal conductivity, the higher its thickness, the lower the temperature of the slab compressive strength, where the concrete effectively acts at the resistant moment. The drawback of this solution is the increased weight of the structure.

From 30 minutes of exposure to fire, the reduction coefficient of the steel deck shows that it has no more structural participation, leaving the concrete with no reinforcement, subjected to bending. Therefore, in numerical analyzes designed based on normative equations, the use of positive reinforcement is necessary to avoid sudden breaking of concrete at high temperatures. However, experimental studies have shown that these slabs have an intrinsic fire resistance, having seen the membrane effect that is difficult to predict numerically.

4. CONCLUSION

Among the items evaluated in this work, the ones that exert the greatest influence on the behavior of composite concrete and steel slabs are the steel deck geometry and the concrete layer thickness, respectively. This is mainly due to the thermal stability generated by the geometry that allows higher concrete consumption and the low thermal conductivity of the concrete.

5. REFERENCES

- Associação Brasileira de Normas Técnicas (2013). *NBR 14323: Projeto de estruturas de aço e de estruturas mistas de aço e concreto de edifícios em situação de incêndio*. Rio de Janeiro.
- Associação Brasileira de Normas Técnicas (2008). *NBR 8800: Projeto de Estruturas De Aço e de estruturas mistas de aço e concreto de edifícios*. Rio de Janeiro.
- Associação Brasileira de Normas Técnicas (2010). *NBR 14762: Dimensionamento de estruturas de aço constituídas por perfis formados a frio*. Rio de Janeiro.
- Associação Brasileira de Normas Técnicas (2012). *NBR 15200: Projeto de estruturas de concreto em situação de incêndio*. Rio de Janeiro.
- Bailey, C. G.; White, D. S.; Moore, D. B. (2000). *The tensile membrane action of unrestrained composite slabs simulated under fire conditions*. Engineering Structures. 22 (12):1583–1595. [https://doi.org/10.1016/S0141-0296\(99\)00110-8](https://doi.org/10.1016/S0141-0296(99)00110-8)

- Costa, C. N.; Figueiredo, A. D.; Pignatta, V. (2002). *O fenômeno do lascamento (“spalling”) nas estruturas de concreto armado submetidas a incêndio – uma revisão crítica*. In: In: 44º Congresso Brasileiro do Concreto- IBRACON 2002. Anais eletrônicos. Belo Horizonte.
- Craveiro, H. D. S. (2010). “*Análise do comportamento estrutural de lajes mistas aço-betão com reforço transversal*”. Dissertação de mestrado. Universidade de Coimbra, Coimbra.
- European Committee for Standardization (2005). *EN 1994-1-2: Design of composite steel and concrete structures – Part 1-2: General rules – structural fire design: Eurocode 4*. Brussels.
- Gillie, M.; Usmani, A. S.; Rotter, J. M. (2001). *A structural analysis of the first Cardington test*. Journal of Constructional Steel Research. 57 (6):581–601. [https://doi.org/10.1016/S0143-974X\(01\)00004-9](https://doi.org/10.1016/S0143-974X(01)00004-9)
- Li, G.; Zhang, N.; Jiang, J. (2017). *Experimental investigation on thermal and mechanical behaviour of composite floors exposed to standard fire*. Fire Safety Journal. 89:63-76. <https://doi.org/10.1016/j.firesaf.2017.02.009>
- Liang, Q. Q. (2015). “*Analysis and Design of Steel and Composite Structures*”. CRC Press, New York. p. 458. ISBN: 9780415532204
- Li, G.; Wang, P. (2013). “*Advanced Analysis and Design for Fire Safety of Steel Structures*”. China: Zhejiang University Press, Springer-Verlag Berlin Heidelberg. p. 357. ISBN: 9783642343933
- Nguyen, T. T.; Tan, K. H.; Burgess, I. W. (2015). *Behaviour of composite slab-beam systems at elevated temperatures: Experimental and numerical investigation*. Engineering Structures, 82: 199–213. <https://doi.org/10.1016/j.engstruct.2014.10.044>
- Omer, E.; Izzuddin, B. A.; Elghazouli, A. Y. (2009). *Failure of lightly reinforced concrete floor slabs with planar edge restraints under fire*. Journal of Structural Engineering, 135 (9): 1068–1080. [https://doi.org/10.1061/\(ASCE\)0733-9445\(2009\)135:9\(1068\)](https://doi.org/10.1061/(ASCE)0733-9445(2009)135:9(1068))
- Selamet, S.; Bolukbas, C. (2016). *Fire resilience of shear connections in a composite floor: Numerical investigation*. Fire Safety Journal, 81: 97–108. <https://doi.org/10.1016/j.firesaf.2016.02.003>
- Vargas, M. R.; Silva, V. P. (2005). *Resistência ao fogo das estruturas de aço*. Rio de Janeiro: IBS/CBCA. Rio de Janeiro. P.78. ISBN: 85-89819-02-7.
- Wang, Y. C. (Ed.). (2002). “*Steel and Composite Structures: Behaviour and Design for Fire Safety*”. 1 ed. London: CRC Press. p. 352. ISBN: 9780429257056. DOI: <https://doi.org/10.1201/9781482267693>

Performance of fire protective coatings in reinforced concrete elements submitted to high temperatures

C. Brites^{1*}, V. P. Silva², M. Carvalho³, P. Helene⁴ 

*Contact author: brites.consultoria@gmail.com

DOI: <http://dx.doi.org/10.21041/ra.v10i1.430>

Reception: 29/07/2019 | Acceptance: 11/12/2019 | Publication: 30/12/2019

ABSTRACT

This article aims to compare different fire-resistant coating systems to 1.5 cm cover and one-year-old reinforced concrete elements for evaluating the performance of these systems by visual inspection and verification of internal temperature evolution after standard fire simulations under the ISO 834 curve by using thermocouples for a time of 120 minutes. The results showed very close correlations with the literature for cement-based mortar coatings, as well as other particularities about plaster coatings and the possibility of using intumescent paints as passive protection in reinforced concrete elements.

Keywords: fire; fire protection coating; concrete; passive fire protection; experimental tests.

Cite as: Brites, C., Silva, V. P., Carvalho, M., Helene, P. (2020), " *Performance of fire protective coatings in reinforced concrete elements submitted to high temperatures.*", Revista ALCONPAT, 10 (1), pp. 79 – 96, DOI: <http://dx.doi.org/10.21041/ra.v10i1.430>

¹ Pesquisador de Pós-Doutorado na Escola Politécnica da USP, Brites Consultoria, São Paulo, Brasil.

² Professor da Escola Politécnica da USP, São Paulo, Brasil.

³ Universidade Presbiteriana Mackenzie, São Paulo, Brasil.

⁴ Professor Titular da Escola Politécnica da USP, PhD Engenharia, São Paulo, Brasil.

Legal Information

Revista ALCONPAT is a quarterly publication by the Asociación Latinoamericana de Control de Calidad, Patología y Recuperación de la Construcción, Internacional, A.C., Km. 6 antigua carretera a Progreso, Mérida, Yucatán, 97310, Tel.5219997385893, alconpat.int@gmail.com, Website: www.alconpat.org

Responsible editor: Pedro Castro Borges, Ph.D. Reservation of rights for exclusive use No.04-2013-011717330300-203, and ISSN 2007-6835, both granted by the Instituto Nacional de Derecho de Autor. Responsible for the last update of this issue, Informatics Unit ALCONPAT, Elizabeth Sabido Maldonado, Km. 6, antigua carretera a Progreso, Mérida, Yucatán, C.P. 97310.

The views of the authors do not necessarily reflect the position of the editor.

The total or partial reproduction of the contents and images of the publication is strictly prohibited without the previous authorization of ALCONPAT Internacional A.C.

Any dispute, including the replies of the authors, will be published in the third issue of 2020 provided that the information is received before the closing of the second issue of 2020.

Desempenho de revestimentos contrafogo em elementos de concreto armado submetidos a temperaturas elevadas

RESUMO

Este artigo visa comparar diferentes sistemas de revestimento contrafogo aderidos a elementos de concreto armado, com um ano de idade e cobertura de 1,5 cm, e avaliar o desempenho desses sistemas por inspeção visual e verificação da evolução das temperaturas internas após simulações de incêndio padrão sob a curva ISO 834, com uso de termopares, por um tempo de 120 minutos. Os resultados demonstraram correlações bem próximas às da literatura consagrada para revestimentos em argamassa base cimento, bem como outras particularidades sobre revestimentos em gesso e ainda a possibilidade do uso de tintas intumescentes como proteção passiva em elementos de concreto armado.

Palavras-chave: incêndio; revestimento contrafogo; concreto; proteção passiva; programa experimental.

Desempeño de recubrimientos protectores contra incendios en elementos de hormigón armado sometidos a altas temperaturas

RESUMEN

El objetivo de este artículo es comparar diferentes sistemas de revestimiento resistentes al fuego aplicados a elementos de concreto armado de un año de edad y 1,5 cm de recubrimiento de concreto, y evaluar el desempeño de estos sistemas mediante inspección visual y verificación de la evolución de las temperaturas internas después de simulaciones de incendio bajo la curva ISO 834, utilizando termopares por 120 minutos. Los resultados mostraron correlaciones muy cercanas con la literatura para recubrimientos de mortero a base de cemento, así como particularidades sobre revestimientos de yeso y la posibilidad de utilizar pinturas intumescentes como protección pasiva en elementos de hormigón armado.

Palabras clave: fuego, revestimiento contra incendios, hormigón, protección pasiva, programa experimental.

1. INTRODUCTION AND LITERATURE REVIEW

Currently, it is complex to technically support the use of fire protective coatings in at least two situations: a) in retrofit construction, where the thickness of the concrete cover of an existing building is not in accordance with the requirements of current Brazilian or foreign standards for a given TRRF (Required Fire Resistance Time); and b) to compensate the covering thickness (aiming at fire action) in concrete elements with constructive faults or design errors (related to insufficient thickness) in “new” construction (built, in theory, with the current standards). ABNT NBR 15200:2012 does not provide clear alternatives to these exceptional cases of non-compliance, except for the automatic reduction of the TRRF, which can, in practice, result in a situation of non-compliance with ABNT NBR 14432:2001 and Fire Department Technical Instructions.

In this context, this research will deal with the fireproof coatings allowed by ABNT NBR 15200:2012, and also examine other solutions, such as intumescent paints, aiming at extending the options for cement mortars and plaster coatings (which should be experimentally proven, as prescribed in the aforementioned standard), for use in situations such as retrofit construction or structural restoration or for execution errors, which may have many limitations, including architectural ones.

Due to its fire behavior, very similar to the concrete, the use of cement-based mortar coatings as passive protection are already well established in the technical field. The current standardization (ABNT NBR 15200:2012) recommends the use of plaster, vermiculite and fiber coatings depending on the performance of an experimental test that proves their efficiency. However, there has been a history of recommendation and use of these materials since the 1980s (Landi, 1986; Almeida, 1984).

The old ABNT NBR 5627:1980, currently canceled, basically stated that if there was a lime and sand mortar coating adhered to the structure, it would be possible to reduce 10mm of concrete covering for each 15mm thickness of this coating (67% efficiency). Still, if plaster, asbestos fibers or vermiculite mortar were used, 10mm of concrete cover could be reduced for each 4mm of these coatings (250% efficiency).

Malhotra (1982) points out that gypsum is calcined at about 150 °C to produce plaster ($\text{CaSO}_4 \cdot 1/2\text{H}_2\text{O}$) which, when mixed with water once again, reverts to gypsum. It can be used mixed with sand, lime or light aggregates such as perlite or vermiculite. On exposure to high temperatures, it changes to the hemi-hydrate between 100 °C and 140 °C, and releases a significant amount of moisture which absorbs significant amount of heat. Between 400 °C and 500 °C, the hemi-hydrate calcines and transforms into an insoluble anhydrite.

In addition, Alexander (1982) points out that the fire resistance of plaster can be attributed to a number of reasons. Gypsum crystals contain 50% water by volume and about 21% by weight. On exposure to intensive heat, structures coated by plaster remain substantially at about 100 °C to 140 °C until the plaster is changed to the hemi-hydrate; and the temperature does not exceed 250 °C until dehydration to anhydrous calcium sulfate is completed. This behavior has advantages such as eliminating thermal shock, preventing premature spalling of concrete or excessive thermal expansion. It further limits the expansion of the protected structure by limiting its temperature rise and thereby increasing the fire resistance time.

Concerning intumescent paints, there are numerous researches on steel structures, where this coating system is widely used as a fire protective coating (Silva; Bilotta; Nigro, 2017; Atefi; Nadjai; Ali, 2017; Ogrin; Saje; Hozjan, 2017; Lucherini; Maluk, 2017), but there are not many records in scientific articles about its application on concrete structures. In this context, in the experimental program of this article, the product employed is a water-based acrylic paint, similar in appearance to conventional paintings. When in contact with temperatures above 200 °C, the protective layer expands up to 60 times the original dry thickness of the material, promoting thermal protection of the concrete substrate at temperatures above 1000 °C.

2. EXPERIMENTAL PROGRAM

Two test events were conducted with four concrete elements each, with 25 MPa compressive strength (f_{ck}) and aged one year, under the ISO 834 fire standard curve during 120 minutes (2 h). The tests took place at the Fire Safety Laboratory and Explosions (LSFEx) of IPT (Institute for Technological Research), located in the University City, at Almeida Prado Street, 532, Butantã, São Paulo. The assessment was performed during and after the test by visual inspection (spalling intensity analysis) and with reference to an uncoated element. Each element was 2.40 m high, 30 cm deep and 40 cm wide.

In addition, the protective capacity of each coating and its insulation were analyzed through the evolution of temperatures inside the concrete elements, which were monitored using seven thermocouples per element (28 thermocouples per test), strategically installed. Per element, six thermocouples were positioned inside the concrete mass and one outside, to measure the temperature insulation capacity), as shown in Figures 1 and 2.

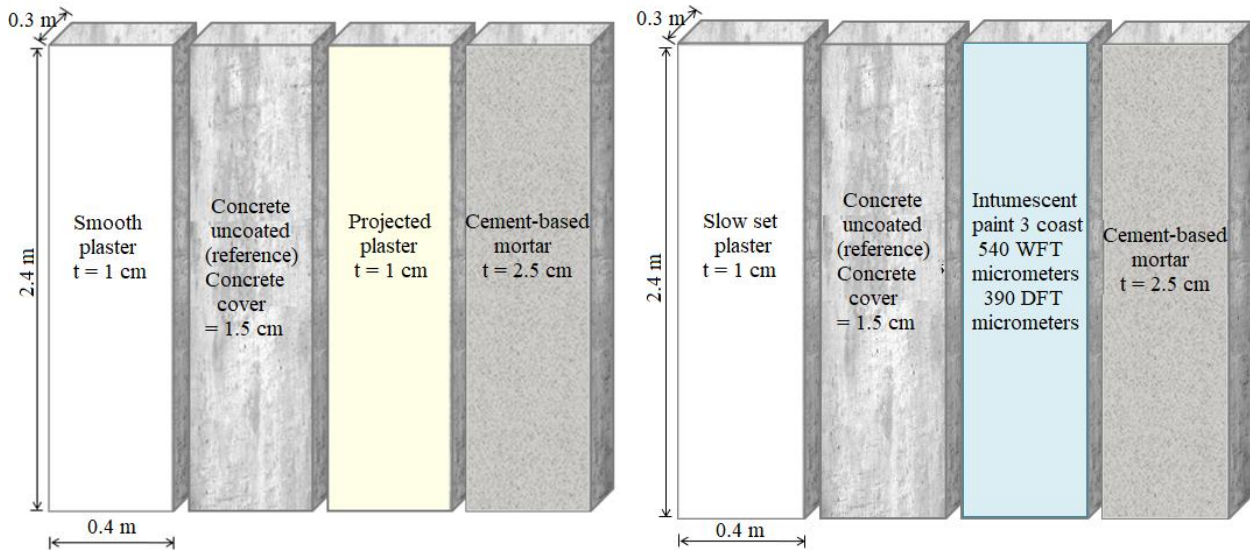


Figure 1. Concrete elements and coating systems that went through tests in both fire simulations (1st test event at left and 2nd test event at right).

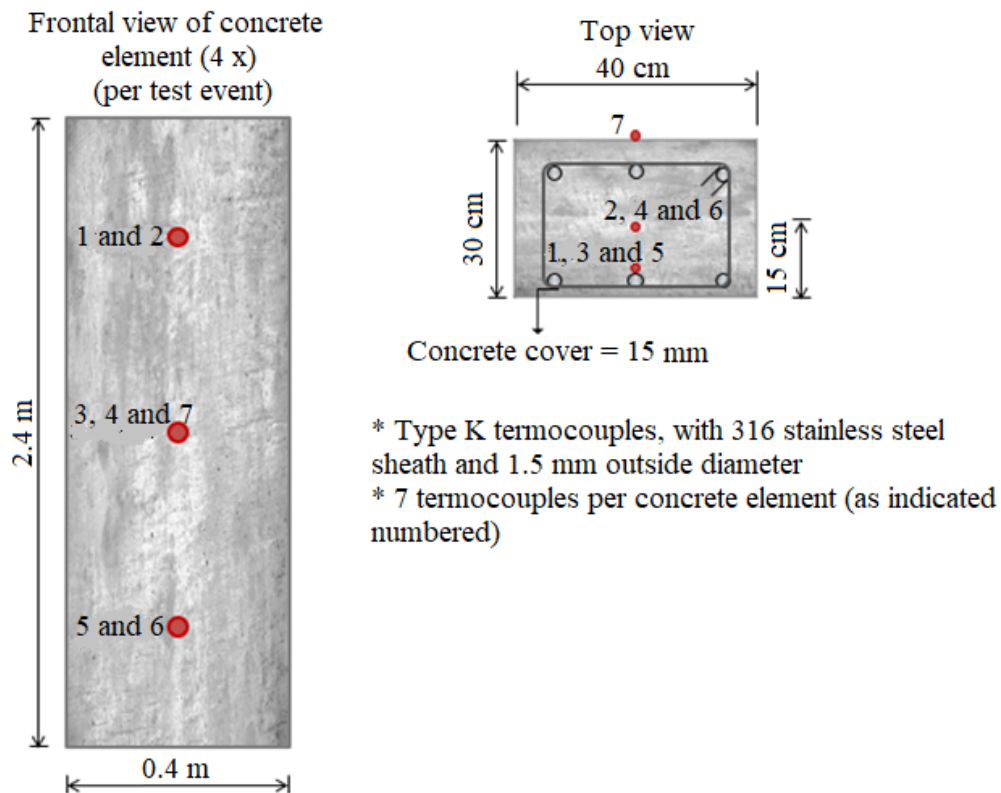


Figure 2. Detail of thermocouples location for both test events.

In all, five types of fire protective coatings were tested: slow-set plaster (popular in Brazilian market) and smooth formulated plaster (both hand applied), industrialized cement-based mortar (prepared on site), intumescent paint and projected plaster (applied with industrial equipment). The slow-set plaster, smooth formulated plaster and projected plaster have different chemical compositions, as will be discussed below, depending on their origin.

2.1 Details of concrete elements construction and coating systems application

In September 2017, the formwork and reinforcement were assembled [(stirrups with hooks, according to Kodur (2005)], thermocouples installed, and the concrete elements themselves were constructed inside the shed provided by IPT, in São Paulo. Concrete was designed with type CP II-E-40 cement, quartz pit natural fine sand, gravel sand and limestone gravel. The water was set at 175 L/m³ and a plasticizer/water reducer admixture was used to get a consistency of 20 ± 3 cm, gauged by slump-test. As planned, only one concrete mixer truck was involved in the pouring of the eight elements, leaving no room for variation of the concrete material when analyzing the results of the experimental tests. The eight samples were constructed under the same conditions and with the same batches of materials (formwork, concrete, reinforcement and thermocouples). The concreting event was controlled and the samples were molded and tested, with compressive strengths of 20.2 MPa (7 days) and 25.6 MPa (28 days), respectively. The values obtained were compatible with the 25 MPa f_{ck} predicted for 28-day age.

After the construction of the eight elements, a 6-month period of concrete hydration degree was waited for the application of fire protective coating systems (preparation of base and coating layer itself). During these six months the elements were stored inside the shed and protected with a non-adherent plastic tarp, just to prevent impregnation of dirt on the surface or other types of damage or even vandalism. In March 2018, as planned, all fire protective coatings were applied.

On the four elements related to the first test event, three types of coating were applied (in one of them, the reference one, no coating was applied): a) type M30 smooth formulated plaster, hand applied with a steel trowel; b) type P80 projected plaster, applied using M280 projection machine; and c) general purpose industrialized mortar, sold in 20 kg bags.

On the four elements related to the second test event, three types of coating were also applied (as in the first event, in one of the elements, the reference one, no coating was applied): a) slow-set plaster, hand applied with a steel trowel; b) intumescent paint, type CKC-333; and c) general purpose industrialized mortar, sold in 20 kg bags.

Both the hand applied plaster and the projected plaster were applied with a thickness of 1.0 cm, controlled using a digital caliper and a thickness jig. The intumescent paint was applied in three coats totaling a wet thickness of 540 micrometers, term internationally known as WFT (Wet Film Thickness), which corresponds to 390 micrometers dry thickness, term known as DFT (Dry Film Thickness).

The coating layers themselves were applied approximately 15 days after the preparation of the roughcast mortar [rolled for plaster and troweled for mortar], following the deadlines that commonly occur on site. From March 2018 to the end of August 2018, the elements were kept uncovered within IPT shed in order to promote enough hydration degree of the coatings, as in a normal work situation, as shown in Figure 3.

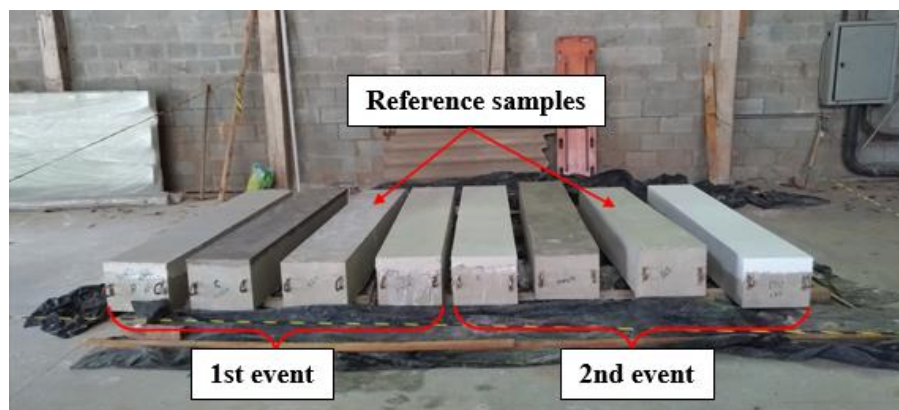


Figure 3. Detail of the finished elements with coatings applied, except for the reference samples.

2.2 Details of the fire simulation tests

The fire simulation tests were carried out in the furnace of the Fire and Explosion Safety Laboratory of the Institute of Technological Research of São Paulo (IPT-SP), a center of excellence in technology in Brazil and a reference in this type of test, with dimensions that meet the planned thermal program. The furnace used in the experimental program has a system with five natural gas burners, arranged on both side walls and positioned so that there is no frontal encounter between them.

2.2.1 First test event (1st event)

The four elements of the first test event were tested at once, unloaded and basically with one face exposed to fire (the largest face, 40 cm wide and 2.40 m high), in order to evaluate the influence of the coating without any interference. This also allowed the rear face (where the thermocouples were installed) to remain freely accessible during the fire simulation test. Prior to the test, after 11 months of the elements' construction, control specimens were tested again, and a compressive strength of 30.4 MPa was found. On August 30th, 2018, the first fire simulation event was carried out, under the ISO 834 curve, for 120 minutes. Table 1 shows the maximum and average temperature values detected by the thermocouples located on the reinforcement, in each of the specimens, at 120 min of test.

Table 1. Temperatures of thermocouples positioned on the reinforcement (concrete cover region), at 120 min of test.

Specimen	Temperatures (°C)	
	Maximum (thermocouple indicated)	Average (thermocouples 1, 3 and 5)
Reference (uncoated)	553 (thermocouple 1)	543
Industrialized cement-based mortar coating (25mm)	198 (thermocouple 3)	195
Smooth formulated plaster coating (10 mm)	206 (thermocouple)	186
Projected plaster coating (10 mm)	283 (thermocouple)	231

24 hours after the end of the test, the furnace was opened for visual inspection of the elements. Surface spalling was observed, uniformly distributed on the face of the reference element. No reinforcement exposure was detected. Partial fall of the coatings was verified on the other elements, but no superficial damage to the concrete, as shown in Figure 4.



Figure 4. Detail of the elements and coatings condition after furnace opening (event 1): smooth formulated plaster coating, reference element, projected plaster coating and cement-based mortar coating.

The smooth formulated plaster sample still had some coating remaining upon the furnace opening (without any integrity or adhesion), an amount of 46% of the total area exposed to the fire. For the cement-based mortar sample, this number was 41%. Carefully investigating the elements using a hammer, it was found that the remaining coatings of smooth formulated plaster and mortar were completely friable and the remaining part almost spontaneously displaced, however, the roughcast mortar applied as adhesion was intact in both elements.

Notably, the sample coated with projected plaster still had part of the plaster adhered (in 100% of the sample), partially intact and with little hollow sound. However, there was not enough integrity for a pullout test by conventional methods, as the sample could easily be removed by mechanical scraping. It was found that the remaining layer was working only as a sacrificial layer (physical barrier) and with poor adherence. Using a digital caliper, it was verified that a delamination of the projected plaster occurred, with a thickness of the order of 5 mm and remaining in the concrete sample a thickness of the order of 6 mm (1 mm deviation from the original predicted thickness of 10 mm).

The reference sample, uncoated, also caught attention for the small amount and depth of spalling, corresponding to an area of the order of 19% of the original sample at a typical (maximum) depth of about 6 mm (measured at several points). In other words, even in the uncoated reference element, there was no exposure of the reinforcement (which had a 15mm concrete cover). In fact, there was no exposure of the reinforcement in any element tested in this first event.

The temperature evolution obtained inside the samples confirmed the visual and qualitative analysis of the fireproof coatings' performance. As observed in Figure 5, the heat distribution was uniform within the samples, according to the depth of each thermocouple. It is also noted that the three thermocouples located in the concrete cover region of the reference element differ greatly from the rest.

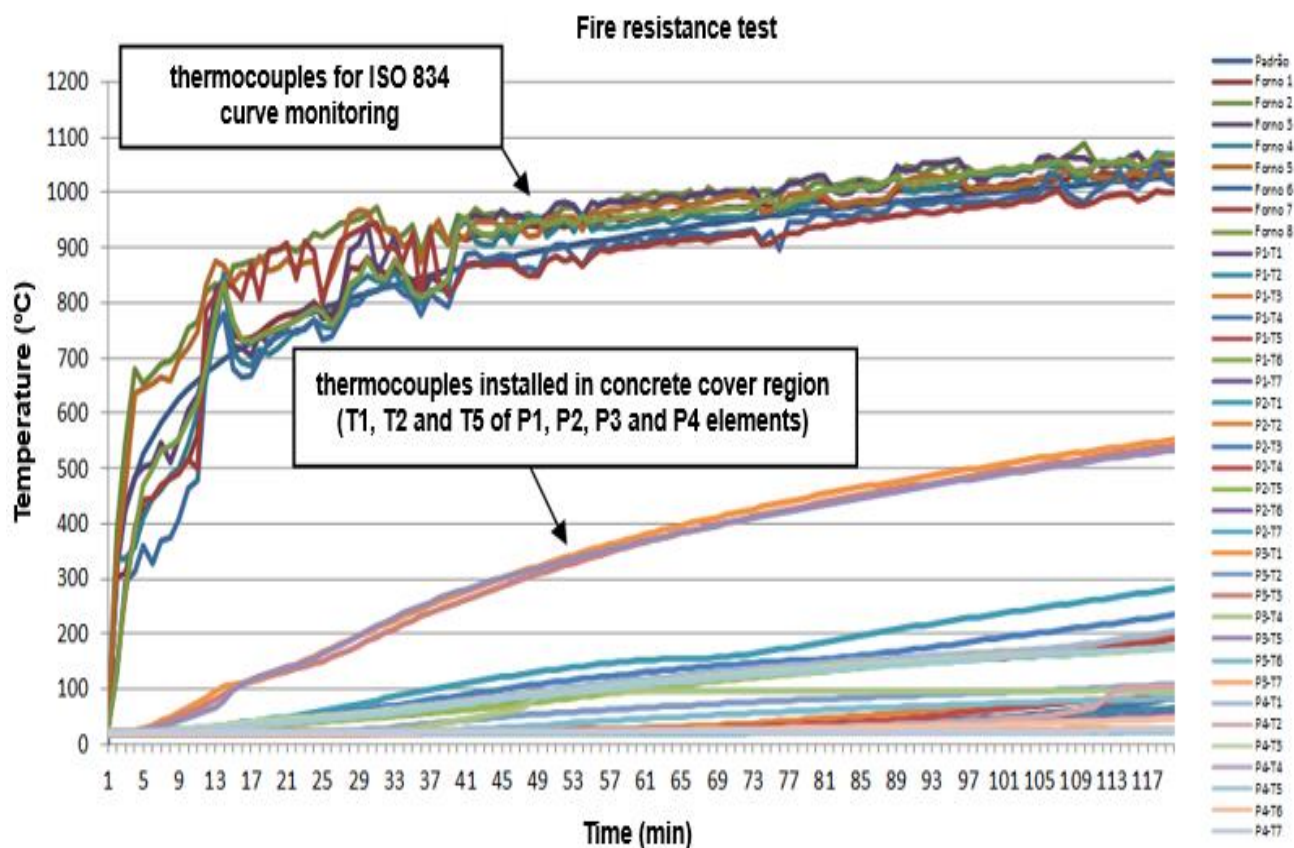


Figure 5. Temperatures obtained inside the furnace and inside the elements of 1st event.

2.2.2 Second test event (2nd event)

On September 5th, 2018, the second fire simulation event occurred, under the ISO 834 curve for 120 minutes. After 53 minutes of testing, it was already observed the flaking of all the slow-set plaster coating, quite different from what occurred in the first test event, taking part of the concrete adhered. Also, at 6 minutes of testing, the intumescent paint started to act. During this period, we also noticed the beginning of small flaking points of the reference element, without coating. At 20 minutes, the intumescent paint had a darker-colored “red-hot element” appearance and small incandescent spots, as shown in Figure 6. Table 2 shows the maximum and average temperature values of the thermocouples located on the reinforcement in each of the specimens at 120 min.

Table 1. Temperatures of thermocouples positioned on the reinforcement (concrete cover region), at 120 min of test.

Specimen	Temperatures (°C)	
	Maximum (thermocouple indicated)	Average (thermocouples 1, 3 and 5)
Reference (uncoated)	557 (thermocouple 3)	533
Industrialized cement-based mortar coating (25mm)	255 (thermocouple 3)	241
Intumescent paint coating (540 micrometers WFT / 390 micrometers DFT)	386 (thermocouple 5)	359
Slow-set plaster coating (10 mm)	559 (thermocouple 1)	487

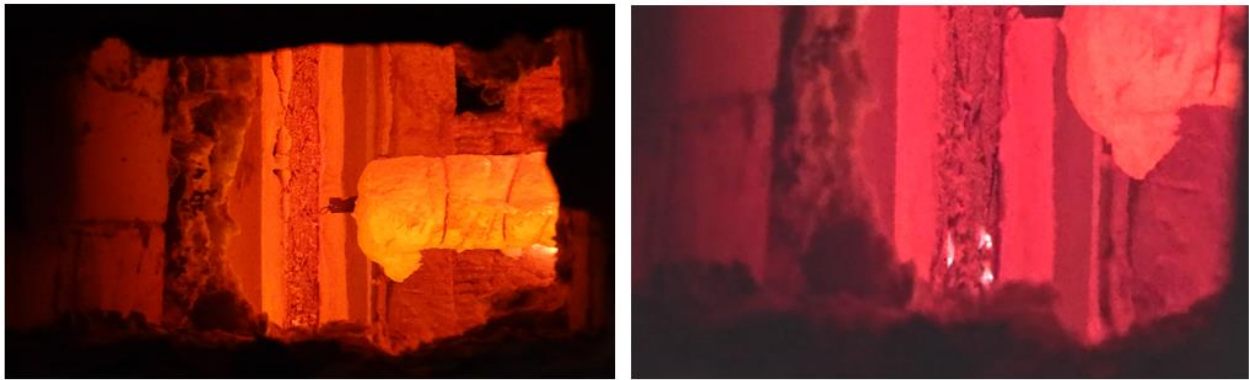


Figure 6. Detail of the “red-hot element” appearance of the intumescent paint-coated element (dark on the left) and small glowing spots on this same element (on the right).

24 hours after the end of the test, the furnace was opened for visual inspection of the elements. Surface spalling was observed, uniformly distributed on the reference element face exposed to fire. No reinforcement exposure was detected.

In the element coated by the slow-set plaster, a large spalling / flaking was observed at its top, and no trace of the roughcast mortar applied as adhesion, as well as 100% of detachment of the plaster coating itself.

In the element coated with cement-based mortar, all the roughcast mortar kept adhered in the element and the coating itself detached almost entirely. Finally, the intumescent paint was detected covering the entire face of its concrete element, expanded and white colored, without exposing the concrete surface or reinforcement, as shown in Figure 7.

Carefully investigating the elements with the use of a hammer, it was found that, in the sample coated by slow-set plaster, besides the large spalling with reinforcement exposure, there was a friable layer with no strength in almost all the area exposed to fire (on the concrete surface). In the reference sample, the material still adhered to the surface was also friable throughout the covering region. Nevertheless, the roughcast mortar applied as adhesion of the mortar-coated element and the concrete surface of the intumescent paint-coated element were intact.

To summarize, the concrete was completely intact and preserved in the case of the elements coated with cementitious mortar and intumescent paint, showing no signs of a typically friable material or exposed reinforcement. The spalling area of the sample coated with slow-set plaster, where the reinforcement exposure occurred, was measured with a measuring tape, representing approximately 20% of the total area, suggesting that the slow-set plaster coating detached from the surface much before that observed in the 1st event and did not protect the concrete substrate.



Figure 7. Detail of the elements and coatings condition after furnace opening (event 2): slow-set plaster coating, reference element, intumescent paint coating and cement-based mortar coating.

Also, among all the reinforcement from the face exposed to fire, it was verified that only 6% was actually exposed. Notably, the intumescent paint-coated sample protected the concrete element well, with no indication of flaking. The surface was so completely well-finished that, in the case it had been clean, it could hardly be said that it had been subjected to a fire simulation test.

Using a digital caliper, it was found that there was severe spalling in the slow-set plaster coated sample, from 19 mm to 27 mm (maximum), over an area of approximately 20% of the total sample area (60 cm x 30 cm), as shown in Figure 7. The remaining friable part, in turn, had a thickness of the order of 2 mm to 3 mm (Figure 7), which was smaller than the reference sample one in of both events, as will be noted below.

In turn, the reference sample also drew attention for the small amount and depth of spalling. The flaking corresponded to an area of the order of 40% of the original sample in a typical (maximum) depth of about 7.5 mm (measured at several points) only, although the sample had turned friable in 100% of the area exposed to fire in this same measured depth. In other words, there was no exposure of the reinforcement (with minimum coverage of 15 mm). In fact, there was only reinforcement exposure in the slow-set plaster coated element at the second test event (underperforming the reference sample, uncoated). The expansion of the remaining intumescent paint, along its entire area exposed to fire, was also measured. In this case, it had no adhesion and was easily removed with a spatula (manually). From the scraped area, it was possible to measure with a caliper an expandability of 110 mm to 112 mm, which corresponds to the order of 30 times the original applied thickness of 390 micrometers dry (DFT), according to the manufacturer's specifications.

The evolution of temperatures obtained inside the samples also confirmed the visual and qualitative analyzes of the performance of the fireproof coatings. As observed in Figure 8, the heat distribution was uniform within the sample according to the depth of each thermocouple. A substantial increase in temperature was also noted in the three thermocouples of the reference sample in the concrete cover region, as well as in the three for slow-set plaster coated sample, from 53 min (highlighted in red), probably when the total detachment of this coating took place, taking with it part of the concrete and exposing the reinforcement. This behavior differs greatly from the exhibited by the rest of the thermocouples.

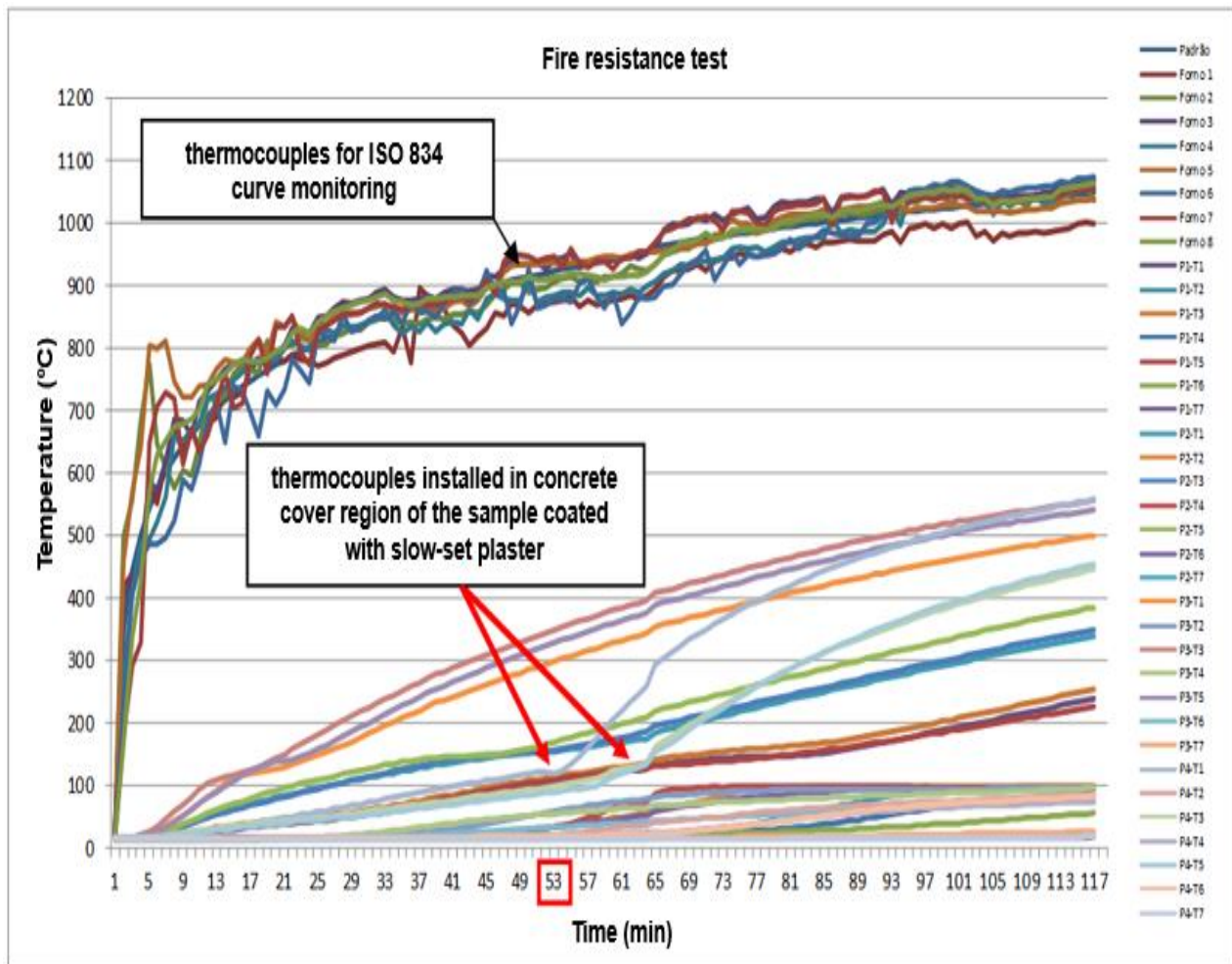


Figure 8. Temperatures obtained inside the furnace and inside the elements of 2nd event.

Although the reinforcement was not exposed to fire by spalling in the region of thermocouples 3 and 5, under these conditions (after spalling), for approximately 65 minutes, due to the thermal conductivity of the steel, the temperature of the reinforcement measured at these points was only 20% lower than in the exposed region. It was expected to be 66% lower, if compared to the first test event involving smooth formulated plaster, where there was no spalling.

3. RESULTS DISCUSSION AND COMPLEMENTARY TESTS

In general, it can be said that all the elements, except for the slow-set plaster sample (which was analyzed separately by complementary examinations), presented good performance when exposed to fire for 120 min (2 h). The concrete practically maintained its original integrity in the coated elements and presented damage (spalling / flaking) lower than 7.5 mm depth in the reference samples for a concrete coverage of only 15 mm (not exposing the reinforcement). In these reference samples, despite an initial flaking measured between 19% and 40% of the total area, after percussion hammer inspection, it can be safely stated that all the area exposed to fire was completely friable at the same depth, that is, in terms of integrity, about 6 mm depth of damage was verified in the reference sample of the first event and the order of 7.5 mm in the second event. These values are considered irrelevant to the 2 h test under the ISO 834 curve.

Also, regarding the measured temperatures (in the reference samples), there are a lot of similarities between the two test events, as it can be seen in Figures 5 and 8 (maximum 10 °C difference). In this case, on the average of the two test events, it can be stated that 15 mm of concrete cover thickness (without any coatings) was enough to record a temperature below 550 °C (on average 538 °C), for a temperature of almost 1000 °C in the furnace within 120 minutes of testing. That is, the 15 mm cover insulated a temperature of the order of 450 °C, without any reinforcement exposure for a maximum flaking of 7.5 mm with the rest of the cover (about 50%) still quite intact, as exposed in Table 3.

Table 3. Performance comparison of each type of coating in insulating the average temperature in thermocouples 1, 3 and 5, positioned in the reinforcement (cover region), at 120 min of test (regarding the reference element).

Test event	Samples in comparison	Average temperature (°C)	Difference	Isolation
Event 1	Reference (uncoated)	543	348	64%
	Cement-based industrialized mortar coating (25 mm)	195		
	Reference (uncoated)	543	357	66%
	Smooth formulated plaster coating (10 mm)	186		
	Reference (uncoated)	543	312	57%
	Projected plaster coating (10 mm)	231		
Event 2	Reference (uncoated)	533	292	55%
	Cement-based industrialized mortar coating (25 mm)	421		
	Reference (uncoated)	533	174	33%
	Intumescent paint coating (540 micrometers WFT / 390 micrometers DFT)	359		
	Reference (uncoated)	533	46	9%
	Slow-set plaster coating (10 mm)	487		

Specifically on the cement-based mortar coatings, it was noted that probably, because of the temperatures obtained, they detached from the roughcast mortar base, either at the end or even after the end of the test, during natural cooling (the furnace was opened 24 h after the end of the test). Interestingly, the roughcast mortar applied directly to the concrete element (with 8mm x 8mm toothed trowel) was completely adhered and intact, providing an absolutely intact concrete in both samples coated with this system. In this context, the 2.5 cm thick mortar coating worked well as a sacrificial layer during the two test events. The temperatures measured within the sample corroborate these considerations. The graphs in Figures 5 and 8 show a linearity in the evolution of the measured temperature values, which is consistent with an interference-free heat transmission, i.e., no flaking during the test event (even considering the coatings in this case). An anomalous behavior, for example, a peak or a discontinuous temperature growth rate, could indicate localized flaking or even reinforcement exposure. It would greatly increase the measured temperature values, with a much faster heating rate compared to concrete one, because of the significant difference in the thermal conductivity of these two materials.

In the case of intumescent paint, it could be seen that it quickly started expanding itself in the first minutes of the test event, which was expected because the action of this type of chemical reaction starts at approximately 200 °C (the ISO 834 curve reaches 550 °C within the first five minutes).

What was striking in this case is that only the thickness of 390 micrometers (three coats / DFT) was enough to guarantee the complete integrity of the structural element, keeping the original sample surface completely preserved. Despite the impression of “red-hot element” and signs of incandescence, there was no damage in 100% of the area exposed to fire, although with internal measured temperatures higher than those registered in the mortar coating, for example.

What caught attention and motivated complementary chemical tests and examinations were the analyzes of the plaster coated samples' integrity. In the first event, it was found that the smooth formulated plaster applied with steel trowel completely preserved the integrity of the concrete element, including clear signs of the still adhered rolled roughcast mortar base. In this case, it is assumed that the same effect of the mortar coatings occurred, that is, the plaster must have detached from the roughcast mortar at the end or even after the end of the test, during natural cooling, providing an absolutely intact concrete in the sample coated with this system. In this context, only 1.0 cm of smooth formulated plaster coating worked well as a sacrificial layer.

In turn, in this same event, the projected plaster presented a delamination of the order of 50% of its thickness. This also greatly preserved the integrity of the concrete sample, which was still protected by approximately 6 mm of plaster. On the other hand, this remaining plaster had little adhesion and had a hollow sound and fluffy surface when subjected to steel hammer percussion tests. This leads to believe, even from the internal temperatures, that the delamination actually occurred during the fire simulation test (from inspections carried out, within 30 to 40 minutes after the start of the test). That is, for a period of 80 to 90 minutes of testing, this element had only been protected by 6 mm of projected plaster thickness. It is interesting to compare these considerations with the recorded temperature values. Despite a remaining plaster thickness after completion of the test, the internal temperatures were slightly higher when compared to the smooth formulated plaster sample, which suggests that there was even a delamination during the test and that a smaller thickness functioned as a layer of sacrifice. At 120 minutes of testing, an average of 231 °C was recorded in the projected plaster-coated element, approximately 25% higher when compared to the smooth formulated plaster (186 °C). We remember that they are materials of the same nature, including very similar chemical, mineralogical and thermal composition, which corroborates with the earlier delamination in the projected plaster (perhaps due to the application method) and the preservation of the smooth formulated plaster throughout the period of the first test event (detachment only after furnace cooling).

Specifically on slow-set plaster coating applied in the second test event, with the same procedures as the smooth formulated plaster (first event), it was noted that there was a significant difference in the results obtained, represented by a severe spalling of concrete, with reinforcement exposure. It was the only sample with reinforcement exposure, among the eight tested in both test events. It is noteworthy that there was no spalling in the uncoated (reference) samples. The observed spalling had an approximate area of 60 cm x 30 cm, with a maximum depth of 27 mm, which was enough to expose the reinforcement, that had a 15 mm covering. Nevertheless, among total area of reinforcement that could be exposed, only 6% was actually exposed.

Based on the monitored temperatures, it is believed that the highest proportion spalling occurred between 40 and 50 minutes, since the behavior of the internal temperature evolution in the covering region changed dramatically at approximately 55 minutes. The behavior up to 55 minutes was very similar to that of the first test event plaster samples. From that moment on, there was a sudden change in the internal heating rate, recorded mainly by thermocouple 1 and later in the other thermocouples, which leads us to believe that the detachment of the coating system had already occurred, with reinforcement exposure and a change in the records, due to thermal conductivity of the steel (the first thermocouple line was fixed on the boundary longitudinal reinforcement concrete cover). The average temperature measured in the three thermocouples was 487 °C, with a maximum of 559 °C, that is, almost the same temperature as the reference samples, which presented peaks of

553 °C and 557 °C in the two test events, respectively.

As the experimental study was designed to have as few variables as possible [elements built at the same time, with the same concrete, procedures and manpower; same worker applying the troweled plaster coatings (smooth formulated and slow-set plaster, regardless of origin) on the elements, fire simulation tests under the same conditions etc.], it was assumed that the agent responsible for the anomalous behavior could be related exclusively to the material applied (slow-set plaster popular in the market). That said, it was decided to elaborate and carry out a plan of tests and complementary chemical and thermal exams in the three samples of plaster involved in the experimental study: M30 smooth formulated plaster, P80 projected plaster and slow-set plaster popular in the market.

Samples from the same batch of plaster used in the experimental study were collected and separated in order to identify any alteration, impurity or strange material. Results from the semiquantitative chemical analysis have already indicated a significant difference in “Loss on ignition” and “Sulfuric Anhydride”, as shown in Table 4.

Table 4. Results from the X-ray fluorescence semiquantitative chemical analysis.

Determinations	Results, in %		
	slow-set plaster popular in the market	P80 projected plaster	M30 smooth formulated plaster
Loss on ignition (LOI)	20,9	9,5	9,5
Sulfuric anhydride (SO ₃)	39,8	51,8	53,7
Calcium oxide (CaO)	32,5	32,2	31,2
Aluminum oxide (Al ₂ O ₃)	2,3	1,7	0,8
Magnesium oxide (MgO)	2,2	0,1	0,2
Silicic anhydride (SiO ₂)	1,9	3,6	3,4
Phosphorus oxide (P ₂ O ₅)	0,2	0,2	0,5
Ferric oxide (Fe ₂ O ₃)	0,1	0,2	0,2
Strontium oxide (SrO)	0,1	0,1	0,2
Potassium oxide (K ₂ O)	n.d.	0,4	0,4

In the slow-set plaster sample, the value obtained for fire loss differed by 120% and sulfuric anhydride about 35% when compared to the smooth formulated and projected plaster samples of the first test event, which in turn were quite high similar. In the case of sulfuric anhydride, it is noted that the value obtained in the test was still 25% below the limit required in the standard ABNT NBR 13207:2017 - Plaster for construction - Requirements, i.e. the sample sold in the market does not follow the limits prescribed by national standards. Concomitantly, thermogravimetric analysis (TG / DTG) (differential thermal and simultaneous thermogravimetric analysis) were performed to identify the mass losses, where the fire loss values were confirmed with minimal differences from those obtained in the X-ray fluorescence semiquantitative chemical analyzes, as shown in Table 5.

Table 5. Mass losses from TG / DTG curves.

Material	Mass loss as a function of temperature range					Total loss (%)	
	°C	28-69	69-168	168-1000			
Slow-set plaster	°C	28-69	69-168	168-1000		20,0	
	%	0,73	3,46	15,8			
Interpretation of mass losses as a function of temperature range:							
1. 23 – 82°C: beginning of free water loss;							
2. 82 – 211°C: end of free water loss and adsorption water;							
3. 211 – 934°C: decarbonation of carbonated phases;							
4. 934 – 1000°C: probable beginning of sulfur loss.							
Smooth formulated Plaster M30	°C	28-78	78-253	253-300	300-934	934-1000	8,63
	%	1,60	5,15	1,61	1,58	0,27	
Interpretation of mass losses as a function of temperature range:							
5. 28 – 78°C: beginning of free water loss;							
6. 78 – 253°C: end of free water loss and adsorption water;							
7. 253 – 300°C: mass gain. Probable oxidation of metallic elements present in Ankerite;							
8. 300 – 934°C: decarbonation of carbonated phases;							
9. 934 – 1000°C: probable beginning of sulfur loss.							
Projected plaster P80	°C	28-82	82-211	211-934	934-1000		8,70
	%	1,60	5,15	1,61	0,34		
Interpretation of mass losses as a function of temperature range:							
1. 23 – 82°C: beginning of free water loss;							
2. 82 – 211°C: end of free water loss and adsorption water;							
3. 211 – 934°C: decarbonation of carbonated phases;							
4. 934 – 1000°C: probable beginning of sulfur loss.							

The high fire loss in the slow-set plaster sample, confirmed by two test methods [X-ray fluorescence semiquantitative analysis and thermogravimetric analysis (TG / DTG) (differential thermal and simultaneous thermogravimetric analysis)] can be associated with the high volume of CO₂ released by the thermal decomposition of the carbonates (dolomite and calcite), as will be verified in the analyzes below. Also, in order to identify any difference that could justify the anomalous behavior of the slow-set plaster coating, semi-quantitative mineralogical X-ray diffraction analyzes were performed, as shown in Table 6.

Table 6. Results of semi-quantitative mineralogical analyzes of the phases analyzed by X-ray diffraction.

Material	Compounds or mineralogical phases	Molecular formula	Results (%)
Slow-set plaster	Bassanite	$\text{CaSO}_4 \cdot \frac{1}{2}\text{H}_2\text{O}$	65,2
	Dolomite	$\text{CaMg}(\text{CO}_3)_2$	22,5
	Calcite	CaCO_3	5,5
	Anhydrite	CaSO_4	2,0
	Alpha-Quartz	αSiO_2	1,1
	Hornblende	$\text{Ca}_{3,32}\text{Si}_{14,56}\text{Al}_{2,00}\text{Mg}_{6,98}\text{Fe}_{2,66}\text{Ti}_{0,12}\text{Mn}_{0,04}\text{K}_{0,03}\text{H}_{4,00}\text{O}_{47,60}\text{F}_{0,40}$	1,0
	Olivine	$\text{Fe}_{0,145}\text{Mg}_{1,854}\text{SiO}_4$	0,8
	Chrysotile	$\text{Mg}_3(\text{Si}_2\text{O}_5)(\text{OH})_4$	0,7
	Ankerite	$\text{CaFe}_{0,23}\text{Mg}_{0,77}(\text{CO}_3)_2$	0,7
	Zeolite	SiO_2	0,5
Projected plaster P80	Bassanite	$\text{CaSO}_4 \cdot \frac{1}{2}\text{H}_2\text{O}$	93,2
	Anhydrite	CaSO_4	4,3
	Dolomite	$\text{CaMg}(\text{CO}_3)_2$	1,3
	Calcite	CaCO_3	0,6
	Gypsum	$\text{CaSO}_4 \cdot 2\text{H}_2\text{O}$	0,4
	Olivine	$\text{CoMg}_7(\text{SiO}_4)_4$	0,1
	Quartz	SiO_2	< 0,1
Smooth formulated plaster M30	Bassanite	$\text{CaSO}_4 \cdot \frac{1}{2}\text{H}_2\text{O}$	88,9
	Anhydrite	CaSO_4	7,1
	Ankerite	$\text{Ca}_{3,15}\text{Fe}_{1,89}\text{Mg}_{0,81}\text{Mn}_{0,15}(\text{CO}_3)_6$	1,2
	Dolomite	$\text{CaMg}(\text{CO}_3)_2$	1,1
	Calcite	CaCO_3	1,2
	Gypsum	$\text{CaSO}_4 \cdot 2\text{H}_2\text{O}$	0,6
	Alpha-Quartz	αSiO_2	< 0,1

To summarize, it was observed a large difference in the slow-set plaster sample when compared to the smooth formulated and projected plaster, mainly in the contents of bassanite and dolomite. Thus, it is believed that the presence of a higher carbonate content (dolomite and calcite), identified in high proportions in the thermal decomposition of the slow-set plaster sample, will certainly

generate a significant volume of carbon dioxide, which combined with a rapid heating rate environment and excessive furnace temperatures (characterized by the ISO 834 curve), will generate larger expansion pressures, resulting in severe spalling, including reinforcement exposure. In other words, we believe that if the slow-set plaster sample complied with the minimum requirements of current standardization (free of high carbonate content), the fire behavior of plaster coatings would be very similar. Thus, it is important to characterize the properties of the plaster which, as observed, has a unique behavior and greatly interferes in the performance of the coating when used with fireproof purposes.

4. CONCLUSIONS

1. In this experiment, 1.0 cm of plaster was equivalent to 2.5 cm of cement-based mortar, as shown in the relevant technical literature, obviously excluding the slow-set plaster sample of 2nd test event, which did not meet current standards. It is essential that the plaster used as fireproof coating meets the basic requirements prescribed in national standardization and does not contain impurities with high levels of carbonate materials;
2. In this experiment, the efficiency of cement-based mortar coating was equivalent to that of concrete (confirmed by thermocouple temperatures), as reported in the literature (Silva, 2012);
3. The intumescent paint obtained about half the efficiency of the mortar and plaster coatings (from test event 1) with a thickness of 540 WFT. It can be assumed that in this experiment, 1.0 mm thickness of intumescent paint would have had the same performance in terms of fireproof coating as the thicknesses of cementitious mortar (25 mm) and plaster (10 mm);
4. It was observed that the concrete spalling, regardless of its magnitude or region of occurrence, can lead to a significant increase of reinforcement temperatures, even in unexposed regions, due to the thermal conductivity of the steel.

5. REFERENCES

- Alexander, B. (1982). *Behaviour of gypsum and gypsum products at high temperatures*. RILEM Committee PHT-44, British Gypsum, East Leake, Loughborough, England.
- Almeida, D. F. (1984). *As estruturas de concreto armado e o fogo, comportamento, consequências, restauração*. Dissertação (mestrado) - Escola Politécnica, Universidade de São Paulo, São Paulo.
- Associação Brasileira de Normas Técnicas. (1980). *NBR 5627: Exigências particulares das obras de concreto armado e protendido em relação à resistência ao fogo*. Rio de Janeiro, 3 p.
- Associação Brasileira de Normas Técnicas. (2014). *NBR 6118: Projeto de estruturas de concreto, procedimentos*. Rio de Janeiro, 238 p.
- Associação Brasileira de Normas Técnicas. (2017). *NBR 13207: Gesso para construção civil - Requisitos*. Rio de Janeiro, 3 p.
- Associação Brasileira de Normas Técnicas. (2001). *NBR 14432: Exigências de resistência ao fogo de elementos construtivos de edificações, Procedimento*. Rio de Janeiro, 14 p.
- Associação Brasileira de Normas Técnicas. (2012). *NBR 15200: Projeto de estruturas de concreto em situação de incêndio*. Rio de Janeiro, 48 p.
- Atefi, H., Nadjai, A., Ali, F. (2017). *Numerical and experimental investigation of the thermal behaviour of coated cellular beams with intumescent coatings at elevated temperatures*. In: IFireSS 2017 – 2nd International Fire Safety Symposium. Naples, Italy, June 7-9. p. 257-264.
- Kodur, V. K. R. (2005). *Guidelines for fire resistance design of high-strength concrete columns*. Ottawa, Ontario, Canadá: IRC/NRC. (Report NRCC-47729). Disponível em: <<http://irc.nrc-cnrc.gc.ca/pubs/fulltext/nrcc47729/>>. Acesso em: novembro de 2007.

- Landi, F. R. (1986). *Ação do incêndio sobre as estruturas de concreto armado*. Boletim técnico nº 01/86. São Paulo: Escola Politécnica, Universidade de São Paulo. 24p.
- Lucherini, A., Maluk, C. (2017). *Novel test methods for studying the fire performance of thin intumescent coatings*. In: IFireSS 2017 – 2nd International Fire Safety Symposium. Naples, Italy, June 7-9. p. 565-572.
- Malhotra, H. L. (1982). *Properties of Materials at High Temperatures — Report on the work of technical committee 44-PHT*. Materials and Structures/Matériaux et Constructions. Vol. 15. N° 86. RILEM, Paris.
- Ogrin, A., Saje, M., Hozjan, T. (2017). *Effect of incomplete expansion of intumescent coating on mechanical response of steel frame in fire*. In: IFireSS 2017 – 2nd International Fire Safety Symposium. Naples, Italy, June 7-9. p. 365-372.
- Silva, D., Bilotta, A., Nigro, E. (2017). *Experimental analysis on the effectiveness of intumescent coatings in fire*. In: IFireSS 2017 – 2nd International Fire Safety Symposium. Naples, Italy, June 7-9. p. 249-256.
- Silva, V. P. (2012). *Projeto de estruturas de concreto em situação de incêndio, conforme ABNT NBR 15200:2012*. São Paulo: Blucher.

Structural masonry walls exposed to high temperatures with thermal expansion control

J. Menegon*¹ , A. G. Graeff¹ , L. C. P. Silva Filho¹ 

*Contact author: menegonjulia@gmail.com

DOI: <http://dx.doi.org/10.21041/ra.v10i1.440>

Reception: 24/09/2019 | Acceptance: 11/11/2019 | Publication: 30/12/2019

ABSTRACT

This study evaluates the behavior of small clay hollow-bricks walls exposed to high temperatures. Blocks measuring 14 and 19 cm thick were used, with strengths of 7 and 10 MPa. The thickness of the joints, the mortar, and the coating influence was evaluated. The temperatures of the furnace, the interior and the surface of the walls, the expansion of the blocks and the crushing of the joints were measured. It was possible to infer that the samples presented good performance, maintaining their integrity, thermal insulation, and load-bearing capacity. The restriction of the boundaries did not cause the spalling of the blocks, however, it was possible to observe the stress transfer to them in samples with rigid joint mortar. The masonry measuring 19 cm wide and the ones with coating showed better thermal performance.

Keywords: high temperatures; structural masonry; masonry walls; clay hollow-bricks; fire resistance.

Cite as: Menegon, J., Gaio Graeff, Â., Silva Filho, L. C. P. (2020), "Structural masonry walls exposed to high temperatures with thermal expansion control", Revista ALCONPAT, 10 (1), pp. 98 – 114, DOI: <http://dx.doi.org/10.21041/ra.v10i1.440>

¹ Universidade Federal do Rio Grande do Sul, Brasil.

Legal Information

Revista ALCONPAT is a quarterly publication by the Asociación Latinoamericana de Control de Calidad, Patología y Recuperación de la Construcción, Internacional, A.C., Km. 6 antigua carretera a Progreso, Mérida, Yucatán, 97310, Tel.5219997385893, alconpat.int@gmail.com, Website: www.alconpat.org

Responsible editor: Pedro Castro Borges, Ph.D. Reservation of rights for exclusive use No.04-2013-011717330300-203, and ISSN 2007-6835, both granted by the Instituto Nacional de Derecho de Autor. Responsible for the last update of this issue, Informatics Unit ALCONPAT, Elizabeth Sabido Maldonado, Km. 6, antigua carretera a Progreso, Mérida, Yucatán, C.P. 97310.

The views of the authors do not necessarily reflect the position of the editor.

The total or partial reproduction of the contents and images of the publication is strictly prohibited without the previous authorization of ALCONPAT Internacional A.C.

Any dispute, including the replies of the authors, will be published in the third issue of 2020 provided that the information is received before the closing of the second issue of 2020.

Paredes de albañilería estructural expuestas a altas temperaturas con medidas de control de dilatación

RESUMEN

Este estudio evalúa el comportamiento de paredes de bloques estructurales cerámicos a altas temperaturas. Se utilizaron bloques de 14 y 19 cm de ancho, con resistencias de 7 y 10 MPa. Se evaluaron los espesores de las juntas, el mortero para asentamiento y la influencia de revestimiento en la cara expuesta. Se midieron las temperaturas del horno, en el interior y en la superficie de las paredes, la dilatación de los bloques y el aplastamiento de las juntas. Se pudo inferir que las muestras presentaron buen desempeño, manteniendo su estanqueidad, aislamiento y resistencia mecánica. La restricción lateral no ocasionó descascaramiento de los bloques, sin embargo, se pudo observar transferencia de tensión entre ellos para morteros poco flexibles. Las mamposterías de 19 cm de ancho y aquellas revestidas presentaron mejor desempeño térmico.

Palabras clave: altas temperaturas; albañilería estructural; paredes de mampostería; bloques cerámicos; resistencia al fuego.

Paredes de alvenaria estrutural expostas a altas temperaturas com medidas de controle da dilatação

RESUMO

Este trabalho analisa o comportamento de miniparedes executadas com blocos estruturais cerâmicos em elevadas temperaturas. Utilizaram-se blocos de 14 e 19 cm de largura, com resistências de 7 e 10 MPa. Foram avaliadas as espessuras das juntas, a argamassa de assentamento e a influência de revestimento na face exposta. Mensurou-se as temperaturas do forno, no interior e na superfície das paredes, a dilatação dos blocos e o esmagamento das juntas. Pôde-se inferir que as amostras apresentaram bom desempenho, mantendo sua estanqueidade, isolamento e resistência mecânica. A restrição lateral não ocasionou deslocamento dos blocos, porém, pôde-se observar transferência de tensão para os mesmos para argamassas pouco flexíveis. As alvenarias de 19 cm de largura e aquelas revestidas apresentaram melhor desempenho térmico.

Palavras-chave: altas temperaturas; alvenaria estrutural; paredes de alvenaria; blocos cerâmicos; resistência ao fogo.

1. INTRODUCTION

Often, laboratory-mandated tests for walls at high-temperature neglect the internal forces that arise in the elements, in a real-world setting, due to the constraints of temperature-induced thermal expansions (LI et al., 2015). This is because some standards, such as the Brazilian (ABNT, 2001), for conducting fire resistance testing on walls, load-bearing or not, recommend that the lateral edges of the analyzed sample have their movement free of restrictions, allowing them to expand laterally. However, international standards such as ISO 834-4 (1994) and BS 476 (1987), while suggesting the use of free vertical edges, allow lateral restrictions to be used, provided that this corresponds to the real situation to which the wall is subjected. More specifically, the abovementioned British standard recommends the use of vertical edge restraints if the wall sample in question is smaller than the real dimensions of the element under evaluation, or if this wall is located between robust pillars. Based on these standards and other studies, it is noted that simply neglecting the real characteristics of the walls that will be analyzed in the laboratory can significantly cause distortions in the final result. Shieids *et al.* (1988), for example, analyzed the

different thermal deformation modes of a small-sized masonry wall model and observed that the maximum deflection for a given situation depends on the boundary conditions to which the element is subjected, this means, it varies according to the displacement restrictions in the edges of the sample. This was also observed by Nguyen and Meftah (2012), that by measuring the deformations at different points of the tested walls, obtained different deformations for different boundary conditions, evidencing the influence of the bonds on the thermal behavior of the element.

The concern about the limitations applied to the samples arises from the fact that the internal forces caused by the thermal expansion constricted in real fire situations have their effects not well explored. In a survey conducted in a building subjected to a severe fire, it was possible to observe occurrences of spalling of clay-brick faces (NAVARRO; AYALA, 2015). At the time, the elements had no structural function. Therefore arises the need to understand under which circumstances such spalling occur, by which mechanisms trigger it and what the possible consequences of this phenomenon on the behavior of the structure, when it's about load-bearing masonry, since such constructive technique is widely used in buildings on multiple floors.

Therefore, the motivation of this work lies in the need to better understand the behavior of masonry structural walls submitted to high temperatures, previously explored in other studies such as Souza (2017), Al-Sibahy and Edwards (2013) and Ayala (2010), including the concept of internal stresses caused by the restrictions of thermal expansions, in order to understand the damage of the elements in real situations. Thus, the objective of this work is to analyze the behavior presented by small-scale masonry walls when exposed to high temperatures, axial loading and having their lateral thermal expansion restricted, in order to simulate conditions close to the reality in a fire situation.

2. MATERIALS AND METHODS

2.1 Materials

Three different types of blocks were used for this research – 7 and 10 MPa, 14 cm-thick and 7 MPa, 19 cm-thick – all made of burnt clay (Figure 1). The dimensions and other characteristics of the units are outlined in Table 1.

Table 1. Properties of the clay hollow blocks.

ID	Characteristic Strength	Dimensions (l x h x c)	Strength of the prism (mortar f_m 4 MPa)	Net area/gross area
B1	7 MPa	14 x 19 x 29 cm	≈ 3,5 Mpa	≈ 0,41
B2	10 MPa	14 x 19 x 29 cm	≈ 6,0 Mpa	≈ 0,48
B3	7 MPa	19 x 19 x 29 cm	≈ 3,0 Mpa	≈ 0,36

Adapted from <http://www.pauluzzi.com.br/produtos.php>

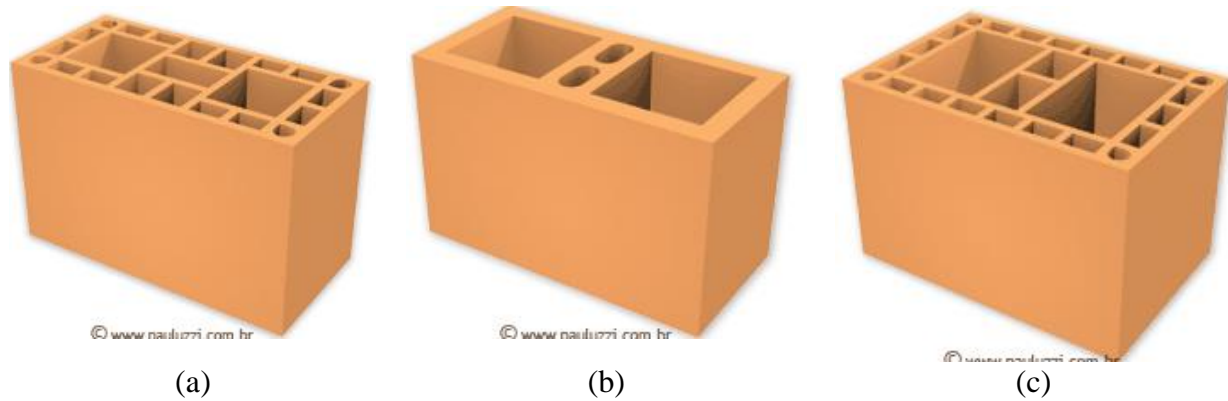


Figure 1. Clay hollow blocks used. (a) B1. (b) B2. (c) B3.
(Fonte: <<http://www.pauluzzi.com.br/produtos.php>>)

Traditional prebatched mortars with resistances of 4, 6 and 10 MPa were used in the joints of the samples - according to the block employed. It was also evaluated the use of polymeric mortar for bedding the blocks, in order to assess its behavior when subjected to excessive heat and loading action, verifying the consequences for the masonry as a whole.

In one of the research stages, the samples were coated with mortar. It was used around 1 cm thick industrialized mortar as the coating material.

2.2 Experimental Program

The experimental program was carried out in three stages: in the first all three types of blocks were compared; the second evaluated the thickness and strength of the mortar of laying joints, and the presence of coating are evaluated for the same block. Finally, in the third stage, the use of polymeric mortar joints are evaluated. The details of each step are described below.

2.2.1 First stage

In the first stage, the mini-walls with three different blocks were exposed to the thermal test, with mortars strength corresponding to a maximum of 70% of the blocks characteristic compressive strengths. The mortar joints in this stage were made with a thickness of 10 ± 3 mm, filled with the mortars specified in Table 2, both vertically and horizontally, the samples had no type of coating whatsoever.

Table 2. First stage mini-walls tested – Group 01.

Mini-wall	Bricks	Mortar type	Joint thickness
P1	B1	$f_m \approx 4,0\text{MPa}$	10 ± 3 mm
P2	B2	$f_m \approx 6,0\text{MPa}$	10 ± 3 mm
P3	B3	$f_m \approx 4,0\text{MPa}$	10 ± 3 mm

2.2.2 Second stage

In the second stage, only the brick B1, 14 cm thick and 7 MPa, was used. In this stage, the thickness of the joints, the mortar used in the samples' execution and the presence of coating were evaluated. In one case (P4), the bed joint was reduced to 5 mm thick, maintaining the compressive strength of the mortar at 4 MPa. Successively, the compressive strength was increased to 10 MPa, with the joint thickness maintained at 10 mm (P5).

Finally, one last situation was imposed at this stage: the coating application. In a sample made with the same characteristics as P1, a 10 mm thick layer of mortar coating was applied. Such coating was applied only on the face exposed to fire, so as not to impair the positioning of the instrumentation on the opposite face.

Thus, three more wall configurations were tested and compared to samples P1, as shown in Table 3.

Table 3. Second stage mini-walls tested – Group 02.

Mini-wall	Brick	Mortar type	Joint thickness
P1	B1	$f_m \approx 4,0\text{MPa}$	$10 \pm 3 \text{ mm}$
P4	B1	$f_m \approx 4,0\text{MPa}$	$\approx 5\text{mm}$
P5	B1	$f_m \approx 10,0 \text{ MPa}$	$10 \pm 3 \text{ mm}$
P6	B1	$f_m \approx 4,0\text{MPa}$ and coating	$10 \pm 3 \text{ mm}$

2.2.3 Third stage

For this stage, the tests evaluated the samples constructed with polymeric mortar joints, compared with those constructed with traditional mortar. In the construction of these walls, the 10 MPa (B2) brick was used to facilitate the application of the polymeric mortar, as they have solid webs. Thus, the comparison was made in relation to the P2 walls, since they were made with the same structural bricks. The sample characteristics are presented in Table 4.

It is relevant that even though usually the head joints of masonry built with polymeric mortar are open, for this research, the polymeric mortar was also applied vertically, aiming to maintain the tightness of the samples against the action of high temperatures and ensure the safety during the test.

Table 4. Third stage mini-walls tested – Group 02.

Mini-wall	Brick	Mortar type	Joint thickness
P2	B2	$f_m \approx 6,0\text{MPa}$	$10 \pm 3 \text{ mm}$
P7	B2	Polymeric	-

2.3 Small-scale Walls

The walls were constructed with the blocks and mortars as specified in item 2.1 and with dimensions of 90 x 80 cm, due to the oven size restrictions; therefore, they were called mini-walls. These were built on a metal profile, with a U-shape folded plate, in order to facilitate its movement. For the loads to be applied and distributed equally along the wall, the samples were covered with cement-rich mortar in the top and both sides, thus obtaining a flat surface.

The samples were cured for at least 56 days so that the moisture present in the mortar was reduced and the results would not be affected due effects present only at the initial ages. Likewise, in the samples that were coated, it was performed after at least 7 days from the construction of the walls, and the tests were performed at least after 56 days.

The samples were accommodated for testing within a loading gantry designed to withstand the applied stresses and prevent lateral expansions. It was also been designed to allow the application of distributed vertical loads in order to simulate the loading of a load-bearing wall. It is a frame made of rail tracks with two hydraulic jacks attached to it: one for vertical loading application and one for lateral confinement. Both hydraulic jacks were attached to strain gages to monitor the increments. The effort made by hydraulic jacks was distributed on wall faces using metallic profiles. The schematic drawing of the planned and assembled equipment can be seen in Figure 2.

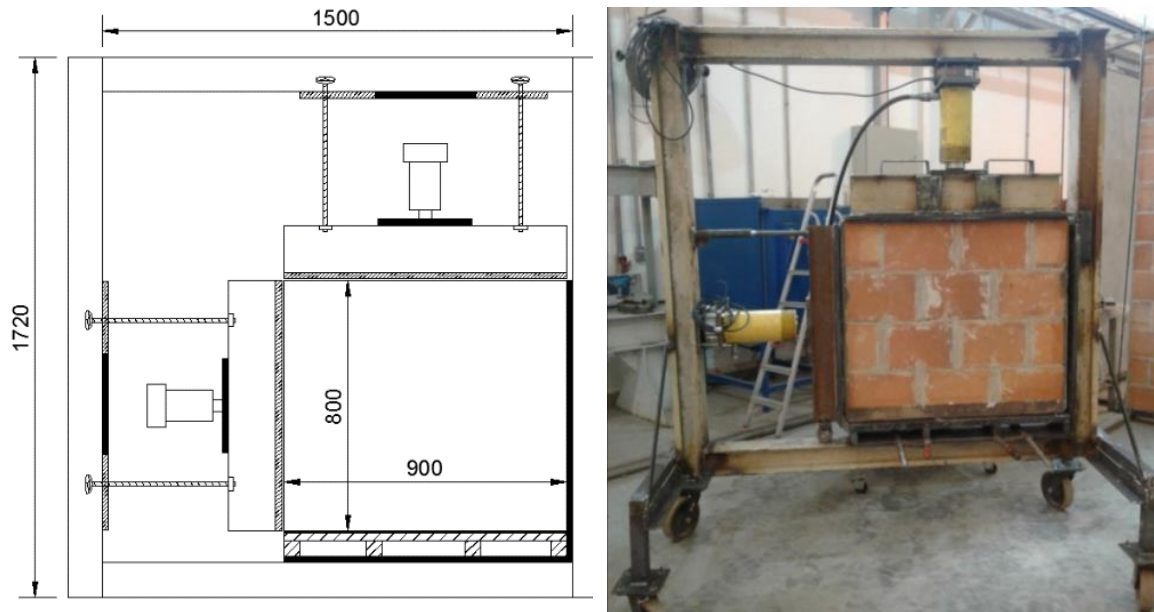


Figure 2. Reaction frame used in the tests.

Once the sample was placed in the reaction frame, it was coupled to a *Sanchis* electrical resistance furnace, in this way one of the mini-wall faces was subjected to heating. The instrumentation monitoring for temperature and displacement was placed onto the unexposed face.

The load applied to the samples was estimated so they were applied in accordance with the requirements of NBR 6120 - Loads for the calculation of building structures (ABNT, 1980). Thus, loading of 97.83 kN/m was applied to the sample before starting the fire resistance test, increasing due to expansion attempts after the beginning of the test

2.4 Temperatures

Due to the limitations of the equipment available in the laboratory, the test required by NBR 5628 (ABNT, 2001) was adapted for small-scale walls that fit the available furnace size. The furnace temperature was increased to a rate like the standard curve described by the NBR 5628 (ABNT, 2001), to a maximum of 950°C, the temperature usually reached during a real fire. The mini-walls were then kept exposed to such temperature for about 4 hours.

To verify the integrity of the samples, the cotton pad test was performed whenever necessary, as described by NBR 5628 (ABNT, 2001). Thermal insulation was verified using thermocouples with copper disc tip to measure the temperature on the unexposed face of the samples, as recommended by NBR 5628 (ABNT, 2001). In addition to the thermocouples placed on the non-heated face, K-type thermocouples were placed through the wall to obtain temperature values inside the oven and inside the blocks. In total seven thermocouples were distributed, five of them on the unexposed face, for thermal insulation control, and the others to collect additional information (Figure 3).

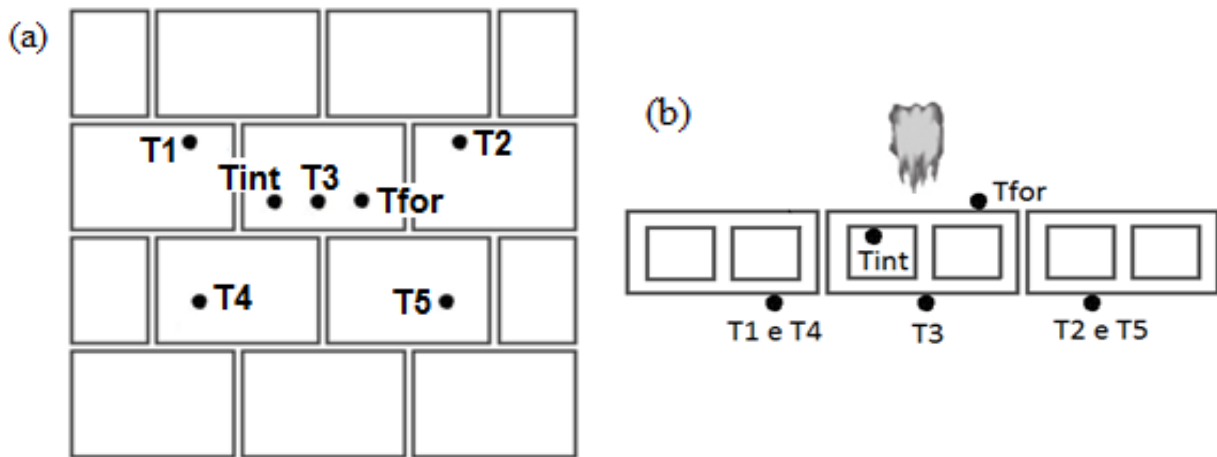


Figure 3. Thermocouple positioning in the samples. (a) Frontal view. (b) Upper View.

2.5 Longitudinal Displacements

Using displacement transducers, also called clip-gages, positioned on the unexposed face of a unit in the center of the mini-walls, the horizontal and vertical deformations were measured during the hearing test. These devices were built based on those used by Beber (2003), and consist of arches with extensometers on their lower and upper faces (Figure 4). These arcs are attached to the surface whose displacements are to be measured. The specific strain determined by the strain gauges in the central section of the arcs is correlated to the relative displacements between the fixed points A and B.

The spacing or approximation between different blocks of the same course and consecutive course was also measured using clip-gages in the joints, which provides an indication of the mortar absorption of the displacements caused by thermal deformation. The positioning of clip-gages in the samples is outlined in Figure 4.

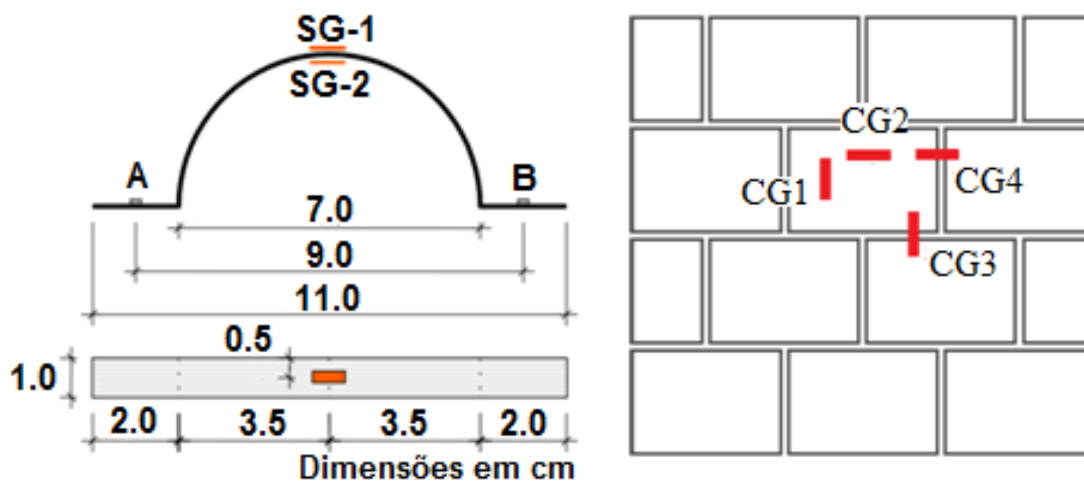


Figure 4. Clip-gages geometry (BEBER, 2003) and placement in the wall.

2.6 Thermography

Thermographic analysis of the samples was also conducted during its exposure to heat treatment. The use of this technique allowed the mapping of the temperature along the surface of the samples, using a FLIR T440 thermographic camera for the detection of the infrared radiation emitted by the samples when submitted to the heat. With this equipment, it was possible to monitor the temperature increase throughout the test and identify zones of possible failures in the masonry. It also rendered it possible to make a comparison of the heat spread in the different types of masonry.

3. RESULTS AND DISCUSSION

3.1 The temperature throughout the samples

In Figure 5 is possible to see the temperature evolution inside the bricks (Tint) for the first three wall configurations, intending to compare the three different blocks. For blocks B1 and B2, the results for the intermediate thermocouple peaked around 600°C. The wall P3 presented values below 600°C, which was due to the fact that it was built with block B3, wider than the others.

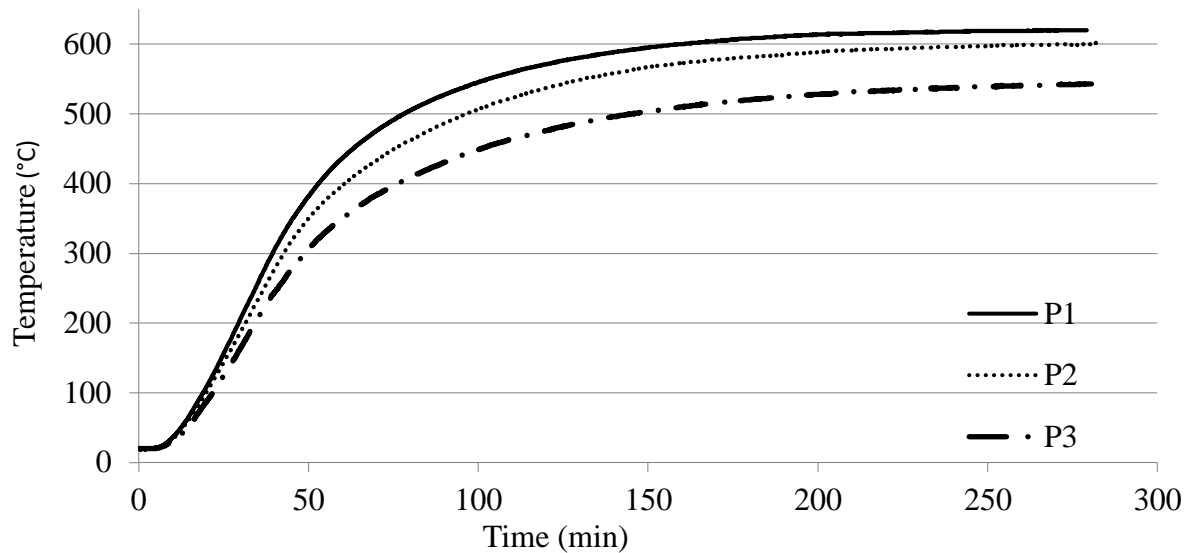


Figure 5. Temperature inside of the masonry in the different brick types (Group 1).

When comparing the samples from the second stage, it can be seen from Figure 6 that the thickness of the joints and the strength of their mortars do not influence heat transfer, with the walls P1, P4 and P5 having temperatures inside the blocks around 600°C, although by adding a coating on the exposed face the temperature reduction is significant, reaching less than 400°C, for the P6 wall.

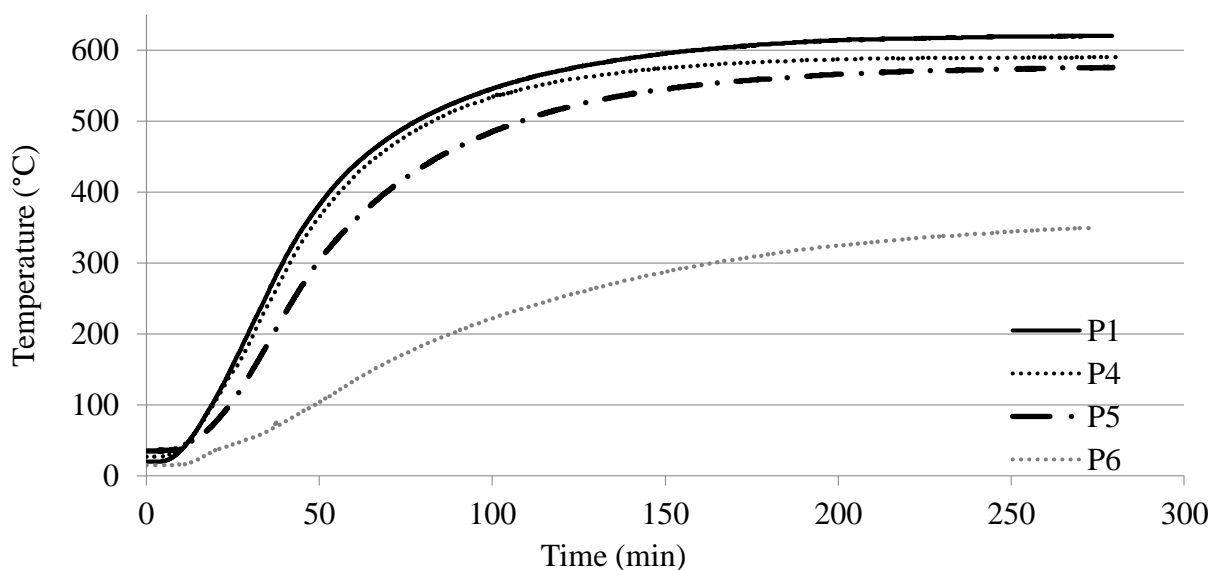


Figure 6. Temperature inside the masonry with respect to the different laying joints and coating (Group 2).

The third group of samples indicates the non-influence of the joint type on the heat transfer along

the wall thickness since the results for the thermocouple readings internal to the wall blocks P2 and P7 were very similar (Figure 7). The use of polymeric mortar, therefore, offers no harm or benefit regarding this item.

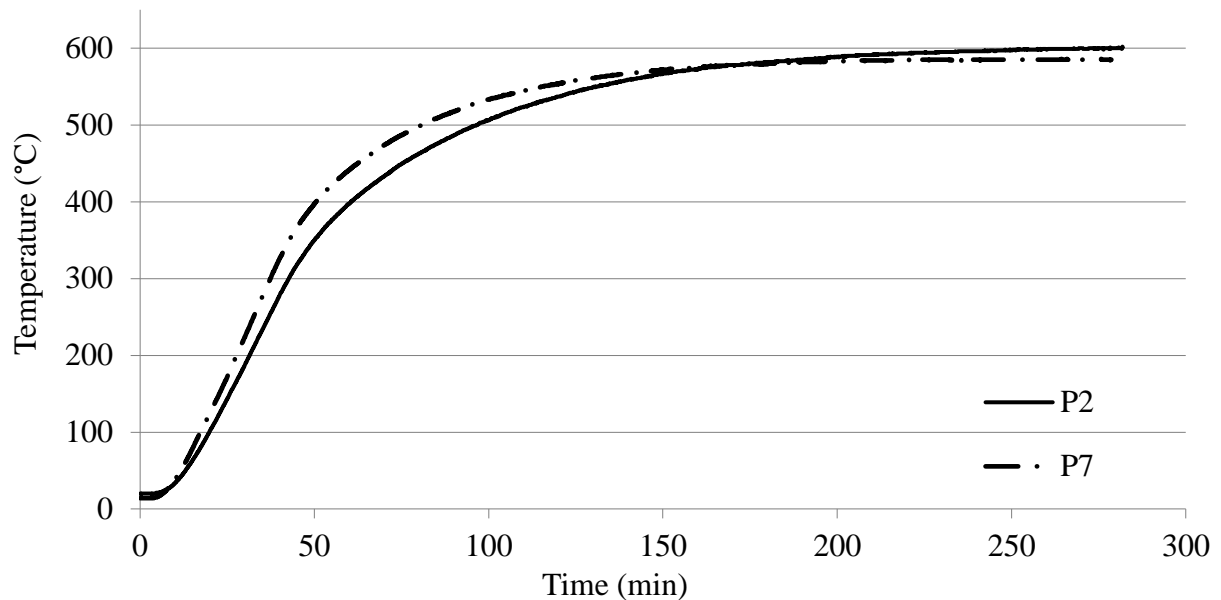


Figure 7. Temperature inside the masonry with respect to the different laying joints with traditional mortar and polymeric mortar (Group 3).

The maximum temperatures recorded on the non-heated face are represented in Figure 8. The values, in general, remained around 140 to 160°C. The exceptions are sample P3, made with the thickest brick (B3), and P6, which had a coating on its exposed face. The latter-maintained temperatures below 90°C, again demonstrating the insulation that the coating provides to the element, even if applied only on one of its faces. These results corroborate the data obtained by Nguyen e Meftah (2012) and Souza (2017), who found similar results with significantly lower temperatures in masonry with coated faces. The former also identified some influence of the increase of block thickness on the thermal insulation of masonry. As expected, block strengths and laying joints have no significant influence on the temperature results of the tested masonry. Regarding the fulfillment of the criteria established by the Brazilian standard NBR 14432 (2001b), none of the samples failed to achieve the required criteria for fire-resistance rating during exposure to the test - integrity, thermal insulation, and load-bearing capacity.

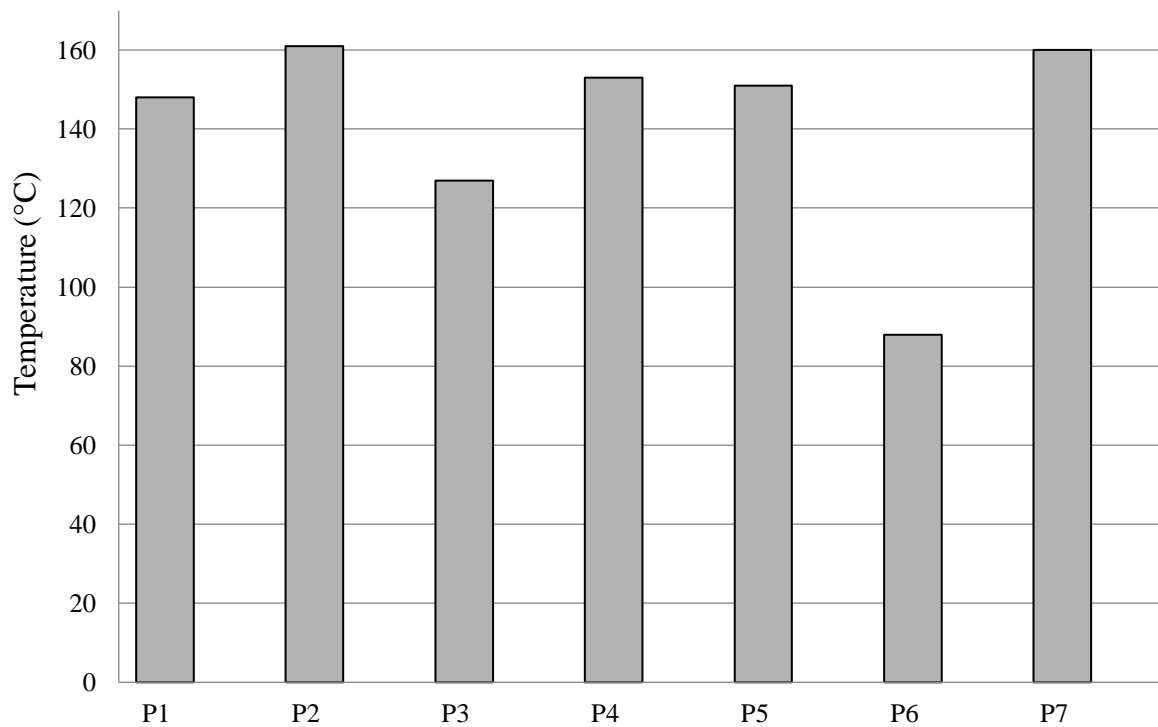


Figure 8. Maximum temperature on the unexposed face.

3.2 Thermographic images

Thermographic images captured every 25 minutes until the first 50 minutes of the test were selected (Figure 9 to Figure 11). The analyses were performed with a comparative purpose between the masonry samples. In the thermographic images, the lighter tone regions represent the highest temperatures.

It was possible, through the images, to ratify the best thermal insulation of the samples with the 19 cm thick block (P3) and with coating on the exposed face (P6).

For the heated sample with a coated face, the heating of the unexposed region was delayed and softened. It is possible to see in the 25-minute capture of Figure 11, however, the higher temperature spots in the upper portion. This is attributed to local cracking and spalling of the coating mortar, which allowed for great heat propagation in these regions.

The difference in color and therefore in the temperature that can be seen between the first images (time 0 min) of each figure is referred to the different room temperatures on the days of the tests, which vary greatly throughout the year in the region where the tests were performed.

0 min

25 min

50min

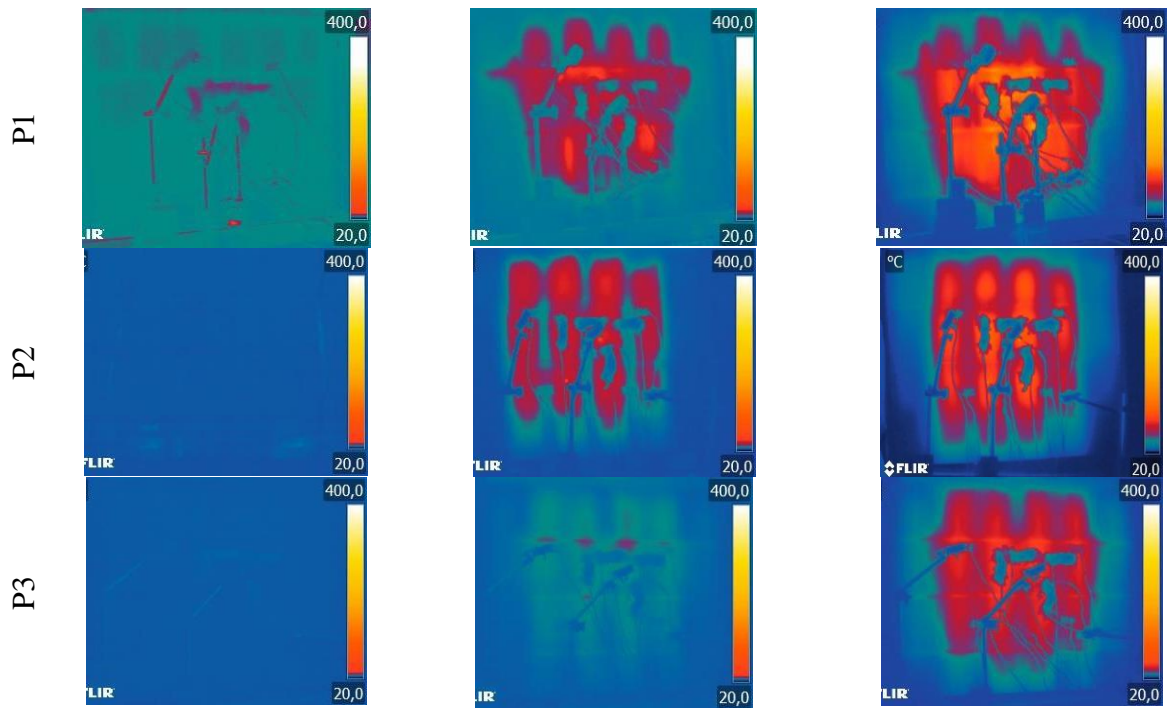


Figure 9. Thermographic Images – Group 01.

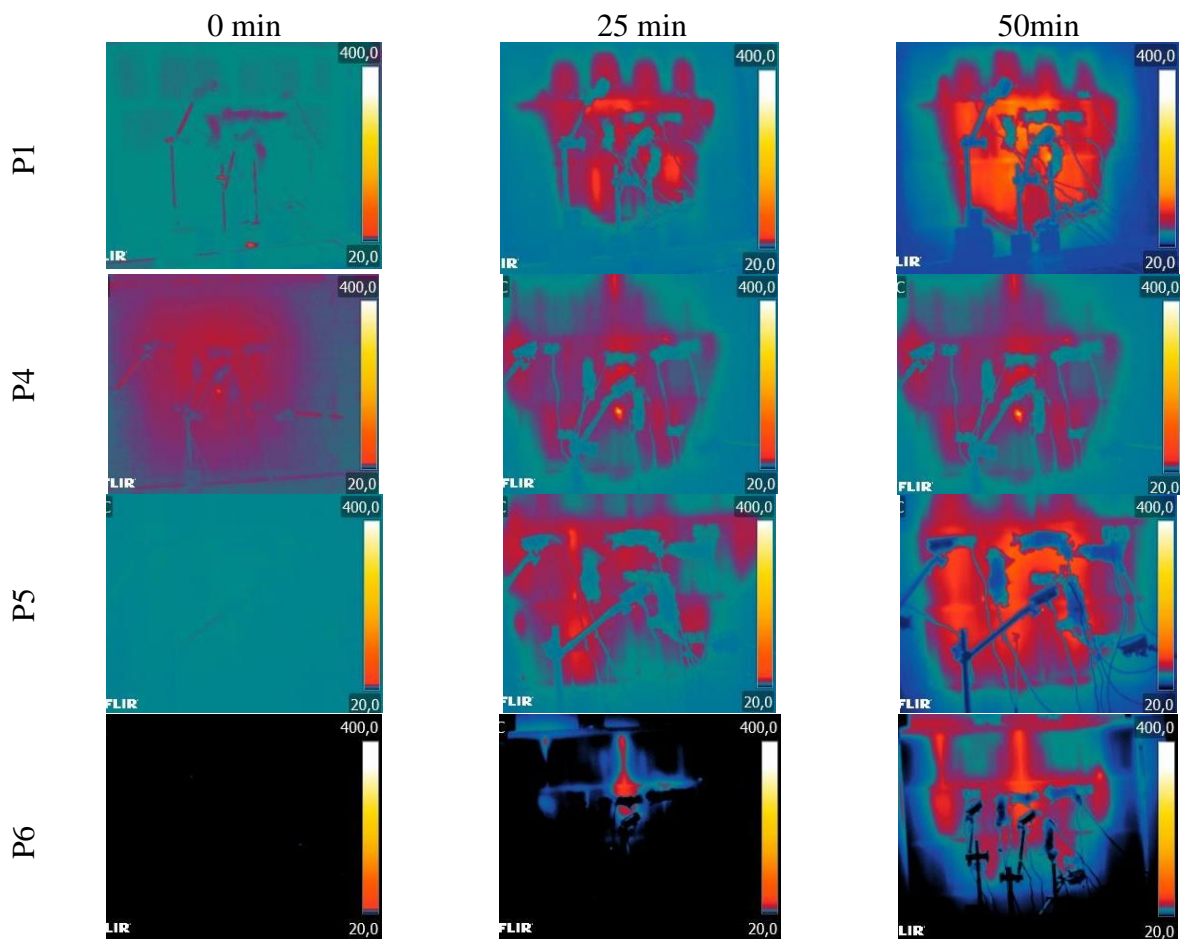


Figure 10. Thermographic Images – Group 02.

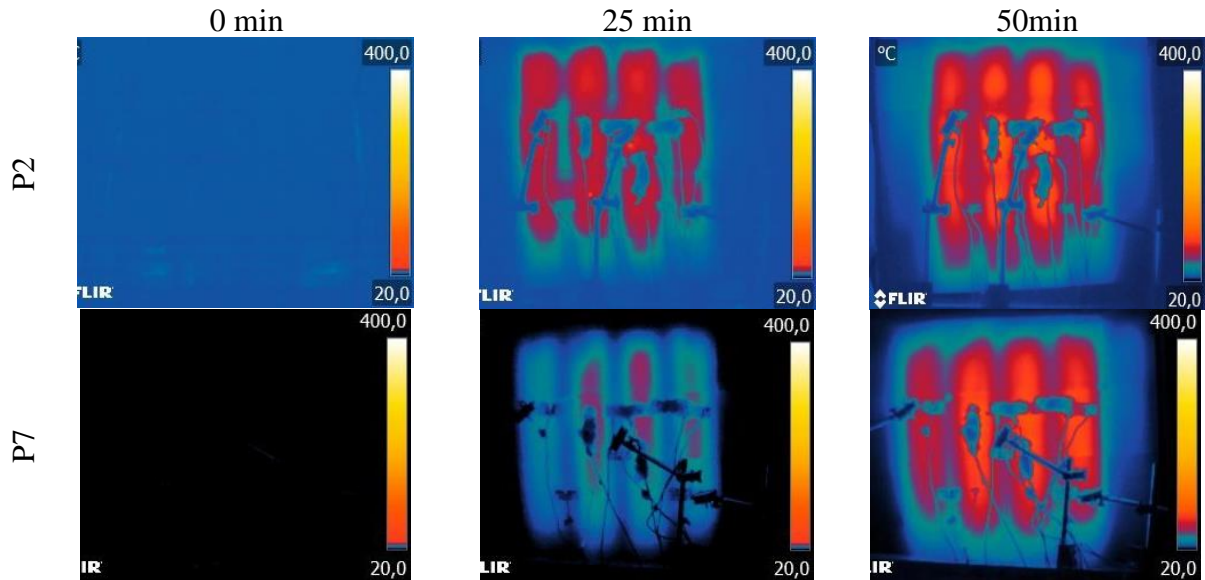


Figure 11. Thermographic Images – Group 03.

A different heating pattern can be also visualized for samples P2 and P7, made with type B2 bricks, of 10 MPa resistance, where the temperature propagates essentially through the cavities (Figure 11). The pattern is like that observed by Nguyen e Meftah (2012), who identified higher temperatures in the alveoli of the blocks. According to the authors, the main heat transfer mechanisms in a wall are convection and radiation, thus, the temperatures measured in the block cavities are higher than those measured in their transverse webs, where heat is propagated by conduction. Therefore, the observed pattern is because the webs of the B2 units are massive and, consequently, the heat propagation is smaller in these regions than in the hollow web bricks.

3.3 Longitudinal Displacement

The displacements presented in this item deal with the movements within the plane of the walls. The dilatations or contractions of the bricks in the vertical and horizontal directions - CG 1 and CG 2, respectively, were measured, as well as the crushing or spacing of the masonry joints, also vertically (CG3) and horizontally (CG4).

To analyze the results the data obtained in the first 150 minutes of exposure were considered. After this point, they could suffer temperature interference, since, at this time of the test, the heating of the unexposed face reached approximately its maximum, also heating the clip-gages used in the instrumentation. The negative values in the graphs represent the closure of the displacement transducers, while positive values indicate their opening.

One of the observations that can be made from the results presented is that samples with more flexible joints tend to allow the block to dilate, forming a more deformable system compared to the others. This behavior can be observed in sample P1, where the transducers fixed to the central block - CG 1 and CG 2 - showed behavior indicating expansion in both directions (Figure 12). The onset of dilation coincides with the moment when the temperature on the outer surface begins to rise.

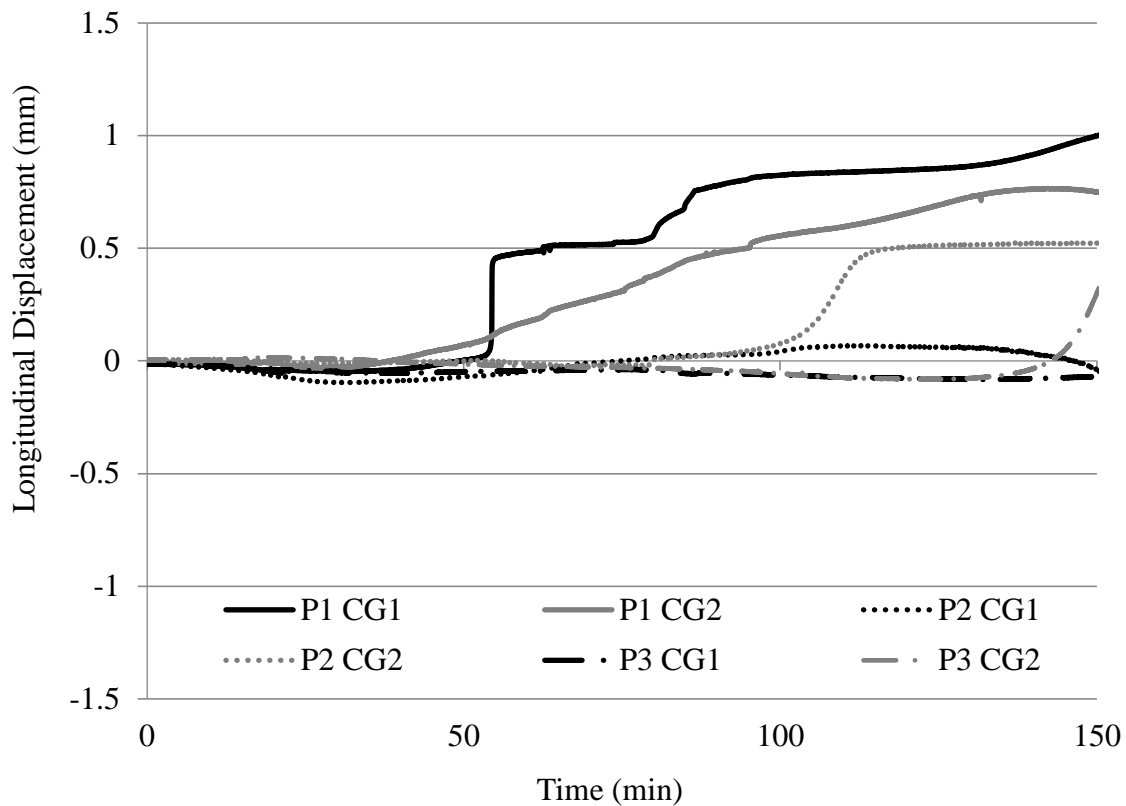


Figure 12. Longitudinal Displacement of the bricks – Group 01.

Although for sample P2 the mortar had a slightly higher resistance than that of the previous ones, the block expansion did not have the same behavior. This may have been because the lateral restraint was more effective, or because of the greater rigidity of the brick, which has massive webs, not hollow, in order to give it greater resistance. In the case of sample P3, the block practically showed no movement during the period considered. This behavior was attributed to the better thermal insulation observed for this sample, which showed little temperature increase in the early periods, thus suffering less thermal movement. The same is true for sample P6, which has better thermal insulation due to the coating of its face.

By improving the joint mortar strength to the point where it reaches or even exceeds the brick strength, as in the case of P5, the joint no longer absorbs the deformations, thus transferring compressive stresses to the brick, denoted by negative values of CG2 (Figure 13). The same is true for the sample with polymeric mortar (P7), which, because it has low deformation, also transfers stresses to the brick, causing it to be compressed in both directions - CG1 and CG2 (Figure 14).

These compressive stress transfers to the brick may indicate a warning signal for the possible occurrence of spalling in masonry when executed with high strength mortar. In sample P7, for example, jointed with polymeric mortar, it was possible to visualize in the brick a significant crack, even though it was a case of a unit with massive webs. This crack may be related to the compressive stresses existing in it.

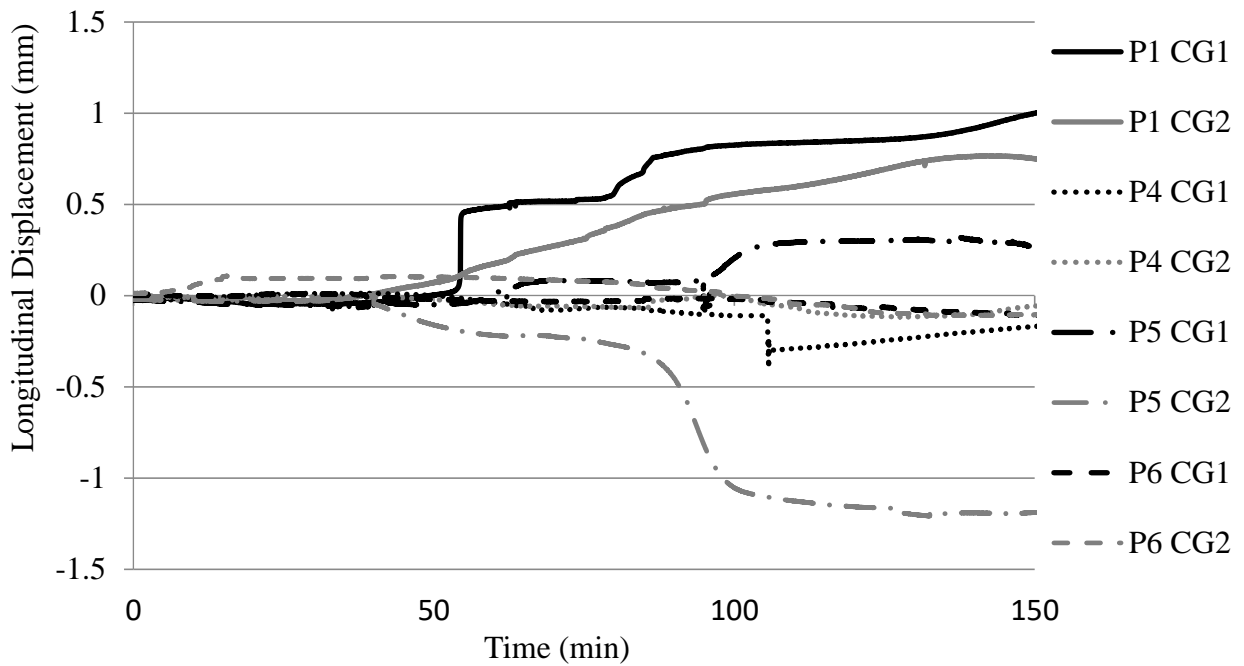


Figure 13. Longitudinal Displacement of the bricks – Group 02.

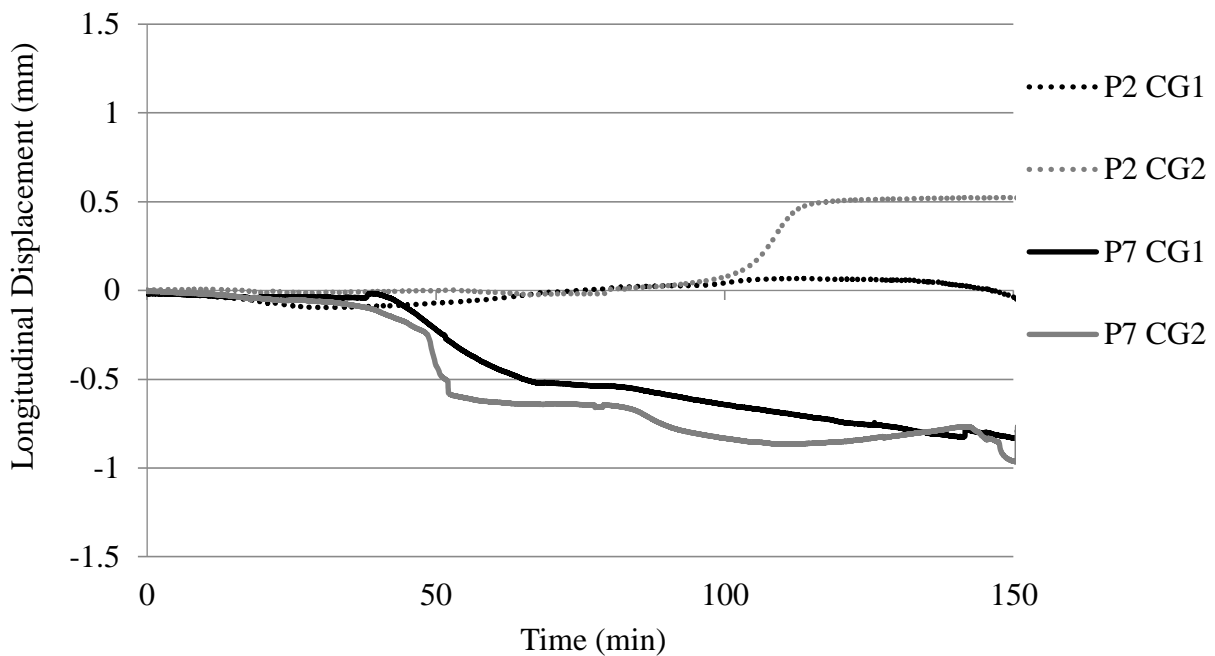
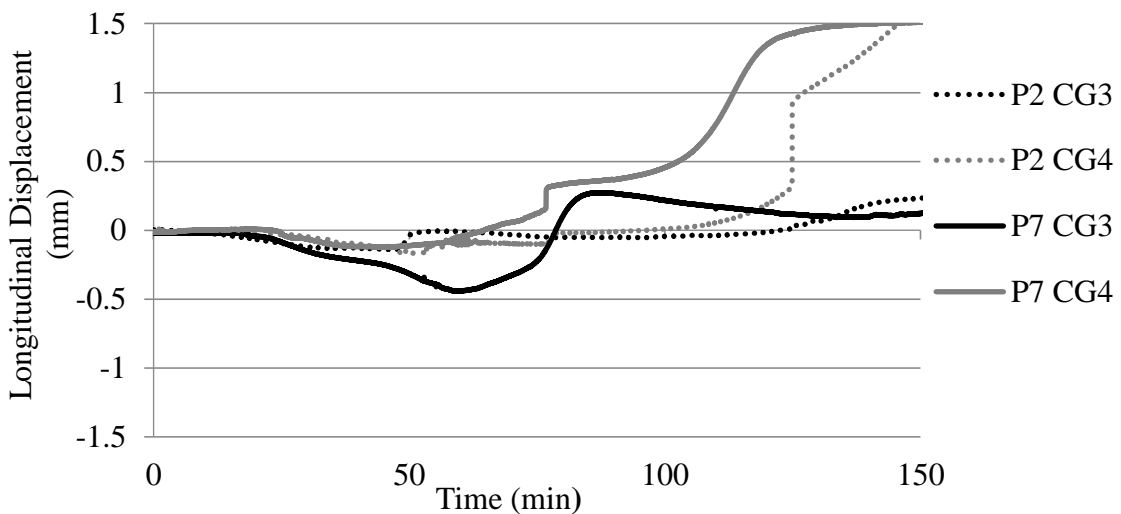
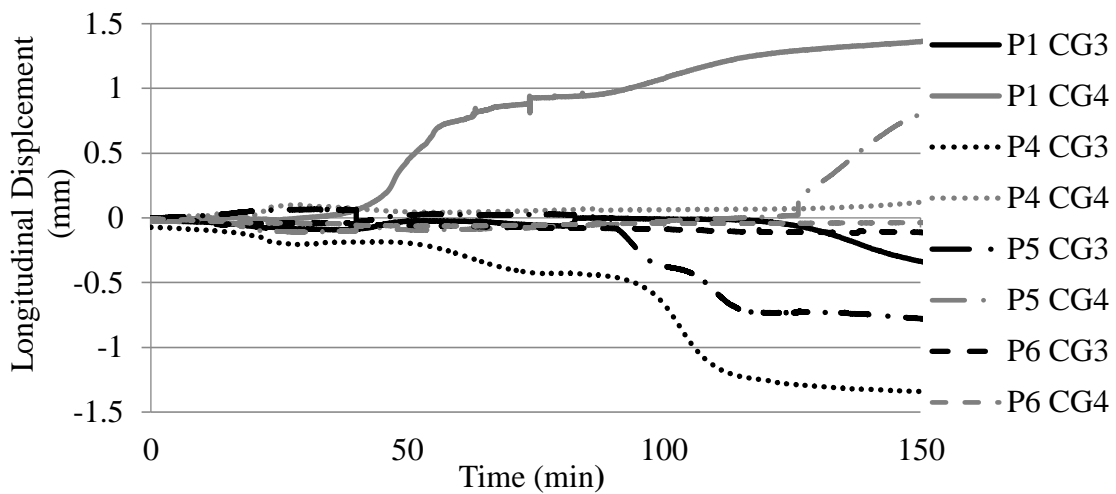
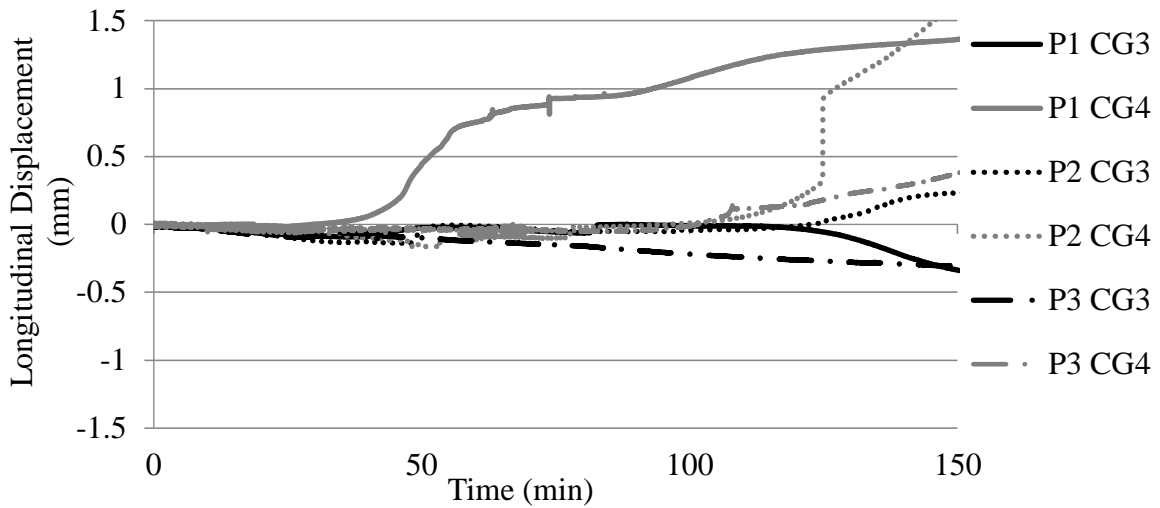


Figure 14. Longitudinal Displacement of the bricks – Group 03.

Although the occurrence of spalling was not observed in the tests performed, it's a beginning to better understand the characteristics that could facilitate this phenomenon in real-sized walls, as observed in the studies by Nguyen e Meftah (2012) and Souza (2017).

For almost every case, the bed joint, monitored by CG 3, shown a closure, that signal compression in the joint (Figure 15 e Figure 16). Such manifestation can be due either by the vertical loading applied to the sample, or by the expansion of the bricks adjacent to it, or by a combination of both. The exception to this pattern occurred in sample P7, where the bed joint initially behaves like the others, showing compression, and later reverses its movement, denoting joint opening (Figure 17). This fact may be caused by the degradation and loss of mortar resistance on the inner face of the

wall.



The opening movement noted on CG 4, which was manifested for most results, may have been the result of a movement of the wall as a whole, which could be expanding laterally due to an inefficient restriction in that direction. It is possible that the mortar used for capping the samples did not offer sufficient strength to prevent deformation. Thus, the crushing effect of the joint between the blocks is best visualized in the vertical direction by clip-gage 3, since in this direction the load application makes the restriction more effective.

In general, the results presented here constitute an important contribution to the development of the research regarding the mechanical behavior of masonry exposed to high temperatures, as well as contribute to the knowledge about the influence of the types of materials used in the masonry construction on the obtained results, subjects classified as scarce or absent in the study by Russo e Sciarretta (2013).

4. CONCLUSIONS

The tested walls showed good performance facing the action of high temperatures. They presented predominantly vertical cracks after exposure, especially on the face exposed to the heat. The masonry laying mortar had a significant strength loss. In the coated samples, the coating mortar completely detached from the substrate as the temperature increased.

It was possible to infer that the increase of block thickness and, above all, the use of mortar coating attenuate the heat transfer to the unexposed face.

Analysis of the data obtained for longitudinal displacements indicated that more flexible joints form a more deformable system compared to the others, allowing the brick to dilate in both directions in the plane. The increase of the mortar strength so it equals or exceeds the strength of the masonry units may pose a risk to the elements, as stress absorption by the joints is reduced thus transferring stresses to the block. The same applies to polymeric mortar due to its low deformability.

With the data obtained it is possible to observe many variables that can influence the behavior of masonry elements, being this a construction method with properties hard to comprehend in a fire situation. It is noteworthy that the scale of the studied samples, being reduced compared to reality, attribute greater rigidity to them, which certainly influences the mechanical behavior of the elements.

5. REFERENCES

- Al-Sibahy, A., Edwards, R. (2013), *Behaviour of masonry wallettes made from a new concrete formulation under combination of axial compression load and heat exposure: Experimental approach*. Engineering Structures, v. 48, p. 193–204, 2013.
<http://dx.doi.org/10.1016/j.engstruct.2012.09.028>
- Associação Brasileira De Normas Técnicas. (2001), *NBR 5628: componentes construtivos estruturais - determinação da resistência ao fogo*. Rio de Janeiro.
- Associação Brasileira De Normas Técnicas. (1980), *NBR 6120 - Cargas para o cálculo de estruturas de edificações*. Rio de Janeiro.
- Associação Brasileira De Normas Técnicas. (2001b), *NBR 14432 - Exigências de resistência ao fogo de elementos construtivos de edificações - Procedimento*. Rio de Janeiro.
- Ayala, F. R. R. (2010). *Mechanical properties and structural behaviour of masonry at elevated temperatures*. Tese (Doutorado) - University of Manchester, Faculty of Engineering and Physical Sciences. p. 294.

- Beber, A. J. (2003). *Comportamento Estrutural de Vigas de Concreto Armado Reforçadas com Compósitos de Fibra de Carbono*, p. 317.
- British Standards Institution. (1987). *BS 476: fire tests on building materials and structures*. London.
- International Organization For Standardization. (1994). *ISO 834: fire-resistance tests - Elements of building construction*. Genève.
- Li, Y., Lu, X., Guan, H., Ying, M., Yan, W. (2015). *A Case Study on a Fire-Induced Collapse Accident of a Reinforced Concrete Frame-Supported Masonry Structure*. Fire Technology. <https://doi.org/10.1007/s10694-015-0491-0>
- Navarro, M. C., Ayala, F. R. R. (2015). *Degradación de Materiales de la Construcción Ante la Acción de Altas Temperaturas*. Congreso Internacional de Ciencias de la Ingeniería, 2., 2015. Los Mochis. Anais... . Los Mochis.
- Nguyen, T. D., Meftah, F. (2012). *Behavior of clay hollow-brick masonry walls during fire. Part I: Experimental analysis*. Fire Safety Journal, v. 52, p. 55–64. <https://doi.org/10.1016/j.firesaf.2012.06.001>
- Russo, S., Sciarretta, F. (2013). *Masonry exposed to high temperatures: Mechanical behaviour and properties - An overview*. Fire Safety Journal, v. 55, p. 69–86, Elsevier.
- Shields, T. J., Connor, D. J. O., Silcock, G. W. H., Donegan, H. A. (1988). *Thermal bowing of a model brickwork panel*. International brick/block masonry conference, 8. Anais. Dublin: Elsevier Applied Science, v. 2. p.846–856.
- Souza, R. P. (2017). *Avaliação da influência da espessura do revestimento argamassado e do carregamento no comportamento de alvenaria frente a altas temperaturas*. Dissertação (Mestrado) - Universidade do Vale dos Sinos. São Leopoldo. 138 p.

Fire and collapse of the Wilton Paes de Almeida building in São Paulo, Brazil. Lessons learned

P. Helene^{1*} , J. Pacheco², D. Couto³ 

*Contact author: paulo.helene@concretophd.com.br

DOI: <http://dx.doi.org/10.21041/ra.v10i1.419>

Reception: 07/06/2019 | Acceptance: 22/11/2019 | Publication: 30/12/2019

ABSTRACT

The objective of this work was to make a diagnosis that explains the mechanism of collapse, in just 80 minutes, of the Wilton Paes de Almeida building, which was surprising for the engineering of structural concrete. Previous fires, such as that of the Andraus Building, the Joelma and the Great Avenue, withstood more than 4 hours of fire without collapsing and are currently in use. To understand this unusual collapse, an experimental investigation of the characteristics and properties of the concrete and the reinforcement used in that structure was carried out, based on a "hypothetical structural project" that considered the actual characteristics of the materials used. Based on the diagnosis, recommendations were established so that cases like this do not recur.

Keywords: collapse, Wilton Paes de Almeida building, diagnosis.

Cite as: Helene, P., Pacheco, J., Couto, D. (2020), "*Fire and collapse of the Wilton Paes de Almeida building in São Paulo, Brasil. Lessons learned*", Revista ALCONPAT, 10 (1), pp. 115 – 131, DOI: <http://dx.doi.org/10.21041/ra.v10i1.419>

¹ Professor Titular da EPUSP. PhD Engenharia, São Paulo, Brasil.

² PhD Engenharia, São Paulo, Brasil.

³ Universidade Estadual de Campinas (UNICAMP). PhD Engenharia, São Paulo, Brasil.

Legal Information

Revista ALCONPAT is a quarterly publication by the Asociación Latinoamericana de Control de Calidad, Patología y Recuperación de la Construcción, Internacional, A.C., Km. 6 antigua carretera a Progreso, Mérida, Yucatán, 97310, Tel.5219997385893, alconpat.int@gmail.com, Website: www.alconpat.org

Responsible editor: Pedro Castro Borges, Ph.D. Reservation of rights for exclusive use No.04-2013-011717330300-203, and ISSN 2007-6835, both granted by the Instituto Nacional de Derecho de Autor. Responsible for the last update of this issue, Informatics Unit ALCONPAT, Elizabeth Sabido Maldonado, Km. 6, antigua carretera a Progreso, Mérida, Yucatán, C.P. 97310.

The views of the authors do not necessarily reflect the position of the editor.

The total or partial reproduction of the contents and images of the publication is strictly prohibited without the previous authorization of ALCONPAT Internacional A.C.

Any dispute, including the replies of the authors, will be published in the third issue of 2020 provided that the information is received before the closing of the second issue of 2020.

El incendio y colapso del edificio Wilton Paes de Almeida en São Paulo, Brasil. Lecciones aprendidas

RESUMEN

El objetivo de este trabajo fue realizar un diagnóstico que explique el mecanismo de colapso, en apenas 80 minutos, del edificio Wilton Paes de Almeida, lo cual fue sorprendente para la ingeniería del concreto estructural. Incendios anteriores, como el del Edificio Andraus, el Joelma y la Gran Avenida, resistieron más de 4 h de fuego sin derrumbarse y se encuentran actualmente en uso. Para entender ese colapso inusitado, se realizó una investigación experimental de las características y propiedades del concreto y de la armadura empleados en esa estructura, con base en un "proyecto estructural hipotético" que consideró las características reales de los materiales empleados. A partir del diagnóstico se establecieron recomendaciones para que casos como éste no se repitan

Palabras clave: colapso, edificio Wilton Paes de Almeida, diagnóstico.

Colapso do Edifício Wilton Paes de Almeida – SP. Lições aprendidas.

RESUMO

O objetivo deste trabalho foi fazer um diagnóstico que explique o mecanismo de colapso, em apenas 80 minutos, do edifício Wilton Paes de Almeida, o que foi surpreendente para a engenharia de concreto estrutural. Incêndios anteriores, como o Edifício Andraus, o Joelma e o Grande Avenida, resistiram a mais de 4 horas de incêndio sem desmoronar e estão atualmente em uso. Para entender esse colapso incomum, foi realizada uma investigação experimental das características e propriedades do concreto e da armadura usada nessa estrutura, com base em um "projeto estrutural hipotético" que considerou as características reais dos materiais utilizados. Com base no diagnóstico, foram estabelecidas recomendações para que casos como esse não se repitam.

Palavras-chave: colapso, edifício Wilton Paes de Almeida, diagnóstico.

1. INTRODUCTION

The experimental study of concrete structures under the action of high temperatures, requires a large amount of financial resources and a large proportions laboratory structure, which allows testing significant parts of a reinforced concrete structure with foundations, columns, beams and slabs, besides the interaction with sealing walls or structural masonry. This capacity does not exist yet worldwide neither in the scientific literature, there is only the record of the experiment carried out at the Cardington Laboratory (CHANA; PRICE, 2003).

Thus, the engineering, until today, has been content to extrapolate results obtained from test bodies and small structural elements, performed isolated and without loads many times, to with a lot of creativity create “models” that allows to predict the behavior of a structure facing a fire. Another significant difficulty is the fact that all the limited laboratory tests results, depend on a standard “fire” designed by a standard curve ISO 834 (1999) or ASTM E119 (2019), that most of times do not corresponds to a true fire.

Considering these limitations until now insurmountable, this paper, as well as others, for example the articles about Windsor Building fire in Madrid, which took place on 2005, researched por Alonso (2008) from IET (Eduardo Torroja Institute of Cement and Concrete) and Calavera Ruiz *et al.* (2005) from INTEMAC (Technical Institute of Materials & Constructions) and the report on the collapse of the World Trade Center Twin Towers, where studies culminated in changing the design standards of tall buildings (NIST, 2005), seek to study thoroughly the cases of true fires, in

search of lessons that many times are no impossible from expensive and limited laboratory tests. For the authors of this paper, the greatest contribution is to gather all possible information from a disastrous event like the collapse occurred in only 80 minutes of Wilton Paes de Almeida building, in order to enable a diagnosis of the incident and thus understand a little bit more about the complexity of the behavior prediction of reinforced concrete structures under fire. Therefore, the scientific contribution is well characterized in the research carried out, seeking information and data that may explain this premature collapse.

2. HISTORIC

Started in the early of 1960s, the Wilton Paes de Almeida building was concluded in 1968 by the construction company Morse & Bierrenbach, Co., serving as the headquarters for the business conglomerate of the politician and businessman Sebastião Paes de Almeida. The building occupied an area of 6,996.54 sq. ft and its built total area was 129,166.93 sq. ft (ALETEIA, 2018).

With characteristics of a typical Miesian building, it had a reinforced concrete structure, with only 04 (four) recessed columns with “H” section, supporting a ribbed concrete slab in the central region and a cantilever slab in the periphery (Figure 1). In the facade, the thin thickness of the slabs made possible to use an equally thin aluminum window frame fixing the “glass skin” blades of green glass made by the *Rayban* house.

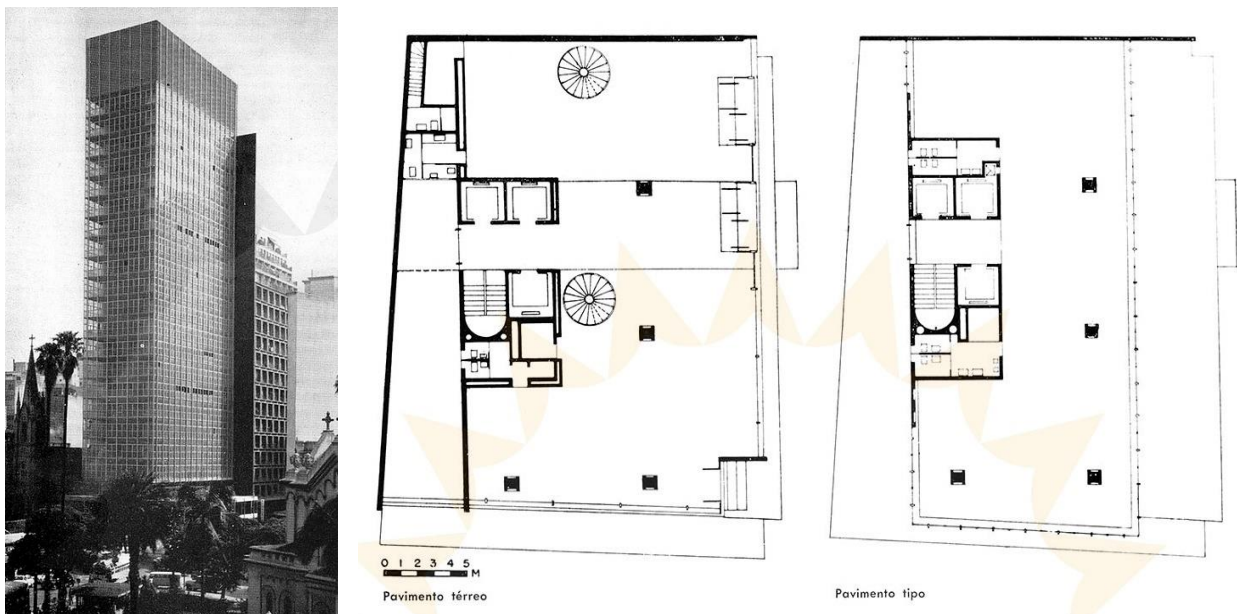


Figure 1. View of the Wilton Paes de Almeida building and ground floor and typical stories (source: Revista Acrópole, 1965)

The main company that occupied the building at its beginning was CVB (Commercial Glass Company of Brazil). After a year of activity by CVB, the building had an agency of the bank *Caixa Econômica Federal* on the ground floor.

Considered a development milestone because it was the first building of Brazil with a glass-skin facade, it was listed in 1992 by the Municipal Council for the Preservation of the Historical, Cultural and Environmental Heritage of the City of São Paulo (CONPRESP).

Subsequently, the building would receive a post from the Brazilian Social Security Institute (INSS) and in the early 2000s began to house the Federal Police. During this period, there are no records of significant renovations to keep the building in good conditions.

Years later, the two public agencies left Wilton Paes de Almeida so that it would be empty for sale by the Ministry of Cities' Union Heritage Secretariat (SPU) in February 2015. With the length of the process and the lack of interested in the purchase, the building was invaded by poor and homeless people (NEWS RONDÔNIA, 2018).

At dawn on the first day of May 2018, a fire caused the collapse of Wilton Paes de Almeida building. The fire started around 1:30 AM, and the flames began with a probable short circuit on the fifth floor (G1, 2018).

In a short time, due to the building's constructive characteristics, fire spread quickly through the other floors, both upwards (as expected) and downwards (unexpected), taking over the entire structure, from the ground floor to the roof. At about 2:50 AM, the entire building, still in flames, collapsed on itself (Figure 2), causing the death of seven people and many damages on the neighbor buildings as well as huge disruption to families and the traffic and free movement of people from the region.



Figure 2. Wilton Paes de Almeida after its collapse (source: Paulo Helene's personal collection).

With the collapse occurred in the Largo do Paissandu Square (Center Region of São Paulo), it is evident that the lack of maintenance and neglect with the patrimony can cause many losses and risks to the society. There were 07 people who lost their lives, about 92 families who lost the roof to the housed; 220 million of Brazilians who have lost a public property belonging to the Government estimated at more than US\$ 7 million, and countless of other inconvenience to people who live and work in properties around the building that collapsed (Figure 3).



Figure 3. Damage to the Lutheran Church, next to Ed. Wilton Paes de Almeida (source: Paulo Helene's personal collection)

Due the unusual collapse of this building, PMSP (City Hall of São Paulo) through Prof. Vitor Castex Aly, Secretary of Infrastructure, and Eng. Julio Timerman, President of IBRACON (Brazilian Concrete Institute), signed a technical cooperation protocol to make the case study feasible, which was under the responsibility of IBRACON's Technical Director, Prof. Paulo Helene.

3. BUILDING FIRE SAFETY

The premature collapse, around 80 minutes, of the Wilton Paes de Almeida (WPA) building surprised the engineering of concrete structures. From the conception of this building system, patented by François Hennebique in 1892, who used as a slogan of his advertising “*plus d' incendies désastreux*”, in other words, never more disastrous fires, it is known that reinforced concrete has high structural strength to the action of the fire and the weather. An example of this statement can be seen in Figure 4, which shows the first building made in 1900 with structural elements in reinforced concrete, located at Rue Danton, 1, Paris - France, with the system Hennebique, which is in full use today.



Figure 4. World's first building designed with the system Hennebique (119 years of good service to the society) (Source: Paulo Helene's personal collection).

Since 1900 there has been a great evolution of concrete and with the advent of high strength

concrete, above 100 MPa, doubts about the good behavior of concrete under fire rise again. Studies by Britez (2013) with high-strength concrete columns (140 MPa) subjected to high temperatures demystified the beliefs and doubts of the time that high-strength concrete could “explode” in a fire situation, with a marked *spalling* effect, which could lead to the premature collapse of buildings designed with this type of concrete.

The tested columns, made of colored reinforced concrete, presented excellent performance, keeping their edges intact. The reduction in concrete compressive strength was only observed in the peripheral regions, about 1.2 inches, even with fire exposure duration of 180 minutes. The steel of the reinforcement did not lose resistance after cooling and the portlandite content present in the sample also indicated that the depth of the nefarious action of the fire was very shallow, about 1.2 inches in 3 h of an ISO standard fire.

Corroborating the claim that the concrete shows excellent performance under the action of fire, previous fires as the Andraus, Joelma and Grande Avenida buildings, all in São Paulo and built in 1960s, withstood more than 4 h of fire without collapse and are currently in normal use.

This premature collapse of the WPA must be considered a serious fact, both from the point of view of the evacuation of buildings by users, and from the point of view of the safety of firefighters in their rescue and firefighting activities, as well as the safety of the surrounding neighborhood that cannot be hit by the wreckage, in other words, buildings cannot collapse so quickly in the face of fire.

4. RECONSTRUCTION OF THE STRUCTURE

Under a hard work of research to obtain the information and design sheets of the building, some architectural sheets describing the geometry of the columns were found in the records of FAU/USP (Faculty of Architecture of the University of São Paulo). Interestingly and surprisingly the outer section of the columns was square and constant with 85cm by side, but its sturdy cross-section with the shape of the letter H was staggered and variable from floor to floor. In addition, two opposing faces defined a “shaft” that was continuous throughout the height of the columns, from the underground floor to the rooftop, as shown in Figure 5. These “shafts” have been designed and constructed for the central air conditioner system.

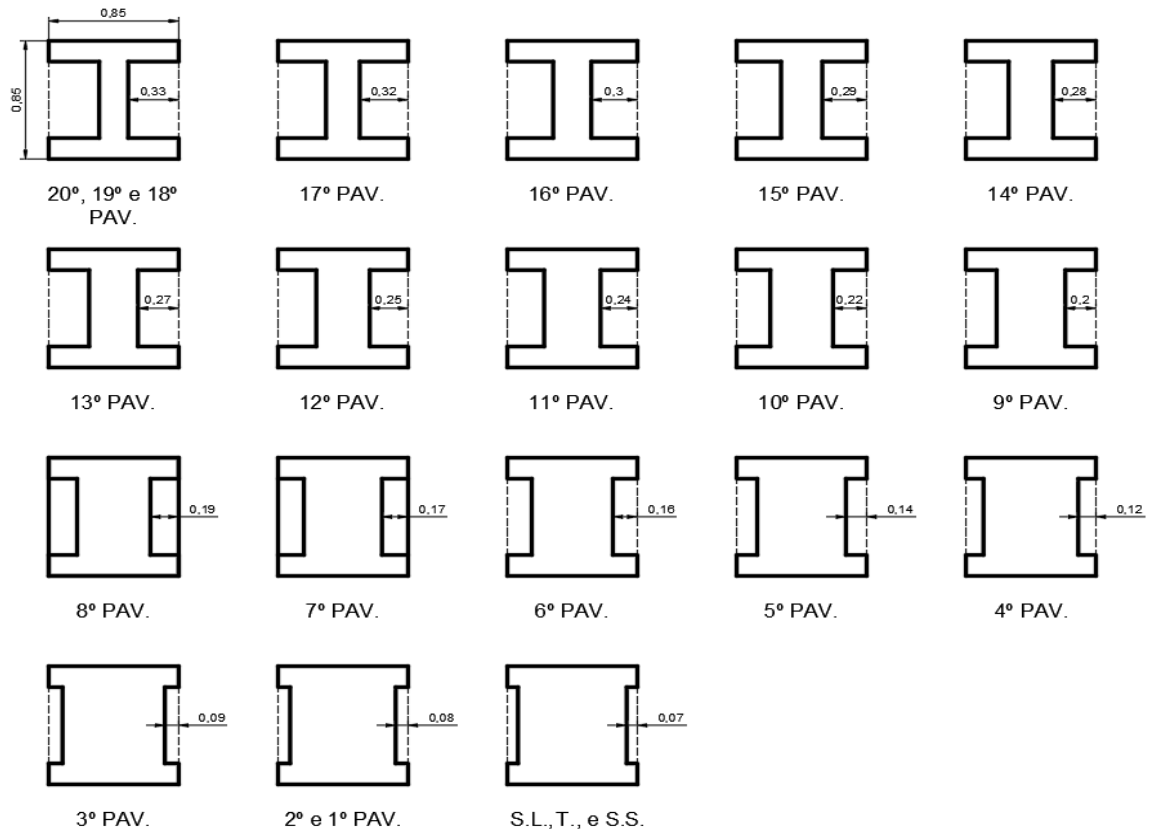


Figure 5. Scheduling of the columns (Source: executive architectural design found in the library of FAU. USP)

Many adaptations of projects and proposals made during the years of building operation that was headquarters of Federal Police, the Savings Bank and other companies were found in the archives of SPU (Union Heritage Department) together with these sheets. Engineer Leandro Coelho from SPU provided photos of his personal collection taken over the years, where it was possible to confirm, with some degree of precision, the structural typology used in the Wilton Paes de Almeida building (Figure 6).



Figure 6. Columns without metal coating, where it is observed the "H" which is actually a shaft of the air conditioner and I grate beam track with AJE still forms wood.
(source: personal collection of Leandro Coelho)

The building slabs were ribbed and were placed *in situ* with thickness of the topping slab of 6 cm (Figure 7). The ribs were 10 cm width and 28 cm high to the bottom of the topping slab, and were spaced every 50 cm. From the columns to the limit where it was installed the glass skin, the slab was a cantilever slab with variable cross-section (Figure 8).

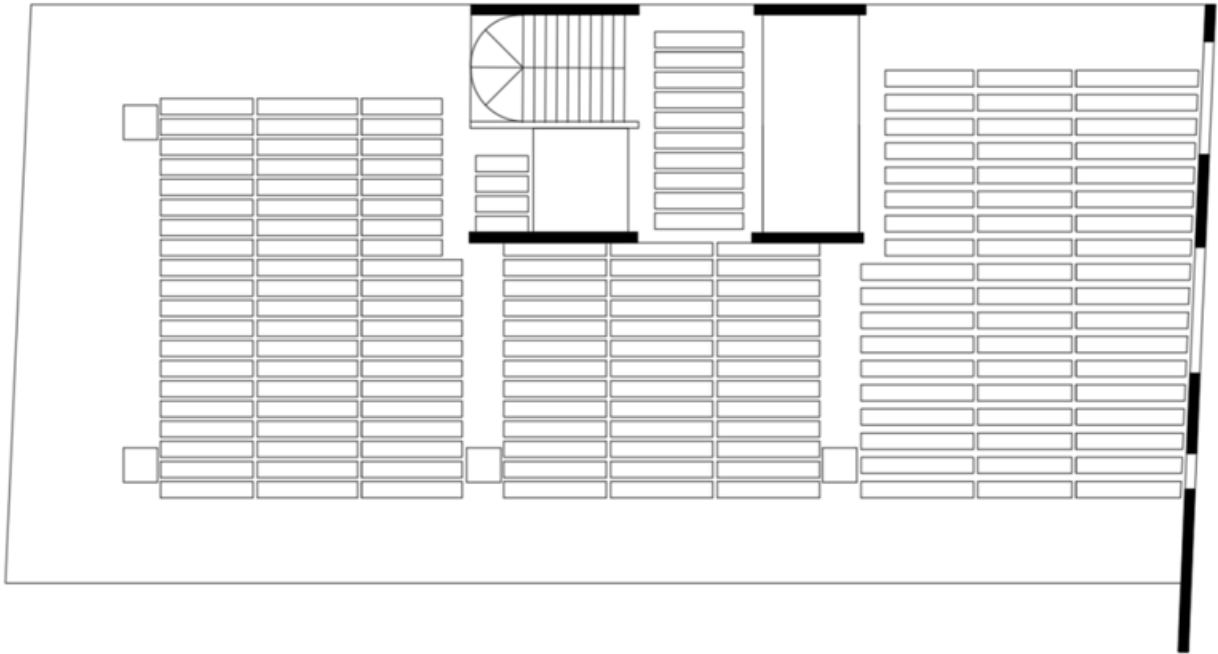


Figure 7. Grid Slab Scheme (Source: FAU-USP)

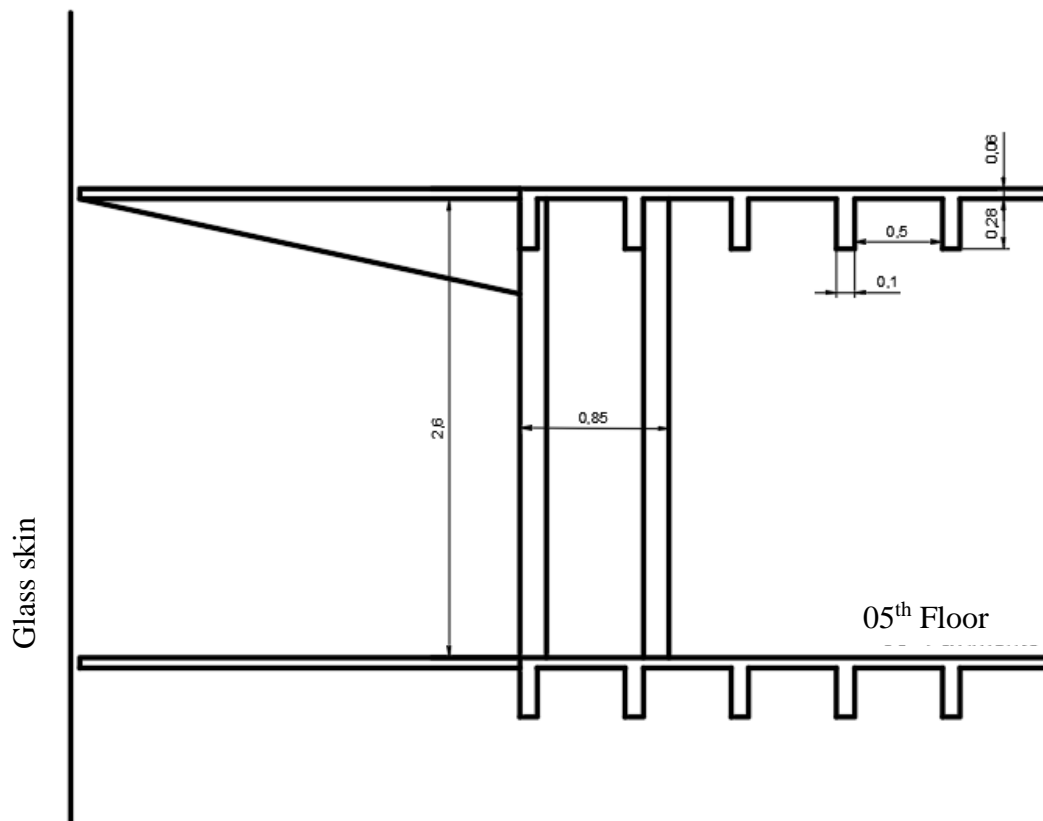


Figure 8. Grate slab cutting (Source: FAU-USP)

Thus, the main structural system of the structure, responsible for its lateral stability, was composed of concrete columns with “H” section, forming frames in one direction with the strip beams with the same height of the slab, added to concrete shear-walls in the lift and staircase and further a large wall crosslinked to the bottom, consisting of columns, beams and masonry, making a structural frame-wall, as can be seen in the hypothetical model shown in Figure 9.

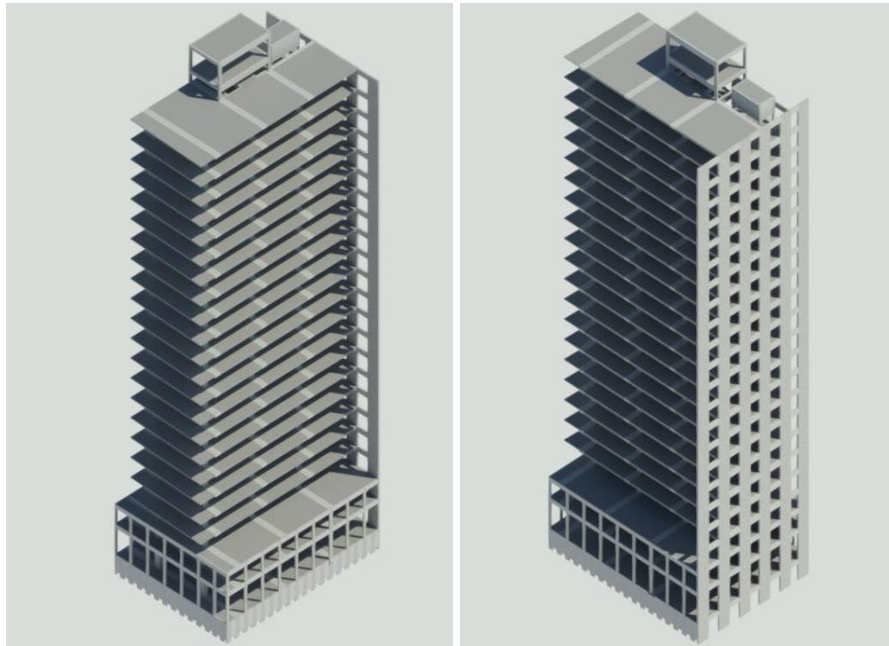


Figure 9. Frontal and posterior perspectives of the structure of Ed. Wilton Paes de Almeida (source: interpretation of existing projects at FAU-USP, SPU and Acrópole Magazine).

5. PROPERTIES OF REINFORCED CONCRETE

The following are the activities of sample collection and the test plan established to know the physical and mechanical properties of the materials present in the structure.

5.1 Sample Collection

Two major parts of collapsed superstructure were selected for collecting samples of the building to performing characterization tests, one slab portion and one column portion (Figure 10).



Figure 10. Excerpts cantilever slab and column collected from the debris for testing (source: Paulo Helene's personal collection)

5.2 Testing Plan

Regarding the concrete samples, the following activities and specific tests were established: geometric survey, core extraction, mineralogical characterization of the aggregate, petrographic appreciation of natural minerals, compressive strength, tensile strength, sclerometer test, ultrasonic test, modulus of elasticity, water absorption test, voids index, specific mass, mix reconstitution, x-ray diffraction, thermodifferential and thermogravimetry analysis, and carbonation.

Regarding the steel samples, the following activities and specific tests were established: typology of the steel employed, chemical and metallurgical composition, traction, folding, stretching and metallography.

5.3 Results - concrete

The results of tests carried out in concrete can be found full in the report made by the authors (Helene et. al., 2019) and is presented here only these analysis.

5.3.1 Sclerometry:

The “surface hardness assessment by the reflection sclerometer” test was performed in the laboratories of Mackenzie Presbyterian University (UPM), according to ABNT NBR 7584: 2013. 224 impacts in 14 different test areas were performed, half of them on fire exposed surfaces, and the other half on cut surfaces (core), called as *exposed face* and *core face*, respectively.

It was observed that there was a significant reduction in the reflection index values obtained from the external faces in relation to the values obtained from the core. All faces were affected by the flames, there was obtained a mean value of 24% reflective index (corresponding to the cylindrical compression resistance of $16 \pm 4,8$ MPa), while the measurements performed on the core sample obtained an average index of 30% (that corresponds to the cylindrical compressive strength of $26 \pm 6,3$ MPa).

5.3.2 Column cross section

After a diamond wire cutting in the column cross section, the layout of the rebars was evident inside the columns, being possible to make a draft with the reconstitution of column's cross section sampled, as shown in Figure 11.

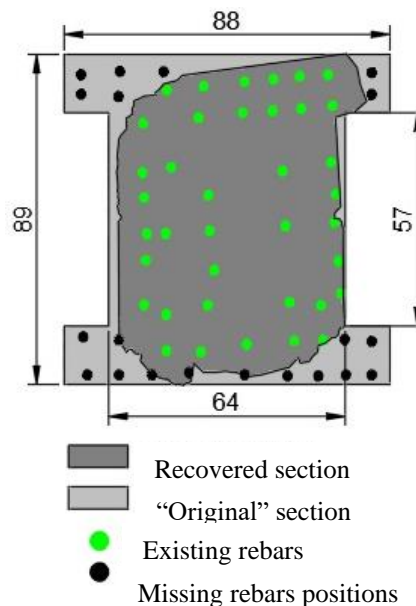


Figure 11. Reconstitution of the cross section of the recovered rubble column.

With the assessment of the cross section, arrangement of reinforcement rebars and their respective average diameters, it was possible to estimate the longitudinal reinforcement rate at approximately 3% of the gross area of the column, which is conventional for multi-story buildings.

The reinforcement cover, an important verification of the durability and fire resistance criteria, range from 1 cm to 5 cm in the collected sample, which, once again, showed a lack of control and construction care, typical and common at the date of execution of this building.

From the point of view of fire resistance, the cover (C1) that is used for the calculation of the resistance to the thermal gradient, extends from the external face of the columns to the center of the rebar reinforcement, which in this case ranged from 2.5 cm to 6.5 cm.

Still in the collected column section, it was found a column-slab intersection, and its evident reinforcement. Therefore, it was possible to determine the arrangement of the reinforcement of the strip-beam (Figure 12).

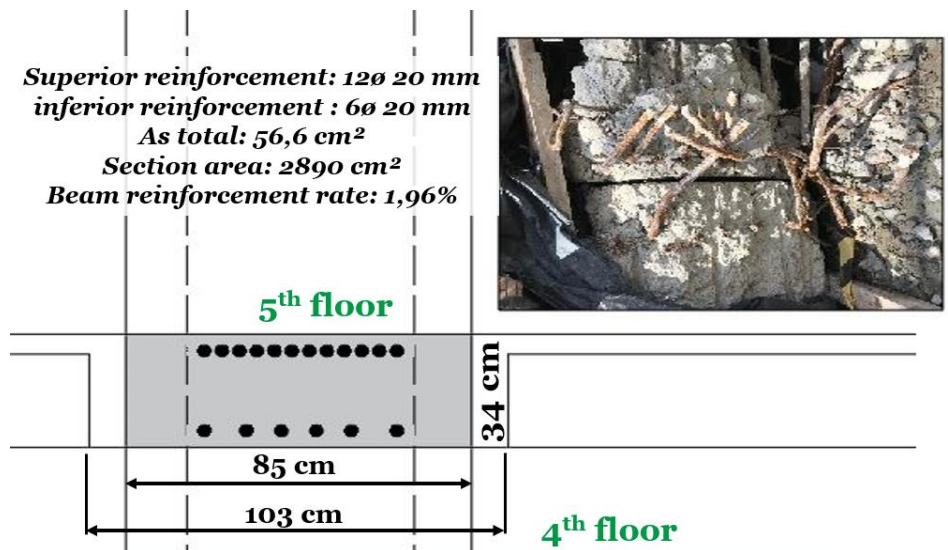


Figure 12. Configuration of the strip-beam reinforcement.

5.3.3 Concrete Cores Obtaining:

Core tests were performed at UPM. In addition, testing of axial compressive strength and diametral tensile strength was performed, several chemical and physical analysis was dependent substantially on the availability of samples in suitable proportions for performing the same; thus, the extraction of cores for these tests was fundamental.

A total of 16 cores were performed, of which only six (06) could be used for mechanical strength, due to the large number of internal cracks, as shown in figure 13. These cracks were possibly caused by poor concrete pouring at the age of the building's construction and, most likely, by the dynamic stresses of the superstructure falling during the building's collapse as well.



Figure 13. Visible cracks during extraction and decomposed core.
(Source: Paulo Helene's personal collection)

5.3.4 Compressive Strength

Tests were performed in UPM's laboratories, following the procedure of the standard ABNT NBR NBR 5739 and 7680, checking the average compressive strength of 21.8 MPa.

The results are consistent with the concretes produced at that time, which specified resistance was around of 135 kgf/cm² (13.5 MPa) to 180 kgf / cm² (18 MPa).

For structural evaluation purposes it was assumed that the characteristic compressive strength of concrete was $f_{ck} = 15$ MPa.

5.3.5 Tensile Strength

The tensile strength test was performed at UPM's laboratories, following the procedure of ABNT NBR 7222, checking an average value of 2,1 MPa.

The result obtained corresponds to approximately 10% of the value obtained for the compressive strength, which is totally satisfactory, coherent and expected for concretes of that time, in São Paulo.

5.3.6 Ultrasonic test and modulus of elasticity

The test for determining the ultrasonic velocity was performed in the PhD laboratories, for determining the dynamic elastic modulus by following the procedure d ABNT NBR 8802, checking an average speed of propagation of waves of 3707 m/s.

The Dynamic Modulus of Elasticity by Impact Stimulus test was also performed by following the procedure of ASTM C215, where values of 19.6 GPa (longitudinal) and 12.3 GPa (transverse) were checked.

Based on the master's dissertation of Bilesky (2016), it was possible to estimate the conventional static modulus of elasticity, ranging from 20 GPa to 26 GPa, that is perfectly compatible for the concrete in question.

5.3.7 Water absorption test, void indices and specific mass

The tests to determining water absorption, void index and density were performed following the procedure ABNT NBR 9778 and carried out in laboratories UPM. Samples were taken from the core of the column.

The following average results were obtained:

Water absorption → 6.52%, voids index → 14.75% and specific mass → 2.260 kg/m³

It is concluded that the results obtained are consistent with the quality of a concrete of the order of

$f_{ck} = 15$ MPa.

5.3.8 Mix Design Reconstitution

The test for Mix reconstitution was performed in the laboratory of the Brazilian Portland Cement Association (ABCP), following the procedure of internal standard ABCP PO-GT 3016.

For mass proportion calculations, a calcium oxide value of 60% was adopted. No account was taken of the possible presence of limestone materials linked to the aggregates.

The concrete mixes founded in the tests were 1: 5.9 in the columns and 1: 6.2 in the slabs, in dried mass of cement / aggregates and can be considered compatible with the age, corresponding to a cement consumption of 309 kg / m³, with a water/cement ratio of 0.65.

The results obtained are appropriate to the aggressiveness class in which the structure was inserted (class II of ABNT NBR 12655: 2015) and represent the concrete found at the time.

5.3.9 X-ray diffractometry, thermodifferential and thermogravimetry

The x-ray diffractometry, thermodifferential analysis and thermogravimetry tests were performed in the ABCP laboratory, following the procedure of the internal standard ABCP PO-GT 5042. These tests aimed to identify the crystalline phases that make up the samples of concrete submitted to high temperatures, which were analyzed in the X-Ray diffractometer and recognized through thermograms the presence of peaks related to cement hydrated to calcium hydroxide and calcium carbonate constituents of the hydrated binder, in addition to those related to the quartz present in the aggregate. By identifying the presence or absence of certain mineralogical compounds, it becomes possible to evaluate the temperature reached by a concrete structural element at different depths in a fire episode. The results of these analyzes can be found in tables 1 and 2.

Table 1. Mineralogical compounds of concrete samples.

Minerals	Approximate Chemism	Main interplanar distance (Å)	Relative Frequency					
			a (top)	b (middle)	c (base)	d (top)	e (middle)	f (base)
Feldspar	(Na _{0,5-0,3} , Ca _{0,5-0,7}) Al (Al _{0,5-0,7} , Si _{0,5-0,3}) Si ₂ O ₈	3,20	*	*	*	**	-	**
Mica	KAl ₂ (AlSi ₃ O ₁₀)(OH) ₈	9,99	**	*	**	**	**	***
Quartz	SiO ₂	3,33	****	**	***	****	**	***
Calcite	CaCO ₃	3,03	**	*	*	*	*	*
Portlandite	Ca(OH) ₂	4,90	***	****	****	**	****	****

Symbology - = not detected ** = uncommon
 tr = dashes *** = frequent
 * = present **** = very common

Note: The semiquantitative evaluation (expressed in number of asterisks) of the phases is based on the height of the diffraction peaks, whose intensity is a function of the content, symmetry and degree of crystallinity of the constituent.

Table 2. Results of Termodiferential and Thermogravimetry tests.

Sample Identification		Weight loss (%)					
		40°C to 200°C (Loss of free and / or adsorbed water and decomposition of hydrated silicates)	200°C to 400°C (Decomposition of hydrated aluminates)	400 ° to 500 ° C [decomposition of Ca (OH) ₂]	500° a 800°C (Decarbonation of the CaCO ₃)	Ca (OH) ₂	CaCO ₃
214424	top	4,59	2,03	1,32	10,34	5,4	23,5
	middle	7,54	4,86	3,85	2,90	15,8	6,6
	base	8,14	4,81	4,16	2,97	17,1	6,8
214425	top	4,35	2,79	1,46	11,53	6,0	26,2
	middle	8,38	5,45	4,18	4,31	17,1	9,8
	base	6,42	4,00	2,84	3,81	11,7	8,7

As seen in Tables 1 and 2, the samples from column surface, in the coatings region, resulted in portlandite levels three times lower than the core samples, which is consistent with the friable appearance found in coatings region *in situ*, being more intact in the region of the reinforcement (columns core).

In conclusion, these tests allow to estimate that the high temperature only acted on the surface of the structural concrete, about less than 1cm. This can also be one of the reasons for the mechanical integrity of the reinforcement, i.e., since it was over 1 cm, it was not affected by high temperatures (below 573° C).

5.3.10 Petrographic assessment of aggregates

The stereoscopic microscopy of the concrete constituents of the Wilton Paes de Almeida Building was performed at the ABCP laboratory by following the procedure of ABCP standard PO-GT 3016 rev. 02.

Four (4) fractions were taken from the column sample, the fractions were taken in function of the distance from the sample to the surface. It was observed that the analyzed concrete is composed of gravel and sand aggregates from rock crushing and river sand. Analyzes suggest a good quality of aggregates. The coarse aggregate comes from igneous rock, petrographically called biotite granite. A smaller amount of mafic rock was probably present, probably coming from a shaft that cut the rock massif.

From the petrographic point of view, aggregates have good characteristics to be used in concretes and no features caused by harmful exposure to fire were observed. For example, the presence of fractured quartz crystals and fractures at their crystalline interfaces that are indicative of allotropic quartz transformations was not observed. Such allotropic transformation of the alpha quartz to beta quartz occur with increased volume when the target temperature reaches 573° C, or it can be an evidence that the concrete has not been subjected to temperatures above 570° C. This is a reasonable conclusion because the exposure time to fire was very short, on the order of 1 h.

5.3.1.1 Carbonation measurement

The determination of carbonation depth was analyzed using a phenolphthalein – based pH chemical indicator. External faces were chosen and, therefore, hypothetical regions exposed to fire.

The measurements were performed for the carbonation layer in the most affected regions depths ranging from 2.5 cm to 3.0 cm, which corroborate the hypothesis that coated structural elements, as was the case of the columns of this building, have a longer durability, since the coating acts as another barrier against the penetration of the carbonation front and heat.

Considering that it was a structure with about 54 years of age, the depth of carbonation found demonstrate a good quality concrete and consistent with its age.

5.4 Results - steel

The results of the steel tests can be consulted in full in the document prepared by the *ArcelorMittal* technical team (Annex I of the report prepared by Helene et. al. 2019), and only a summary of them is presented here.

5.4.1 Steel typology employed

The steel used in the WPA reinforcement was of two types, and they were named notched and smooth due to their surface conformation. Due to the original format, the rebars "notched" presented with depressions arranged uniformly so vary their angle of 90°, as shown in Figure 14.



Figure 14. Classification of steel samples according to his gauge (Source: Arcelor Mittal)

After researches and contributions by Prof. Dr. Eduardo Thomaz, it is believed that steel rebars for reinforced concrete were manufactured by Peristahl S/A, at that time operating in the Brazilian market. These bars are cold hardened by bite in both normal and orthogonal directions, and in the case presented the following diameters: 8, 10, 16, 20 and 22mm.

5.4.2 Chemical Composition

A comparison between building samples with the current parameters for each chemical element present was performed, and the limits set by the ABNT NBR 8965, which for the components present in the standard (maximum values: C = 0.29; Mn = 0, 91; Si = 0.41; P = 0.14; S = 0.07 and Ceq = 0.47) were mostly below the maximum limits (0.38, 1.56, 0.55, 0.058, 0.058 and 0.59, respectively), and are therefore suitable for the weldability, ductility and strength parameters required for use in reinforced concrete.

5.4.3 Traction / Stretching

All samples were tested for tensile strength (f_{st} ranging from 470MPa to 760MPa; f_{yk} ranging from 320MPa to 640MPa; elongation ranging from 3% to 35% and all showed ductile rupture). Comparing with the current standardization of ABNT NBR 7480, it can be inferred that this reinforcement can be considered as CA-60 grade steel.

5.4.4 Metallography

Metallographic analyzes performed at different magnifications showed that the samples of 22, 20, and 16 mm gauge longitudinal notched bars correspond to the CA 60 steel and the 10 mm gauge smooth crossbars and the 8 gauge flat complementary bars. mm correspond to AC 37 steel. An example of metallographic analysis can be seen in Figure 15.

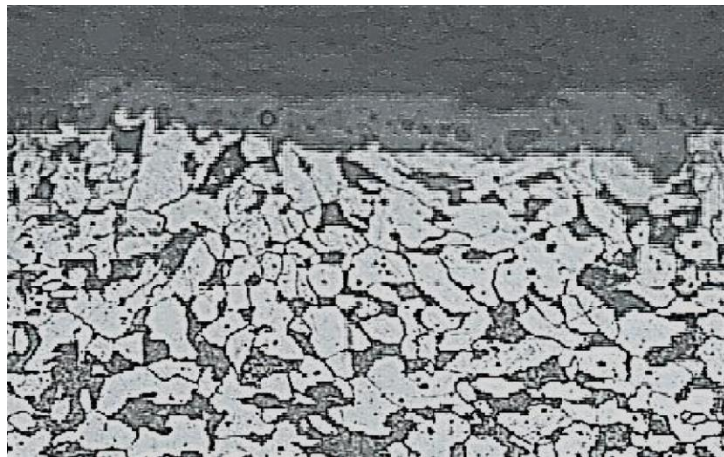


Figure 15. 22 mm diameter, 200x magnified steel bar sample surface
(Source: ArcelorMittal Laboratory)

6. FINAL CONSIDERATIONS

Based on extensive testing program carried out, in different and even contradictory sources of information available, and in the simulations of the structural model made, it can be concluded that:

1. Concrete had a mean compressive strength of 21,8 MPa with f_{ck} assumed of 15 MPa and MoE of 20 GPa to 26 GPa, besides other properties and characteristics very common to the age of construction in the city of São Paulo, not being the responsible for the collapse;
2. The X-ray Diffractometry, the thermodifferential and thermogravimetry analysis have shown that the maximum thickness of concrete not calcined reached 1 cm and the maximum temperatures of the concrete surface did not reach 573° C;
3. Coating studies have shown that concrete coating was enough to keep steel below 500° C, generally considered as a tolerable limit for reinforcement;
4. The results of the characterization tests of the rebar reinforcement showed that it was a kind of steel available in the Brazilian market at that time and still meeting the current standards, but not being the responsible for the premature collapse as well;
5. The reconstruction of the structural elements, column and beam, with respective cross section and reinforcement section, has demonstrated that the structure was designed to withstand the vertical loads, however when performing lateral loads checks and lateral stability with current criteria, the structure showed to be eccentric and with great potential of torsion. It must be considered the neighborhood mitigating factor, that in a way, could be

- a shield of lateral wind loads for this building, that stay in service for 54 years;
6. The structural model associated with the calculation thermal loads effects for the temperature gradient of 250° C showed that torsional moments due the thermal expansions of the structural elements, are about 20 times higher than those due to wind loads and vertical loads. This assessment is extensive and will be the subject of another specific paper, but this fact is recorded here, because it was the best explanation for the early collapse of the WPA building.

Finally, the diagnosis showed that from a “hypothetical structural design”, because the original structural design was not found, it was possible to explain the collapse by a global torsion effect generated by the high temperatures. Being a building with asymmetric structure the thermal deformations induced torsional stress and bending moments far above the resistance of the structure.

As recommendations, it stands out:

- a) In existing buildings, which are thousands in the city of São Paulo, demand through the Fire Department Active and Passive Fire Protection, with training people because in case of an uncontrollable fire, they could have a serious risk of collapse, like to WPA.
- b) In existing glass facade buildings, which are also hundreds in the city of São Paulo, there would be required, through City Hall, the construction of a 1.2 m minimum partitioning between twinned buildings and between stories with insulating and incombustible material.

7. ACKNOWLEDGMENTS

The authors acknowledge and thank the following companies and entities: ArcelorMittal, Brazilian Portland Cement Association (ABCP), Brazilian Association of Structural Engineering and Consulting (ABECE), Technological and Industrial Research and Services Cooperative (CPTI), Police Fire Department State Military Service (CBPMESP), Demolisher Santos Filho, Engefuro , Polytechnic School of the University of São Paulo (EPUSP), Institute of Technological Research (IPT), PhD Engenharia, São Paulo City Hall (PMSP), São Paulo Works (SPObras), São Paulo Urbanismo (SPU), Municipal Secretariat of Urban Infrastructure and Works (SIURB), Union Heritage Secretariat (SPU) , Superintendence of the Technical-Scientific Police (SPTC), University of Rio dos Sinos Valley (UNISINOS) , Federal University of Goiás (UFG), Federal University of Santa Maria (UFSM) and Mackenzie Presbyterian University (UPM).

8. REFERENCES

- Alonso, C. (2008), *Assessment of post-fire reinforced concrete structures: Determination of depth of temperature penetration and associated damage*. Concrete Repair, Rehabilitation and Retrofitting II – Alexander et al (eds)© 2009 Taylor & Francis Group, London, ISBN 978-0-415-46850-3.
- Aleteia (1992), “A trajetória do prédio que desabou no centro de São Paulo”. 28/05/2018. Disponível em: <https://pt.aleteia.org/2018/05/02/a-trajetoria-do-predio-que-desabou-no-centro-de-sao-paulo/> , acesso em 08/03/2019.
- Andrade, C. (1992), *Manual para diagnóstico de obras por corrosão de armaduras*. PINI, 104p
- American Society of Test Materials. (2000), *ASTM E119: standard methods of fire test of building construction and materials: fire and flammability standards, test method*. West Conshohocken, PA.
- Bilesky, P. (2016), *Contribuição aos estudos do módulo de elasticidade do concreto*. Dissertação. IPT Instituto de Pesquisas Tecnológicas, 298 p. Orientador: Paulo Helene.
- Britez, C., Castro-Borges, P., Berto, A., Helene, P. (2013), *Experimental evaluation of colored*

- HSC column in fire conditions*. Revista ALCONPAT, CONPAT, vol. 3 n° 1, p. 39-54, DOI: 10.21041/ra.v3i1.42
- Calavera Ruiz, J. et. al. (2005), *Comportamiento de la estructura del edificio Windsor de Madrid frente al incêndio sufrido*. *Ingenieria Estructural*, n. 37, p. 27-39.
- Chana, P., Price, B. (2003), *The Cardington fire test*. *Concrete (London)*, v.37, n.1, p. 28-33.
- G1 (2018), “*Incêndio em prédio de SP foi causado por curto-circuito em tomada no 5º andar, diz secretário*”. 03/05/2018. Disponível em: <https://g1.globo.com/sp/sao-paulo/noticia/incendio-em-predio-de-sp-foi-causado-por-curto-circuito-em-tomada-no-5-andar-diz-testemunha.ghtml>, acesso em 20/03/2019
- Helene P., et. al. (2019), *Edifício Wilton Paes de Almeida*. Histórico, anamnese, estudos, ensaios e análises da estrutura de concreto armado do edifício Wilton Paes de Almeida, que sofreu incêndio e colapso no dia 1o de maio de 2018, sito a Rua Antônio de Godoy, 581, Largo do Paissandu, São Paulo, SP. Recomendações Técnicas. Parecer Técnico PhD 324/2019. Abril, 2019. 100p. Disponível em www.phd.eng.br.
- International Organization for Standardization. (1999). *ISO 834: fire resistance tests: elements of building construction: part 1. General requirements*. Geneva.
- National Institute of Standards and Technology. (2005). *Final report on the collapse of the World Trade Center Towers. NIST NCSTAR 1*. September, 302p.
- News Rondônia (2018). “*A história do edifício Wilton Paes de Almeida no Largo do Paissandu*”. 03/05/2018. Disponível em www.newsrodonia.com.br/noticias/a+historia+do+edificio+wilton+paes+de+almeida+no+largo+do+paissandu/110221. Acesso em 08/03/2019.
- Revista Acrópole (2019). Ano 27 - N° 323, Nov. 1965. Disponível em: www.acropole.fau.usp.br/edicao/323/14, acesso em 08/03/2019.
- François Hennebique (2019). Disponível em: www.fr.wikipedia.org/wiki/Fran%C3%A7ois_Hennebique, em 08/03/2019.

Fires in concrete structures - Significant case studies in São Paulo

A. F. Berto* 

*Contact author: aberto@ipt.br

DOI: <http://dx.doi.org/10.21041/ra.v10i1.438>

Reception: 13/09/2019 | Acceptance: 11/11/2019 | Publication: 30/12/2019

ABSTRACT

In this article, the normative aspects related to fire safety will be approached and case studies of buildings in São Paulo that suffered the fire action and its consequences will be presented. Fire safety must be considered from the conception and development of the preliminary design of the building, through the design and construction and into the operation and maintenance phase. In the design phase, the issue should be especially considered, as it establishes the basic structure of the building's fire safety. It must be based on a thorough knowledge of the relationships with the provisions that give the building adequate levels of fire safety.

Keywords: fire, design, concrete structures.

Cite as: Berto, A. F. (2020), "*Fires in concrete structures - Significant case studies in São Paulo*", Revista ALCONPAT, 10 (1), pp. 132 – 146, DOI: <http://dx.doi.org/10.21041/ra.v10i1.438>

¹ IPT - Instituto de Pesquisas Tecnológicas, Brasil.

Legal Information

Revista ALCONPAT is a quarterly publication by the Asociación Latinoamericana de Control de Calidad, Patología y Recuperación de la Construcción, Internacional, A.C., Km. 6 antigua carretera a Progreso, Mérida, Yucatán, 97310, Tel.5219997385893, alconpat.int@gmail.com, Website: www.alconpat.org

Responsible editor: Pedro Castro Borges, Ph.D. Reservation of rights for exclusive use No.04-2013-011717330300-203, and ISSN 2007-6835, both granted by the Instituto Nacional de Derecho de Autor. Responsible for the last update of this issue, Informatics Unit ALCONPAT, Elizabeth Sabido Maldonado, Km. 6, antigua carretera a Progreso, Mérida, Yucatán, C.P. 97310.

The views of the authors do not necessarily reflect the position of the editor.

The total or partial reproduction of the contents and images of the publication is strictly prohibited without the previous authorization of ALCONPAT Internacional A.C.

Any dispute, including the replies of the authors, will be published in the third issue of 2020 provided that the information is received before the closing of the second issue of 2020.

Incendios en estructuras de concreto – Casos de estudio significativos ocurridos en São Paulo

RESUMEN

En este artículo se abordarán los aspectos normativos relacionados con la seguridad contra incendios y se presentarán estudios de casos de edificios en São Paulo que sufrieron la acción del fuego y sus consecuencias. La seguridad contra incendios debe considerarse desde la concepción del edificio, pasando por el diseño y la construcción, hasta la fase de operación y mantenimiento. En la fase de diseño, el tema debe considerarse especialmente, ya que establece la estructura básica de la seguridad contra incendios del edificio. Debe basarse en un conocimiento profundo de las relaciones que hay con las disposiciones que le dan al edificio niveles adecuados de seguridad contra incendios.

Palabras clave: fuego, diseño, estructuras de hormigón.

Incêndios em estruturas de concreto - Estudos de caso significativos em São Paulo

RESUMO

Neste artigo serão abordados os aspectos normativos com relação a segurança contra incêndio e apresentados estudos de casos de edifícios em São Paulo que sofreram a ação do incêndio e suas consequências. A segurança contra incêndio deve ser considerada desde a concepção e o desenvolvimento do anteprojeto do edifício, passando pelo projeto e construção e adentrando a fase de operação e manutenção. Na fase de projeto, a questão deve ser especialmente considerada, pois aí se estabelece a estrutura básica da segurança contra incêndio do edifício; ele deve ser elaborado a partir de um conhecimento aprofundado das relações que mantem com as disposições que conferem ao edifício, níveis adequados de segurança contra incêndio.

Palavras-chave: incêndio, projeto, estruturas de concreto.

1. INTRODUCTION

Fire, when reaching the phase of widespread inflammation in the origin environment, gradually promotes, due to its severity, structural elements' gradual weakening and assumes, under critical conditions, the ability to promote the building structural collapse. This destructive capacity increases as larger portions of the structure are affected by its action, as the fire spreads to other building environments.

Because of this, the design of structural building elements must consider the resolution of fire resistance. Currently, in Brazil there are state regulations regarding this issue, whose service in the buildings design and construction are compulsory. As a regulatory reference, the State Decree No. 63.911 / 2018, of the São Paulo State Fire Department, can be quoted, in which, the Technical Instruction No. 08/2019 - Fire resistance of building elements and the Technical Instruction No. 09 - Horizontal and vertical compartmentation is inserted.

The requirement to provide structural elements resistant to fire actions is strongly linked to the horizontal and vertical compartmentation of buildings, after all, the slabs and associated beams always integrate vertical compartmentation and the walls with horizontal compartmentation function always have structural elements incorporated or not to the main structure of the building.

From the perspective of the integral fire safety solution, vertical partitioning is an aspect that interferes with the resolution of the fire resistance of the structural elements. Certainly, it will be extremely complex to ensure (control the risk with a high level of confidence), in the development of the structural design, that building failure will not occur if large portions of the structure on various floors of the building are simultaneously subjected to fire. This situation is discussed in the present article, taking as reference some major fires that occurred in the city of São Paulo.

2. FIRE RESISTANCE REQUIRED TIME

The State Decree No. 63.911 / 2018 of the São Paulo State Fire Department, through the Technical Instruction No. 08/2019 establishes conditions to be met by structural and buildings compartmentation elements and defines the fire resistance required time (TRRF) under the justification that in the event of a fire, structural collapse is avoided, enabling personnel safe escape and access to fire brigade operations. This TRRF of structural and partitioning constructive elements is conditioned to the occupation and height of the building.

The TRRF is a design parameter and it does not represent the duration of the fire, the building evacuation time or even the Fire Department response time to the beginning of fighting the fire. The TRRF is established empirically, taking into account the likely severity of the fire, the difficulties of controlling the fire's progress and the consequences of the structural collapse caused by the fire, either in terms of risk to combat teams or in terms of collapse, considering the increasing gravity due to the height of the building.

As an example, the occupancy class of office buildings, the State Decree No. 63.911 / 2018 establishes TRRF values between 30 min to 180 min. For single-store buildings up to 6 m high the TRRF requires 30 min, above 6 m up to 23 m it requires 60 min, above 23 m up to 30 m it requires 90 min, above 30 m up to 120 m it requires 120 min, over 120 m to 150 m it requires 150 min and above 150 m to 250 m it requires 180 min.

For this occupancy class vertical compartmentation is required only for buildings over 12 m. Despite that, for buildings above 12 m (usually more than five floors), the decree referred allows such compartmentation to be replaced (partly as it makes exception for penetration and facade seals) by an automatic fire detection system, sprinkler system and smoke control system (lobby only for buildings up to 23 m in height). Above 90 m vertical compartmentation is indeed mandatory and must be accompanied by smoke detection, sprinkler and control systems.

It is important to emphasize that automatic fire detection and sprinkler systems are already mandatory, respectively, for heights greater than 12 m and 30 m, even if vertical compartmentation has been adopted. This way, they do not represent any additional benefit to those situations in terms of fire safety to allow eliminating vertical partitioning.

Analyzing the proposed values of TRRF, and the typical fire loads for office buildings (700 MJ / m², according to the State Decree No. 63.911 / 2018), among other factors, it can be considered that 60 minutes is the basic amount required for the structure supporting the action of the fire. The value of 30 min would be an option for smaller buildings and the values of 90 min, 120 min, 150 min and 180 min would correspond to aggravations considering what was placed until now. It should be noted that such aggravations do not account for the risk that portions of the structure associated with subsequent pavements are concomitantly subjected to fires of severity consistent with the 60 min TRRF, which represents extremely severe action on the structure.

Despite this, the State Decree No. 63.911 / 2018 provides benefits of easing the requirements concerning TRRF. It allows the TRRF to be reduced by 30 minutes through an equivalent time calculation, which takes into account (among other factors) the existence of a sprinkler system and automatic fire detection system (and which does not take into account the existence of vertical and horizontal compartmentation). In many situations considered, these active protective measures are mandatory or have already been taken into account to abolish the need for vertical

compartmentation and horizontal compartmentation.

In the case of office buildings, as an example, the TRRF equivalent time of 30 min is accepted for buildings up to 23 m in height. The easing granted is far beyond reasonable from the point of view of the risk of structural collapse in a fire situation.

The approach described here repeats for nearly all other types of occupation. What stands out here is the case of office buildings because of the tragedies that have occurred in Brazil involving these buildings and the collapses that have already occurred in its concrete structures.

3. SYSTEMIC APPROACH TO FIRE SAFETY

The lack of consistency that the regulation existing in Brazil presents in relation to issues that affect the structure of buildings in a fire situation, results in the risk conditions possibility that will give rise to the occurrence of major tragedies. Regarding structures fire resistance, this regulation lacks the systemic meaning, which is an essential issue to make it possible, since the complexity of solving the fire safety problem, to adopt an approach that leads to solutions safe.

This approach starts in the project and extends throughout the building's lifespan, considering the subdivision of the general problem into partial problems, which addresses the risks complexity, taking into account the objectives set. Such an approach should allow each of these partial problems to be solved independently, ensuring that they maintain between themselves and interact synergistically enough to establish, appropriately, the fire safety solution as a whole. An example of this division is presented next and includes eight elements:

- a) Precaution against the onset of fire, composed by preventive actions to control the fire onset risk;
- b) Safe abandonment of the building, consisting by protective actions aimed at ensuring the fast and safe building population evacuation;
- c) Occurrence limitation of generalized inflammation, consisting of protective actions aimed at controlling the risk of fast growth of fire in the environment of origin;
- d) Initial fire extinguishing, consisting of protective actions aimed at ensuring the means to fight the fire in its early stages;
- e) Limiting the spread of fire within the building, consisting of protective actions aimed at controlling the risk of fire spread beyond the original environment;
- f) Fire spreading precaution for adjacent buildings, consisting of protective actions to control the risk of fire spreading to adjacent buildings;
- g) Precaution against structural collapse, consisting of protective actions to control the risk of total or partial collapse of the building affected by fire;
- h) Facilitation of combat and rescue operations, consisting of protective actions to ensure speed and efficiency of combat operations.

Each of these elements, except the first, is composed of protective actions, that is, fire protection measures, which are divided into active and passive. The first, which there is greater familiarity in Brazil, correspond to the building systems of fire protection, including fire hydrants, sprinklers, detection and alarm etc.

Passive actions, which make up the portion of fire protection associated with the largest number of elements of the systemic approach mentioned, include the control of fire reaction characteristics of materials used in buildings, horizontal and vertical compartmentation, fire resistance of structural elements etc.; and condition, especially, the elements solutions: building safe abandonment; occurrence limitation of generalized inflammation; spread limitation of fire within the building; precaution against the spread of fire to adjacent buildings; precaution against structural collapse; and facilitation of combat and rescue operations.

One of the fire safety fundamental objectives is to preserve the building structural stability in case

of fire. This can be achieved more reliably if the fire safety solution is considered as a whole from a systemic approach.

A fire onset that finds favorable conditions in the building to grow and quickly reaches the phase of widespread inflammation will hardly be controlled by the use of manual combat systems. The rapid-fire growth does not leave time for the fire brigade action and the environment will be taken by smoke and heat making it impossible to the human presence. A situation like this, not protected by automatic combat system (or in case of failure of this system), may allow the occurrence of a fire that completely gets out of control, to the point of affecting extensively the building structure. From the human life standpoint, the conditions favorable to the fire growth may set insufficient time for the safe evacuation of the building, surprising people, who may be affected by the smoke and heat that are developed by the fire in frightening proportions when generalized inflammation is reached. There were two major fires in office buildings in the city of São Paulo. The first, in 1972, the Andraus building. And the second, in 1974, the Joelma building. Together they caused more than 200 deaths, undoubtedly highlighted this situation. In both cases, the fast occurrence of generalized inflammation surprised the buildings occupants.

These are just two examples that fully justify the need for the systemic approach to fire safety, which is characterized by the solutions interaction of its elements in order to solve the safety problem as a whole in the building. In these cases it can be said that the solution of the precautionary element against structural collapse, in addition to relying on intrinsic issues in the structure in the design, sizing and structure execution phases, will depend on extrinsic factors associated with other system elements, such as limiting the occurrence of widespread inflammation, initial fire extinguishing, limiting the spread of fire within the building, precaution against spreading fire to adjacent buildings, and facilitating combat and rescue operations. The following cases of fire presented here, prove these statements.

4. IMPORTANCE OF PARTITIONING

Automatic fire detection and smoke control do not directly play a role in containing the vertical spread of the fire. The sprinkler system, in turn, can do this to the extent that it contains fire development at its place of origin. If this system fails, or it does not count on the necessary support actions due to manual combat, the fire can spread vertically in the building. Overall in Brazil, these three systems have low reliability due to design, installation, operation and maintenance deficiencies (Berto et.al, 2018 and Berto et.al. 2019). Given this situation, it can be considered that the dispensation of vertical partitioning in the design of tall buildings becomes a temerity.

If the building is not equipped with proper vertical compartmentation, the Fire Department will have very little time and great difficulty to contain the vertical spread by soaking and cooling upper floors near the facades. Aggravating this situation is that the Fire Department in Brazil, in general, is slow to reach the fire scene. The response time of the fire brigade in the city of São Paulo and Brazil, understood as the time required for the fire brigade to reach the fire scene and start fire-fighting operations, is generally very high. The reasons that can be enrolled for this are: narrow streets; heavy volume of traffic; not planned growth of the city (Kodur et.al, 2019).

It is necessary to recognize that the vertical compartmentation of tall buildings finds a great fragility in the facades. This situation is characterized by two aspects. The first concerns the fire materials reaction characteristics that make up the façade. In São Paulo there are no rules for evaluating the façade fire behavior as a whole and the rules for the selection of facades materials in relation to fire reaction characteristics are relatively new and systematically disregarded.

Facades in tall office buildings, for example, are often lined with aluminum composite panels, which behave the same as those on the Grenfell Tower facade, where the fire spread vertically, killing more than 70 people.

Assessments of fire reaction characteristics of a major part of these materials used in São Paulo

building facades were carried out by the Fire Safety and Explosions Laboratory of the São Paulo State Institute of Technological Research - IPT and prove the poor performance and the ability of facades solutions composed of these materials to easily engage in fire and promote their spread. The second aspect mentioned is characterized by the following situation: the fire, reaching widespread inflammation in the original environment, can spread horizontally and dominate large areas in the pavement, thereby increasing the risk of vertical spread through the façade, since a large portion of the façade may be subjected to intense convection heat exchange that can determine the spread of fire to higher floors. This condition can be easily met in office buildings, which typically feature open space plan. Even if there are vertical separations between consecutive floor openings usually composed by the combination of the edge beam and the sill, the absence of combat action by cooling the facade above the fire floor can be crucial.

According to the indicated above and also because of the possibility that a large portion of the structure can be simultaneously attacked by a fire that dominates the entire floor of the building, the horizontal compartmentation also plays a very important role for the structure performance.

If vertical compartmentation is already poorly addressed in regulation, horizontal compartmentation is even more so. Recalling the case of office buildings, buildings up to 12 m height may have the horizontal partitioning replaced by the sprinkler system arrangement; over 12 m to 30 m in height the replacement should add the automatic fire detection system (although the detection system is already mandatory for buildings over 12 m height). Just above 30 m height there can't be a replacement of the horizontal partitioning by these two active fire protection systems. From this height the sprinkler system is required. Nevertheless, the admitted horizontal compartmental area is 2,000 m². It happens that automatic detection systems are mandatory for heights above 12 m, even if horizontal partitioning has been adopted, which does not represent any additional benefit for these situations.

One thing that cannot fail to be mentioned is that, according to State Decree No. 63.911 / 2018 of São Paulo State Fire Department, when required vertical compartmentation, it will be allowed, in above ground floors, the interconnection of up to three consecutive floors, through the atriums, stairs, circulation ramps or escalators, provided that the sum of areas of these floors does not exceed the values established for the compartmentation of areas. It can be seen therefore another weakness that threatens the performance of building structures in a fire situation.

The scenario presented here determines that the concrete structures of buildings, even if they were designed to comply with the TRRF, considering the dimensioning of the structural members separately, according to the Brazilian standard ABNT NBR 15200: 2012- Design of concrete structures in a fire situation, may suffer collapse when considerable portions of the whole are affected by the intense fire heat.

Fire Safety regulations emerged in the city of São Paulo in 1974, a few days after the major fire in the Joelma building, where 179 people died. It was already being prepared after the fire in the Andraus building, with the expectation that it would be incorporated into the next Municipal Works Code revision. The Joelma building tragedy led to the publication of rules that had been developed in the form of a Municipal Decree proposing that were observed in the design, construction and use of buildings. The first consistent regulation of the São Paulo State Fire Department was published only nine years later, in 1983.

Building designs prepared prior to these dates were not required to comply with any fire safety rules. Old buildings in São Paulo, that is, those designed prior to the validity of the Decrees mentioned, generally did not incorporate fire protection measures.

Despite this, from the moment that it was established the need to obtain the Fire Department Inspection Report - AVCB (document issued by the Fire Department certifying that, during the survey, the building had the fire safety conditions provided for by law, establishing a revalidation period), the São Paulo State Fire Department created rules for their adaptation in order to incorporate mandatory, at least basic, set of fire protection measures.

These rules are currently consolidated in the Fire Department regulations, that is, State Decree No. 63.911 / 2018, under the title Adaptation to Fire Safety Regulations - Existing Buildings. Old buildings, according to the Decree, must be regularized with the Fire Department by obtaining the AVCB, that is, they must be provided with basic fire protection measures which correspond to: fire extinguishers; emergency lights; emergency signaling; fire alarm; electrical installations in accordance with technical standards; fire brigade; fire hydrants; Emergency Exit; sealing shafts and installation ducts for buildings over 12 m high. Note that the horizontal and vertical compartmentation requirements and the structure fire resistance are not included as basic. In this way, old buildings, even AVCB holders, may have a structure unable to withstand the action of fire.

5. CONCRETE STRUCTURES IN A FIRE SITUATION

The lack of knowledge of several structural designers about the specificities associated with fire safety, in particular the ability of fire to cause severe damage to concrete structures, associated with the fact that the inspection processes do not include the verification of the structures dimensioning in a fire situation, leads to non-compliance of regulations and standards that impose a mandatory resolution of the issue. Besides this feeling, often decisive, that the design of concrete structures in fire situation is an unnecessary penalty, it leads to the adoption of wider sections and higher coatings of longitudinal reinforcement.

In fact, the need to adopt larger sections and coatings applies in some situations, which is evident when adopting the tabular sizing method included in the ABNT NBR 15200: 2012 standard and seeking to meet TRRF values greater than 60 min. This method is based on design tables derived from fire resistance test results and incorporates issues such as: preservation of a resistant concrete core; preservation of adequate reinforcement temperatures and acceptable steel-concrete adhesion conditions. It turns out that the stability preservation of concrete structures in fire situation goes well beyond what the tabular method predicts, because other important aspects interfere with the behavior of concrete structures, which can be: the static structure system as a whole; the major stresses that arise on the structure in fire caused by thermal expansion of heated parts of the structure; and the explosive chipping that concrete can suffer in a fire situation.

Regarding the expansion efforts, ABNT NBR 15200: 2012 textually proposes the following:

“The heat transmitted to the structure in this time interval (TRRF) generates in each structural element a function of its shape and exposure to fire, a certain temperature distribution. This process reduces the materials strength and the structural elements capacity, as well as stressing forces due to axial elongation or thermal gradients. While with heating, the stiffness of parts decreases greatly and the plastic adaptability increases proportionally, the stresses generated by heating can generally be neglected.”

It is not difficult to understand, and the large fires that occurred in Brazil that affected buildings with concrete structure reaffirm this situation, that this loss of stiffness does not occur, indicated in the concrete structure standard in the region affected by the fire and, much less, in the structure as a whole.

Inside the section of concrete parts, during the fire, the structure preponderant part is kept at proportionally low temperatures. Nevertheless, the surface portion of the parts reaches high temperatures, and determines on average, considering the entire section and parts length, enough temperatures to cause thermal expansion extremely greater than any structure plastic adaptability as a whole.

In fact, the structural elements thermal expansion, such as beams and columns, submitted on three or four faces to the fire action, produce efforts that the structure will hardly be able to absorb, without at least causing serious local damage (collapses) to the concrete structure. The problem of thermal expansion, in relation to the structure collapse, is accentuated in the situations presented

below and can lead to disasters:

- a) The efforts are predominantly directed to a structure sector, due the great stiffness of the building opposite sector, which offers a reaction to the stresses without significant deformation;
- b) The efforts are predominantly directed towards a structure sector, due to the asymmetrical arrangement of columns or beams;
- c) The efforts are predominantly directed to columns that integrate multiple frames, where the beams between them overcome great gaps and, consequently, have larger section;
- d) The structural lattice does not present great stiffness, that is, they present low degree of hyperstaticity, as precast structures, where prefabricated horizontal and vertical elements are solidified in the work, and the expansion stresses displace the supports.

When more than one of these conditions coexists, the situation may become critical and the total or partial building collapse may occur. This can be achieved early in the fire situation, that is, even before the effects of heat determine local damage that provide the structural elements collapse directly affected by the fire.

The situation seems to get worse when the horizontal structure is composed of ribbed slabs, which present in relation to the flat slabs, a larger heat transfer surface. A much more significant and stiffened concrete surface reaches high temperatures before it suffers significant mechanical damage, that is, while still able to transfer expansion stresses to the structural elements to which they are attached (beams and columns). They correspond to shear forces for which these structural elements are not prepared to withstand.

The concrete exposed to intense heat in fire, suffers physical and chemical changes that decisively compromise its mechanical properties. The reinforcement in the interior of the gradually heated concrete pieces has its adherence with the concrete compromised and also suffer a significant yield strength reduction. Still, the problem of fragmentation surface can promote the cross-section reduction of the parts and, consequently, its bearing capacity, in addition to exposing the reinforcement directly to the high temperatures reached in a fire. The concrete mix, including the water-cement ratio and admixtures used, are decisive factors for the occurrence of this phenomenon.

Some of these situations are illustrated in Figures presented next, corresponding to major fires in the metropolitan area of São Paulo and which led to tragedies that together caused many deaths.

The case of the Grande Avenida building fire occurred in São Paulo in 1981, illustrated in Figures 1, 2 and 3, which developed severely on two consecutive floors of its front podium, evidenced that the thermal expansion stresses of the concrete structural elements that composed the beams and slabs of these pavements, found in the tower the stiffness necessary to direct the thermal expansion stresses to the large section columns in the front podium portion, causing them to collapse.

The Wilton Paes de Almeida building fire case, which occurred in São Paulo in 2018, illustrated in Figures 4, 5 and 6, which concomitantly dominated a dozen floors, evidenced the coincidence of two harmful factors that caused the total collapse of its concrete structure just 80 minutes after the fire start: the thermal expansion stresses of the concrete structural elements that made up the beams and slabs of the floors affected by the fire, found on the face composed of a structural wall (twinned with a large building block) the stiffness necessary to direct the thermal expansion stress to the pillars that made up the building structure, especially for those associated with the central circulation core; The asymmetric set distribution of columns determined the predominant direction of this effort towards the columns integrated with the central circulation core (Helene, 2018). This situation caused the columns collapse and, consequently, caused the entire structure collapse. This situation was further aggravated by the reckless structural design of the concrete structure as a whole, which currently would not meet the Brazilian standard for sizing concrete structures.

The fire case illustrated in Figures 11 and 12 in 1995 in the São Paulo city metropolitan region

shows the collapse of a large precast concrete structure where the expansion efforts of the concrete structural elements displaced the supports. The absence of solidarity between the horizontal and vertical elements led to the structure collapse.

The most impressive case of fire reported here, due to the large concomitantly built area dominated by fire (over 20,000 m²), which defined the collapse of concrete structure part, occurred in São Paulo in 1987 and is illustrated in Figures 7, 8, 9, 10, 13, 14, 15, 16 and 17. This case is commented in the next topic.



Figure 1. Grande Avenida Building, highlighting front podium associated with 22-story tower



Figure 2. Podium of the Grande Avenida building, submitted to fire on 02/14/1981

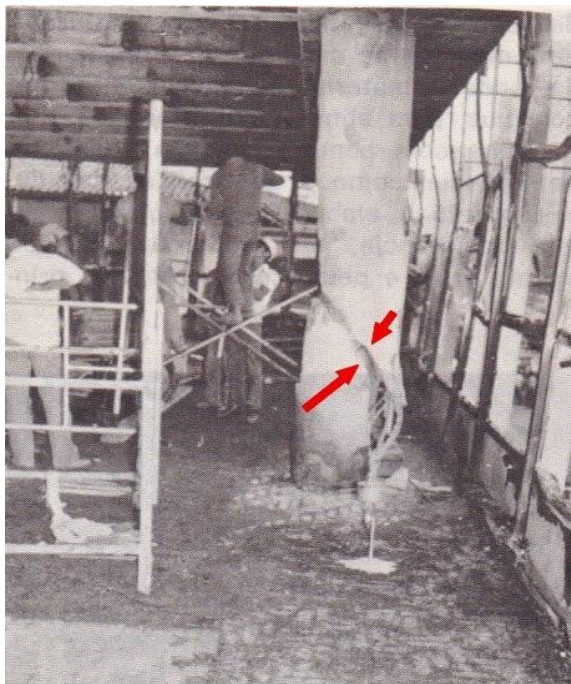


Figure 3. Column break located on the podium of the Grande Avenida building due to slab expansion stresses



Figure 4. Wilton Paes de Almeida Building, located downtown São Paulo

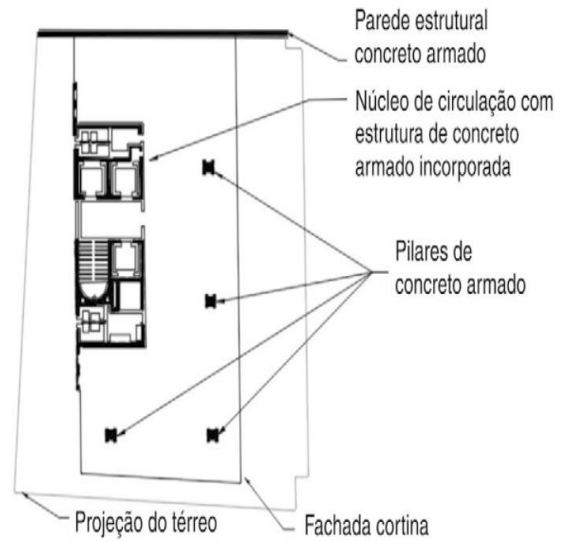


Figure 5. Wilton Paes de Almeida building subjected to fire on 05/01/2018

Figure 6. Schematic Floor plan of the building Wilton Paes de Almeida

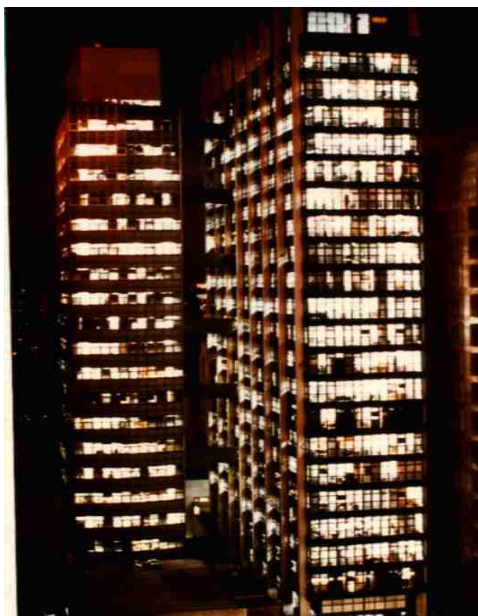


Figure 7. Sede I and Sede II Buildings of Companhia Energética de São Paulo - CESP

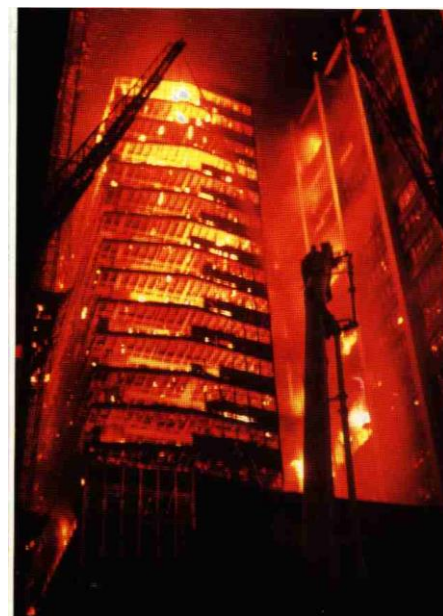


Figure 8. CESP Sede I and Sede II buildings submitted to fire on 05/21/1987

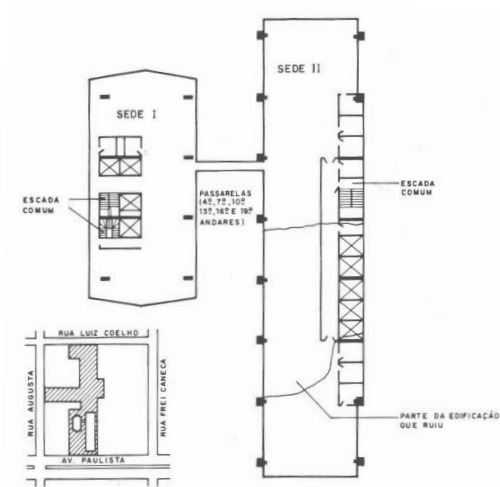


Figure 9. Schematic plan of the type pavement of CESP Sede I and Sede II buildings showing the sector that collapsed

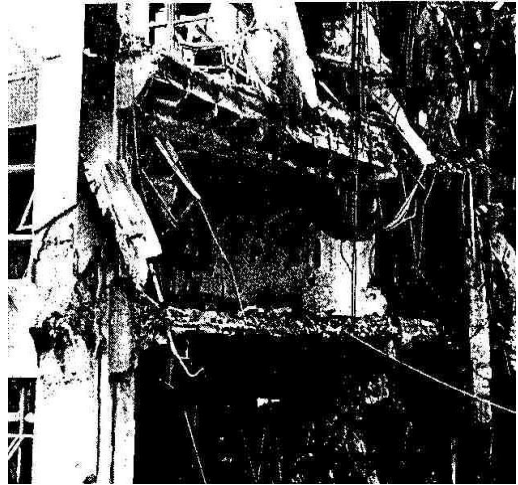


Figure 10. Collapse detail of the concrete structure of CESP Sede II building



Figure 11. Collapse of building with precast structure subjected to fire



Figure 12. Support displacement of pre-molded fire structure

All these conditions must be considered and addressed in the design of concrete structures, since the concrete structure collapse should not occur in a fire situation, as their catastrophic consequences, especially in the case of tall buildings, are absolutely unacceptable.

6. CONCRETE STRUCTURE COLLAPSE CASE STUDY

An exemplary case of concrete structure collapse corresponded to CESP Sede II building in a fire that took place on May 21, 1987. This building was part of a large building, forming a block with basement, podium and two towers. The basement had three levels, two of them were used for vehicle parking. The podium consisted of the ground floor and two mezzanines, which occupied the entire ground area. Above this podium there were two towers, called Sede I and Sede II, which had 19 and 21 floors respectively. Both towers had a standard floor size of approximately 12 m x 30 m and 12 m x 60 m, respectively.

The Sede I Building lining was composed of agglomerated cellulose fiber boards and the Sede II Building lining consisted of plasterboard. Over both there were wooden slabs forms, which were ribbed. The two towers facades were predominantly made of glazed metal frames.

The Sede I building had two unclosed stairs, one of which reached up to the 8th floor. The Sede II building had only one staircase, which was not enclosed.

The fire broke out on the 5th floor of the Sede I building, in the electric lighting network arranged

over the fuel ceiling. The lining quickly ignited, and the flames spread on its bottom surface. Ignited portions of the liner dropped off the combustible materials contained in the office and ignited them. Generalized inflammation on the 5th floor was reached very quickly.

The fire spread between floors in the Sede I building with great ease. This happened by two ways: through the building interior, through the stairs; and the outside of the building through windows and aluminum rails. The vertical fire spread was so fast that all floors of the building from the 5th onwards coincided with the widespread ignition phase, meaning they burned intensely at the same time. Although the distance between the Sede I and Sede II buildings facades is 9.5 m, the fire spread between them by thermal radiation. The fire in the Sede II building began intensely and concomitantly on several floors. The fire found no obstacles in the pavements to reach the whole floors area, since the floors only had subdivisions opposite the Sede I building, there where were the stairs, elevators, pantries and bathrooms.

Approximately two hours after the fire spread to the Sede II building, its central part collapsed, as shown in Figure 2. The building structure consisted of a set of multiple parallel frames of cast-in-place reinforced concrete, whose horizontal elements consisted of T-beams, large section and great rigidity that overcame gaps ranging from approximately 8 m to 11 m. The spacing between the frames was approximately 8 m. The locking between them was promoted by the ribbed slabs of the floors.

The fire, prior to the collapse of the Sede II building, was developing most intensely on the upper and building middle floors. In these regions the vertical elements of the frames were subjected to stresses due to the T-beams thermal expansion and their constituent materials were gradually losing their mechanical strength as they were being heated.

The building central region collapse was due to the fire that was developing at its mid-height, resulting from the expansion stresses introduced by two consecutive T-beams in the vertical elements of their respective frames. These two consecutive frames had significantly more stiffened vertical elements on one side of the building, as their cross sections were larger and formed the columns that made up the elevator shaft. The less stiff parts of the two gantries received greater efforts due to these dilations, ruled by the geometric relationship of the column sections on both frames sides, and suffered severe shear, breaking up.

The same type of structural design was adopted for Sede I building. Despite that, the gaps overlapped by the beams that made up the multiple gantries were significantly smaller, reaching about 4.5 m where there was a distinction between the vertical elements sections of the frames, and the beams had smaller sections than those of the Sede II building. This situation has not determined the emergence of critical shear forces in the vertical elements of the frames.

It was found in the Sede I building that the horizontal structural elements (beams and slabs) presented two problems capable of seriously compromising the stability of the structure in a fire situation. One of them was related to coatings of armor, generally very reduced, being next to the concrete surface in some regions. The other related to the reduced cross sections of the ribbed slab beams, which were insufficient to ensure fire resistance of more than 1 h. As a result, a significant part of the horizontal structural elements suffered great deformation.

Although only a structure part of the Sede II building collapsed, splitting it in two, what was left of its structure and also the Sede I structure, suffered serious damage, so that after the fire, there was an imminent risk of collapse of both buildings. Such a situation justified the urgent need for two buildings demolition.

The structural solution fragility of the two buildings facing the fire situation, associated with the absence of vertical compartmentation, clearly shows how fragile the static system adopted for the two towers structure. The collapse that has occurred shows that this structural solution, from the point of view of fire safety, must be avoided.

Part of the situations relating to the two buildings structures reported here are shown in Figures 9, 10, 13, 14, 15, 16 and 17. It is clear that on Sede II building, the efforts to expand the beams sheared

the columns of two frames, causing the central tower part to collapse.

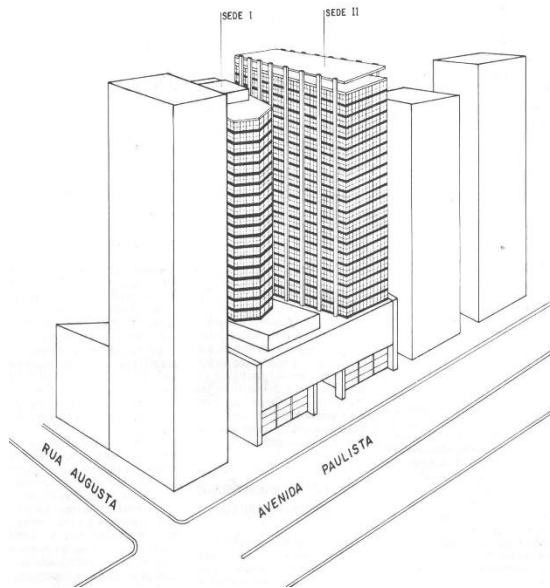


Figure 13. Block affected by fire: Podium and Sede I and II buildings I



Figure 14. Detail of the Sede II building concrete structure collapse, showing the two remaining parts of the tower.



Figure 15. Front view of the Sede II building structure, from its rear, highlighting the void left by the collapse of the central part



Figura 16. Building Sede II Remaining front

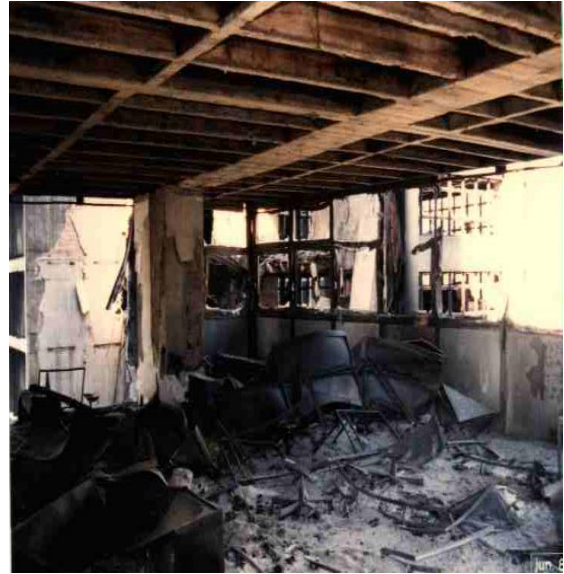


Figura 17. Fire damaged Sede I building structure

7. FINAL CONSIDERATIONS

The cases of collapse presented affected buildings built when there were no mandatory requirements in Brazil to ensure adequate conditions of fire safety. Currently there are regulations such as the State Decree No. 63.911/2018 of the Fire Department, with details set forth in Technical Instruction No. 08/2019 - Fire Resistance of Building Elements - which determines, in most situations, such as the case of larger buildings, that concrete structures and any other type of material (steel, wood and structural masonry) should be designed and constructed to be fire resistant, that is, so as to be capable of withstanding the action of fire, preserving the structural stability of buildings.

Despite this, the norm cited in this regulation, concerning the design of concrete structures in fire situation, needs to be urgently improved and designers should be aware of the importance of giving structures the real ability to withstand the action of a fire while preserving the stability of buildings. The cited regulation, which serves as a reference to other existing regulations in Brazil, should be improved and ensure a consistent approach that prevents properly sized structures from being affected by extremely severe actions, represented, among other situations, by large portions of the structure exposed, concomitantly or successively, to the action of the fire.

8. REFERENCES

- Associação Brasileira de Normas Técnicas. (2012). *ABNT NBR 15200: Projeto de estruturas de concreto em situação de incêndio*.
- Berto, A. F., Bottger, I. F., Paula D. J. (2018), *Segurança contra Incêndio? – ParteI*. Revista Emergência. p. 46 – 55, 12 dez. 2018.
- Berto, A. F., Bottger, I. F., Paula D. J. (2019), *Segurança contra Incêndio? – ParteII*. Revista Emergência. p. 34 – 41, 10 jan. 2018.
- Berto, A. F., Bottger, I. F., Paula D. J. (2019), *Segurança contra Incêndio? – ParteIII*. Revista Emergência. p. 30 – 38, 19 fev. 2018.
- Berto, A. F., Bottger, I. F., Paula D. J. (2019), *Segurança contra Incêndio? – ParteIV*. Revista Emergência. p. 42 – 51, 18 mar. 2018.
- Corpo de Bombeiros da PMESP. (2019). *Instrução Técnica nº 08 - Resistência ao fogo dos*

elementos de construção.

Corpo de Bombeiros da PMESP. (2019). *Instrução Técnica n° 09 - Compartimentação horizontal e compartimentação vertical.*

Corpo de Bombeiros da PMESP. (2018). *Decreto Estadual n° 63.911.* 10 de dezembro

Helene et. al. (2019), *Edifício Wilton Paes de Almeida. Histórico, anamnese, estudos, ensaios e análises da estrutura de concreto armado do edifício Wilton Paes de Almeida, que sofreu incêndio e colapso no dia 1o de maio de 2018*, sito a Rua Antônio de Godoy, 581, Largo do Paissandu, São Paulo, SP. Recomendações Técnicas. Parecer Técnico PhD 324/2019. Abril. 100p. Disponível em www.phd.eng.br.

Kodur, V. R., Kumar, P., Rafi, M. M. (2019). *Fire Hazard in Buildings: Review, Assessment and Strategies for Improving Fire Safety.* PSU Research Review - Emerald PUBLISHING. <https://doi.org/10.1108/PRR-12-2018-0033>